

339

RECEIVED

NOV 15 1991

ID. TRANSPORTATION DEPT

NATIONAL COOPERATIVE
HIGHWAY RESEARCH PROGRAM REPORT

339

EFFECTS OF THE QUALITY OF TRAFFIC SIGNAL PROGRESSION ON DELAY

TRANSPORTATION RESEARCH BOARD
NATIONAL RESEARCH COUNCIL

TRANSPORTATION RESEARCH BOARD EXECUTIVE COMMITTEE 1991

OFFICERS

Chairman: *C. Michael Walton, Bess Harris Jones Centennial Professor and Chairman, College of Engineering, The University of Texas at Austin*
Vice Chairman: *William W. Millar, Executive Director, Port Authority of Allegheny County*
Executive Director: *Thomas B. Deen, Transportation Research Board*

MEMBERS

JAMES B. BUSEY IV, *Federal Aviation Administrator, U.S. Department of Transportation (ex officio)*
GILBERT E. CARMICHAEL, *Federal Railroad Administrator, U.S. Department of Transportation (ex officio)*
BRIAN W. CLYMER, *Urban Mass Transportation Administrator, U.S. Department of Transportation (ex officio)*
JERRY R. CURRY, *National Highway Traffic Safety Administrator, U.S. Department of Transportation (ex officio)*
TRAVIS P. DUNGAN, *Research & Special Programs Administrator, U.S. Department of Transportation (ex officio)*
FRANCIS B. FRANCOIS, *Executive Director, American Association of State Highway and Transportation Officials (ex officio)*
JOHN GRAY, *President, National Asphalt Pavement Association (ex officio)*
THOMAS H. HANNA, *President and Chief Executive Officer, Motor Vehicle Manufacturers Association of the United States, Inc. (ex officio)*
HENRY J. HATCH, *Chief of Engineers and Commander, U.S. Army Corps of Engineers (ex officio)*
THOMAS D. LARSON, *Federal Highway Administrator, U.S. Department of Transportation (ex officio)*
GEORGE H. WAY, JR., *Vice President for Research and Test Departments, Association of American Railroads (ex officio)*
ROBERT J. AARONSON, *President, Air Transport Association of America*
JAMES M. BEGGS, *Chairman, Spacehab, Inc.*
J. RON BRINSON, *President and Chief Executive Officer, Board of Commissioners of The Port of New Orleans*
L. GARY BYRD, *Consulting Engineer, Alexandria, Virginia*
A. RAY CHAMBERLAIN, *Executive Director, Colorado Department of Highways*
L. STANLEY CRANE, *Consultant, Boynton Beach, Florida*
RANDY DOI, *Director, IVHS Systems, Motorola Incorporated*
EARL DOVE, *President, Earl Dove Company*
LOUIS J. GAMBACCINI, *General Manager, Southeastern Pennsylvania Transportation Authority (Past Chairman 1989)*
THOMAS J. HARRELSON, *Secretary, North Carolina Department of Transportation*
KERMIT H. JUSTICE, *Secretary of Transportation, State of Delaware*
LESTER P. LAMM, *President, Highway Users Federation*
ADOLF D. MAY, JR., *Professor and Vice Chairman, University of California Institute of Transportation Studies, Berkeley*
DENMAN K. McNEAR, *Vice Chairman, Rio Grande Industries*
WAYNE MURI, *Chief Engineer, Missouri Highway & Transportation Department (Past Chairman, 1990)*
ARNOLD W. OLIVER, *Engineer-Director, Texas State Department of Highways and Public Transportation*
DELLA M. ROY, *Professor of Materials Science, Pennsylvania State University*
JOSEPH M. SUSSMAN, *Director, Center for Transportation Studies, Massachusetts Institute of Technology*
JOHN R. TABB, *Director, Chief Administrative Officer, Mississippi State Highway Department*
FRANKLIN E. WHITE, *Commissioner, New York State Department of Transportation*
JULIAN WOLPERT, *Henry G. Bryant Professor of Geography, Public Affairs and Urban Planning, Woodrow Wilson School of Public and International Affairs, Princeton University*

NATIONAL COOPERATIVE HIGHWAY RESEARCH PROGRAM

Transportation Research Board Executive Committee Subcommittee for NCHRP

C. MICHAEL WALTON, *University of Texas at Austin (Chairman)*
WAYNE MURI, *Missouri Highway & Transportation Department*
FRANCIS B. FRANCOIS, *American Association of State Highway and Transportation Officials*

Field of Traffic

Area of Operations and Control

Project Panel G3-28C

DONALD S. BERRY, *Murphy Northwestern University (Chairman)*
KEN G. COURAGE, *University of Florida*
DAVID B. HILL, *Frederic R. Harris, Inc.*
WILLIAM C. KLOOS, *City of Portland, Oregon*
RALPH A. LEWIS, *City of Overland Park, Kansas*
BLAIR G. MARSDEN, *Kimley-Horn & Associates, Inc.*

Program Staff

ROBERT J. REILLY, *Director, Cooperative Research Programs*
LOUIS M. MacGREGOR, *Program Officer*
DANIEL W. DEARASAUGH, JR., *Senior Program Officer*
IAN M. FRIEDLAND, *Senior Program Officer*

WILLIAM W. MILLAR, *Port Authority of Allegheny County*
THOMAS D. LARSON, *U.S. Department of Transportation*
L. GARY BYRD, *Consulting Engineer*
THOMAS B. DEEN, *Transportation Research Board*

RAYMOND S. PUSEY, *Delaware Department of Transportation*
STEPHEN E. ROWE, *City of Los Angeles, California*
GEORGE W. SCHOENE, *D.C. Department of Public Works*
ALBERTO SANTIAGO, *FHWA Liaison Representative*
DAVID K. WITHEFORD, *TRB Liaison Representative (Now, Retired)*

CRAWFORD F. JENCKS, *Senior Program Officer*
KENNETH S. OPIELA, *Senior Program Officer*
DAN A. ROSEN, *Senior Program Officer*
HELEN MACK, *Editor*

NATIONAL COOPERATIVE HIGHWAY RESEARCH PROGRAM
REPORT

339

EFFECTS OF THE QUALITY OF TRAFFIC SIGNAL PROGRESSION ON DELAY

DANIEL B. FAMBRO, EDMOND C. P. CHANG, CARROLL J. MESSER
Texas Transportation Institute
Texas A & M University
College Station, Texas

RESEARCH SPONSORED BY THE AMERICAN
ASSOCIATION OF STATE HIGHWAY AND
TRANSPORTATION OFFICIALS IN COOPERATION
WITH THE FEDERAL HIGHWAY ADMINISTRATION

AREAS OF INTEREST

Traffic Flow, Capacity, and Measurements
Operations and Traffic Control
(Highway Transportation)

TRANSPORTATION RESEARCH BOARD

NATIONAL RESEARCH COUNCIL
WASHINGTON, D.C.

SEPTEMBER 1991

NATIONAL COOPERATIVE HIGHWAY RESEARCH PROGRAM

Systematic, well-designed research provides the most effective approach to the solution of many problems facing highway administrators and engineers. Often, highway problems are of local interest and can best be studied by highway departments individually or in cooperation with their state universities and others. However, the accelerating growth of highway transportation develops increasingly complex problems of wide interest to highway authorities. These problems are best studied through a coordinated program of cooperative research.

In recognition of these needs, the highway administrators of the American Association of State Highway and Transportation Officials initiated in 1962 an objective national highway research program employing modern scientific techniques. This program is supported on a continuing basis by funds from participating member states of the Association and it receives the full cooperation and support of the Federal Highway Administration, United States Department of Transportation.

The Transportation Research Board of the National Research Council was requested by the Association to administer the research program because of the Board's recognized objectivity and understanding of modern research practices. The Board is uniquely suited for this purpose as: it maintains an extensive committee structure from which authorities on any highway transportation subject may be drawn; it possesses avenues of communications and cooperation with federal, state and local governmental agencies, universities, and industry; its relationship to the National Research Council is an insurance of objectivity; it maintains a full-time research correlation staff of specialists in highway transportation matters to bring the findings of research directly to those who are in a position to use them.

The program is developed on the basis of research needs identified by chief administrators of the highway and transportation departments and by committees of AASHTO. Each year, specific areas of research needs to be included in the program are proposed to the National Research Council and the Board by the American Association of State Highway and Transportation Officials. Research projects to fulfill these needs are defined by the Board, and qualified research agencies are selected from those that have submitted proposals. Administration and surveillance of research contracts are the responsibilities of the National Research Council and the Transportation Research Board.

The needs for highway research are many, and the National Cooperative Highway Research Program can make significant contributions to the solution of highway transportation problems of mutual concern to many responsible groups. The program, however, is intended to complement rather than to substitute for or duplicate other highway research programs.

NCHRP REPORT 339

Project 3-28C FY '84

ISSN 0077-5614

ISBN 0-309-04862-1

L. C. Catalog Card No. 91-65200

Price \$11.00

NOTICE

The project that is the subject of this report was a part of the National Cooperative Highway Research Program conducted by the Transportation Research Board with the approval of the Governing Board of the National Research Council. Such approval reflects the Governing Board's judgment that the program concerned is of national importance and appropriate with respect to both the purposes and resources of the National Research Council.

The members of the technical committee selected to monitor this project and to review this report were chosen for recognized scholarly competence and with due consideration for the balance of disciplines appropriate to the project. The opinions and conclusions expressed or implied are those of the research agency that performed the research, and, while they have been accepted as appropriate by the technical committee, they are not necessarily those of the Transportation Research Board, the National Research Council, the American Association of State Highway and Transportation officials, or the Federal Highway Administration, U.S. Department of Transportation.

Each report is reviewed and accepted for publication by the technical committee according to procedures established and monitored by the Transportation Research Board Executive Committee and the Governing Board of the National Research Council.

Special Notice

The Transportation Research Board, the National Research Council, the Federal Highway Administration, the American Association of State Highway and Transportation Officials, and the individual states participating in the National Cooperative Highway Research Program do not endorse products or manufacturers. Trade or manufacturers names appear herein solely because they are considered essential to the object of this report.

Published reports of the

NATIONAL COOPERATIVE HIGHWAY RESEARCH PROGRAM

are available from:

Transportation Research Board
National Research Council
2101 Constitution Avenue, N.W.
Washington, D.C. 20418

Printed in the United States of America

FOREWORD

*By Staff
Transportation Research
Board*

The findings of this report will be of special interest to traffic engineers concerned with techniques for computing highway capacity. The techniques addressed in the report are those currently contained in the 1985 "Highway Capacity Manual" (*TRB Special Report 209*), Chapter 9, Signalized Intersections, which presents methods for computing the level of service for intersections controlled by traffic signals.

One of the more important factors in determining the level of service of a signalized intersection is the quality of progression of traffic. To the driver of a vehicle traveling along a street or arterial highway, good quality of progression would be seen as not having to stop too often or for too long. To traffic engineers, the quality of progression is expressed by a "progression adjustment factor" (PF) that is used to adjust the delay calculated from analytical equations for uniform arrival rates. The importance of PF in computing level of service is evidenced by the range of PF values, from 0.40 to 1.85, in Table 9-13 of Chapter 9, of the 1985 HCM.

Because the values of PF in the 1985 HCM were based on limited field data, the work reported herein was one of the highest priorities for further research in highway capacity following publication of that manual.

Under NCHRP Project 3-28C, "Effects of the Quality of Traffic Signal Progression on Delay," research was undertaken by the Texas Transportation Institute, College Station, Texas, to evaluate the effects of changes in the quality of traffic signal progression on level of service.

To accomplish the objective the researchers performed a critical review of the literature and theoretical modeling approaches and combined the results with the findings from controlled simulation and field studies. The research has resulted in an improved set of adjustment factors and more flexible methods for computing the capacity and level of service for signalized intersections. NCHRP Report 339 documents the research methodology and provides well-illustrated examples of how to apply the results. In addition, a supplement to this report contains a summary of the field data collected at each of the four study sites: Houston Suburban, Houston Urban, Los Angeles Suburban, and Los Angeles Urban. Copies of the supplement are available at a cost of \$8.00, on written request to the Cooperative Research Programs, Transportation Research Board, 2101 Constitution Avenue, NW, Washington, D.C. 20418.

The results of this research have been provided to the Transportation Research Board's Committee on Highway Capacity and Quality of Service. The Capacity Committee is currently reviewing, and considering for publication, a revised version of Chapter 9 of the HCM. Because progression issues are only one of many topics covered in Chapter 9, and there is ongoing research on the other topics, it may be some time

before a revised Chapter 9 is published. The Committee, however, has reviewed the report, endorses its findings, and has begun preparing an appendix to Chapter 9 for future publication. This report will be particularly useful because of the significance of progression issues to traffic engineers, the improved capacity analysis techniques that have resulted, and the exemplary documentation of a complex subject:

CONTENTS

1 SUMMARY

PART I

3 CHAPTER ONE Introduction and Research Approach
Research Objectives and Scope, 3
Research Approach, 3

4 CHAPTER TWO Findings
Summary of Previous Research, 4
Progression-Delay Models, 12
Simulation Studies, 15
Field Studies, 20
Results, 24

30 CHAPTER THREE Interpretation, Appraisal, and Application
Uniform Delay, 30
Revised Delay Equations, 30
Proportion Volume Arriving on Green, 30
Platoon Dispersion, 30
Early and Late Arrivals, 31
Progression Adjustment Factor, 32

33 CHAPTER FOUR Conclusions and Recommendations
Conclusions, 33
Recommendations, 34

35 REFERENCES

PART II

37 APPENDIX A Development of Progression-Delay Models

51 APPENDIX B Field Data

69 APPENDIX C Statistical Analysis

ACKNOWLEDGMENTS

This work was sponsored by the American Association of State Highway and Transportation Officials, in cooperation with the Federal Highway Administration, and was conducted in the National Cooperative Highway Research Program, which is administered by the Transportation Research Board of the National Research Council.

The research reported herein was performed under NCHRP Project 3-28C by the Texas Transportation Institute. The majority of the work was performed by personnel in the Traffic Operations Program of the Texas Transportation Institute. Dr. Edmond C. P. Chang and Dr. Daniel B. Fambro, Assistant Research Engineers, served as the principal and co-principal investigators for Project 3-28C. The primary author of this report is Dr. Daniel B. Fambro, and contributing authors, in alphabetical order, include Mr. James A. Bonneson, Dr. Edmond C. P. Chang, Dr. Carroll J. Messer, and Mr. Michael S. Ross. Specifically, Mr. Bonneson developed the platoon dispersion model described in Appendix A, and Mr. Ross coordinated the data reduction effort and designed and conducted the statistical analysis described in Appendix C. Other project staff members at TTI who assisted with the data collection and reduction

included Ms. Jeannette H. Arnold, Ms. Kristine A. Bachtel, Ms. Marggie N. Bass, Mr. Gilmer D. Gaston, Ms. Karen M. George, Mr. Tom R. Hammons, Ms. Wanda M. Hinshaw, Ms. Patricia A. Jackson, Mr. Said Majdi, Mr. Carl W. Ogden, Ms. Karen L. Pate, Mr. Joseph T. Short, Mr. Donald J. Szczesny, Mr. Kevin D. Tyer, Mr. Joseph F. Weesner, Mr. Marc D. Williams, Mr. Way En Yong, and Mr. Michael A. Zube.

The staffs of the Texas State Department of Highways and Public Transportation, City of Houston Department of Traffic and Transportation, City of Los Angeles Department of Transportation, and the California Department of Transportation were of great assistance during the data collection and analysis for this project. The Research Team is especially grateful for the contributions of Mr. H.F. Garrison and Mr. Doug Vanover of the Texas State Department of Highways and Public Transportation in Houston, Mr. Harvey Hawkins and Mr. Chi Ping Ha of the City of Houston Traffic and Transportation Department, Mr. Stephen E. Rowe and Mr. Kang Hu of the City of Los Angeles Department of Transportation, and Mr. Fred Erbe and Mr. Gene Woo of the California Department of Transportation in Los Angeles.

EFFECTS OF THE QUALITY OF TRAFFIC SIGNAL PROGRESSION ON DELAY

SUMMARY Chapter 9 of the 1985 Highway Capacity Manual (HCM), *Transportation Research Board (TRB) Special Report 209*, uses average stopped delay per vehicle as the sole determinant to establish threshold criteria for defining levels of service at signalized intersections. As described in Chapter 9 of the HCM, stopped delay can either be measured in the field or estimated using analytical equations. Of all the variables impacting delay, quality of progression has the largest potential effect as evidenced by the wide range of progression adjustment factors (PFs), 0.40 to 1.85 in Table 9-13 of the HCM. Of concern, however, to TRB's Highway Capacity and Quality of Service Committee and traffic engineers in general are the facts that the PFs in Table 9-13 are based on limited field data, and selection from a reasonable range of PFs in the table often results in changes in the level of service designation for the approach. In addition, guidelines for selecting the appropriate PFs to apply in practical applications are difficult to interpret. Because of these concerns and the importance of PFs in level-of-service determination, a research program was identified to verify variations in delay resulting from changes in the quality of progression.

The objective of NCHRP Project 3-28C was to evaluate the effects of changes in the quality of traffic signal progression on stopped delay. The general approach to this research was to combine the findings from the literature and theoretical modeling with the findings from controlled simulation and field studies to obtain a comprehensive evaluation of the effects of changes in the quality of traffic signal progression on stopped delay. A critical review of the literature was conducted to examine the HCM methodology together with the development of the existing progression adjustment factors, and to identify those variables that appeared to have significant influence on the quality of progression. Dependent variables that were investigated included signal offset and spacing, cycle length and splits, bandwidth, platoon volume, volume-to-capacity ratios, arterial speed, and platoon dispersion. Primary emphasis was given to through movements at pretimed signals on multilane arterials in urban and suburban areas. Secondary emphasis was given to the same conditions under semiactuated control. Several controlled simulation studies were conducted to examine the relationship between stopped delay and the variables identified as potentially influencing quality of progression. The variables examined included traffic volume, cycle length, green splits, travel time, and platoon dispersion. Results from the simulation studies were used to verify expected trends and define boundary conditions.

A pilot and four field studies were conducted to collect the data necessary to calibrate the analytical progression-delay models. Data were collected for two arterial signal systems, one urban arterial and one suburban arterial, in each of two metropolitan areas, Houston and Los Angeles. Standard statistical analysis techniques were used to analyze the field data and calibrate the progression-delay models. These models provide continuous relationships between variables rather than the discrete thresholds currently defined, and were used to validate a revised uniform delay equation and to prepare a revised version of Table 9-13, both for possible inclusion in the HCM. Use of these equations eliminates two problems noted by users of the 1985 HCM, discrete thresholds and the need for a wider range of adjustment factors to account for extremely good and extremely bad progression. Adjustment factors to account for early and late platoon arrivals (before or after the start of green) were also developed as part of this research. A methodology for estimating the proportion of the total volume arriving on green, platoon ratio, and/or arrival type was also developed.

Conclusions and recommendations based on the results of this research were as follows:

1. Progression adjustment factors should only be applied to the uniform delay term of the HCM's delay equation.
 2. Delay equations incorporating the proportion of the total volume arriving on green can explicitly account for the effects of progression on delay.
 3. The proportion of the total volume arriving on green, rather than platoon ratio, is a better predictor of the effects of quality of progression on delay.
 4. Platoon dispersion affects the minimum and maximum percentage of the volume that can reasonably be expected to arrive on green.
 5. Early platoon arrivals generally decrease the expected delay; late platoon arrivals generally increase the expected delay.
 6. Progression adjustment factors can provide reasonable estimates of delay at signalized intersections in a coordinated system.
-

INTRODUCTION AND RESEARCH APPROACH

Chapter 9 of the 1985 Highway Capacity Manual (HCM), *Transportation Research Board (TRB) Special Report 209*, uses average stopped delay per vehicle as the sole determinant to establish threshold criteria for defining levels of service at signalized intersections (1). The rationale for this decision is that delay is a measure of driver discomfort, frustration, fuel consumption, and lost travel time, i.e., a measure to which drivers can easily relate to their own travel experiences. As described in Chapter 9 of the HCM, stopped delay can either be measured in the field or estimated using analytical equations. Also, as noted in the HCM, delay is a complex measure that is dependent on a number of variables, including cycle length, effective green time to cycle length (g/C) ratio, demand volume to signal capacity (v/c) ratio, saturation flow, and quality of progression.

Of all the variables impacting delay, quality of progression has the largest potential effect as evidenced by the wide range of progression adjustment factors (PFs), 0.40 to 1.85, in Table 9-13 of the HCM (1). The appropriate adjustment factor from Table 9-13 is multiplied by the delay calculated from analytical equations for uniform arrival rates to estimate delay and a level of service designation for the intersection approach. Of concern, however, to TRB's Highway Capacity and Quality of Service Committee and traffic engineers in general are the facts that the PFs in Table 9-13 are based on limited field data, and selection from a reasonable range of progression adjustment factors in the table often results in changes in the level of service designation for the approach. In addition, guidelines for selecting the appropriate PFs to apply in practical applications are difficult to interpret.

Because of these concerns and the importance of PFs in level-of-service determination, field data supplemented by simulation data for a variety of conditions are needed to verify variations in delay resulting from changes in the quality of progression. These data should include the effects on stopped delay of individual factors, singly and in combination with one another, which may influence the quality of progression along an arterial street.

RESEARCH OBJECTIVES AND SCOPE

The objective of NCHRP Project 3-28C was to evaluate the effects of changes in the quality of traffic signal progression on stopped delay. Dependent variables that were investigated included signal offset and spacing, cycle length and splits, bandwidth, platoon volume, volume-to-capacity ratios, arterial speed, and platoon dispersion. Primary emphasis was given to through movements at pretimed signals on multilane arterials in urban and suburban areas. Secondary emphasis was given to the same conditions under semiactuated control.

The products of this research are fourfold:

1. A revised uniform delay equation which includes a term for quality of progression.
2. A calibrated set of progression adjustment factors in the form of a revised version of Table 9-13.
3. A continuous relationship for estimating the progression adjustment factors in the revised version of Table 9-13.
4. A methodology for estimating the proportion of the total volume arriving on green, platoon ratio, and/or arrival type.

This material is suitable for application to the general stopped delay model of Chapter 9 and to the urban arterials procedure in Chapter 11 of the 1985 HCM.

RESEARCH APPROACH

The general approach to this research was to combine the findings from the literature and theoretical modeling with the findings from controlled simulation and field studies to obtain a comprehensive evaluation of the effects of changes in the quality of traffic signal progression on stopped delay. Analytical modeling was necessary to provide a better understanding of the underlying progression-delay process and to provide the foundations for the simulation studies. This modeling resulted in the development of stronger statistical relationships from the simulation data.

A critical review of the literature was conducted to examine the HCM methodology together with the development of the existing progression adjustment factors, and to identify those variables that appeared to have significant influence on the quality of progression. For each of the variables identified, practicality of measurement and potential effect on stopped delay were considered. Analytical progression-delay models utilizing these variables were prepared and used in the design of controlled simulation and field studies.

Several controlled simulation studies were conducted to examine the relationship between stopped delay and the variables identified as potentially influencing quality of progression. The variables examined included traffic volume, cycle length, green splits, travel time, and platoon dispersion. Results from the simulation studies were used to verify expected trends and define boundary conditions. These findings guided the data reduction effort required in this research.

A pilot and four field studies were conducted to collect the data necessary to calibrate the analytical progression-delay models. Data were collected for two arterial signal systems, one urban arterial and one suburban arterial, in each of two metropolitan areas, Houston and Los Angeles. Each of the systems was operated in the pretimed mode, and exhibited a range of cycle lengths, green splits, volumes, geometrics, and platoon arrival types. In addition, the Los Angeles suburban system was operated in the semiactuated mode during the last day of data collection.

Standard statistical analysis techniques were used to analyze the field data and calibrate the progression-delay models. These models provide continuous relationships between variables rather than the discrete thresholds currently defined, and were used to validate a revised uniform delay equation and to prepare a revised version of Table 9-13, both for possible inclusion in the HCM. A methodology for estimating the proportion of the total volume arriving on green, platoon ratio, and/or arrival type was also developed.

CHAPTER TWO —

FINDINGS

The research examined the effects on stopped delay of the quality of traffic signal progression. This chapter presents the major findings from the summary of previous research, progression-delay model development, simulation and field studies, and statistical analysis of the collected data. Each of these topics is discussed in the following sections.

SUMMARY OF PREVIOUS RESEARCH

The summary of previous research describes the final formulation and application of the progression adjustment factors (PFs) used in the 1985 HCM. In particular, the reader will find that the present PFs are based on empirical as well as theoretical evidence, and are not as arbitrarily defined as they appear in the HCM. This section also discusses those variables that appear to have significant influence on the quality of progression and on the progression-delay models.

Highway Capacity Manual Methodology

Chapter 9: Signalized Intersections. The operational analysis section of Chapter 9 of the HCM contains level-of-service evaluations for signalized intersections (1). Figure 1 presents a brief overview of the methodology used. Module 1 defines the intersection problem; Module 2 determines the traffic demand; Module 3 determines the geometric and traffic capacity (saturation flow); Module 4 determines the signal capacity; and Module 5 determines the level-of-service based on calculated stopped delay. The effects on delay of the quality of signal progression are estimated in the initial calculations of Module 5.

Level-of-Service. The 1985 HCM uses average stopped delay per vehicle to establish threshold criteria for defining level-of-service for signalized intersections. Stopped delay is defined as the time a vehicle spends stationary while waiting in a queue of vehicles on an approach to a signal during the red signal display, or while waiting for the queue to begin moving during the early portion of the green signal display. Deceleration time, running travel time through the approach, and acceleration time are not considered as stopped delay time.

The HCM level-of-service criteria for signalized intersections are given in Table 1. Increasing average stopped delay per vehicle results in progressively lower levels of service for motorists. The specific delay criteria were selected by the Highway Capacity and Quality of Service Committee of the Transportation Research Board (TRB). In the HCM, delay-based levels of service are identified for three conditions:

1. lane groups within approach;
2. approaches to intersection; and
3. composite average of intersection.

Table 1. 1985 HCM Level-of-Service Criteria for Signalized Intersections.

Level of Service	Stopped Delay Per Vehicle (sec)		
A	≤	5.0	
B	5.1	to	15.0
C	15.1	to	25.0
D	25.1	to	40.0
E	40.1	to	60.0
F	>	60.0	

Source: Table 9-1 of Reference (1).

Delay Estimations. Numerous factors influence the amount of stopped delay experienced by the through lane group at an intersection. Strictly empirical studies using statistical regression analysis techniques on large data sets have noted some of these factors. One recent study (2) observed that all delay measures decreased significantly with increasing g/C ratios and increased with increasing cycle lengths. Stopped delay for through movements decreased as percent volume arriving on green increased and increased as left and right turning volumes increased. In this same study, overall delay was found to equal stopped delay for random arrivals when multiplied by a constant of 1.3.

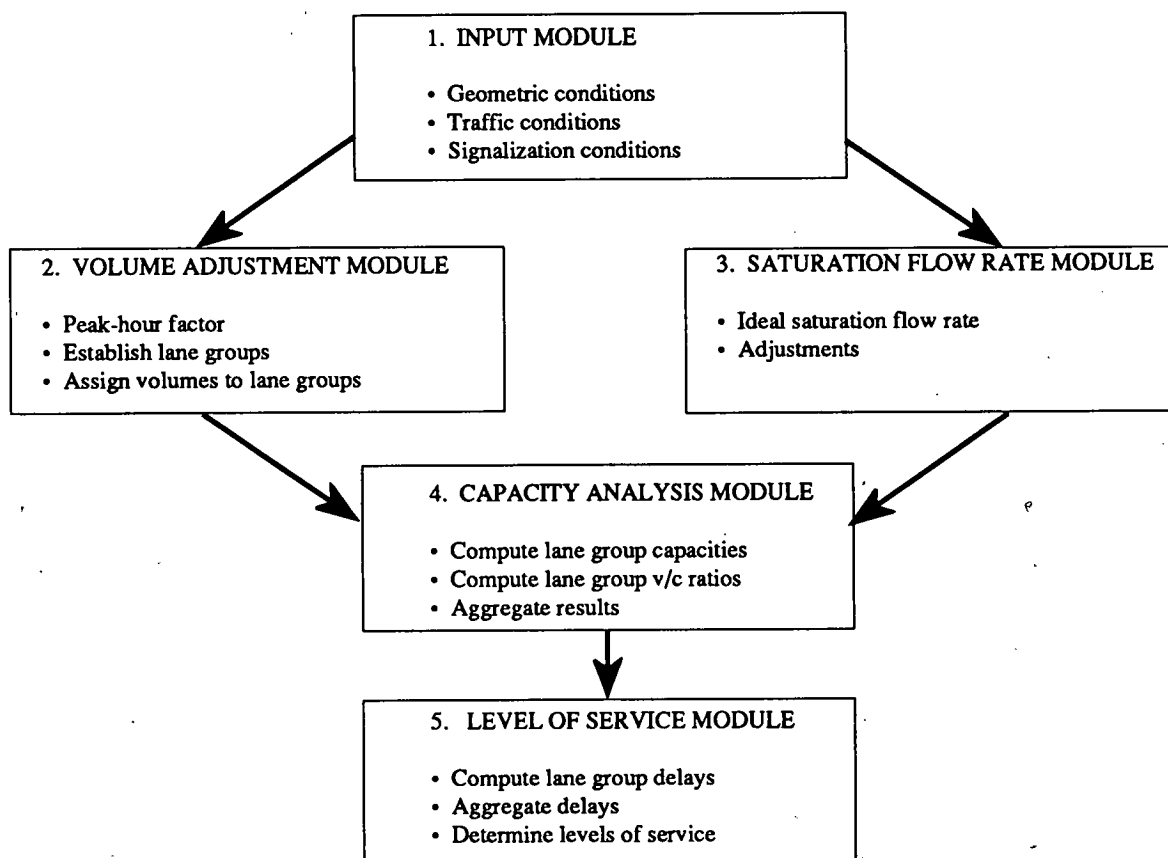


Figure 1. Operational Analysis Procedure.

Stopped delay is estimated in the HCM by an equation based on empirical data as well as theoretical relationships (1,2,3). Undersaturated (v/c ratio ≤ 1.0) and oversaturated (v/c ratio > 1.0) flow can be addressed. The basic form of the delay equation is for random (Poisson) arrivals having a constant (uniform) average flow rate throughout the cycle. Random arrivals typically occur when there is no upstream signal within one-half mile in coordinated signal systems and one-fourth mile in uncoordinated, actuated signal systems. Other factors, including turning traffic and stream friction, influence the type of arrival traffic flow (4). The 1985 HCM delay equation for random arrivals is as follows:

$$d = d_1 + d_2$$

and

$$d_1 = 0.38 * C * \frac{(1 - g/C)^2}{[1 - (g/C) * X]}$$

$$d_2 = 173X^2 * \left[(X - 1) + \sqrt{(X - 1)^2 + (16X/c)} \right]$$

where:

d = average stopped delay per vehicle for the lane group, sec/veh;

- d_1 = first-term delay for uniform arrivals, sec/veh;
- d_2 = second-term delay for incremental random and overflow effects, sec/veh;
- C = cycle length, sec;
- g/C = green ratio for the lane group; the ratio of effective green time to cycle length;
- X = demand volume to signal capacity (v/c) ratio for the lane group; and
- c = capacity of the lane group, veh/hr.

The first term of the equation accounts for delay due to a uniform or average flow rate throughout the cycle. It is the same as the first term in Webster's equation (5), adjusted for stopped delay, i.e., the coefficient $0.38 = 0.50/1.3$. To be technically correct, X cannot exceed 1.0 in Webster's first term because X is equivalent to $y/(g/C)$, where $y = v/s$ and is less than g/C . This limitation is not explicitly recognized in the 1985 HCM.

The second term of the delay equation estimates both the additional delay due to random arrivals over uniform arrivals and, for the long-term, the additional delays that arise when demand exceeds capacity for a period of 15 minutes; i.e., when $X > 1.0$ for 15 minutes. The square-root portion of the second term was derived from work by Kimber and Hollis (6). Embedded in this term is an assumed study period of 15 minutes.

During subsequent testing, it was envisioned that arrival types would be selected by experienced traffic engineers based on field observations. Type estimation studies conducted at that time indicated that type estimates were almost always identical or only off by a difference of one, e.g., Type 4 versus Type 3.

Further guidance was provided (9) in estimating the appropriate arrival type for a through movement to an intersection. Field observations were suggested to determine the percentage of total approach volume contained in the largest platoon. With this data, and with a classification of the quality of signal coordination (good, random, or poor), an arrival type could be identified. Table 3 provides the guidelines necessary to make this selection.

Modified Factors. During preparation of the new HCM, it became apparent that additional research and development would be necessary to estimate the effects of progression. No data useful for further calibration of the progression adjustment factors of Table 2 and Table 3 were available. As a result of this lack of data, a more generalized equation to estimate total delay due to progression was used as the analytical model for further testing and refinement of the PFs of Table 2. Development of this analytical model is presented in Appendix A. This delay model (which is affected by progression) was used in PASSER II-84 (10) and is illustrated as follows:

$$d_1 = 0.38 * C * (1 - g/C)^2 * q_r/q * \left(1 + \frac{q_r}{s - q_g}\right)$$

where:

- d_1 = first term delay for uniform arrivals, sec/veh;
- C = cycle length, sec;
- g = effective green time of phase, sec;
- q = average flow rate during cycle, vps;
- q_g = average flow rate during effective green time, vps;
- q_r = average flow rate during effective red time, vps; and
- s = saturation flow rate, vps.

Using the PASSER II-84 modeling concept, the following platoon ratio was defined in the 1985 HCM:

$$R_p = PVG/PTG$$

where:

- R_p = platoon ratio;
- PVG = proportion of all vehicles in the movement arriving during the green phase; and
- PTG = proportion of the cycle that is green for the movement.

As noted and used in Chapter 9 of the HCM, PVG is observed in the field, and PTG can be observed or calculated. Both values are computed internally in PASSER II. Thus, the theory behind the platoon ratio adjustment for delay is conceptually sound; it is related directly to progression concepts and has been tested through field and simulation studies. Figure 2 shows the results of one of the earliest simulation studies of the effects of platoon ratio on delay (4).

The principal investigators for the preparation of the 1985 HCM used this existing technology to refine the original progression adjustment factors from NCHRP 3-28. Explicit ranges of R_p were given to each of the five arrival types. Midpoints of the five categories were defined as 2, 4, 6, 8, and 10 of 6. Threshold criteria were then defined as midpoint values of 3, 5, 7, and 9 of 6, i.e., 3 = 3/6 or $R_p = 0.50$. The resulting relationships between the five arrival types and platoon ratios (slightly rounded) were derived and are presented in Table 4 (Table 9-2 in the HCM).

Using the progression delay theory in PASSER II, new PFs for delay estimation were derived. Figure 3 shows these PFs for pretimed signal operations and compares them with the original values of Table 2. Note that volume-to-capacity ratio effects were added as a refinement step.

Table 3. Guidelines Provided to Establish Arrival Types Within NCHRP 3-28 (2).

	Coordination			
	Good	Random	Poor	
Dense Platoon	5	3	1	Platoon is dense and contains over 80% of total approach volume.
Platoon contains 40-80% of total approach volume	4	3	2	Platoon is somewhat dispersed, and contains between 40-80% of total approach volume.
Predominantly random arrivals	3	3	3	Random arrivals. Platoon contains less than 40% of total approach volume.

Source: Table F-1 of Reference (10).

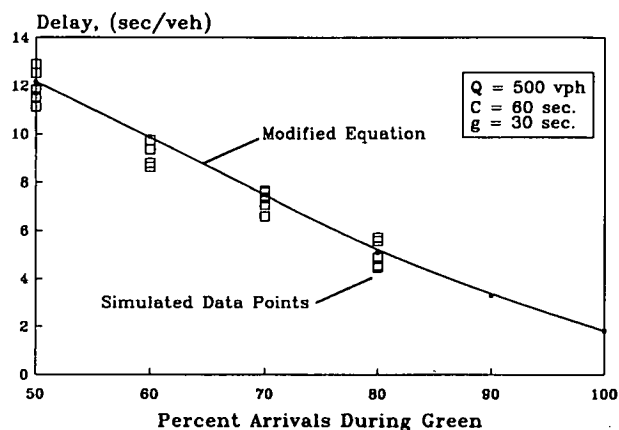


Figure 2. Simulated Effects of Progression on Individual Vehicle Delay.

Table 4. Relationship Between Arrival Type and Platoon Ratio.

Arrival Type	Range of Platoon Ratio, R_p
1	≤ 0.50
2	0.51 to 0.85
3	0.86 to 1.15
4	1.16 to 1.50
5	> 1.50

Source: Table 9-2 of Reference (1).

The following steps were then taken to derive the remainder of the HCM's progression adjustment factors, shown herein as Table 5 (Table 9-13 in the HCM). The basic performance differences between pretimed control and the three actuated types of signal control observed in the original study were retained. Direct proportioning with the PASSER II delay model formulation was performed using the following relationship:

$$PF_{T,X,A} = PF_{P,X,A} * \frac{PF_{T,A}}{PF_{P,A}}$$

where:

- $PF_{T,X,A}$ = progression factor for Signal Type T, for v/c ratio X, and Arrival Type A (Table 5 and HCM values);
- $PF_{P,X,A}$ = progression factor for pretimed signals P, for v/c ratio X, and Arrival Type A;
- $PF_{T,A}$ = progression factor for Signal Type T and Arrival Type A in Table 2; and
- $PF_{P,A}$ = progression factor for pretimed signals P and Arrival Type A in Table 2.

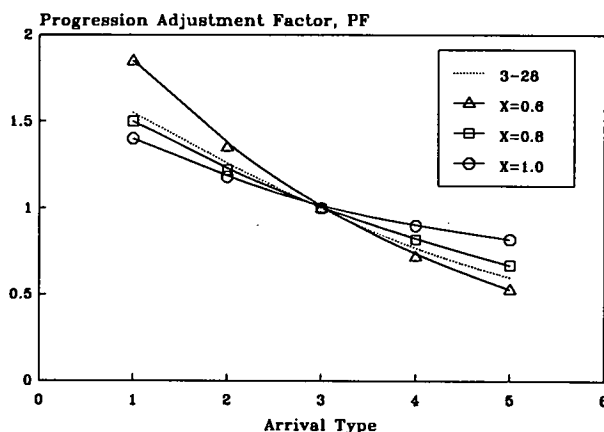


Figure 3. Comparison of Original and Final HCM Progression Factors.

As a case in point, note in Table 5 that the PF for actuated signals and v/c ratio X of 0.6 is 1.54 for Arrival Type 1. This factor was obtained as follows:

$$PF_{A,0.6,1} = 1.85_{P,0.6,1} * \frac{1.25_{T,A}}{1.50_{T,A}}$$

Application of the proportional method reveals a minor inconsistency in the HCM progression adjustment factors given in Table 5. Factors for main street lane groups having Arrival Type 5 and semiactuated control are about 5 percent too low. This is not considered a serious error, but rather an inconsistent application of the proportioning technique to derive all factors. Note in Table 5 that all left-turn factors are assumed to be 1.0. This assumption is a carryover from the results of the original NCHRP 3-28 study. The arrival type characterizations in the HCM remained identical to the original descriptions.

Progression and Delay Relationships

Many field studies (2,11) have shown that delay can be reduced from that occurring for random flow if good progression of platoons traveling along an arterial street is provided. As noted in these studies, it is desirable to have one coherent platoon of traffic per cycle, preferably of a length not exceeding the through green for the maximum progression flow. It is also desirable to achieve, through signalization control techniques, the repeated arrival of these platoons on green, and not on red. For pretimed signal systems, implementation of an optimized set of cycle lengths, greens splits, phase sequences, and offsets is required. For coordinated, actuated systems, either prescheduled time-space solutions or platoon-identification techniques applied in real time are required.

Stopped delay for a through movement on a signalized arterial may be related to the following four factors:

$$\text{delay} = f(\text{bandwidth, offset, volume, dispersion})$$

Progression bandwidth, signal offset, platoon volume, and platoon dispersion would be calculated for the approach in question

Table 5. Final 1985 Highway Capacity Manual Progression Adjustment Factors, PF.

Type of Signal	Lane Group	v/c Ratio, X	Arrival Type ^a				
			1 (bad)	2	3	4	5 (good)
Pretimed	TH, RT	≤ 0.6	1.85	1.35	1.00	0.72	0.53
		0.8	1.50	1.22	1.00	0.82	0.67
		1.0	1.40	1.18	1.00	0.90	0.82
Actuated	TH, RT	≤ 0.6	1.54	1.08	0.85	0.62	0.40
		0.8	1.25	0.98	0.85	0.71	0.50
		1.0	1.16	0.94	0.85	0.78	0.61
Semiactuated ^b	Main Street TH, RT	≤ 0.6	1.85	1.35	1.00	0.72	0.42
		0.8	1.50	1.22	1.00	0.82	0.53
		1.0	1.40	1.18	1.00	0.90	0.65
Semiactuated ^b	Side Street TH, RT	≤ 0.6	1.48	1.18	1.00	0.86	0.70
		0.8	1.20	1.07	1.00	0.98	0.89
		1.0	1.12	1.04	1.00	1.00	1.00
	All LT ^c	All	1.00	1.00	1.00	1.00	1.00

Source: Table 9-13 of Reference (1).

- ^a See Table 4 [Table 9-2 of Reference (1)]
- ^b Semiactuated signals are typically timed to give all extra green time to the main street. This effect should be taken into account in the allocation of green time.
- ^c This category refers to the exclusive LT lane groups with protected phasing only. When LTs are included in a lane group encompassing an entire approach, use the factor for the overall lane group type. Where heavy LTs are intentionally coordinated, apply factors for the appropriate through movement.

based on related linkage relationships (of distance, speed, offset, etc.) from the upstream signal(s) to the downstream signal. A discussion of these four sets of factors follows.

Progression Bandwidth. Progression is an abstract term used to describe the non-stop movement of vehicular platoons along a signalized arterial system. In pretimed signal systems, progression along a street may arise through the proper selection of cycle length, green splits, phase sequence, and offsets. Progression bandwidth is a resulting geometric quantity of potential platoon flow bands in a time-space model (diagram) that only estimates the potential for progression of platoons to occur. On a link-by-link basis, there is a strong correlation between increasing bandwidth and reductions in delay.

Bowers (12) graphically illustrated the relationships involved in maximizing bandwidth as related to signal system variables of cycle length, green splits, speed, and spacings between adjacent signals along an arterial. For the limiting case of equal green splits (e.g., $g/c = 0.5$) and uniform speed in both

directions, it can be demonstrated that the bandwidth progression efficiency shown in Figure 4 applies between two signals (13).

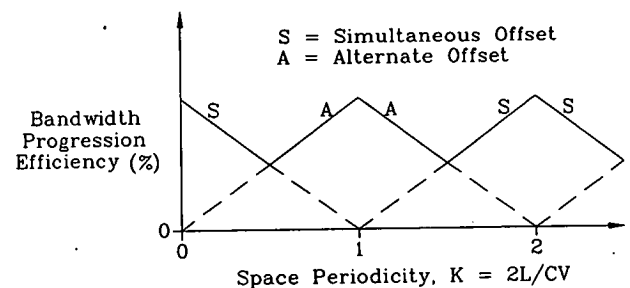


Figure 4. Bandwidth Progression Efficiency Between Two Traffic Signals.

where:

- E = average progression bandwidth efficiency, the average bandwidth divided by the cycle, C ;
 K = space periodicity, $2L/CV$;
 L = arterial signal spacing, ft;
 C = cycle length, sec;
 V = average speed, ft/sec; and
 S, A = simultaneous (S) or alternate (A) offsets.

The bandwidth, B , and bandwidth efficiency, B/C (the percentage of the cycle available for progression), are related to the value of the space periodicity, K , (13), which relates C , V , and L into one single parameter. This general wave form is applicable along arterials in most cases, particularly where signals are evenly spaced. The previous illustration (see Figure 4) of progression efficiency was originally solved for all pairs of signals (i,j) by Morgan in 1964 (14) using dynamic programming techniques.

Signal Offset. One of the earliest studies of measured delay versus signal offset (and progression) was conducted in West London during the formulative development of TRANSYT in the early 1960s (8). Signal offsets were incremented by two seconds for each data set for each of four volume levels. Volume-to-capacity ratios of 0.6, 0.8, 0.9, and 0.95 resulted. Figure 5 shows the observed changes in delay with offset and degree of saturation. An important finding of this study was that "there exists a progression speed, approximately equal to the mean running speed of the traffic stream, that minimizes total delay" (7).

Platoon Volume. There is no need to provide progression in a system of intersections if the arrival volume levels are uniform and balanced throughout each cycle. Due to the different green times available in each signal of the progression system, however, the amount of delays and stops could be affected by the coordinated offsets under normally fluctuating arrival conditions. Several of the factors which may contribute to the uniform arrival of vehicles at an intersection (15) are listed below:

1. an intersection isolated by distance relative to the other upstream signalized intersections;
2. consequential traffic volumes entering at mid-block and from upstream turns; and
3. significant truck movement between intersections.

Thus, a desirable condition for good progression is an imbalance in through volume entering from the upstream intersection. In addition, significant traffic entering at mid-block or large truck traffic between intersections will force arriving flows to slow down and good progression cannot be provided due to this traffic congestion.

The arrival flow on an approach is the sum of four upstream flows minus side-street exiting losses. These upstream input flows are as follows:

1. through flow from intersection "i";
2. cross-street, right-turn flow from intersection "i";
3. cross-street, left-turn flow from intersection "i"; and
4. intra-link (side street) entry flow (from non-signalized intersections, driveways, etc.).

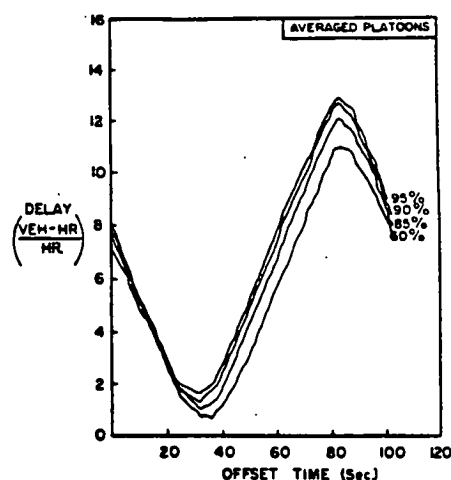


Figure 5. Signal Offset and Delay Relationships.

In most cases, the progressed platoon is created from the arterial through flow from intersection "i". The arterial through flow should compose much more than 25 percent of the total flow for the through volume arriving at intersection "j"; thus, the greater the arterial through flow, the better the potential platoon formation. The through volume probably should exceed 60 percent of the total flow before major link coordination and progression benefits (or disbenefits) can be expected.

Consider the typical link flow pattern between two adjacent intersections. The entry volume for the downstream intersection consists of the right-turn, through, and left-turn volumes from the upstream intersection. The degree of flow imbalance from the upstream intersection "i" is represented by the ratio between the maximum link traffic flow rate feeding from the upstream intersection and the sum of all the link traffic volumes arriving at the downstream intersection "j" over the cycle. This ratio can be stated by the following equation:

$$I_p = \frac{[q / (g/C)]_{i_{\max}}}{q_j}$$

where:

- I_p = platoon index;
 $q_{i_{\max}}$ = maximum upstream flow rate during green, usually from through movement, vph;
 g = effective green of phase associated with $q_{i_{\max}}$; and
 q_j = average arrival flow rate at downstream intersection j, vph.

The arrival flow on the downstream intersection is influenced by the arriving flow over the cycle. The platoon index, as calculated from the maximum upstream flow rate over a period of time divided by the average arrival flow, is an index representing the fluctuation of traffic volume along the downstream link. It varies as:

$$1 \leq I_p \leq \frac{1}{\lambda}$$

where:

$$\lambda = \text{green time to cycle length ratio, (g/C)}.$$

When the platoon index I_p equals 1.0, uniform flow exists. That is, cross street, mid-block, and turning traffic flow rates at the upstream intersection are approximately equal to the major entering flow rate. Interconnection of upstream and downstream signalized intersections is not desirable in this case. When the platoon index significantly exceeds 1.0, however, the heavy imbalance condition creates a desirable situation for progression. The relationship between flow rates and vehicle platoon formation define the magnitude of the imbalance. This equation, however, should also consider the additional effects of platoon dispersion on the upstream flow.

Platoon Dispersion. Platoons are groups of high-density vehicles traveling along an arterial street. Platoons tend to

disperse, or spread out, with increasing travel time and distance until a uniform arrival rate is attained. This dispersion is primarily the result of different drivers having different desired speeds. Faster drivers begin to pull away, while slower ones lag behind. Because the lead driver sometimes restricts other drivers, however, the platoon tends to disperse from the back at a faster rate. This phenomenon is illustrated in Figure 6. Notice that the platoon disperses faster to the right (back) as it moves down the street.

Platoon dispersion results from the drivers adjusting the relative distance between their vehicle and adjacent leading and trailing vehicles. The dispersion of a platoon of vehicles leaving a signalized intersection can be approximated by a dispersion rate given in terms of percent of original platoon length according to the model presented below (11):

$$\text{Rate of dispersion} = \frac{L + \Delta L}{L * (1 + t)}$$

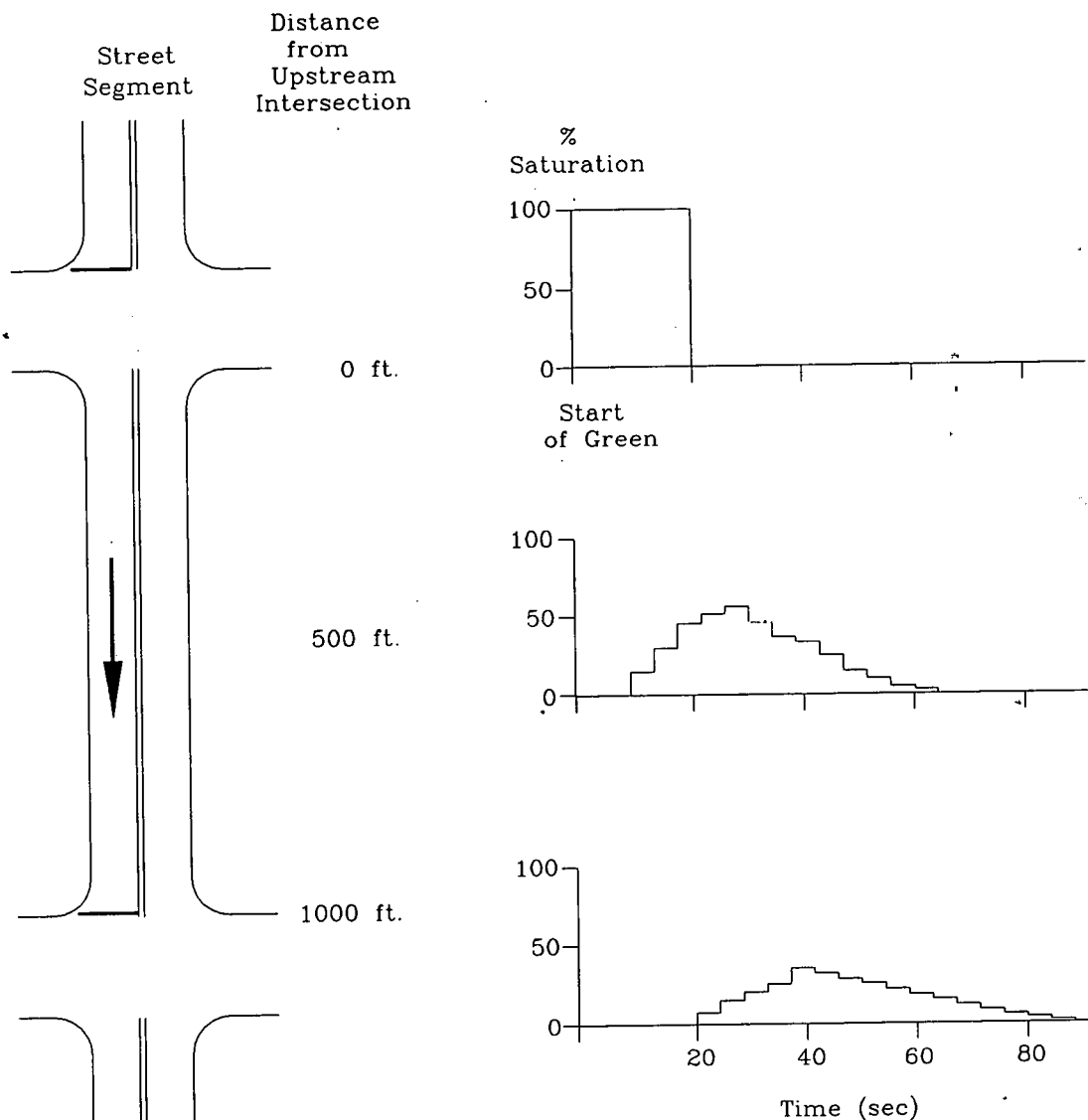


Figure 6. Simple Case of Platoon Dispersion.

where:

- L = length of the original standing platoon, sec;
 ΔL = change in length over distance and time, sec; and
 t = average travel time, sec.

Several researchers have attempted to analyze and/or model platoon dispersion. Some concepts common to most of these models include increasing dispersion rates with increasing travel time and distance, increasing dispersion rates with decreasing platoon size, and increasing dispersion rates with increasing traffic friction. Dispersion models have been included both in PASSER II (4) and TRANSYT-7F (8) to account for platoon dispersion in a progressive signal system.

The effects of dispersion on vehicular delay in such systems are illustrated in Figure 7. The damped sinusoidal (Fresnel integral) shape is a direct result of dispersion, i.e., the platoon dispersing because of increased distances, and the platoon's flow rate is approaching the average rates for the link (16).

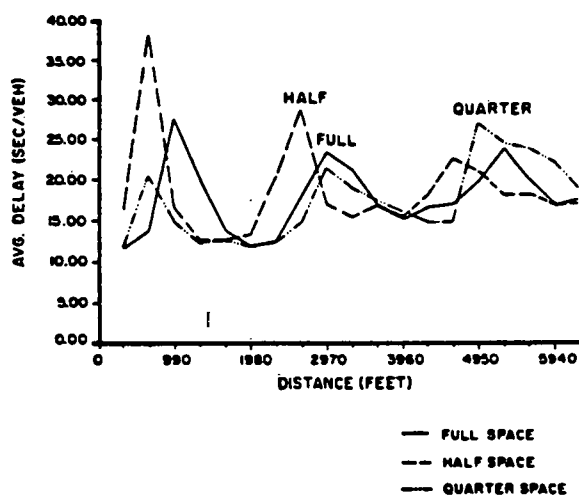


Figure 7. Summary of Simulation Study Results -- Effects of Traffic Volume Level.

The procedure used in TRANSYT to predict platoon behavior is very simple to apply and uses the following recurrence relationship:

$$q_{2(i+1)} = F * q_{1(i)} + (1 - F) * q_{2(i+1-1)}$$

where:

- $q_{2(i)}$ = derived flow in the i -th time interval of the predicted platoon at a point "2" along the road;
 $q_{1(i)}$ = flow in the i -th time interval of the initial platoon at a point "1" along the road;
 t = 0.8 times the average journey time over the distance for which the platoon dispersion is being calculated;
 F = smoothing factor $F = 1/(1 + \alpha * t)$; and
 α = platoon dispersion rate.

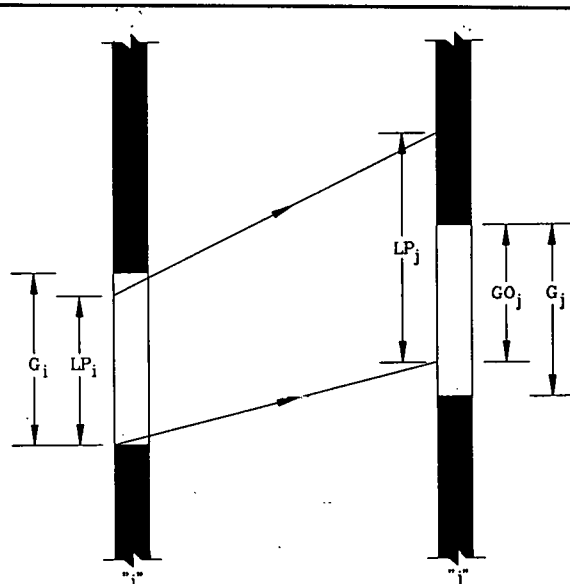


Figure 8. PASSER II Model of Platoon Projection from Intersection "i" to "j".

Selection of a realistic value of " α " in the smoothing factor equation is important because it controls the predicted rate of dispersion. Robertson (8) recommended a value of 0.5 be used, whereas Seddon (17) found values of 0.4 and 0.6 best fit the data for his two test sites. A recent study in the U.S. by McCoy (18) concluded that even lower values were appropriate for low traffic friction roadways in American cities. Clearly, no simple value is applicable to all conditions. This point is reflected in Table 6, which was taken from FHWA's TRANSYT-7F User's Manual (19). As stated in the manual, however, there has not been much research to substantiate these recommended values.

Perhaps the most widely used U.S.-developed platoon dispersion model is an analytical projection method developed by Messer and Fambro in 1975 (4). The basic theory behind this model is presented in Figure 8. By calculating the platoon's size at intersection "i" and the average travel time from "i" to "j", the arrival of a dispersed platoon at intersection "j" is projected into a time-space diagram. Knowing the green time available for platoon flow and the start and end of the through green allows benefits of the timing plan to be calculated. Rate of dispersion in the Messer-Fambro model is a function of travel time and platoon size (4).

PROGRESSION-DELAY MODELS

As documented in the state-of-the-art summary, there are a number of variables affecting the relationship between progression and delay. In addition, there is uncertainty whether to apply progression adjustment factors to the entire delay equation, including the overflow delay term, or to only the first term of the delay equation excluding the overflow delay term. The methodology presented in the following discussion addresses these uncertainties and offers a possible solution.

Table 6. Recommended Values for TRANSYT-7F's Dispersion Factor.

Dispersion Factor	Roadway Characteristics	Description of Conditions
0.50	Heavy friction	Combination of parking, moderate to heavy pedestrian traffic, narrow lane widths. Traffic flow typical of urban CBD.
0.35	Moderate friction	Light turning traffic, light pedestrian traffic, 11- to 12-foot lanes, possibly divided. Typical of a well-designed CBD arterial.
0.25	Light friction	No parking, divided, turning provisions, 12-foot lanes. Typical of urban high-type arterials.

Progression Adjustment Factor Application

Figure 9 presents a representative plot of the HCM delay equation for a single-lane, lane group. The cycle time is 90 seconds, the green time is 45 seconds ($g/C = 0.5$), and the saturation flow rate is 1800 vehicles per lane per hour of green. Flow rate, v , increases from 0 to 1,080 vehicles per hour, thereby increasing the v/c ratio, X , from 0 to 1.2. The incremental effects of the uniform and overflow delay terms are identified as d_1 and d_2 , respectively.

Several observations concerning the relationships depicted in Figure 9 are of interest to this research. First, until X reaches a value of 0.6, the incremental effect of overflow delay is negligible. Second, as X approaches 0.8, the incremental effect of overflow delay is noticeable; however, most of the total delay is still due to the uniform delay term. Third, as X approaches 1.0, most of the total delay is due to the overflow delay term. Finally, after X exceeds 1.0, the overflow delay term is entirely dominant.

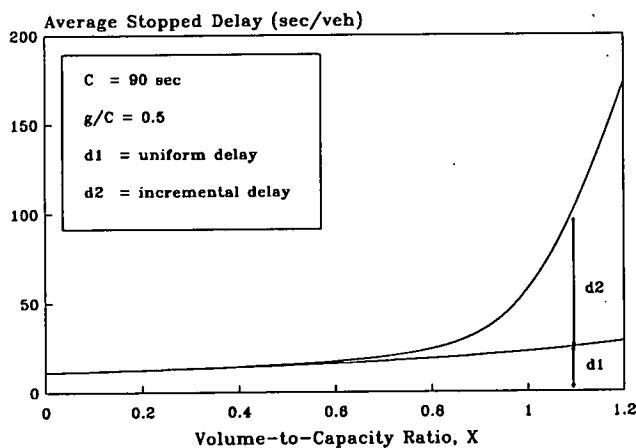


Figure 9. HCM Delay Equation Response to Increasing Volume-to-Capacity.

A close examination of Figure 10 reveals that the application of the progression adjustment factor to the entire delay equation or to only the first term of the delay equation, makes no difference in the results below X -ratios of 0.6; makes little difference in the results between X -ratios of 0.6 and 0.8; makes some difference in the results between X -ratios of 0.8 and 1.0; and makes large differences in results above 1.0 due to the dominance of the overflow delay term.

Recalling that the first term of the HCM equation accounts for delay due to uniform flow over a cycle, it is reasonable to assume that platoon flow due to progression is also uniform (for each cycle) and should be multiplied by an adjustment factor to account for its effects on delay. The magnitude of this adjustment is not appreciably affected by volume. If the additional delay due to random arrivals (i.e., uniform delay plus overflow delay) is also adjusted, there is a volume effect above X -ratios of 0.6 which necessitates different adjustment factors for different volume levels.

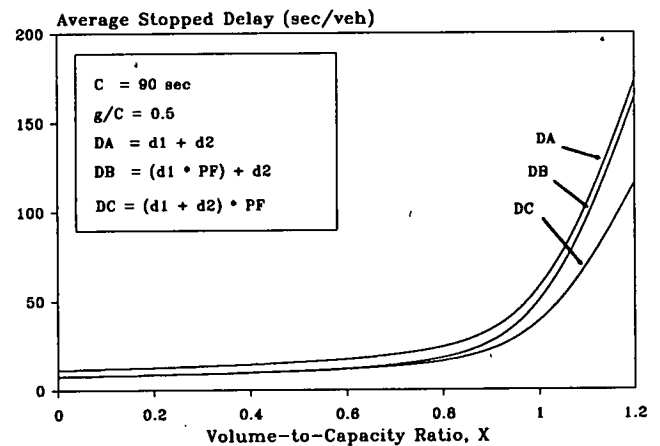


Figure 10. HCM Delay Equation Response to Progression Adjustment Factors for Arrival Type 5.

Intuitively, a factor that is not dependent on volume levels would be easier to understand and apply. Therefore, in the remainder of this report preference will be given to developing a factor for the first delay term only. The differences between the two alternative approaches, however, will be compared by simulation and field data.

Platoon Ratio

As mentioned previously, Platoon ratio, R_p , is defined in the 1985 HCM as the ratio between the percent of the total volume that arrives on green (PVG) and the percent of the cycle that is green (PTG). When PVG equals PTG; i.e., $R_p = 1$, uniform flow is said to exist and the progression adjustment factor is 1.0. When PVG is less than PTG ($R_p < 1$), a disproportionate share of the total flow arrives on red and the progression adjustment factor should be greater than 1.0. When PVG is greater than PTG ($R_p > 1$), a disproportionate share of the total flow arrives on green and the progression adjustment factor should be less than 1.0.

There are, however, no stated limits on the minimum and maximum values of R_p . In addition, several researchers have documented lower progression factors for extremely good progression and higher progression factors for extremely bad progression (20, 21). Theoretically, as shown in Appendix A, the maximum values of R_p and PF are dependent on the g/C ratio of the subject approach. This relationship is illustrated in Figure 11 and can be expressed by the following inequality:

$$0 \leq R_p \leq 1/\lambda$$

where:

$$\begin{aligned} R_p &= \text{platoon ratio (PVG/PTG); and} \\ \lambda &= \text{green time to cycle length ratio (g/C).} \end{aligned}$$

Note that R_p can assume values both greater than and less than those presented in the 1985 HCM. The exact boundary conditions are dependent on λ .

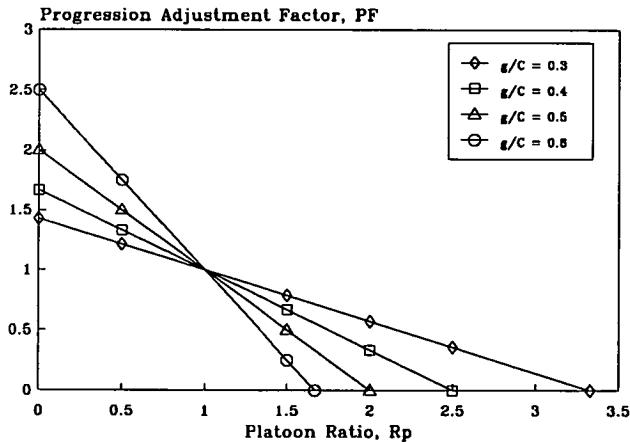


Figure 11. Relationship Between Progression Adjustment Factors and Platoon Ratio.

Proportion of Volume Arriving on Green

Because R_p 's boundary conditions are dependent on λ , it would appear that platoon ratio may not be the best descriptor of the effects of quality of progression on delay. The term $R_p * \lambda$, however, has a constant boundary between 0.0 and 1.0 and also has an intuitive appeal because, as shown in Appendix A, it is equivalent to the HCM's proportion of the total volume arriving on green, PVG. Thus, P or PVG, appears to be a better descriptor of the effects of progression on delay. The relationship between PF and P is illustrated in Figure 12 and can be expressed as follows:

$$P = R_p * \lambda$$

where:

$$0 \leq P \leq 1$$

and

$$P = \text{proportion of volume arriving on green.}$$

and, as shown in Appendix A,

$$PF_s = \frac{1-P}{1-\lambda}$$

where:

$$PF_s = \text{simplified progression adjustment factor.}$$

such that

$$0 \leq PF_s \leq \left(\frac{1}{1-\lambda} \right)$$

The relationship between R_p and P is important because (PVG) is required in order to determine R_p . Thus, if the proportion of volume arriving on green were adopted as the descriptor of the quality of progression, its determination would not require information beyond that currently required by the HCM (1). The relationship between R_p and P is illustrated in Figure 13.

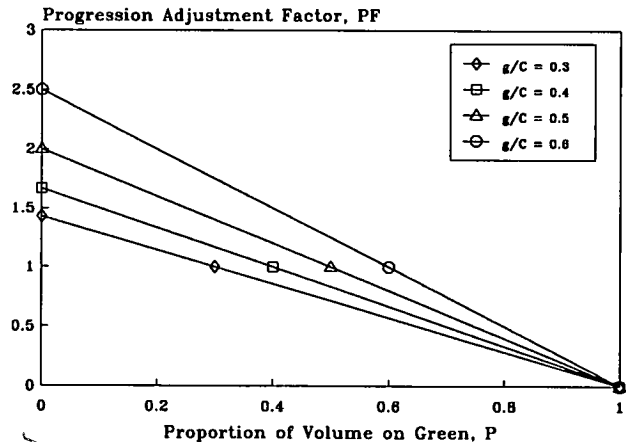


Figure 12. Relationship Between Progression Adjustment Factors and Proportion of Volume on Green.

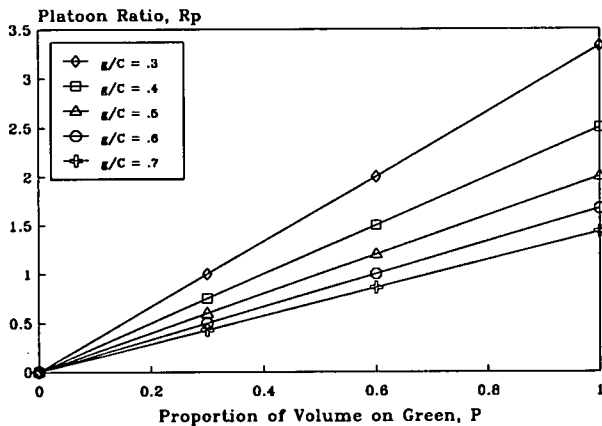


Figure 13. Relationship Between Platoon Ratio and Proportion of Volume on Green.

Progression-Delay Equation

An alternative to applying a progression adjustment factor to the HCM's uniform delay term would be to reformulate the uniform delay term to explicitly account for the effects of progression. This proof is shown in Appendix A and can be expressed as follows:

$$d = d_u * PF_p + d_o$$

where:

$$d_u = 0.38 * r * (1 - \lambda) / (1 - y)$$

and

$$PF_p \equiv (1 - P) / (1 - \lambda)$$

then:

$$d \equiv .38 * r * \frac{1 - \lambda}{1 - y} * \frac{1 - P}{1 - \lambda} + d_o$$

Note that when P is equal to λ , the flow rate is uniform; i.e., $PF_p = 1.0$, and the progression delay equation can be shown to be equivalent to the first term of the HCM delay equation. If P is less than λ (bad progression), delay will be greater than that predicted by the HCM's uniform delay term, and if P is greater than λ (good progression), delay will be less than that predicted by the HCM's uniform delay term. These relationships are illustrated in Figure 14.

Estimating Proportion Volume on Green

Unfortunately, one is still left with the problem of estimating P ; as noted by Rouphail (22), different delays can result depending upon what point in time the front of the platoon arrives at the downstream signal. In regard to this problem, green splits, platoon volumes, and travel time are known to affect P . Knowing these parameters, one can estimate P using Courage's bandwidth formulation (21) or a TRANSYT-like platoon dispersion model as suggested by Rouphail (22) and modified in this research. Both methods are described in Appendix A.

In order to avoid estimating P , one could actually measure the proportion of the total volume arriving on green in the field. This measurement can be accomplished by a modification of Berry's methodology for collecting data to measure overflow delay (23). The key components of this methodology are the counting of both arrival and discharge volumes on a cycle-by-cycle basis. Specifically, the following steps should be followed when measuring volume arriving on green.

1. Observe the lane or lane group to be observed during the period of interest.
2. Begin counting the arrival volume when the signal changes to red. Count each vehicle that joins the end of the queue, and record this value in the arrival on red column at the end of the red indication (beginning of the green indication). One should also identify the vehicles at the end of the queue at this time.
3. Begin counting the departure volume at the start of the green indication. Count each vehicle as it crosses the stopline of the lane group, and record this value in the total volume column at the end of the yellow indication.
4. If the queue clears, the difference between the departure volume on green and the arrival volume on red is the arrival volume on green. The proportion of the total volume arriving on green is the arrival volume on green divided by the discharge volume on green.
5. If the queue does not clear, the difference between the departure volume on green plus the overflow queue represented total volume, and the difference between departures on green plus the overflow queue and the arrival volume on red is the arrival on green. In this case, Berry's overflow delay procedure (23) should be used for calculating delay.

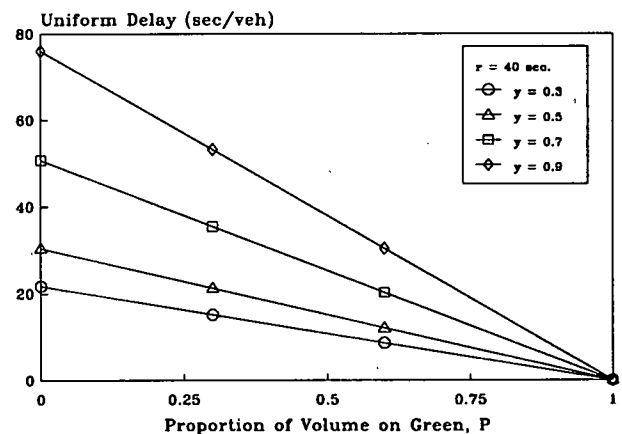


Figure 14. Relationship Between Proportion of Volume on Green and Stopped Delay.

SIMULATION STUDIES

In order to further examine the interrelationships between the variables that may affect the quality of traffic signal progression, several simulation studies were conducted with the PASSER III-88 (24) and TRANSYT-7F (19) microcomputer programs. PASSER III-88 was used first to study the effects of different traffic volumes and signal timing parameters without having to

consider the effects of platoon dispersion. Then, TRANSYT-7F was used to study the detailed effects of different intersection spacings and platoon dispersion rates on the traffic volumes and signal settings already modeled by PASSER III-88. As mentioned previously, emphasis was given to studying the progression effects for the first delay term only. The following discussion summarizes the results of these simulation studies.

Study Approach

PASSER III-88 and TRANSYT-7F were used to examine the relationships between traffic volumes, signal timing, arterial geometrics, and the quality of traffic signal progression. PASSER III-88, by isolating the effects of platoon dispersion, was used first to study the effects of different traffic volumes and signal timing parameters. The different traffic characteristics that were examined by PASSER III-88 include volume-to-capacity (v/c) ratios from 0.2 to 1.0 in increments of 0.2; cycle lengths of 60, 75, 90, and 120 seconds; and green-to-cycle (g/C) ratios of 0.5, 0.7, and 0.9 at each of the intersections in question. Each of the 60 variable combinations (5 v/c ratios * 4 cycle lengths * 3 g/C ratios) was evaluated for each of 10 different offsets, with each offset representing a different platoon arrival condition. Thus, 600 different conditions were simulated.

TRANSYT-7F was then used to study the effects of different intersection spacings and platoon dispersion rates on the resultant traffic volumes and traffic signal settings already modeled by PASSER III-88. The TRANSYT-7F platoon dispersion factors (PDF) that were examined include 25, 35, and 50. These values represent the characteristics of the roadway in terms of side and/or internal friction, with 25 being low friction and 50 being heavy friction. Travel times of 20, 40, 80, and 120 seconds were also examined. These travel times correspond to intersection spacings from less than 400 feet to more than 5000 feet.

For each of the conditions simulated by PASSER III-88 and TRANSYT-7F, progression adjustment factors (delay ratios) were calculated by dividing the simulated delay at the downstream intersection by the delay predicted by the HCM equation. These simulated progression adjustment factors were then plotted versus travel time minus offset, platoon ratio, and proportion of the total volume arriving on green for the different variable combinations and several analytical relationships.

PASSER III-88 and TRANSYT-7F Comparison

The traffic models in PASSER III-88 and TRANSYT-7F are based on different assumptions concerning the behavior of a platoon of vehicles as it leaves a signalized intersection and travels down the street. PASSER III-88 was developed to assist traffic engineers in analyzing signalized diamond interchanges. Its traffic model assumes no dispersion as a platoon of vehicles travels from one intersection of the interchange to the other. This is not an unreasonable assumption, given the fact that the two intersections are located in close proximity to each other (less than 300 feet). This unique feature of PASSER III-88 allows the effects of traffic volumes and signal timing to be isolated and studied separately from the effects of platoon dispersion. More important to this study, however, PASSER III-88 can output the proportion

of total volume arrivals on green and resultant delay for every possible offset between the two signals.

TRANSYT-7F's traffic model, on the other hand, assumes that the platoon disperses as a function of its size and travel time along the street. The rate of dispersion is controlled by a dispersion factor which is an input to the program. Thus, by using the results from PASSER III-88 as a basis for comparison, the effects of platoon dispersion could be isolated and studied separately from the effects of traffic volumes and signal timings. As TRANSYT-7F is widely used and accepted by the traffic engineering profession, the first step in this study was to verify that the two programs give similar results whenever their input data is the same. To accomplish this objective, a synthetic, two-intersection signal network was coded and analyzed by both programs. The intersections were spaced 10 seconds apart so as to eliminate dispersion in the TRANSYT results. To avoid the effects of secondary platoons, turning movements were not coded in either program.

Comparisons between PASSER III-88 and TRANSYT 7-F were made for several levels of traffic volume and signal timings, and the resultant delay was plotted versus offset between the two greens. In each of these plots the vertical axis represents the ratio of the average delay when the traffic flow is progressed or pulsed to the average delay when the traffic flow is random or uniform. These delay ratios can also be thought of as progression adjustment factors, i.e., measured delay divided by predicted delay. The horizontal axis represents the travel time between the two intersections minus the relative offset between the two through greens. Thus, the value of "0" represents a platoon's arrival at the start of the downstream intersection green phase; negative values represent a platoon's arrival before the start of the downstream green (early arrivals); and, positive values represent a platoon's arrival after the start of the downstream green (late arrivals). Data points were plotted at increments of tenths of the cycle length for each condition studied, i.e., 10 data points per condition.

To verify the fact that dispersion effects had been removed from the TRANSYT-7F results, runs were made with three different platoon dispersion factors (PDF) with the value at 25, 35, and 50, respectively. As expected, the short travel times allowed little opportunity for dispersion, and as shown in Figure 15, the resultant

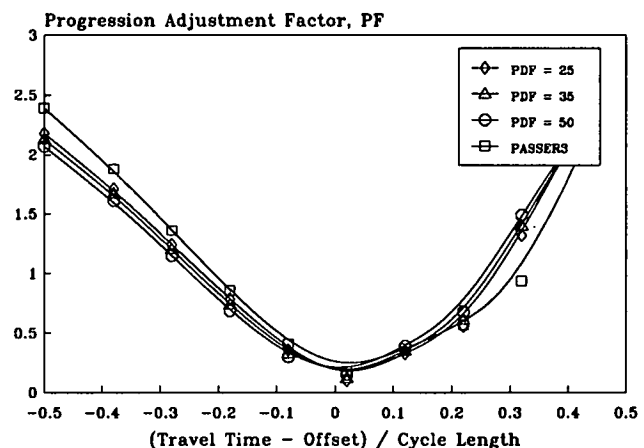


Figure 15. Comparison of PASSER III and TRANSYT-7F Simulation Results.

data points plotted on top of one another. These results indicated the small or nonexistent difference between the three dispersion rates at short travel times. The general shape of the plots was consistent with expected behavior. The least signal delay due to coordination occurred when vehicular platoon or the majority of vehicles arrived at the start of green; the most delay occurred when the platoon arrived at the start of red.

These results were then compared to those output by PASSER III-88 for several levels of traffic volume and signal timing. One of the PASSER III delay-offset plots is also shown in Figure 15. As expected, the TRANSYT-7F results were in close agreement with the results from the PASSER III-88 program in all cases of short intersection spacing. These comparisons verified the fact that these two computer programs do indeed give similar results for the same set of signal progression conditions.

Sensitivity Analysis

Cycle Length. PASSER III-88 was first applied to study the detailed effects of cycle lengths on the estimation of progression adjustment factors. One of the resultant plots of the relationships from this simulation analysis is shown in Figure 16. The horizontal axis in this figure is labeled in tenths of a cycle length so as to establish a common comparison basis for evaluating effects of different cycle lengths. The vertical axis represents the simulated progression adjustment factor, i.e., delay due to progressed arrivals divided by delay due to uniform arrivals. This plot and others not shown in this report indicated that cycle length has little effect on the quality of progression. Therefore, cycle length was removed from the list of variables to be explicitly considered in the field evaluation study. This deduction should be valid as long as the traffic signal systems were properly timed to accommodate the different traffic loading conditions during the different field operation conditions.

One of the interesting outcomes of this analysis was the different slopes and the relative magnitude of stopped delay that result as one moves away from perfect signal progression. For example, as shown in Figure 16, the vehicular platoons arriving two-tenths of a cycle before the start of green are delayed less than platoons arriving two-tenths of a cycle after the start of green. This result is not surprising, since in the first case the vehicles are only delayed for the end of the red period and in the second case, they

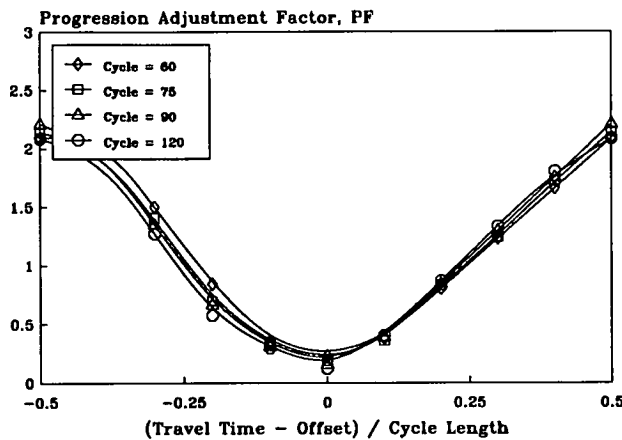


Figure 16. PASSER III Simulation Results -- Effects of Cycle Length.

are delayed for the entire red period. This does, however, create a rather confusing situation in which two different average delays can result from the same platoon depending on whether it arrives before or after the start of green.

Green Times. PASSER III-88 was then used to investigate the effect of green times on progression adjustment factors. One of the resultant plots of the effect of green time or the green-to-cycle length ratio from this analysis is shown in Figure 17. The horizontal and vertical axes represent the simulated platoon ratio, PVG/PTG , and progression adjustment factors, PF , respectively. As illustrated, the general shape of the relationships between the platoon ratio's green time and the arterial progression adjustment factors was also consistent with expected behavior, i.e., as platoon ratios increased, progression adjustment factors decreased, and as green ratio increased, the range of resultant progression adjustment factors also increased.

Evaluation of this particular variable verified that the maximum possible platoon ratio is dependent on the movement's green ratio. To provide a comparison with a descriptor that has a constant boundary, the platoon ratios in Figure 17 were converted to the proportion of the total volume arriving on green and replotted as shown in Figure 18. These simulated results are consistent with the analytical relationships shown in Figures 12 and 13 (pages 12 and 13). Again, note that the range of progression adjustment factors increases as green ratios increase.

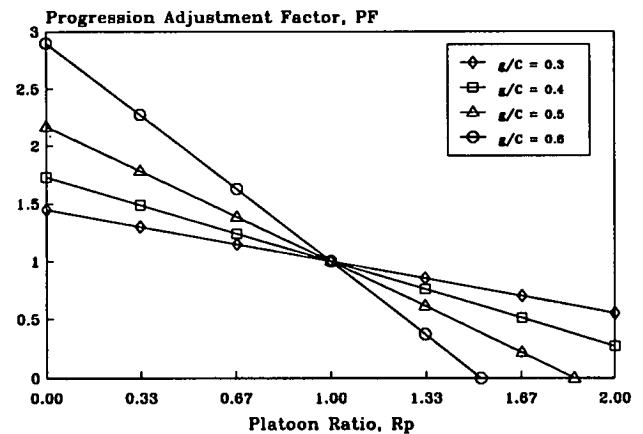


Figure 17. PASSER III Simulation Results -- Effects of Green Time, Platoon Ratio.

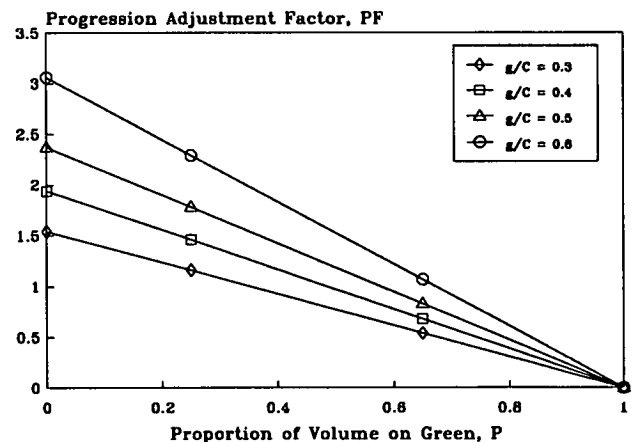


Figure 18. PASSER III Simulation Results -- Effects of Green Time, Proportion Volume on Green.

Traffic Volume. The last variable studied with PASSER III-88 was the effect of different levels of traffic volume on progression adjustment factors. One of the resultant plots from this analysis is shown in Figure 19. Note that volume has little effect on the value of the progression adjustment factor when it is applied to the uniform delay term only. These results substantiate the premise that the significant differences between v/c ratios of 0.6, 0.8, and 1.0 in Table 9-13 of the 1985 HCM (1) are a result of adjustments to both the uniform and incremental delay terms. The curves shown in Figure 19 are also consistent with expected behavior of the progression adjustment factors, i.e., the closer the front of the platoon's arrival is to the start of green the higher the proportion of the volume that will arrive on green, and the smaller the delay the platoon will incur.

Travel Time. TRANSYT-7F was then used to study the effects of travel times on progression adjustment factors. As observed earlier, the traffic volumes and traffic signal settings, as modeled by PASSER III-88, were used as the starting solution point for this analysis. It should be noted that travel time is a combined function of the interactions between the intersection distance and travel speed. For example, two intersections spaced 440 feet apart, at a travel speed of 30 miles per hour equals 10 seconds of travel time. For TRANSYT-7F, the traffic can be modeled using either travel time or speed, with the program generating the same results for either input variable.

One of the resultant progression factor-platoon ratio plots from the travel time analysis is shown in Figure 20. As expected, increasing the travel time decreased the effects of progression. In other words, the farther down the street the platoon traveled, the less dense it became, the fewer vehicles arrived on green, and the flatter the progression adjustment factor line becomes; i.e., the more dispersed the platoon became, the closer the resultant progression factor was to 1.0. The data in this particular figure represent a moderate degree of side friction (a platoon dispersion factor of 35 specified as input to the TRANSYT-7F program). Again, these simulation study results are consistent with expected behavior. The longer the platoon travels and the more dispersed it becomes, the smaller the effect progression has on delay.

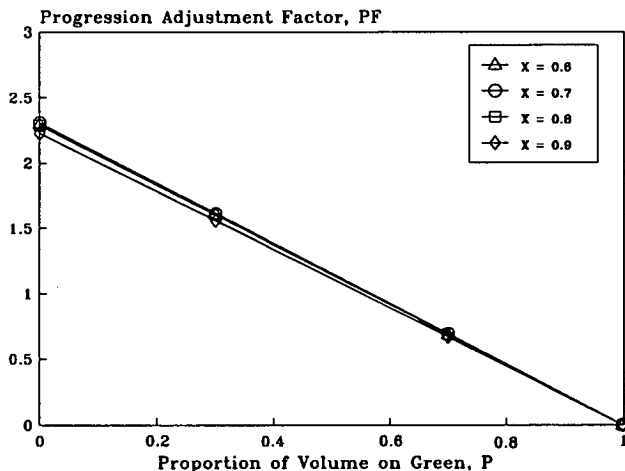


Figure 19. PASSER III Simulation Results -- Effects of Traffic Volumes.

If Figure 20 is converted to a progression factor-proportion of total volume arriving on green plot, the practical implications of platoon dispersion are clearly indicated (See Figure 21). Note that for a given green ratio, the slope of the progression factor line is independent of travel time. Boundary conditions, however, are not independent of travel time. As shown in Figure 21, a wide range of PFs and Ps are possible at short spacings; i.e., the platoon is still compact, and depending on where it arrives in the cycle at the downstream intersection, it can have a very large impact on average delay. Conversely, only a very narrow range of PFs and Ps are possible at long spacings; i.e., the platoon has dispersed to near uniform flow, and where it arrives at the downstream intersection in the cycle has very little impact on average delay. In other words, dispersion causes the progression adjustment factor to approach 1.0.

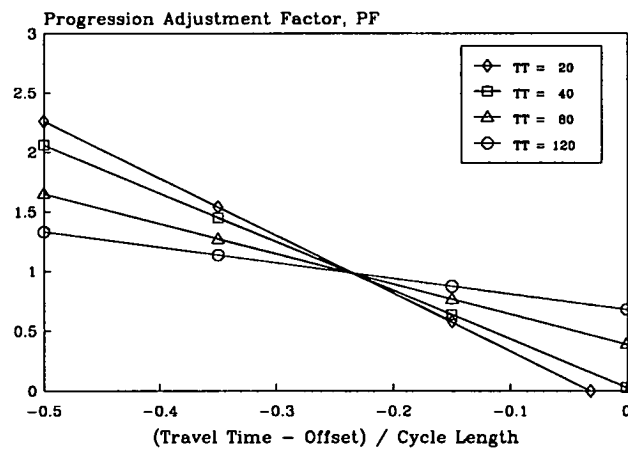


Figure 20. TRANSYT-7F Simulation Results -- Effects of Travel Time, Offset.

Simulated Progression Adjustment Factors

As a final step in these analyses, a comparison was made between the progression adjustment factors calculated by the simplified analytical equation, $PF_s = (1 - P)/(1 - \lambda)$, and those calculated from the simulation studies. The results of this comparison are shown in Table 7 and illustrate the relationship between progression factors (PFs) and the proportion of the total volume arriving on green (P) for various green ratios (g/C) and travel times. The top block of numbers in Table 7 represents the progression adjustment factors from the analytical equations, whereas the bottom four blocks represent progression adjustment factors from the simulation study. Note that as travel time (dispersion) increases, the range of allowable progression factors decreases. In other words, the farther down the street the platoon travels, the closer to uniform flow it becomes and the less its potential effect on uniform delay.

These findings point out the importance of considering dispersion in the selection of appropriate progression adjustment factors. Fortunately, counting the proportion volume arriving on green or estimating it with the techniques in Appendix A automatically account for the effects of dispersion. In the event, however, that P is neither known nor estimable from a valid analytical procedure it should be assumed equal to g/C; i.e., $PF = 1.0$. This assumption minimizes the potential error in predicting delay.

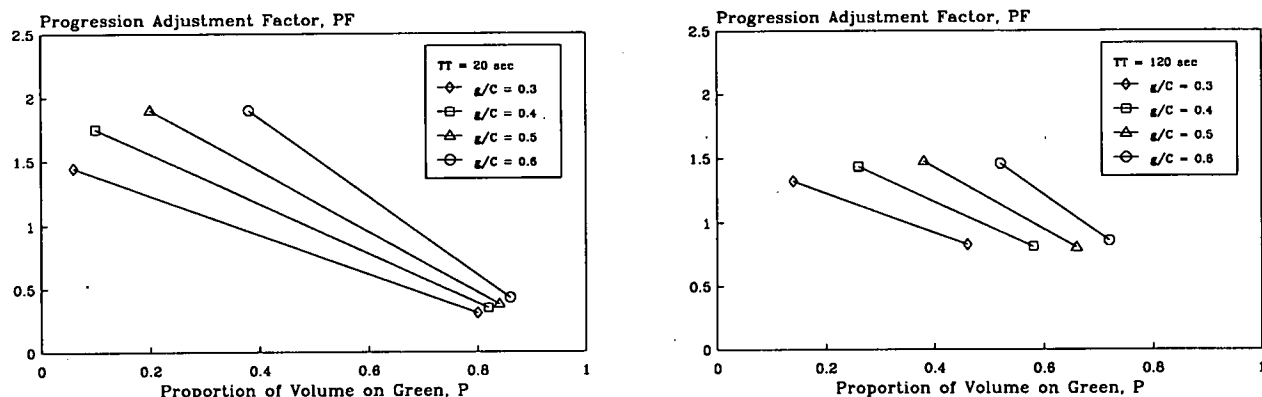


Figure 21. TRANSYT-7F Simulation Results -- Effects of Travel Time, Proportion Volume Arriving on Green.

Table 7. Comparison of Analytical and Simulated Progression Adjustment Factors.

		Proportion of Total Volume Arriving on Green, P								
		Green Ratio, g/C	.20	.30	.40	.50	.60	.70	.80	.90
Analytical Equation	.60		2.00	1.75	1.50	1.25	1.00	0.75	0.50	0.25
	.50		1.60	1.40	1.20	1.00	0.80	0.60	0.40	0.20
	.40		1.33	1.17	1.00	0.83	0.67	0.50	0.33	0.17
	.30		1.14	1.00	0.86	0.71	0.57	0.43	0.29	0.14
Simulation TT = 20	.60		-	2.14	1.84	1.53	1.22	0.92	0.61	0.31
	.50		1.90	1.66	1.42	1.19	0.95	0.71	0.47	0.24
	.40		1.55	1.36	1.16	0.97	0.78	0.58	0.39	0.19
	.30		1.23	1.08	0.92	0.77	0.62	0.46	0.31	-
Simulation TT = 40	.60		-	-	1.84	1.53	1.22	0.92	0.61	0.31
	.50		1.90	1.66	1.42	1.19	0.95	0.71	0.47	0.24
	.40		1.55	1.36	1.16	0.97	0.78	0.58	0.39	-
	.30		1.23	1.08	0.92	0.77	0.62	0.46	0.31	-
Simulation TT = 80	.60		-	-	-	-	1.22	0.92	0.61	-
	.50		-	-	1.42	1.19	0.95	0.71	0.47	-
	.40		-	1.36	1.16	0.97	0.78	0.58	0.39	-
	.30		1.23	1.08	0.92	0.77	-	-	-	-
Simulation TT = 120	.60		-	-	-	-	1.22	0.92	-	-
	.50		-	-	-	1.19	0.95	-	-	-
	.40		-	1.36	1.16	0.97	-	-	-	-
	.30		1.23	1.08	0.92	-	-	-	-	-

FIELD STUDIES

A pilot and four field studies were conducted to collect the necessary data to calibrate the analytical progression-delay models and supplement the results of the simulation studies. The following discussion summarizes the basic study design, data collection techniques, and major findings from these studies.

Study Design

Site Selection. The problem statement of NCHRP Project 3-28C identified three basic factors to be considered when selecting study sites — area type, arterial type, and control type. Replication was required for area type and arterial type, but not for control type (except for a one-shot pairing, where a semiactuated site was also to be studied in the pretimed mode). The site selection criteria specified were as follows:

Primary Criteria:

1. \geq two metropolitan areas;
2. \geq two arterial sites per metro area;
3. \geq one urban arterial per metro area;
4. \geq one suburban arterial per metro area;
5. \geq one pretimed control per metro area; and
6. \geq one semiactuated control per metro area.

Secondary Criteria:

1. sufficient left-turn storage;
2. sufficient phase selection capability;
3. $1.0 \leq X_i \leq 1.1$, for at least one intersection in each system;
4. range of platoon arrival types; and
5. range of traffic volume, signal timing, and geometric conditions.

Some additional characterization criteria were provided. These criteria specified that urban arterials should not have free-flow speeds exceeding 30 mph and suburban arterials should not have free flow speeds less than 40 mph.

Two additional system features were considered before individual sites were selected. First, the signal system should encompass a range of intersection spacings so that the effect of spacing could be investigated. Second, features such as critical or floating intersections and adjacent systems were desirable, as they could be added to or dropped from the progressive system being evaluated. This action would provide changes in timing plans without adversely affecting traffic flow. This research approach was an important liability consideration to operating agencies.

Field studies were conducted in the Houston and Los Angeles metropolitan areas. These two areas had the following attributes:

1. separated geographically;
2. located topographically on level terrain;
3. backed by local support and facilities; and
4. conformed to the site selection criteria.

It should be noted that both a pilot and a field study were conducted at one of the sites and both a pretimed and semiactuated study were conducted at another of the sites. Thus, as shown in Table 8, there were a total of six studies and four sites. Descriptions of each of the four sites are provided in Appendix B.

Study Variables. The data collection plan was designed to provide a data base for the estimation of the coefficients for the progression-delay model and for calibration of the PASSER II and TRANSYT-7F traffic simulation models. The variables necessary to satisfy both potential uses of the data set can be broken down into six major categories as shown in Table 9. The following paragraphs discuss each of the variables' relation to the progression-delay and/or simulation programs, and also address the range of values considered practical for this study. An attempt was made to identify reasonable extremes and provide data for both good and bad conditions.

Physical features were the basic geometric attributes of a particular signal system. These features included such things as distance between intersections, lane width, and presence or absence of exclusive turning lanes. Spacing was important, as distance has an effect on platoon dispersion; therefore, a study site with both long (1600 to 2000 feet) and short approach spacings (400 to 800 feet) was desirable. Lane width was a concern only if it negatively affected traffic flow. For this study, lane widths of at least 12 feet (no effect) were sought. Exclusive turning lanes were important in that the turning traffic should not interfere with the through movement quality of progression. Selected sites had sufficient storage capacity to ensure that left-turn interference did not occur and at least two through lanes were provided for each progression movement.

Traffic characteristics were those attributes of a particular signal system that tended to change with time. These features included volumes, turning movements, and vehicle classification. Volume might have had an effect on quality of progression, as evidenced by the three volume-to-capacity ratios contained in Table 9-2 of the HCM (1); therefore, it was desirable to collect data

Table 8. Study Sites for Pilot and Field Studies.

Study	Metro Area	Arterial Type	Control Type	Study Site
1	Houston	Pilot	Pretimed	NASA Road 1
2	Houston	Suburban	Pretimed	NASA Road 1
3	Houston	Urban	Pretimed	Richmond Avenue
4	Los Angeles	Urban	Pretimed	Normandie Avenue
5	Los Angeles	Suburban	Pretimed	Azusa Avenue
6	Los Angeles	Suburban	Semiactuated	Azusa Avenue

for a range of volumes. To accomplish this objective, data were collected for both peak and offpeak conditions. Turning movements were important if they were sufficient enough in number to create secondary platoons or interfere with the primary platoon at the downstream signal. For this reason, locations with both high and low turning movements were studied. Large percentages of heavy vehicles can have a negative impact on the quality of progression because of their slower acceleration characteristics. Data were collected where the percentage of heavy vehicles was low (less than 5 percent).

Basic traffic signal control parameters of interest included cycle length, splits, bandwidth, offsets, and type of control. Cycle length and splits affect the size of the progression bandwidth, and thus the quality of progression; therefore, it was desirable to study a range for each variable. Recommended values for this study were cycle lengths of 60, 75, 90, and 120 seconds, splits (main/cross) of 50/50, 60/40, and 70/30, and bandwidths of less than 15 seconds and greater than 30 seconds. Offsets probably had the biggest single impact on the quality of progression. The following

general offset categories should document the extremes of this effect:

1. perfect offsets for one-way progression (HCM Arrival Type 5);
2. good offsets for two-way progression (HCM Arrival Type 4);
3. poor offsets for two-way progression (HCM Arrival Type 2); and
4. worst offsets for one-way progression (HCM Arrival Type 1).

Study sites were selected where the above conditions already existed or could be implemented without worsening existing traffic conditions. Both pretimed and semiactuated control were studied; as mentioned previously, data at one of the metropolitan sites were collected under both types of control.

Environmental characteristics included site location, side friction, midblock traffic, and pedestrian interference. Location

Table 9. Variables of Interest, The Range Studied, and Their Potential Uses.

Variable of Interest	Range Studied	Potential Uses		
		Coefficient Estimation	Control Variables	Simulation Calibration
1. Physical Features				
a. Intersection Spacing	short, long	X		X
b. Number of Lanes	≥ 2	X		
c. Lane Widths	≥ 12		X	
d. Exclusive Turning Lanes	yes		X	
2. Traffic Characteristics				
a. Volumes	low, medium, high	X		X
b. Turning Movements	low, high	X		X
c. Heavy Vehicles	< 5%		X	
3. Control Parameters				
a. Cycle Length	60 to 120	X		X
b. Splits	50/50, 60/40, 70/30	X		
c. Bandwidth	small, large	X		
d. Offset	bad to good		X	
e. Type of Control	pretimed, semiactuated	X		
4. Environmental Characteristics				
a. Site Location	urban, suburban	X		
b. Side Friction	low, high			X
c. Midblock Traffic	none		X	
d. Pedestrian Interference	none		X	
5. Flow Characteristics				
a. Progression Speeds	< 30, ≥ 40	X		
b. Travel Time	short, long	X		
c. Platoon Profiles				X
d. Saturation Flow Rates		X		X
6. Performance Measures				
a. Queue Counts				X
b. Stopped Delay		X		X

refers to urban or suburban and is self-explanatory. The amount of side friction can have an impact on quality of progression and, data is needed to calibrate the simulation models; therefore, it was desirable to have sites with high and low levels of side friction. Significant amounts of pedestrians and/or midblock traffic may impede the platoon and decrease the quality of progression. These site characteristics were avoided.

Flow characteristics were important to the understanding of platoon dispersion and quality of progression. They included such things as speeds, travel times, and platoon data. Unfortunately, these characteristics are sometimes difficult to measure. The speeds of interest were less than 30 and greater than 40 miles per hour. Travel times are related to speed and distance; thus, both relatively short (short distance and fast speed) and relatively long (long distance and slow speed) travel times were examined. Platoon data of interest were the arrival times of individual vehicles at several intermediate points between the two signals. These data were then used to construct flow profiles for the simulation models or to estimate the proportion of vehicles arriving on green at the downstream intersection.

Queue counts and stopped delay were performance measures that resulted from a combination of other variables. Because the models contain both uniform and overflow components, it was important to collect data that would allow the two components to be separated. Therefore, both arrivals and departures were counted on a cycle-by-cycle basis.

Data Collection Techniques

The data collection techniques and procedures in this study called for an inventory form for the collection of static and historical data; an environmental computer for the automatic collection of traffic flow data; and manual counts and video recorders for obtaining additional flow data, calculating performance measures, and keeping a permanent record of the study. The techniques and equipment used in this study are described in the following paragraphs.

Inventory. Much of the data was obtained from the operating agencies before the site was visited. This data included the physical features, traffic characteristics, existing control parameters, environmental characteristics, and the desired progression speeds. An inventory form and pre-study visits by the research staff were used to solicit this information.

Environmental Computer. An automatic data collection system was used for collecting the flow traffic and signal timing data required by this study. The basic component of this system was a Golden River Corporation Environmental Computer (EC). This system was used to measure the following variables:

1. turning movement and volume counts at the intersections;
2. vehicle arrival times at intermediate points;
3. vehicle speeds at intermediate points;
4. platoon dispersion effects along the arterial; and
5. green times, offsets, and cycle lengths.

The EC is battery-powered (making it portable) and can accept up to 24 sensor inputs from inductive loops, pneumatic tubes, piezoelectric devices, or manual pushbuttons. It has 128K of memory for data storage and can be provided additional storage by interconnecting the system to a battery-powered Zenith Z-170 PC portable computer. Collected data is stored on 5-1/4" flexible diskettes in the field and later transferred to an IBM PC-XT microcomputer for further processing. Once in the IBM PC, the data are processed into more usable formats and stored on flexible diskettes.

At each of the study sites, two EC systems were installed, along with a series of tape switches and manual input boxes. Communication links between the ECs and the tape switches were provided by a multiconductor cable laid along the edge of the roadway. Time-based coordination between the traffic signal and the EC was provided by small photoelectric sensors placed over the LED indicators on the load switch in the controller cabinet and connected to one of the EC's sensor input lines. These sensors allowed a signal change to be detected without making an electrical connection, thus eliminating the possibility of the data collection equipment causing a signal malfunction.

Manual Counts. Two manual counting procedures were used to determine average stopped delay and the proportion of the total volume arriving on green. These counts were recorded on a cycle-by-cycle basis and required two observers per study approach — one observer for stopped delay counts and one observer for volume counts. The procedures are summarized below.

Stopped delay was measured using the procedure described in Chapter 9 of the 1985 HCM (1). Basically, this procedure consisted of counting the number of vehicles stopped at regular intervals between 10 and 20 seconds. The total number of vehicles stopped during the analysis period was multiplied by the interval length and the product divided by the total number of vehicles that entered the intersection during the same time period.

Proportion volume arriving on green was measured by a modification of Berry's procedure for measuring overflow delay (23). Basically, arrival volumes were counted for each red interval and departure volumes were counted for each green interval. As long as overflow did not occur, departures on green represented the total volume and the difference between departures on green and arrivals on red represented the arrivals on green. When overflow did occur, departures on green plus the overflow queue represented total volume and the difference between departures on green plus the overflow queue and the arrivals on red represented the arrivals on green.

Video Recording. For the pilot and all field studies, a permanent photographic record of the collected data was made. Two time-lapse video cameras were installed and operated, and the film from these cameras served as the primary source of data for turning movements and queue counts and for estimates of stopped delay. It also served as the backup data source for volume counts and vehicle classification. These data were manually reduced by multiple viewing of the film records. As with the data from the EC, the video was reviewed daily in order to ensure the proper operation of the cameras. Camera locations for the field studies are discussed in a subsequent section.

Study Procedure

Study Setup. Typical setup for conducting a field study incorporated several of the attributes that were previously discussed. Data was collected on one short and one long link, which were back-to-back, i.e., there was a control intersection common to both links. This configuration assured the most efficient use of field personnel, because two observers were required for each link being studied. The primary purpose of the observers was to monitor the data collection equipment to insure its proper operation.

The first day's activities at a study site consisted of the data collection team installing the tape switches and connecting them to the EC's sensor input lines, mounting the cameras, and testing the entire data collection system. Some traffic control was required while the tape switches were being installed, because the switches had to be manually placed in the traffic lanes, taking approximately 5 minutes each to install. To minimize impact on traffic flow, this activity began at the conclusion of the AM peak. The activities of Days 2 through 5 consisted of collecting the data described in the proposed sampling plan.

As mentioned previously, data were collected in four, 2-hour time periods of each day — AM peak, off peak, PM peak, and evening. This was believed to be the maximum amount of usable data that could be collected in a 24-hour period. Two-hour time periods were selected because this was about the longest that relatively consistent traffic volumes could be expected to occur, and is also a standard length of video cassettes. Because of this fact, data could be recorded in real-time, and there was no lost time

while film was being changed. The ECs also ran for two continuous hours.

Data Collection Plan. The data collection plan for this study met the requirement that a variety of volume conditions, cycle lengths, green splits, and offsets be studied. All data were collected on a cycle-by-cycle basis and aggregated over nominal 15-minute periods. Both existing operations and temporary modifications to control parameters were studied. This sampling plan was designed to collect the maximum amount of data possible in a day's time period and to make the most efficient use of available resources.

The data collection plan for this study is illustrated in Table 10. Although not shown in the table, it should be noted that traffic volumes and cycle lengths varied by time of day. In addition, the green splits used on Monday were different from those used on Thursday, and these variables in combination with the various offsets which were implemented resulted in a wide range of expected platoon arrival types for this study. Project time and money constraints prohibited data collection for every variable combination, but an effort was made to study as many combinations as possible. Field conditions also dictated what could and could not be studied.

One feature of this data collection plan was the presumed inverse relationship between the HCM platoon arrival type and opposing directions of flow along the arterial. This feature is a result of the planned daily reduction in quality of progression in the other direction.

Table 10. Data Collection Plan.

Day of Week	Offsets Studied	Expected Platoon Arrival Types ^a			
		AM Peak (2 hours)	Off Peak (2 hours)	PM Peak (2 hours)	Evening (2 hours)
Sunday	----	Set up and test data collection system.			
Monday	best one-way	5 and 2	5 and 2	5 and 2	5 and 2
Tuesday	good two-way	4 and 2	4 and 4	4 and 3	2 and 4
Wednesday	poor two-way	2 and 3	2 and 5	2 and 4	2 and 4
Thursday	worst one-way	1 and 4	1 and 4	1 and 3	1 and 5
Friday	----	Optional day for studies that need repeating.			

^a Platoon arrival type as defined by the HCM (1) for AM, or inbound, and corresponding outbound directions of flow.

RESULTS

The field study data were used in the statistical evaluation of the analytical delay and progression factor equations presented previously. The following discussion summarizes the major findings from these analyses, the details of which are presented in Appendix C.

Summary Data

The summary data from each of the four field study sites are presented in Table 11. As shown, both two- and three-lane arterials, long and short block spacings, and mid-block speeds from 30 to 40 miles per hour were studied. Observed cycle lengths and saturation flow rates ranged from 60 to 120 seconds and approximately 1600 to 2100 vehicles per hour per lane, respectively. Interestingly, at all four sites the offpeak saturation flow rates were noticeably less than the peak period saturation flow rates. Thus, the resultant data set incorporates a wide range of geometric and operational conditions.

In terms of size, there are 256 hours, 12,280 cycles, 64,800 stopped delay queue counts, and 222,233 individual vehicles included in the data set. As mentioned previously, all data were recorded on a cycle-by-cycle basis. Specific variables for which information is available include green times, cycle lengths, and offsets for the upstream and downstream intersections; volumes on green, volumes on red, and total volumes; proportion of the total volume arriving on green, X-ratios and platoon ratios; and the average measured stopped delay at the downstream intersection.

Frequency Analysis

Prior to the detailed statistical analysis of the data, a frequency analysis on several of the more important variables affecting delay was conducted. The variables included green ratio (g/C), volume-to-capacity or X-ratio (X), proportion of the total volume arriving on green (P), and measured delay (d_m). The entire pretimed data set, which contained 855 15-minute observations,

Table 11. Study Sites and Their Attributes.

	NASA Road 1		Richmond		Normandie		Azusa	
	WB	EB	WB	EB	NB	SB	NB	SB
Physical Features								
• No. of Lanes	2	2	3	3	2	2	2	2
• Intersection Spacing	1066	680	900	1800	1320	1320	871	2561
A.M. Peak Conditions								
• Ideal Saturation Flow	1853	1857	1957	1918	1808	1839	2085	2085
• Adj. Saturation Flow	3695	3692	5754	5668	3598	3616	4070	4108
• Mid-block Speed	35	35	35	35	34	36	35	41
• Travel Time	23	20	18	35	-	-	17	41
A.M. Off-Peak Conditions								
• Ideal Saturation Flow	1809	1809	1842	1842	1618	1618	1953	1953
• Adj. Saturation Flow	3582	3582	5383	5334	3220	3188	3789	3820
• Mid-Block Speed	35	35	35	35	35	39	34	36
• Travel Time	23	20	18	35	-	-	17	50
P.M. Off-Peak Conditions								
• Ideal Saturation Flow	1809	1809	1871	1871	1618	1618	1953	1953
• Adj. Saturation Flow	3582	3593	5485	5418	3213	3188	3789	3867
• Mid-Block Speed	35	35	35	35	33	36	31	40
• Travel Time	23	20	18	35	-	-	19	44
P.M. Peak Conditions								
• Ideal Saturation Flow	1853	1857	1957	1918	1808	1839	2012	2012
• Adj. Saturation Flow	3687	3695	5708	5565	3598	3630	3984	3996
• Mid-block Speed	35	35	35	35	32	32	32	39
• Travel Time	23	20	18	35	-	-	19	45
Data Collected								
• Hours	30	30	32	29	28	29	39	39
• Cycles	1287	1276	1382	1384	1860	1860	1614	1617
• Queue Counts	7680	7680	7680	7680	7440	7440	9600	9600
• Vehicles	30659	30005	24344	27126	23707	21641	33252	31499

was analyzed in the initial analysis and then broken down by site for a more detailed analysis. The by-site frequency analyses were used as the basis for selecting the calibration and validation data sets used in the statistical analysis of the delay equations. The semiactuated data set was only used for validation because of its small size.

Figure 22 shows the frequency distributions of the variables of interest for the entire pretimed data set. Because the green ratio was preset and constant for each two-hour time period of data collection, the observed green ratios tend to follow a rectangular rather than normal distribution. Observed values ranged from 0.25 to 0.65, with most of the observations occurring at green ratios less than 0.60. The observed X-ratios, on the other hand, followed a normal distribution with values ranging from 0.10 to 1.00. The majority of the observations occurred in the range of 0.40 to 0.80, which indicates that the data represents low to moderately high traffic volumes.

The relative frequencies of the proportion of the total volume arriving on green and measured delays showed negatively and positively skewed distributions, respectively. These distributions were not surprising given the fact that relatively high values of P ; i.e., relatively good progression, should result in relatively low values of delay. Large numbers of low P s and high delays were not observed because the signal timing adjustments to

achieve such observations were not considered desirable and were therefore not attempted.

The frequency distribution information for the semiactuated data set represents 56 observations that were collected on the last day of data collection at the Los Angeles suburban site. When compared to the pretimed data set, the semiactuated data set contained slightly higher green and X-ratios. The distributions of the proportion of the total volume arriving on green and measured delay in the two data sets were essentially the same. Thus, while the semiactuated control behaved as expected, there was not much difference in the values of the variables that were measured.

Delay Equation Analysis

The delay equation regression analysis examined how well, from both a statistical and practical standpoint, the uniform delay equations developed in this research were able to predict the measured delays under both pretimed and semiactuated operating conditions. After checking the applicability of the HCM delay equation (1) and whether or not any of the assumptions used in linear regression analysis were violated, the pretimed data set was broken down into two parts. The first part of the data was used to develop least squares fit calibration factors for the uniform and incremental delay terms of the delay equation. The second part of

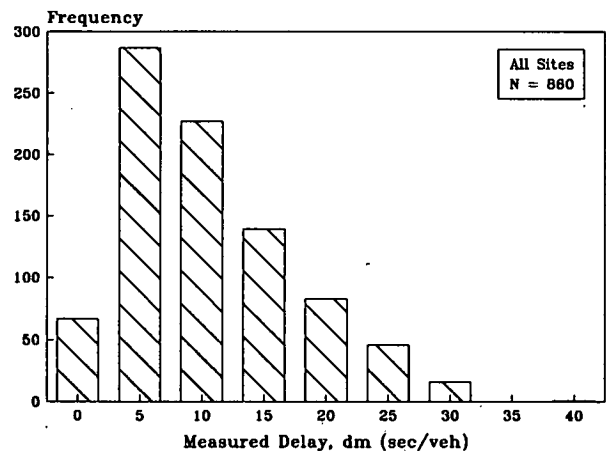
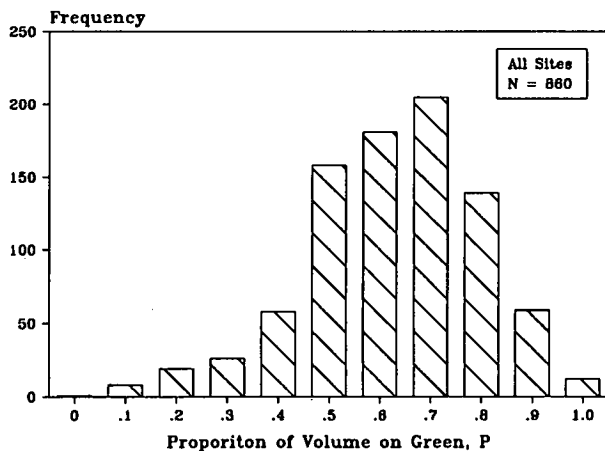
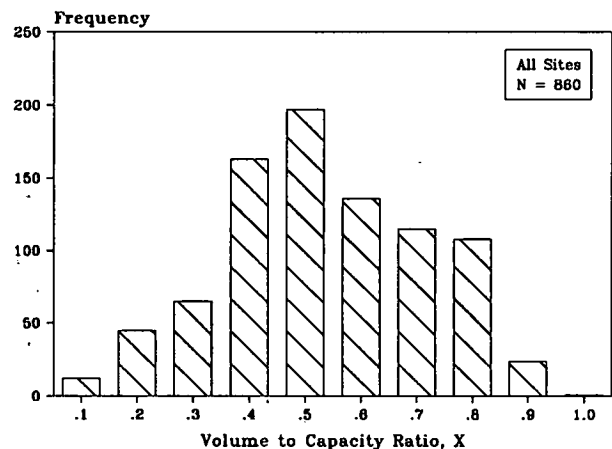
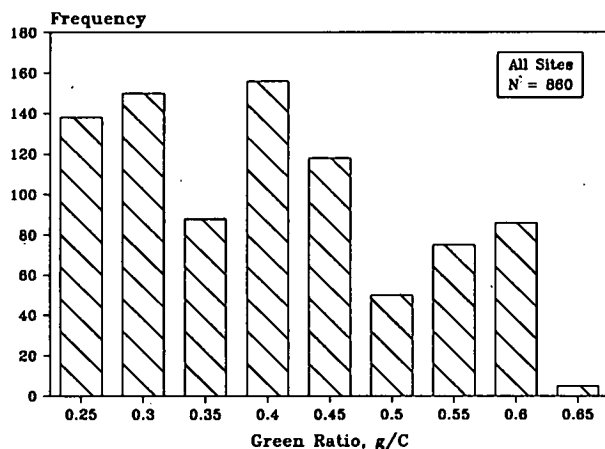


Figure 22. Frequency Distribution of Study Variables.

the data was used to validate the predictive ability of the calibrated delay equation using a simple two-tailed T-test for the slope parameter estimate being equal to 1.0. The findings from these analyses are summarized below.

The first step in the delay equation analysis was to perform a regression analysis on measured versus predicted delay using the HCM's uniform and incremental delay adjustments of 0.38 and 173, respectively. The results of this analysis for the pretimed data set are illustrated in Figure 23. As shown, the regression equation fit the data very well ($R^2 = 0.89$); however, the HCM equation overestimated measured delay. In other words, when 10 seconds of delay were predicted, 8 seconds of delay were measured. Thus, it was apparent that alternative adjustment factors were needed if more accurate estimates of measured delay were to be obtained. Before proceeding with the subsequent analysis, however, the assumptions of constant variance and normality of the residuals were checked and verified as being appropriate.

Because the data used to calibrate a model should not be used to test its predictive ability, the second step in the delay equation analysis was to separate the pretimed data set into two separate data sets. The first part of the calibration analysis developed adjustment factors for the incremental term of the HCM delay equation only whereas the second part of the calibration analysis developed adjustment factors for both the uniform and incremental terms. The two sets of adjustment factors are given in Table 12.

From this table, it is apparent that the least squares adjustment required for the uniform delay term of the delay equation is

the same as the HCM's uniform delay adjustment. The large decrease in the adjustment for the incremental delay term (from the current value of 173 to 69 and 63) was due in part to the lack of the high X-ratio, overflow delay, observations in the data set. Had such observations been available, the least squares adjustments for incremental delay would undoubtedly have been closer to the current adjustment factor of 173.

The final step in the delay equation analysis was to compare the measured delay in the validation data set to the predicted delay with the calibrated adjustment factors. The results of this analysis for both the pretimed and semiactuated data sets are summarized in Table 13. As shown, either set of adjustment factors will produce delay predictions within the allowable confidence intervals. Because the equations produced similar results, it was recommended that the adjustment factors closest to those in the HCM, a uniform adjustment of 0.38 and an incremental adjustment of 69, be used in the subsequent analysis. The relationship between measured and predicted delay with the recommended calibrations factors is illustrated in Figure 24.

Table 12. Calibration Factors Derived from Least Squares Analysis.

Analysis	f_u	f_i	r^2
0.38 fixed, d_i varied	0.38	69	0.93
both d_u and d_i varied	0.38	63	0.93

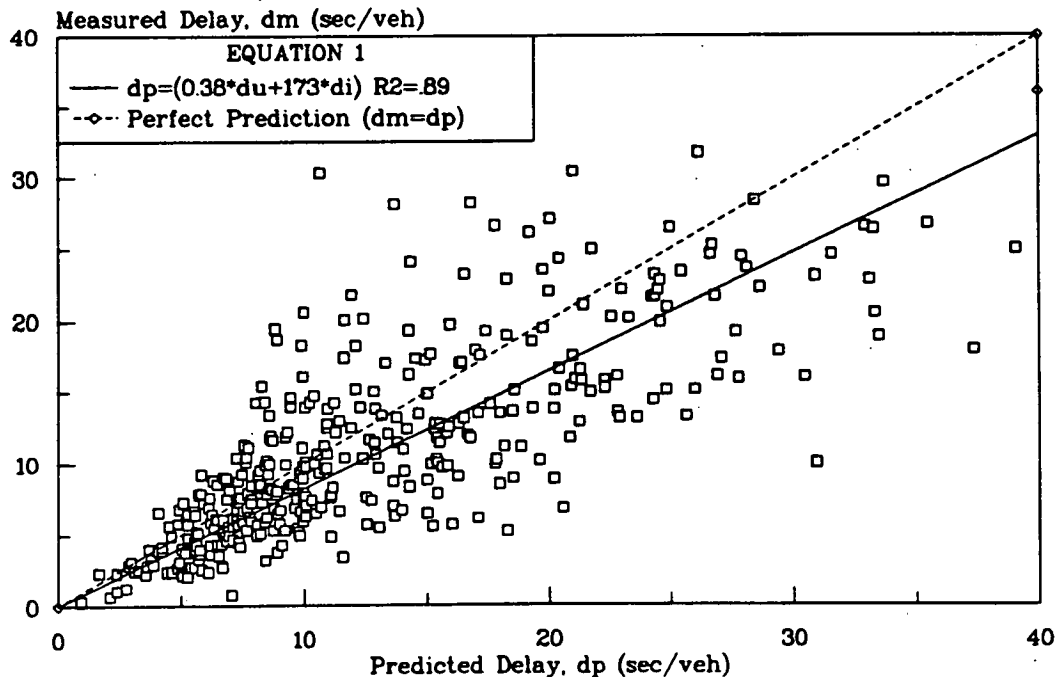


Figure 23. Comparison of Measured Versus Predicted Delay, HCM Delay Equation.

Table 13. Results of Regression Analysis for Measured Versus Predicted Delay.

Equation/ Interval	Number of Observations	Slope Parameter Estimate	R-Square	Standard Error	Confidence Interval (+/-)	T for Ho: Parameter = 1.0	Level of Significance
$f_u = 0.38$ AND $f_l = \text{VARIABLE}$							
<i>Pretimed</i>							
Validation Data	391	0.996	0.93	0.014	0.028	- 0.308	0.242
$g/C = 0.35$	29	1.128	0.95	0.047	0.097	2.704 *	0.988
$g/C = 0.40$	126	0.910	0.95	0.018	0.035	- 5.057 *	> 0.999
$g/C = 0.45$	88	0.964	0.93	0.028	0.055	- 1.320	0.810
$g/C = 0.50$	45	1.055	0.94	0.040	0.080	1.380	0.825
$g/C = 0.55$	43	0.931	0.88	0.054	0.108	- 1.284	0.794
$g/C = 0.60$	60	0.984	0.93	0.036	0.072	- 0.450	0.346
<i>Semiactuated</i>							
All Data	49	0.905	0.96	0.027	0.054	- 3.540 *	> 0.999
$g/C = 0.30$	20	0.896	0.95	0.045	0.094	- 2.323 *	0.969
$g/C = 0.35$	29	0.917	0.97	0.033	0.067	- 2.558 *	0.984
f_u AND f_l VARIABLE							
<i>Pretimed</i>							
Validation Data	391	1.006	0.93	0.014	0.028	0.419	0.325
$g/C = 0.35$	29	1.137	0.95	0.048	0.098	2.871 *	0.992
$g/C = 0.40$	126	0.918	0.95	0.018	0.036	- 4.569 *	> 0.999
$g/C = 0.45$	88	0.977	0.93	0.028	0.055	- 0.823	0.587
$g/C = 0.50$	45	1.064	0.94	0.040	0.080	1.616	0.887
$g/C = 0.55$	43	0.941	0.88	0.054	0.109	- 1.085	0.716
$g/C = 0.60$	60	0.992	0.93	0.036	0.072	- 0.217	0.171
<i>Semiactuated</i>							
All Data	49	0.922	0.96	0.027	0.054	- 2.877 *	0.994
$g/C = 0.30$	20	0.916	0.96	0.045	0.094	- 1.863	0.922
$g/C = 0.35$	29	0.929	0.97	0.034	0.069	- 2.118 *	0.957
* Statistically significant difference at the 95 percent confidence level.							

Progression Factor Analysis

The progression factor regression analysis examined how well the progression factors calculated from the field data (observed progression factors) compared to the progression factors calculated from the analytical equations (analytical progression factors) developed in this research. Observed progression factors were calculated using the calibrated adjustment factors from the delay equation analysis. An additional refinement of the progression factor analysis was the development of a methodology to identify whether the individual observations represented early or late arrivals; i.e., whether the front of the platoon arrived before or after the start of green.

The point in time at which the front of the platoon arrives at the downstream intersection is important because, as noted in the simulation analysis, two different delays can result for the same value of P (proportion of the total volume arriving on green). In other words, for a given P , the delay will be less than that predicted by the analytical equation if the front of the platoon arrives before the start of green and the rear of the platoon arrives before the start of red (early arrivals). For that same P , delay will be greater than that predicted by the analytical equation if the front of the platoon arrives after the start of green and the rear of the platoon arrives after the start of red (late arrivals).

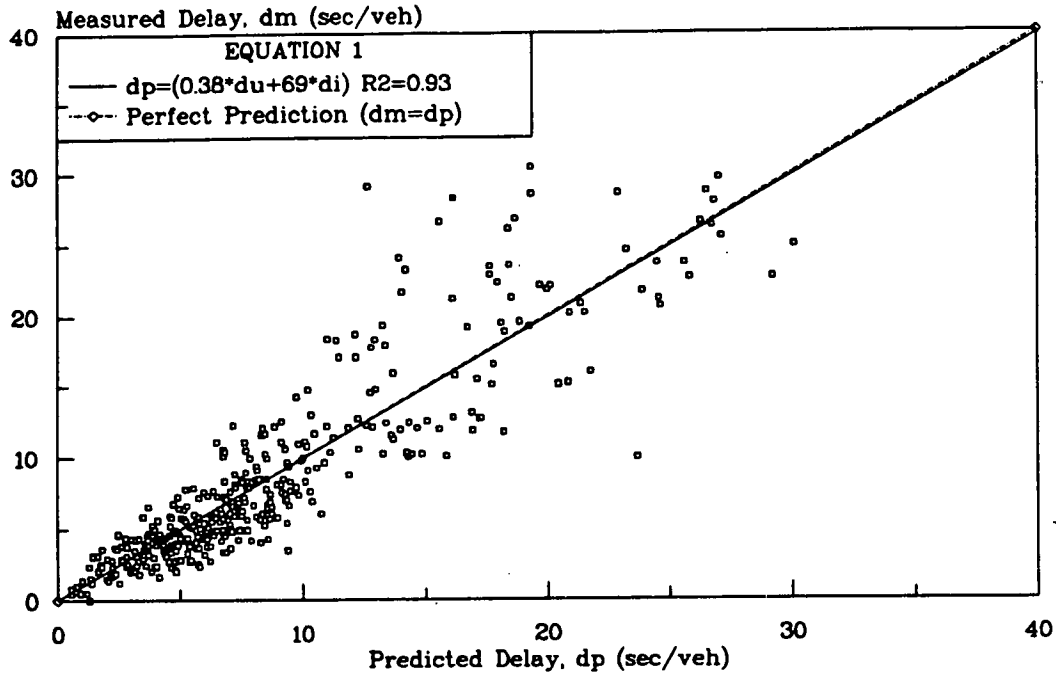


Figure 24. Comparison of Measured Versus Predicted Delay, Calibrated Delay Equation.

The concept of early and late arrivals is described in Table 14 and illustrated in Figure 25. Note that early arrivals result in less delay and late arrivals result in more delay than that predicted by the analytical progression adjustment factor equations. Additionally, the least delay occurs when the progression is good (high P_s and Arrival Types 3, 4, and 5); average or uniform delay occurs when the progression is fair (moderate P_s and Arrival Types 1, 2, 5, and 6); and the most delay occurs when the progression is bad (low P_s and Arrival Types 1, and 7). These observations reinforce the need for developing separate relations for early and late arrivals.

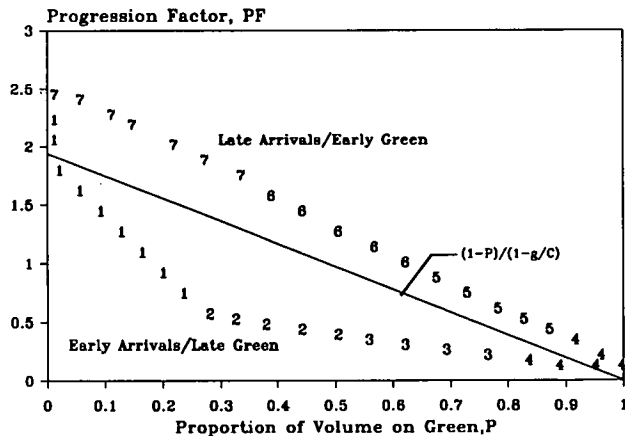


Figure 25. Effects of Early and Late Arrivals on Progression Adjustment Factors.

The results of the progression factor regression analyses for both types of arrivals and each green ratio in the data set are shown in Table 15. As expected, five of the nine equations for early arrivals predicted lower progression factors (less delay) than the analytical equation, and eight of the nine equations for late arrivals predicted higher progression factors (more delay) than the analytical equation. Thus, it appears that an additional adjustment factor to account for early and late arrivals would further increase the accuracy of the predicted delay. This factor, f_{AT} , would be multiplied by either the analytical progression factor equation or to the proposed uniform delay equation as shown below:

$$PF_s = \left(\frac{1-P}{1-g/C} \right) * f_{AT}$$

or

$$d_u = 0.38 * r * \left(\frac{1-g/C}{1-y} \right) * \left(\frac{1-P}{1-g/C} \right) * f_{AT}$$

Based on the findings from this research, the recommended values for f_{AT} are 0.85 for early platoon arrivals and 1.30 for late platoon arrivals. Whenever the front and rear of the platoon both arrive on green or both arrive on red, f_{AT} should be 1.00.

Table 14. Relationship Between Arrival Type and Platoon's Arrival at the Downstream Intersection.

Arrival Type	Progression Type	Description	
1	Bad	Front of platoon arrives during first third of red.	} Early Arrivals or Late Green
2	Poor	Front of platoon arrives during middle third of red.	
3	Good	Front of platoon arrives during last third of red.	
4	Perfect	Front of platoon arrives near the start of green.	
5	Good	Front of platoon arrives during first third of green.	} Late Arrivals or Early Green
6	Poor	Front of platoon arrives during middle third of green.	
7	Bad	Front of platoon arrives during last third of green.	

Table 15. Results of Regression Analysis for Observed Versus Predicted Progression Factors for Early and Late Arrivals.

	Number of Observations	Slope Parameter Estimate	R-Square	Standard Error	Confidence Interval (+/-)	T for Ho: Parameter = 1.0	Level of Significance
EARLY ARRIVALS							
All Data	475	0.873	0.91	0.012	0.02	- 10.19 *	> 0.999
g/C = 0.35	84	0.971	0.91	0.034	0.06	- .85	0.602
g/C = 0.40	45	0.719	0.90	0.036	0.06	- 7.85 *	> 0.999
g/C = 0.45	53	0.985	0.94	0.033	0.06	- .45	0.345
g/C = 0.50	134	0.818	0.91	0.022	0.04	- 8.41 *	> 0.999
g/C = 0.55	58	0.830	0.93	0.030	0.05	- 5.60 *	> 0.999
g/C = 0.60	10	0.935	0.95	0.071	0.13	- 0.91	0.613
g/C = 0.30	29	0.810	0.91	0.048	0.08	- 3.96 *	> 0.999
g/C = 0.35	62	1.013	0.93	0.035	0.06	0.37	0.287
LATE ARRIVALS							
All Data	302	1.309	0.93	0.021	0.03	14.91 *	> 0.999
g/C = 0.35	37	1.550	0.92	0.076	0.13	7.26 *	> 0.999
g/C = 0.40	88	1.314	0.96	0.029	0.05	10.84 *	> 0.999
g/C = 0.45	35	1.339	0.97	0.038	0.06	8.92 *	> 0.999
g/C = 0.50	51	1.357	0.92	0.055	0.09	6.46 *	> 0.999
g/C = 0.55	34	1.107	0.93	0.053	0.09	2.03 *	0.950
g/C = 0.60	44	1.294	0.93	0.054	0.09	5.41 *	> 0.999
g/C = 0.35	13	1.014	0.87	0.112	0.20	0.12	0.094

* Statistically significant difference at the 95 percent confidence level.

INTERPRETATION, APPRAISAL, AND APPLICATION

On the basis of the results of this research, the following was concluded:

1. Progression adjustment factors should only be applied to the uniform delay term of the HCM's delay equation.
2. Delay equations incorporating the proportion of the total volume arriving on green can explicitly account for the effects of progression on delay.
3. The proportion of the total volume arriving on green, rather than platoon ratio, is a better predictor of the effects of quality of progression on delay.
4. Platoon dispersion affects the minimum and maximum percent of the volume that can reasonably be expected to arrive on green.
5. Early platoon arrivals decrease the expected delay; late platoon arrivals increase the expected delay.
6. Progression adjustment factors can provide reasonable estimates of delay at signalized intersections in a coordinated signal system.

Interpretation, appraisal, and application of these conclusions are discussed in the following sections.

UNIFORM DELAY

The first term for the HCM delay equation accounts for delay due to uniform flow over a cycle. Platoon flow due to progression is also uniform; i.e., the pulsed waveform repeats itself every cycle, and can have a significant effect on delay. The magnitude of this effect in terms of an adjustment factor is not appreciably affected by volume. If the additional delay due to random arrivals is also adjusted, there is a volume effect necessitating different adjustment factors for different volume levels.

Intuitively, progression adjustment factors that are not dependent on volume levels would be easier to understand and apply. Application of these factors to only the uniform delay term would also eliminate the possible erroneous conclusion that good or bad progression causes large changes in predicted delay during oversaturated conditions; i.e., quality of progression would not have a significant impact on overflow delay whenever demand exceeded capacity. The combination of these observations strongly supports changing the method by which progression adjustment factors are currently applied in the HCM.

REVISED DELAY EQUATIONS

Because the length of red is the real cause of delay, reformulation of the HCM's uniform delay equation in terms of red has a certain intuitive appeal. The resultant equation is also a much simpler equation. The additional incorporation of a term to explicitly account for the effects of progression would eliminate the need to apply a separate progression adjustment factor.

The practical application of the revised delay equation is illustrated in Figure 26. Solid lines (middle) represent predicted delay that is equivalent to that predicted by the HCM delay equation. Dashed and dotted lines (lower and upper) represent predicted delay that is a result of either good (P greater than g/C) or bad (P less than g/C) progression. Thus, as shown, the revised equation is equivalent to the HCM equation when flow rates are uniform throughout the cycle, and sensitive to the effects of quality of progression. This behavior, in addition to its simpler form, supports adoption of the revised delay equation.

PROPORTION VOLUME ARRIVING ON GREEN

Platoon ratio, the HCM's current description of quality of progression, has no stated limits on its minimum and maximum values. In fact, its maximum value is theoretically dependent on the green ratio on the approach. Proportion of the total volume arriving on green, P , a variable used to calculate platoon ratio, does have a constant boundary between 0 and 1, and would appear to be a better predictor of the effects of progression on delay.

Adoption of the proportion of the total volume arriving on green has several other advantages in addition to its constant boundaries. First, because P is an input in the determination of platoon ratio, its determination would not require additional information. Second, P is a variable that can be directly measured in the field. Finally, the concept that the higher P is, the lower the resultant delay, can be easily understood by non-technical people.

PLATOON DISPERSION

Platoon dispersion's biggest impact on progression adjustment factors is limiting the minimum and maximum proportions of the total volume that can reasonably be expected to arrive on green. In other words, the farther down the street the platoon travels, the more dispersed and closer to uniform flow it becomes; i.e., the progression adjustment factor approaches 1.0. Consequently, dispersion lessens a platoon's potential effect on uniform delay. The analytical, simulation, and field studies verified this diminishing effect.

The implication of the effect of dispersion is in regard to selection of appropriate progression adjustment factors as their range is dependent on travel time. That is, a wide range of factors are possible at short intersection spacings whereas only a very narrow range of factors are possible at long intersection spacings. Thus, it would not be appropriate to select very large or very small progression factors at long intersection spacings. Fortunately, counting the proportion volume arriving on green or estimating it with the techniques in Appendix A automatically account for the effects of dispersion. If P can neither be counted nor estimated, however, it should be assumed equal to g/C (i.e., $PF_g = 1.0$).

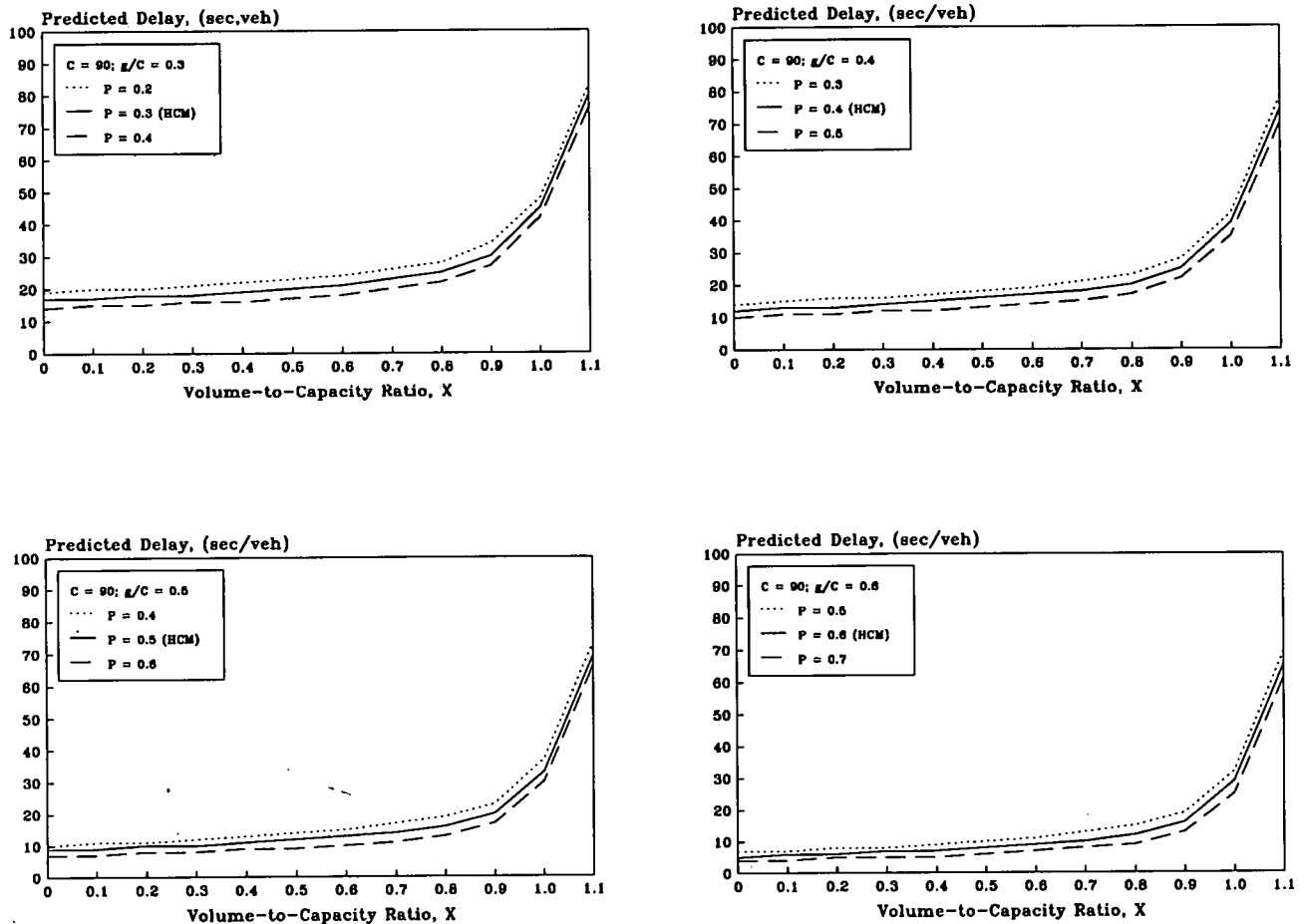


Figure 26. Effects of Proportion of the Total Volume Arriving on Green, P, on Predicted Delay.

EARLY AND LATE ARRIVALS

The point in time at which the front and rear of the platoon arrives at the downstream intersection has a definite effect on delay. The measured delay for a given value of proportion of the total volume arriving on green will be less than that predicted by the revised delay equation whenever the front of the platoon arrives before the start of green and the rear of the platoon arrives before the start of red (early arrivals). Conversely, the measured delay, for the same value of proportion of the total volume arriving on green, will be greater than that predicted by the revised delay equation whenever the front of the platoon arrives after the start of green and the rear of the platoon arrives after the start of red (late arrivals).

The implication of this effect is the need for an additional adjustment factor to account for early and late arrivals. This factor would be multiplied by either the predicted delay from the revised delay equation or by the progression adjustment factors. The

practical effect of an adjustment for arrival type is illustrated in Figure 27. Solid lines represent predicted delays that have not been adjusted for arrival type. Dotted and dashed lines represent predicted delays that have been adjusted to account for early and late arrivals. As shown, the adjusted delays exhibit the expected trends, early arrivals result in smaller delays and late arrivals result in larger delays. This behavior, in addition to its theoretical basis, support adoption of an arrival type adjustment factor.

Although use of these discrete adjustment factors for arrival type creates a discontinuity in the delay equation, the discontinuity occurs near the minimum delay point (i.e., perfect progression) which corresponds to the smallest progression adjustment factors. Thus, because the arrival type adjustment factor is being multiplied by an already small progression adjustment factor, the magnitude of the discontinuity in predicted delay is usually negligible.

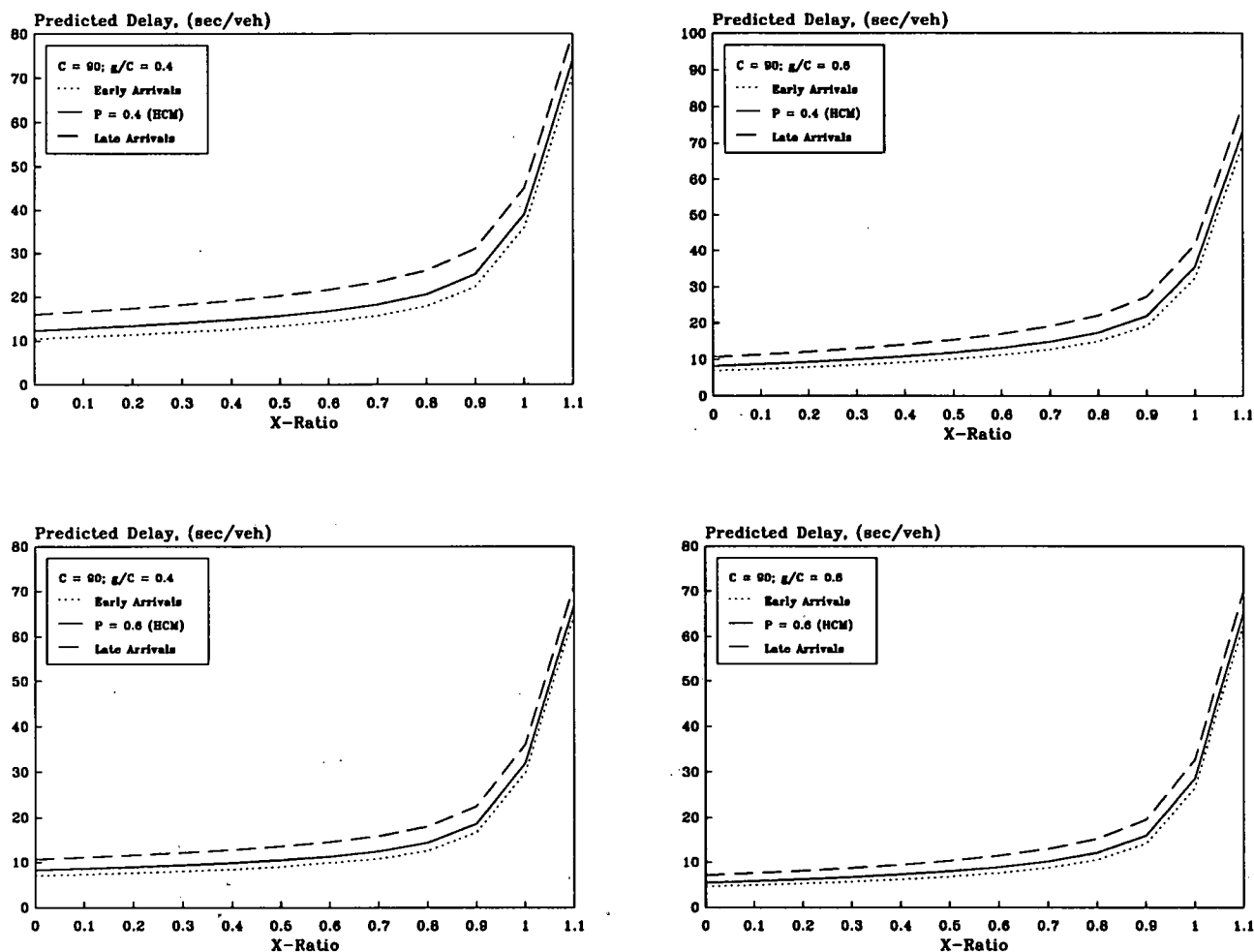


Figure 27. Effects of Early and Late Arrivals on Predicted Delay.

PROGRESSION ADJUSTMENT FACTOR

Quality of progression can have a significant effect on delay at signalized intersections. The progression adjustment factors (with additional adjustment for arrival type) developed in this research can provide reasonable estimates of this effect. The accuracy of these factors has been verified by analytical and statistical modeling of both simulation and field data. Thus, it is logical to recommend them as replacements for the values in Table 9-13 in the HCM.

The changes to the HCM methodology that are required as a result of this recommendation are threefold. First, progression factors are related to green ratios rather than x-ratios. Second, quality of progression is described by the proportion of the total volume arriving on green rather than by the platoon ratio. Finally, arrival type adjustments are made for two (early and late) rather than five arrival types. Adoption of the changes would result in a methodology that is simpler to understand, easier to explain and apply, and more accurate in its estimate of delay.

CONCLUSIONS AND RECOMMENDATIONS

The major conclusions and recommendations of this research address revised procedures for evaluating the effects of changes in the quality of traffic signal progression on average stopped delay. The procedures realistically estimate delay and are suitable for inclusion in the 1985 HCM (1). A brief summary of each conclusion and recommendation is given below.

CONCLUSIONS

As a result of this study, two methodologies for evaluating the effects of progression on stopped delay at signalized intersections (revised uniform delay equations and revised progression adjustment factors) have been developed. Both methodologies are based on theoretical concepts, and validated with over 250 hours of field data. They also yield identical results.

REVISED UNIFORM DELAY EQUATION

The revised uniform delay equation is written in terms of the length of red and eliminates the need for a separate progression adjustment factor. The revised equation was able to predict measured delays from the field studies extremely well, i.e., $R^2 = .93$. It does, however, require the estimation or measurement of the proportion of the total volume arriving on green. This equation can be expressed as follows:

$$d_u = 0.38 * r * (1 - P)/(1 - y)$$

where:

- d_u = first term delay for uniform arrivals, sec/veh;
- r = effective red time for the phase, sec;
- P = proportion of the total volume arriving on green; and
- y = flow ratio for the phase (Q/S).

Note that the above delay equation is directly related to the length of red, r , and the proportion of total volume arriving on red, $(1 - P)$.

REVISED PROGRESSION ADJUSTMENT FACTORS

Continuous equations have been developed to predict a revised set of progression adjustment factors. These equations are a function of the proportion of the total volume arriving on green and the green ratio. Use of these equations eliminates two problems noted by users of the 1985 HCM, discrete thresholds and the need for a wider range of adjustment factors to account for extremely good and extremely bad progression. This equation can be expressed as follows:

$$PF_g = (1 - P)/(1 - \lambda)$$

where:

- PF_g = revised progression adjustment factor; and
- λ = effective green-to-cycle length ratio.

Note that when the proportion of the total volume arriving on green equals the effective green-to-cycle length ratio, $PF_g = 1.00$. The revised progression adjustment factors should be multiplied by the uniform term of the HCM delay equation rather than by both the uniform and incremental terms as is presently done. This change better fits the field data and removes the need to adjust progression factors for changes in volume. The revised progression adjustment factors are applied as follows:

$$d = (d_u * PF_g) + d_i$$

or

$$d = [0.38 * r * (1 - \lambda)/(1 - y) * PF_g] + 173 * d_i$$

where:

- d = average stopped delay per vehicle, sec/veh; and
- d_i = second-term delay for incremental random and overflow effects, sec/veh.

By substituting the value for PF_g and cancelling the $(1 - \lambda)$ s, this equation can be further simplified as follows:

$$d = 0.38 * r * (1 - P)/(1 - y) + 173 * d_i$$

ADDITIONAL ADJUSTMENT FACTORS

Adjustment factors to account for early and late platoon arrivals (before or after the start of green) were also developed as a part of this research. These adjustments produce better estimates of delay and are appropriate whenever the front and rear of the platoon consistently arrive either before or after the start of green (front) and red (rear). They are applied as follows:

$$d = (d_u * PF_g * f_{AT}) + 173 * d_i$$

or

$$d = [0.38 * r * (1 - P)/(1 - y) * f_{AT}] + 173 * d_i$$

where:

- f_{AT} = 0.85 if the front of the platoon arrives before the start of the green and the rear of the platoon arrives before the start of red (early arrivals);
- f_{AT} = 1.00 if the front and rear of the platoon both arrive on either green or red; or

$f_{AT} = 1.30$ if the front of the platoon arrives after the start of green and the rear of the platoon arrives after the start of red (late arrivals).

RECOMMENDATIONS

Both the revised delay equations and the progression adjustment factors developed in this research realistically estimate the effects of changes in the quality of signal progression on delay. It is recommended that these findings be adopted by TRB's Highway Capacity and Quality of Service Committee. Specifically, it is recommended that only the uniform term of the HCM delay equation be adjusted for progression rather than adjusting the sum of the uniform and incremental terms as is presently done.

If progression adjustment factors are retained, Table 16 is recommended as the replacement for Table 9-13 in the 1985 HCM.

Note that progression adjustment factors are a function of green ratio, proportion of the total volume arriving on green, and whether the front and rear of the platoon arrive before or after the start of green and red. These factors should be multiplied by the uniform term of the HCM delay equation rather than the sum of the uniform and incremental terms as is presently done. It also should be noted that P should be assumed equal to g/C whenever it cannot be estimated by field data or from a valid analytical procedure such as provided in the Appendix.

It is recommended that adopting the revised uniform delay equation is the better of the two alternative methodologies because of its simpler form. Adoption of this recommendation would eliminate the need for separate progression adjustment factors as the new equation would explicitly account for the effects of progression.

If more accurate estimates of these effects are desired, it is suggested that the signal timing programs TRANSYT-7F or

Table 16. Recommended Progression Adjustment Factors, PF^a , for both Pretimed and Semiactuated Signals.

Green Ratio, g/C	Proportion of Total Volume Arriving on Green, P							
	.20	.30	.40	.50	.60	.70	.80	.90
.60	N/A ^b	1.75	1.50	1.25	1.00	0.75	0.50	0.25
.55	1.78	1.56	1.33	1.11	0.89	0.67	0.44	0.22
.50	1.60	1.40	1.20	1.00	0.80	0.60	0.40	0.20
.45	1.45	1.27	1.09	0.91	0.73	0.55	0.36	0.18
.40	1.33	1.17	1.00	0.83	0.67	0.50	0.33	0.17
.35	1.23	1.08	0.92	0.77	0.62	0.46	0.31	0.15
.30	1.14	1.00	0.86	0.71	0.57	0.43	0.29	0.14
.25	1.07	0.93	0.80	0.67	0.53	0.40	0.27	0.13

Note: If P cannot be estimated by field data or a valid analytical procedure, $PF = 1.0$.

$$PF = (1 - P) / (1 - g/C)$$

and
$$d = (.38 * d_u * PF * f_{AT}) + (173 * d_l)$$

where:

$f_{AT} = 0.85$ if the front of the platoon arrives before the start of green and the rear of the platoon arrives before the start of red (early arrivals);

$f_{AT} = 1.00$ if the front and rear of the platoon both arrive on either green or red; and

$f_{AT} = 1.30$ if the front of the platoon arrives after the start of green and the rear of the platoon arrives after the start of red (late arrivals).

^b N/A indicates a condition that simulation analysis shows to be extremely unlikely.

PASSER II be used. These programs have embedded traffic models that respond to changes in progression and automatically calculate the resultant delay and other measures of effectiveness. Manual computations of delay are eliminated.

FUTURE RESEARCH

It also is recommended that future research efforts in assessing the effects of the quality of traffic signal progression on delay be directed at the following four areas:

1. To avoid discontinuities associated with discrete adjustment factors for arrival type, continuous adjustment factors should be developed.
2. Calibration of the incremental delay term to account for the effects of progression at moderate and high volume-to-capacity ratio conditions should be reexamined. Based on the results of this research, such a calibration will probably require computer simulation to study high volume to capacity ratio conditions.
3. Even though this study does not recommend a revision of the 0.85 delay adjustment factor to account for the effects of vehicle-actuated signals, the validity of this adjustment factor should be verified with field data.
4. The procedure presented in Appendix A for estimating the proportion volume arriving on green, P , should be validated with field data and/or additional computer simulation data. Identification and evaluation of secondary platoons should be a part of the validations.

REFERENCES

1. "Highway Capacity Manual — 1985". TRB Special Report 209, Washington, D.C.: Transportation Research Board, National Research Council, 1985.
2. REILLEY, W.R., S.L. BOLDUC, J.H. KELL, and M.L. GALLAGHER. "Urban Signalized Intersection Capacity." NCHRP Report 3-28(2), Washington, D.C.: Transportation Research Board, National Research Council, 1983.
3. "Data Experiment Results." Documentation Report for NCHRP 3-28(2), Washington, D.C.: Transportation Research Board, National Research Council, 1981.
4. MESSER, C.J., D.B. FAMBRO, and D.A. ANDERSEN. "Study of Effects of Design and Operational Performance of Signal Systems." Report 203-2F. College Station, Texas: Texas Transportation Institute, Texas A&M University System, 1975.
5. WEBSTER, F.V. "Traffic Signal Settings." Road Research Technical Paper No. 39: Her Majesty's Stationary Office, 1958.
6. KIMBER, R.M., and E.M. HOLLIS. "Traffic Queues and Delays at Road Junctions." TRRL, Laboratory Report 909, Crowthorne, Berkshire, England: Transport and Road Research Laboratory, 1979.
7. HILLIER, J.A., and R. ROTHERY. "The Synchronization of Traffic Signals for Minimum Delay." *Transportation Science*, Vol. 2, 1967, pp.81-93.
8. ROBERTSON, D.I. "TRANSYT: A Traffic Network Study Tool." *Road Research Laboratory Report No. LR 253*. Crowthorne, England, 1969.
9. "NCHRP Signalized Intersection Capacity Method." Documentation Report for NCHRP Report 3-28(2), Washington, D.C.: Transportation Research Board, National Research Council, 1982.
10. CHANG, E.C., C.J. MESSER, and B.G. MARSDEN. "Analysis of Reduced Delay and Other Enhancements to PASSER II-80 — PASSER II-84." Report 375-1F, College Station, Texas: Texas Transportation Institute, Texas A&M University System, 1984.
11. CHANG, E.C., and C.J. MESSER. "Warrants for Interconnection of Isolated Traffic Signals." Report 293-1F, College Station, Texas: Texas Transportation Institute, Texas A&M University System, 1985.
12. BOWERS, D.A. "Progressive Timing for Traffic Signals." *Proceedings, Institute of Traffic Engineers*, 1947.
13. YARDENI, L.A. "Vehicular Traffic Control, A Time-Space Design Model." *Proceedings, Institute of Traffic Engineers*, 1964.
14. MORGAN, J.T., and J.D.C. LITTLE. "Synchronizing Traffic Signals for Maximal Bandwidth." *Operations Research*, Vol. 12, 1964.
15. *Traffic Control Systems Handbook*. Report No. FHWA-IP-76-10, Washington, D.C.: Federal Highway Administration, U.S. Department of Transportation, 1976.
16. ROUPHAIL, N.M. "Analysis of TRANSYT Platoon Dispersion Algorithm." *Transportation Research Record 905*, Washington, D.C.: Transportation Research Board, National Research Council, 1983, pp.72-80.
17. SEDDON, P.A. "Another Look at Platoon Dispersion: 1. The Recurrence Relationship." *Traffic Engineering and Control*, Vol. 13, No. 10, 1972, pp. 442-444.
18. MCCOY, P.T., ET AL. "Calibration of TRANSYT Platoon Dispersion Model for Passenger Cars Under Low-Friction Traffic Flow Conditions." *Transportation Research Record 905*, Washington, D.C.: Transportation Research Board, National Research Council, 1983, pp. 48-52.

REFERENCES CONTINUED

19. WALLACE, C.E., ET AL. "TRANSYT-7F User's Manual." Office of Traffic Operations, Federal Highway Administration, 1983.
 20. PREVEDOUROS, P.D., and P.P. JOVANIS. "Validation of Saturation Flows and Progression Factors for Traffic Actuated Signals." *Transportation Research Record 1194*, Washington, D.C.: Transportation Research Board, National Research Council, 1988, pp. 147-159.
 21. COURAGE, K.G., C.E. WALLACE, and R. ALQASEM. "Modeling the Effect of Traffic Signal Progression on Delay." *Transportation Research Record 1194*, Washington, D.C.: Transportation Research Board, National Research Council, 1988, pp. 139-146.
 22. ROUPHAIL, N.M. "Delay Models for Mixed Platoon and Secondary Flows." *Journal of Transportation Engineering*, Vol. 114, No. 2, 1988, pp. 131-152.
 23. BERRY, D.S. "Volume Counting for Computing Delay at Signalized Intersections." *Institute of Traffic Engineers Journal*, Vol. 57, No. 3, 1987, pp. 21-23.
 24. FAMBRO, D.B., N.A. CHAUDHARY, C.J. MESSER, and R.U. GARZA. "A Report on the Users' Manual for the Microcomputer Version of PASSER III-88." Report 478-1, College Station, Texas: Texas Transportation Institute, Texas A&M University System, 1988.
 25. HURDLE, V. F. "Signalized Intersection Delay Models -- A Primer for the Uninitiated." *Transportation Research Record 971*, Washington, D.C.: Transportation Research Board, National Research Council, 1984, pp. 96-105.
 26. SAS/STAT User's Guide. Release 6.03 Edition, Cary, North Carolina: SAS Institute, Inc., 1988.
 27. OTT, L. "An Introduction to Statistical Methods and Data Analysis." PWS-Kent Publishing Co. Boston, Massachusetts (1988).
-

APPENDIX A --

DEVELOPMENT OF PROGRESSION-DELAY MODELS

Operational delay on approaches to signalized intersections is primarily caused by vehicles arriving at the intersection when the signal is red. If traffic flow were uniform over the cycle, the proportion of vehicles arriving on the red would be equal to the fraction of the cycle that is red for the subject approach and the fraction of vehicles not arriving on red would equal the fraction of the cycle that is green for the subject approach. If traffic flow were not uniform over the cycle, i.e., platoon or pulsed flow, the average flow rates during red and green might not be equal.

Platoon or pulsed flow is characteristic of coordinated signal systems. The basic objective of signal coordination is to minimize arrival flow on red by increasing the proportion of arrival flow occurring on green. Figure A-1 illustrates the quality of this coordination effort.

Definition of terms:

- C = cycle length, sec;
- g = effective green time of phase, sec;
- r = effective red time of phase, sec;
- q = average movement flow rate during cycle, vps;
- s = saturation flow rate of phase, vpsg;
- λ = green time to cycle length ratio (g/C);
- y = flow rate of phase (q/s);
- X = demand volume to signal phase capacity ratio (qC/gs);
- q_g = average movement flow rate during effective green time, vps;
- q_r = average movement flow rate during effective red time, vps;
- P = proportion of all vehicles in the movement arriving during the green phase ($P=PVG$);
- R_p = HCM platoon ratio ($P/\lambda = PVG/PTG$);
- d = uniform delay, seconds/vehicle;
- d_u = uniform delay based on an average arrival rate, seconds/vehicle;
- PVG = proportion of all vehicles in the movement arriving during the green phase ($PVG=P$); and
- PTG = proportion of the cycle that is green ($PTG = \lambda$).

QUALITY OF PROGRESSION PARAMETERS

The following expression, extracted from Figure A-1, can be used to characterize the quality of signal progression or coordination and the resulting effects on delay. The overall cycle length is the sum of the effective red and green times for the subject approach; e.g., the arterial through movement.

$$C = r + g \quad [A-1]$$

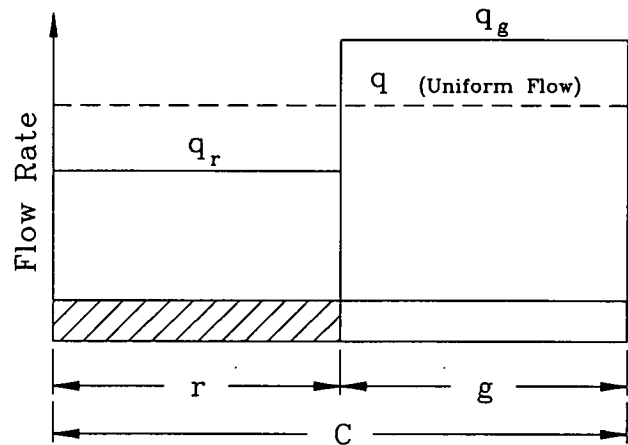


Figure A-1. Effect of Progression on Traffic Flow.

The average number of vehicles arriving during the cycle is expressed as:

$$q * C = q_r * r + q_g * g \quad [A-2]$$

Dividing the previous equation by the average flow during the cycle, q , yields:

$$C = \frac{q_r}{q} * r + \frac{q_g}{q} * g \quad [A-3]$$

Further dividing by the cycle, C , and rearranging terms yields the following equation:

$$1 = \frac{q_r}{q} * \frac{r}{C} + \frac{q_g}{q} * \frac{g}{C} \quad [A-4]$$

In other words, the proportion of total arrivals on red (PVR) plus the proportion of total arrivals on green (PVG) equals 1:

$$1 = PVR + PVG \quad [A-5]$$

The 1985 Highway Capacity Manual (HCM)(1) defines the platoon ratio, R_p , as the ratio of the proportion of arrivals on green to the proportion of time that is green within the cycle. This definition can be stated in the equation on the following page:

$$R_p = \frac{PVG}{PTG} = \frac{(q_g * g) / C}{g / C} \quad [A-6]$$

or

$$R_p = \frac{q_g}{q} \quad [A-7]$$

Thus, the platoon ratio is simply equal to the ratio of the average flow rate during the green to the average flow rate during the cycle.

There are, however, practical limitations on the allowable range of values for the platoon ratio, R_p . For example, the arrival flow during green, q_g , cannot exceed the saturation flow of the approach; i.e., $q_g \leq s$. Similarly, the average flow rate, q , cannot exceed $s * g / C$. The net result of these limitations can be expressed as follows:

$$R_p = \frac{q_g}{q} = \frac{q_g}{X * s * g / C} \quad [A-8]$$

or

$$R_p = \frac{q_g}{X * s * \lambda} \quad [A-9]$$

In general, the platoon ratio increases proportionally with an increase in q_g . This increase is limited by the X ratio and λ . For example, when X equals 1.0, then the upper bound on R_p is equal to:

$$R_p \leq \frac{1}{\lambda}$$

This result suggests that the present definition of platoon ratio is not a robust characterization index for progression quality, because its allowable range depends on the process it is trying to characterize; i.e., the allowable range depends on the g/C ratio and X ratio on the subject approach. Thus, it would appear that R_p may not be a superior descriptor of the quality of progression. The term $R_p * \lambda$, however, does appear to have the desired constant bound between 0.0 and 1.0. This new term is defined as P , such that:

$$P = R_p * \lambda \quad [A-10]$$

where:

$$0 \leq P \leq 1$$

This new term can be manipulated to show its relationship with the previously described variables. In particular, Equations A-6 and A-10 can be combined to show the relation between P and the volume arriving on green.

$$P = \frac{q_g}{q} * \frac{g}{C} = PVG \quad [A-11]$$

In this relationship, P is equal to the proportion of the total traffic arriving on green, PVG . Consequently, the average arrival flow on green is expressed as:

$$q_g = \frac{P}{\lambda} * q \quad [A-12]$$

The average arrival flow on red, determined from Equations A-12 and A-4, is as follows:

$$q_r = \left(\frac{1 - P}{1 - \lambda} \right) * q \quad [A-13]$$

The previous formulations can now be used to estimate delay as a function of P . Intuition would suggest that delay decreases as P approaches 1.0, because there would be more volume arriving on green and less volume arriving on red.

ESTIMATION OF UNIFORM DELAY

The first term of the 1985 HCM delay equation is often referred to as being the uniform delay component because it is based on the assumption that the arrival flow rate during the cycle is uniform. Progression adjustment factors are then applied to account for the effects of progression quality on delay. An alternative delay formulation includes progression effects within the model, and is described in the following derivation.

The total delay that would occur per cycle, assuming the arrival flow profile of Figure A-1, can be estimated as the area under the queue length curve depicted in Figure A-2. The total delay, D , is expressed as:

D = shaded area under arrival/departure curve.

$$D = \left[r * (q_r * r) + (q_r * r) * \left(\frac{q_r * r}{s - q_g} \right) \right] / 2 \quad [A-14]$$

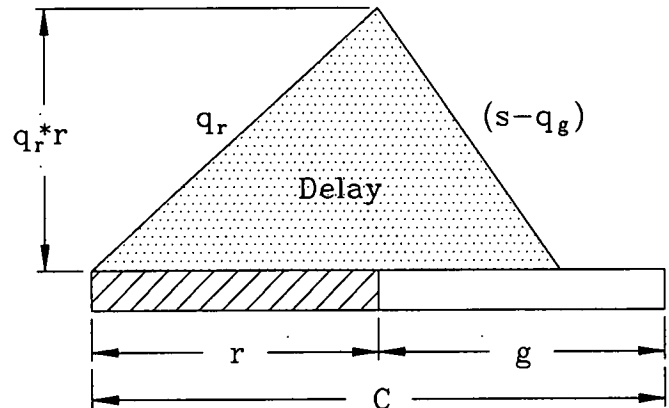


Figure A-2. Total Delay on an Intersection Approach.

$$D = \frac{q_r * r^2}{2} * \left(1 + \frac{q_r}{s - q_g}\right) \quad [A-15]$$

The average delay per vehicle arriving per cycle, d , is computed from $d = D/(q * C)$ as:

$$d = \left(\frac{q_r * r^2}{2 * q * C}\right) * \left(1 + \frac{q_r}{s - q_g}\right) \quad [A-16]$$

Substituting $r = C * (1 - \lambda)$ and rearranging terms yields:

$$d = \frac{C}{2} * (1 - \lambda)^2 * \left(1 + \frac{q_r}{s - q_g}\right) * \frac{q_r}{q} \quad [A-17]$$

This equation can be shown to equal the first term of Webster's delay equation when arrival flows on red and green are uniform. Thus, substituting a uniform average flow, q , for q_r and q_g in the above equation yields the Webster delay term for uniform flow:

$$d_u = \frac{C}{2} * \frac{(1 - \lambda)^2}{1 - y} \quad [A-18]$$

An alternative formulation of Equation A-17 substitutes for the ratio q_r/q from Equation A-13, yielding:

$$d = \frac{C}{2} * (1 - \lambda)^2 * \left(1 + \frac{q_r}{s - q_g}\right) * \left(\frac{1 - P}{1 - \lambda}\right) \quad [A-19]$$

$$d = \frac{C}{2} * (1 - \lambda) * \left(1 + \frac{q_r}{s - q_g}\right) * (1 - P) \quad [A-20]$$

$$d = \frac{r}{2} * \left(1 + \frac{q_r}{s - q_g}\right) * (1 - P) \quad [A-21]$$

Again, should the equivalent uniform flow delay equation be desired, it is found by letting $q_r = q_g = q$ and $(1 - P) = (1 - \lambda)$ resulting in:

$$d_u = \frac{r}{2} * \left(\frac{1}{1 - y}\right) * (1 - \lambda) \quad [A-22]$$

Alternatively, by letting $r = C * (1 - \lambda)$, the Webster delay term is again obtained as:

$$d_u = \frac{C}{2} * \frac{(1 - \lambda)^2}{1 - y} \quad [A-23]$$

DERIVING PROGRESSION ADJUSTMENT FACTORS

The present methodology in the 1985 HCM uses a progression adjustment factor, PF, to adjust both the uniform delay term and the overflow delay term. This research has shown, and most related current research also suggests, that progression adjustment factors should only adjust (be multiplied by) the uniform delay term. More explicitly:

$$d_T = (d_u * PF) + d_i \quad [A-24]$$

where:

d_u = total uniform delay; and

d_i = random and overflow delay, which are not at issue here.

By combining Equations A-21 and A-22, the progression adjustment factor, PF, can be derived as follows:

$$d = d_u * PF \quad [A-25]$$

or

$$\frac{r}{2} * \left(1 + \frac{q_r}{s - q_g}\right) * (1 - P) = \frac{r}{2} * \left(\frac{1 - \lambda}{1 - y}\right) * PF \quad [A-26]$$

Dividing both sides of the equation by $r/2$ and rearranging terms yields:

$$PF = \left(\frac{1 - P}{1 - \lambda}\right) * \left(1 + \frac{q_r}{s - q_g}\right) * \left(1 - \frac{q}{s}\right) \quad [A-27]$$

which is approximately equal to:

$$PF \approx \frac{1 - P}{1 - \lambda} \quad [A-28]$$

By substituting this approximate progression factor and Equation A-22 into Equation A-25, the uniform delay due to progression can be expressed as follows:

$$d = d_u * PF \approx \frac{r}{2} * \left(\frac{1 - \lambda}{1 - y}\right) * \left(\frac{1 - P}{1 - \lambda}\right) \quad [A-29]$$

Removing the $(1 - \lambda)$ term yields the simple equation for the first component of delay:

$$d = \frac{r}{2} * \left(\frac{1 - P}{1 - y}\right) \quad [A-30]$$

A sensitivity analysis of PF to the various input variables in Equation A-27 has been conducted. Three green splits (λ) of 0.25, 0.33, and 0.50 were examined for volume-to-capacity ratios of 0.6, 0.8, and 1.0. The results of these analyses are depicted in Figures A-3, A-4, and A-5. It should be pointed out that Equation A-27 defaults to Equation A-28 at $X=1.0$. Thus, these figures also illustrate the relationship between Equations A-27 and A-28.

The main conclusion reached from an examination of these figures is that the volume-to-capacity ratio, X , does not appear to be a major contributor to the progression adjustment factor, PF. In other words, PF is not sensitive to X , as long as $X \leq 1.0$. The range of values for PF, however, is strongly dependent on the signal's g/C ratio.

It could also be concluded that Equations A-27 and A-28 yield very similar estimates of PF for g/C ratios less than 0.50. Small differences between the two equations begin to emerge as

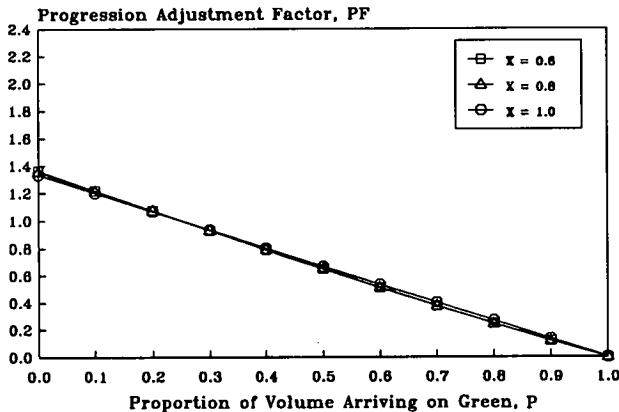


Figure A-3. Progression Factor Versus P for $g/C = 0.25$.

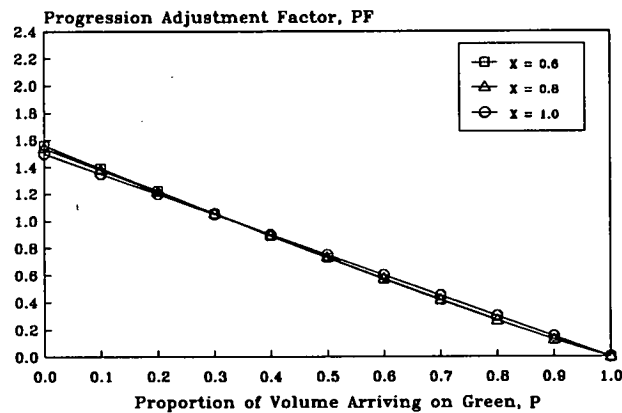


Figure A-4. Progression Factor Versus P for $g/C = 0.33$.

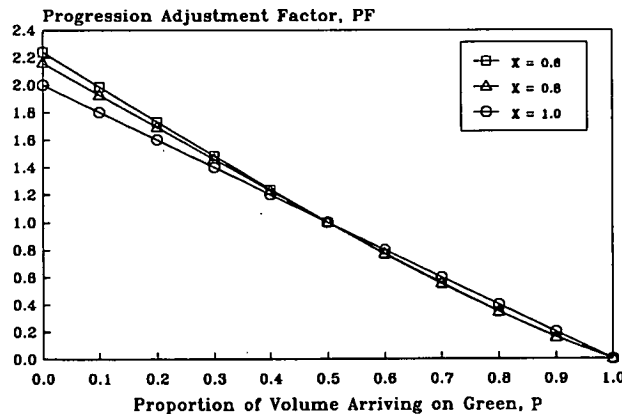


Figure A-5. Progression Factor Versus P for $g/C = 0.50$.

the g/C ratio increases. For example, when the g/C ratio is 0.50, the differences between the estimated values of PF from Equations A-27 and A-28 are only about 10 percent for values of P less than 0.20 or greater than 0.70.

ESTIMATION OF PROGRESSION DESCRIPTORS

Several methods could be used to estimate the numerical value of P between adjacent traffic signals. Two methods will be provided herein. The first method, based on a recent TRB paper by Courage, et. al. (21), uses progression bandwidth to estimate P. The second method, based on a TRANSYT-like platoon dispersion model as suggested by Rouphail (22) and modified in this research, uses green splits, offsets, and travel times to estimate P. The first method is described below, whereas the second method is more fully described in the following section.

Courage formulated an expression for calculating the band ratio, R_b , which he uses as a surrogate for the platoon ratio, R_p . Since R_p is directly related to P (i.e., $P = R_p * \lambda$), Courage's equation for R_b can be rewritten in terms of P as follows:

$$P = \left[p * \left(\frac{b}{g_i} \right) + (1 - p) * \left(\frac{g - b}{C - g_i} \right) \right] \quad [A-31]$$

where:

- p = proportion of arrival traffic at the downstream signal that originates from the coordinated phase at the upstream signal i ;
- b = progression bandwidth from the upstream intersection i through the downstream intersection, sec; and
- g_i = effective green time at upstream intersection, i , sec.

Courage tested a form of this model using TRANSYT-7F and found that the model predicted about 49 percent of the delay variation within a study network in Michigan that contained 49 signalized intersections. Courage concluded his paper by noting that "... the band ratio is an adequate predictor of the platoon ratio for most purposes" (21).

PLATOON DISPERSION MODELS

Traffic flowing between signalized intersections exhibits a wide range of speed and densities. In particular, the stop/go operation of the traffic signal creates dense platoons that decrease in density as their travel time increases. Ideally, platoons of traffic would be progressed from one traffic signal to the next such that lead vehicles arrive at the start of the green phase. In this ideal situation motorist delays and stops would be minimal. On the other hand, if the platoon were to arrive during the red phase, delays could be quite lengthy.

Several approaches to modeling platoon dispersion are shown in Figure A-6. In each case, a platoon of vehicles is projected from the upstream to the downstream intersection. Typically, the reduction in platoon density is described by a reduced flow rate spread over a wider progression band.

Figure A-6a illustrates the dispersion model used in TRANSYT-7F (8). This model is based on a recurrence equation used to predict the dispersed flow rate for each successive increment of time.

Figure A-6b shows the dispersion model used in PASSER II (4). This model projects a dispersed platoon downstream. Unlike TRANSYT, however, the flow rate within the platoon is averaged over the dispersed arrival period.

A third model, shown in Figure A-6c, has been proposed by Rouphail (22). This model assumes a constant progression band unlike the approach of TRANSYT and PASSER II. The effect of progression is accounted for by calculating a reduced flow rate within this progressed band. Any flow outside of this band is averaged over the remaining portion of the cycle.

These three models are also quite different in the technique used to estimate uniform delay. In particular, TRANSYT uses a numeric integration technique over the entire cycle. PASSER II, on the other hand, uses progression information to calculate an average arrival rate on downstream red and green phases. These estimates are then used in an equation similar to Equation A-17 to estimate delay. Rouphail's model is composed of several deterministic delay models that are sensitive to when the progression band arrives during the cycle and to the band's width.

Figure A-6d illustrates the model proposed by this research. This model extends the progression concept employed by Rouphail and the delay calculation technique used in PASSER II. The model's formulation is directed toward a methodology that yields good estimates of delay but is not too difficult to calculate with a hand calculator. It should be noted that the proposed model, consistent with the preceding models, assumes that progression primarily affects the uniform delay component.

PROPOSED MODEL

The proposed model is conceptually similar to that described by Rouphail (22). The approach is based on the transformation of the traffic flow into two flow regions: one representing the progressed platoon and the other representing all secondary flows. This model is shown in Figure A-7. All variables not previously defined on page A-1 are described below.

Traffic Characteristics

- q_{pi} = average flow rate inside of platoon window, vps;
- q_w = average flow rate of progressed traffic inside of platoon window, vps;
- q_p = average flow rate of progressed traffic outside of platoon window, vps;
- q_u = average flow rate outside of platoon window, vps;

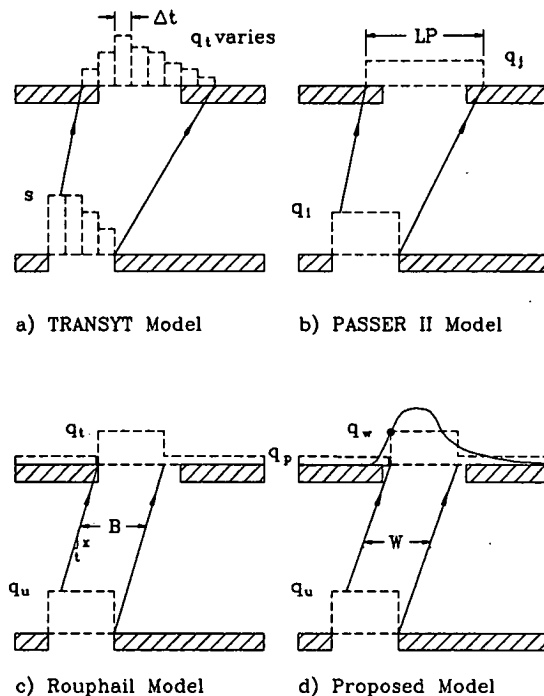


Figure A-6. Overview of Platoon Dispersion Concepts.

- q_u = average flow rate in the platoon window at the upstream intersection, vps;
- q_o = average flow rate from preceding platoon that overlaps the end of the previous cycle, vps.
- p = proportion of arrival traffic at the downstream signal that originates from the coordinated phase at the upstream signal;
- α = platoon dispersion factor, assumed equal to 0.35;
- β = ratio of leading edge of platoon arrival time to average travel time, assumed equal to 0.80;
- F = platoon smoothing factor;

Signal Timing

- g_i = effective upstream green, sec;
- W = window of time spanning progressed movement, sec;
- O = time offset between start of green phases serving progressed movement, sec;
- t = average travel time between intersections, sec;
- g_{pi} = effective green time that receives platooned arrivals, sec;
- t_i = average travel time between the upstream intersection and its preceding intersection, sec;
- W_1 = time after first platooned vehicle arrives at downstream intersection that platoon flow rate exceeds $p \cdot q$, sec;
- W_o = time after first platooned vehicle arrives at downstream intersection that platoon ends, sec.

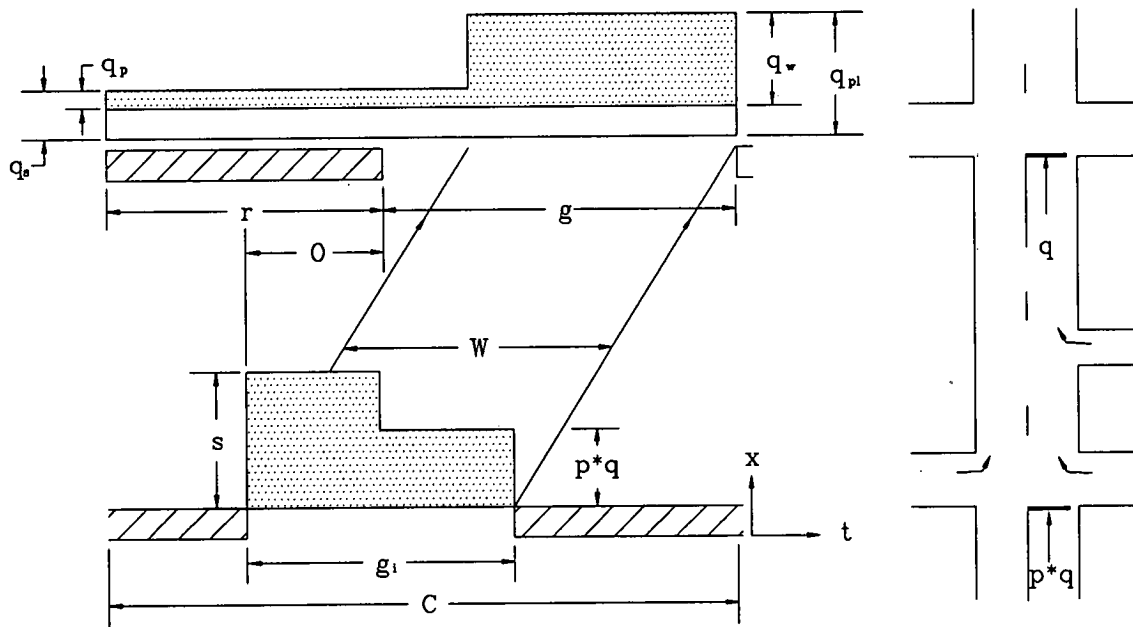


Figure A-7. Progression Model Characteristics.

Assumptions and Definitions

The principal assumption for the proposed method is that the magnitude of secondary flows is small compared to the primary progressed flow; i.e., $p > 0.50$. Based on this assumption, the proposed model only accounts for the dispersion of the primary movement. This is a reasonable assumption since the underlying premise of this methodology is that secondary flow patterns do not significantly affect approach delay.

In recognition of the first assumption, a second assumption is that the secondary flow can be distributed uniformly throughout the cycle. It could be argued that secondary flows would not join a dense platoon of traffic and thus should not be added to the platooned flow (see Figure A-7). However, the width of the progression window is purposely large, such that a secondary flow could still join a low-density platoon or enter just behind the high-density portion but still travel within the window. In addition to its simplicity, the assumption of uniform secondary flows has the advantage of being well-behaved throughout the range of travel times. In particular, the platoon window flow rate, q_p , has the desirable feature of approaching the average arrival rate (i.e., uniform flow) as travel time increases.

The following section describes a technique that is simple enough to be applied using a hand calculator. In this regard, a fundamental decision was made that Equation A-17 would be the only delay model used. Experience with the model suggests that it will yield reasonable results in spite of the model's insensitivity to the platoon arrival time during the cycle (i.e., early versus late arrivals during the green phase).

The model is based on the assumption that the following variables are known: C , q , p , g , s , O , t , t_r .

A fundamental deviation of the proposed model from the other models is in the definition of progression band. In this model, the band of dense, platooned traffic does not have its edges sloped at the average travel speed. Rather, the proposed model calculates the densest portion of the platoon and defines it as the band of progressed flow. The implication here is that the densest portion of the platoon does not always move down the street at exactly the average travel speed. Because of the disparity between this definition and previous definitions of progression band, the band calculated by this model will be redefined as the platoon window (W).

Methodology

The following ten steps describe the proposed model for calculating the platoon ratio, R_p , the proportion of vehicles arriving on green, P , and the uniform delay component. The first two variables describe the quality of traffic progression, while the last variable describes the level of traffic service provided by the downstream signal.

1. Establish platoon window. The platoon window is defined as the upstream green time that spans the densest portion of the platoon. In this regard, the flow rate throughout the platoon must equal or exceed $p * q$. In general, W must be greater than or equal to the saturated portion of the upstream green phase and less than or equal to g_1 . Thus:

$$\frac{(C - g) * p * q}{s - p * q} \leq W \leq g_1$$

If arrivals to the upstream intersection are assumed to be spread uniformly over the cycle, then W should equal g_u . If better information suggests that arrivals to the upstream intersection are platooned, then W may be less than g_u .

2. Platoon flow rate. Once W has been determined, the following equation can be used to estimate the flow rate in the upstream platoon window. Thus:

$$q_u = p * q * \frac{C - f * (g_i - W)}{W} \quad [A-32]$$

$$q_u \leq s$$

where:

$$f \cong 0.064 * \sqrt{t_i}$$

$$f \leq 1.0$$

In this last equation, f is an empirical adjustment to account for progressive effects at the upstream intersection. If t_i is unknown, it can be assumed equal to the travel time between the up- and downstream intersections, t .

3. Smoothing factor. This methodology is mathematically based on the recurrence equation used in TRANSYT. Specifically, this recurrence equation can be written as:

$$q_{(j+T)} = F * q_j + (1 - F) * q_{(j+T-1)} \quad [A-33]$$

where:

$q_{(k)}$ = flow rate of the platoon at time k ;

$$T = B * t$$

$$F = \frac{1}{1 + \alpha * \beta * t} \quad [A-34]$$

By expanding the recurrence equation terms for the interval $i = 1, 2, \dots, j$ seconds it has been shown that the result has the form of a truncated geometric series (17).

$$q_{(j+T)} = \sum_{i=1}^j q_{(i)} * F * (1 - F)^{j-i}$$

If the flow rate over the interval $i = 1, 2, \dots, j$ can be assumed as constant (i.e., $q_{(i)} = q$), then the truncated series can be reformulated as a closed-form solution (16).

$$q_{(j+T)} = q * [1 - (1 - F)^j] ; \text{ if } q \text{ is constant over } j$$

The smoothing factor, F , is needed for the remaining steps of the proposed procedure and can be calculated using Equation A-34. In general, this factor weighs the current upstream inflow rate, q_j , with the flow rate of the previous time interval, $q_{(j+T-1)}$, in calculating the downstream flow rate, $q_{(j+T)}$, arriving T seconds later.

4. Cyclic platoon dispersion overlap flow rate. By applying the closed-form solution, the overlapped flow rate from the preceding platoon that exists at the end of the previous cycle can be estimated from the following equation:

$$q_o \cong 1.26 * p * q * (1 - F)^{(C - G_i)} \quad [A-35]$$

5. Time of platoon arrival. As shown in Figure A-8, the first vehicles in the platoon are assumed to arrive $\beta * t$ seconds after their release upstream. The platoon flow rate, however, does not exceed the average flow rate of $p * q$ until an additional W_1 seconds have passed. This time, in seconds, can be calculated using the following equation:

$$W_1 = \frac{\ln [(p * q - s) / (q_o - s)]}{\ln (1 - F)} \quad [A-36]$$

$$W_1 \geq 0.0$$

Thus, the start of the platoon window occurs W_1 seconds after the first vehicles in the platoon arrive. Using the same point of reference, the platoon is assumed to end $W_1 + W$ seconds later. Thus:

$$W_e = W_1 + W \quad [A-37]$$

6. Flow rate within the platoon window. Because the truncated series can be reformulated into a continuous, closed-form solution, it can also be integrated over the period W_1 to W_e to obtain the total flow in the platoon window. The average flow rate of progressed traffic in the platoon window, q_w , can then be obtained by averaging the total flow over the platoon window, W . Thus, the integrated equation for estimating q_w is as follows:

$$q_w = q_u + \frac{(q_o - q_u) * [1 - (1 - F)^{-W}] * (1 - F)^{(W_e + \beta * t)}}{W * \ln (1 - F)} \quad [A-38]$$

$$q_w \geq p * q$$

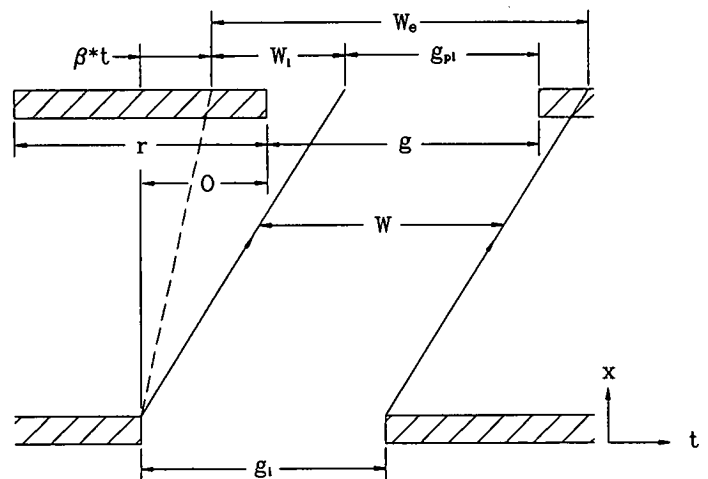


Figure A-8. Platoon Window Relationships.

where:

$$f = \text{empirical adjustment (use 4.0)}$$

Although the integrated equation is exact, the assumption of a uniform flow, q_w , feeding the platoon is an approximation that necessitates a slight modification of the integrated equation. Thus, an adjustment factor, f , has been included to improve the estimate of q_w .

By integrating the closed-form solution, a theoretical relationship between flow rate and travel time has been maintained. Although the integration has resulted in a fairly complicated equation, this complexity is partly offset by the equation's adaptability. Specifically, it can be calibrated to local driving conditions via the smoothing factor, F , calculated in Step 3. The equation is also sensitive to signal timing variables via the platoon window definition and the overlap flow rate, q_o .

7. Flow rates at downstream intersection. Using the values calculated in the previous steps, the downstream flow rates can now be calculated. In particular, the following equations can be used to estimate q_{pl} and q_o , the flows inside and outside the platoon window, respectively (22).

$$q_{pl} = q_w + (1 - p) * q \quad [A-39]$$

$$q_p = \frac{p * q * C - W * q_w}{C - W} \quad [A-40]$$

$$q_o = q_p + (1 - p) * q \quad [A-41]$$

8. Duration of downstream green experiencing platoon arrivals. The determination of where the platoon arrives with respect to the downstream green phase requires knowledge of the signal offset, O , relative to the start of the green phase of the progressed movement.

Initially, four values must be calculated to locate the relative beginning and ending times of both the downstream green phase, g , and the platoon window, W .

$$\begin{aligned} G_1 &= O + g; & G_2 &= O; \\ P_1 &= W_o + \beta * t; & P_2 &= W_1 + \beta * t; \end{aligned}$$

Occasionally, the combination of large travel times and/or cycle lengths may require adjusting these four values as follows:

$$\begin{aligned} \text{If } G_1 - C > W_1 + \beta * t & \text{ then } \begin{cases} G_1 = O + g - C \\ G_2 = O - C \end{cases} \\ \text{If } P_1 - C > O & \text{ then } \begin{cases} P_1 = W_o + \beta * t - C \\ P_2 = W_1 + \beta * t - C \end{cases} \end{aligned}$$

Once the four values have been calculated, the green time experiencing platooned arrivals can be calculated as follows:

$$g_{pl} = \text{MIN} \left\{ \begin{matrix} G_1 \\ P_1 \end{matrix} \right\} - \text{MAX} \left\{ \begin{matrix} G_2 \\ P_2 \end{matrix} \right\} \quad [A-42]$$

One additional check is necessary to insure that g_{pl} has been accurately calculated. This check is as follows:

$$\begin{aligned} \text{If } W > (C - g) & \text{ then } g_{pl} \geq W - (C - g) \\ \text{If } W \leq (C - g) & \text{ then } g_{pl} \geq 0.0 \end{aligned}$$

9. Arrival rate during downstream green and red phase. Once the value of g_{pl} has been calculated, the arrival rate during the green and red phases can be calculated by a simple proportioning technique.

$$q_g = \frac{q_{pl} * g_{pl} + q_o * (g - g_{pl})}{g} \quad [A-43]$$

$$q_r = \frac{q * C - q_g * g}{C - g} \quad [A-44]$$

10. Platoon performance parameters and delay estimate. At this point, the platoon ratio, R_p ; the proportion of volume arriving on green, P ; and the progression adjustment factor, PF , can be calculated using the following relations:

$$R_p = \frac{q_g}{q} \quad [A-45]$$

$$P = \frac{q_g * g}{q * C} \quad [A-46]$$

$$PF = \frac{q_r}{q} * \left(1 - \frac{q}{s}\right) * \left(1 + \frac{q_r}{s - q_g}\right) \quad [A-47]$$

Once the value of PF is known it can also be used with Equations A-18 and A-25 (which are reproduced below as Equation A-48) to estimate the average uniform delay for a progressed traffic stream.

$$d = \frac{C}{2} * \frac{(1 - g/C)^2}{1 - q/s} * PF \quad [A-48]$$

Equation A-48 should yield a reasonable estimate of delay because of its sensitivity to arrival rates on the green and red phases. Of course, at any instant the arrival rate of platooned traffic is not likely to equal these average rates; however, the difference should be small in most situations. To illustrate this difference, Figure A-9 shows the actual and average cumulative arrival rates found on one intersection approach. Although the average rates do not vary precisely with the actual rates, the use of average rates should still yield reasonable estimates of total delay.

The variation in flow rates during either the green or red phase can be further examined to determine the error variability in Equation A-47. In this regard, Figure A-10 was developed to illustrate the region of feasible flow rates during the red and green phases that would yield the same cumulative demand. As the figure suggests, the maximum flow rate can never exceed the saturation flow rate, s , nor can it be less than zero.

Although initial inspection of the feasible regions may lead to the conclusion that there could be significant error in delay estimation using average rates, this is seldom the case in practical application. In general, the error decreases as the travel time, t , increases or the proportion of the flow that is progressed, p , decreases. Additional experience with the proposed procedure indicates better delay estimates for g/C ratios in the range of 0.4 to 0.6 and for higher X ratios.

The following section describes an evaluation of the proposed model using the TRANSYT program.

Preliminary Evaluation

To test the ability of the proposed method to predict delays for progressed movements, the TRANSYT-7F simulation program was used to estimate delays for a simplified arterial system. In this regard, the TRANSYT-7F program was used to estimate uniform delays for various offsets between two signalized intersections. These delays were then compared to those predicted by the proposed model.

The arterial chosen was assumed to have the following characteristics:

$$\begin{aligned} g_r/C &= 0.50; & g/C &= 0.50; & v/c &= 0.80; \\ t &= 30 \text{ seconds}; & p &= 0.80; & \text{and} & C &= 90 \text{ seconds.} \end{aligned}$$

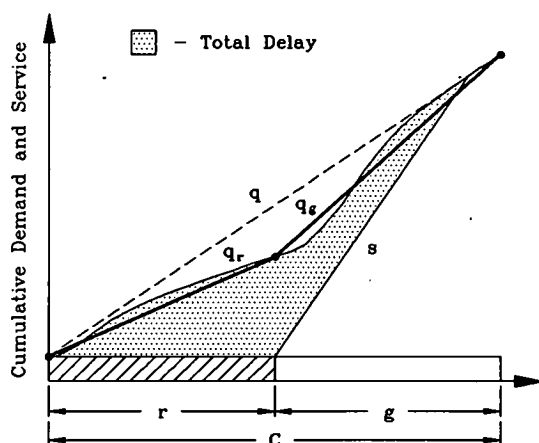


Figure A-9. Comparison of Actual and Average Arrival Rates.

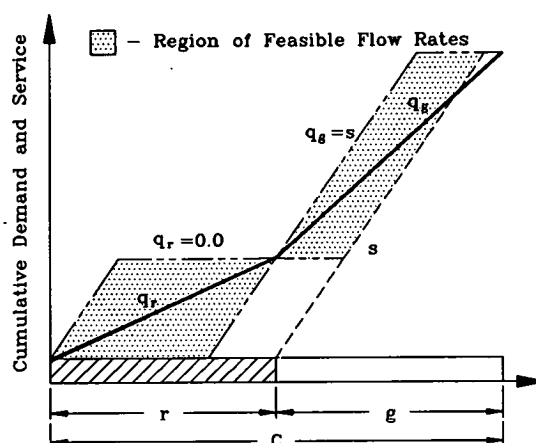


Figure A-10. Region of Feasible Flow Rates During Red and Green Phases.

In addition to examining the proposed model's predictive ability, a second examination was conducted to specifically test one of the assumptions in the model. In particular, the model formulation assumed that secondary arrivals were uniform. In other words, non-progressed traffic (such as upstream turn movements) was assumed to arrive uniformly throughout the cycle.

To test the reasonability of model assumptions, two scenarios were evaluated over the entire range of offset intervals. One employed 20 percent midblock arrivals (i.e., uniform arrivals) and the other used 10 percent left and 10 percent right turns at the upstream intersection (i.e., secondary platoons).

The results of this evaluation are shown in Figure A-11. In general, delays predicted by the proposed model appear to be very close to those calculated by the TRANSYT-7F program. As might be expected, the agreement was best between the proposed model and the TRANSYT-7F scenario with midblock arrivals.

The agreement between the proposed model and TRANSYT-7F was not as close when secondary platoons (i.e., the upstream turn movements) were introduced. The most noticeable difference was at the 30 percent offset. Further investigation of the TRANSYT-7F flow profile diagrams for this scenario indicated the nature of this discrepancy. Although this offset resulted in perfect through movement progression, it also resulted in the subsequent upstream left-turn phase releasing a secondary platoon that arrived at the beginning of the downstream red phase. Since the progressed model assumes uniform arrivals over the entire red phase, it is not sensitive to the early arrival of secondary platoons.

In most situations, there is likely to be both secondary platoons and midblock arrivals that would yield results somewhere between the two TRANSYT-7F scenarios. As a result, the underlying assumption of uniform secondary arrivals is believed to be a reasonable assumption for the given level of computational complexity.

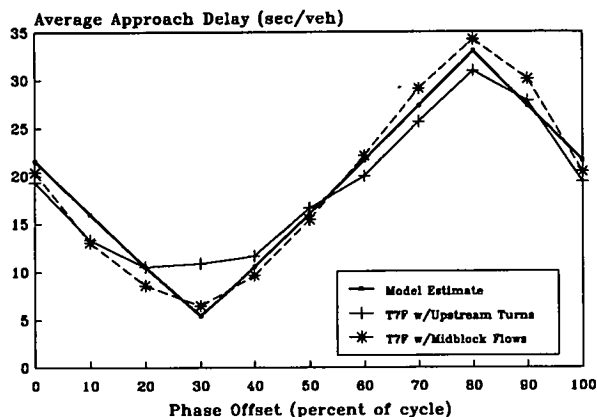


Figure A-11. Delay-Offset Analysis Comparing the Proposed Model with TRANSYT-7F.

Example Application

The following example is presented to illustrate the application of the proposed model. As previously discussed, certain input variables are assumed to be known by the analyst prior to conducting this analysis. In particular, it is assumed that the following variables are known: cycle length, C ; upstream and downstream effective green times, g and g_i ; average downstream through movement flow rate, q , and the proportion of it that is progressed, p ; downstream saturation flow rate, s ; time offset between the start of progressed movements, O ; and the average travel time, t , between signals.

One final piece of information that is needed is the platoon window, W . In general, this can be assumed equal to the upstream green, g_i . If it is known that the upstream flow is progressed, then a portion of the upstream green phase may have little or no flow. In this situation W may be less than g_i .

To simplify the analysis process, a supplemental worksheet has been prepared. This worksheet, shown in Figure A-12, has been patterned after the worksheets provided in Chapter 9 of the 1985 HCM.

For this example assume the following is known:

$C = 60$ seconds;	$q = 0.20$ vpspl (720 vphpl)
$p = 0.80$;	$s = 0.50$ vpsgpl (1800 vphgpl)
$g_i = 30$ seconds;	$g = 30$ seconds
$O = 27$ seconds;	$t = 30$ seconds

The solution would proceed as follows:

1. Establish platoon window. Calculate the duration of saturated flow at the upstream intersection.

$$W \geq \frac{(C - g_i) * p * q}{s - p * q}$$

$$W \geq \frac{(60 - 30) * 0.80 * 0.20}{0.50 - 0.80 * 0.20}$$

$$W \geq 14.1 \text{ seconds}$$

Thus:

$$14.1 \leq W \leq 30$$

Since the nature of arrivals to the upstream intersection is not known, it will be assumed that the arrival rate during green exceeds the average arrival rate, $p * q$. Thus:

$$W \equiv g_i = 30 \text{ seconds}$$

2. Platoon flow rate. Assuming that the arterial has signalized intersections every one-fourth mile, an estimate of t_1 would be t which equals 30 seconds. Thus:

$$f = 0.064 * \sqrt{30} = 0.35$$

and

$$\begin{aligned} q_u &= p * q * \frac{C - f * (g_i - W)}{W} \\ &= 0.80 * 0.20 * \frac{60 - 0.35 * (30 - 30)}{30} \\ &= 0.320 \text{ vps} \end{aligned}$$

3. Smoothing factor.

$$F = \frac{1}{1 + \alpha * \beta * t}$$

For lack of better information, α and β are assumed equal to 0.35 and 0.80 respectively. Thus:

$$\begin{aligned} F &= \frac{1}{1 + 0.35 * 0.80 * 30} \\ &= 0.106 \end{aligned}$$

SUPPLEMENTAL WORKSHEET FOR PROGRESSION ADJUSTMENT FACTOR, PF							
INPUT VARIABLES		EB	WB	NB	SB		
Cycle Length, C (sec)							
Effective Green, g (sec)							
Upstream Effective Green, g _i (sec)							
Offset, O (sec)							
Travel Time, t (sec)							
Progressed Flow Proportion, p							
Average Flow Rate, q (vpspl)							
Saturation Flow Rate, s (vpsgpl)							
Platoon Window, W (sec)							
COMPUTATIONS		EB	WB	NB	SB		
$f = 0.064 \cdot \sqrt{t}$							
$q_u = p \cdot q \cdot [C - f \cdot (g_i - W)] / W$							
$F = 1 / [1 + \alpha \cdot \beta \cdot t]; \alpha = 0.35 \beta = 0.80$							
$q_o = 1.26 \cdot p \cdot q \cdot (1 - F)^{(C - g_i)}$							
$W_1 = \frac{\ln [(p \cdot q - s) / (q_o - s)]}{\ln (1 - F)}$							
$W_e = W_1 + W$							
$q_w = q_u + \frac{(q_o - q_u)[1 - (1 - F)^W](1 - F)^{(W_e + 4)}}{W \cdot \ln (1 - F)}$							
$q_{pl} = q_w + (1 - p) \cdot q$							
$q_p = (p \cdot q \cdot C - W \cdot q_w) / (C - W)$							
$q_s = q_p + (1 - p) \cdot q$							
$G_1 = 0 + g$ ^{1.}	$G_2 = 0$ ^{1.}						
$P_1 = W_e + \beta \cdot t$ ^{2.}	$P_2 = W_1 + \beta \cdot t$ ^{2.}						
MIN = Minimum of {G ₁ , P ₁ }							
MAX = Maximum of {G ₂ , P ₂ }							
$g_{pl} = \text{MIN} - \text{MAX}$ ^{3.}							
$q_g = [q_{pl} \cdot g_{pl} + q_s \cdot (g - g_{pl})] / g$							
$q_r = (q \cdot C - q_g \cdot g) / (C - g)$							
$P = (q_g \cdot g) / (q \cdot C)$							
$PF = \frac{q_r}{q} \cdot \left(1 - \frac{q}{s}\right) \left(1 + \frac{q_r}{s - q_g}\right)$							

1. IF $G_1 - C > W_1 + \beta \cdot t$ then $G_1 = 0 + g - C$ and $G_2 = 0 - C$ ☐

2. IF $P_1 - C > 0$ then $P_1 = W_e + \beta \cdot t - C$ and $P_2 = W_1 + \beta \cdot t - C$ ☐

3. IF $W > (C - g)$ then $g_{pl} \geq W - (C - g)$ ☐

IF $W \leq (C - g)$ then $g_{pl} \geq 0$ ☐

Figure A-12. Supplemental Worksheet for Progression Adjustment Analysis.

4. Cyclic platoon dispersion overlap flow rate.

$$\begin{aligned}
 q_p &= 1.26 * p * q * (1 - F)^{(C \cdot 80)} \\
 &= 1.26 * 0.80 * 0.20 * (1 - 0.106)^{(60 - 30)} \\
 &= \boxed{0.007} \text{ vps}
 \end{aligned}$$

5. Time of platoon arrival.

$$\begin{aligned}
 W_1 &= \frac{\ln [(p * q * - s) / (q_p - s)]}{\ln (1 - F)} \\
 W_1 &= \frac{\ln [(0.80 * 0.20 * - 0.50) / (0.007 - 0.50)]}{\ln (1 - 0.106)} \\
 &= \boxed{3.3} \text{ seconds}
 \end{aligned}$$

Use 3.0 seconds.

$$\begin{aligned}
 W_e &= W_1 + W \\
 &= 3 + 30 \\
 &= \boxed{33} \text{ seconds}
 \end{aligned}$$

6. Flow rate within platoon window.

$$\begin{aligned}
 q_w &= q_p + \frac{(q_p - q_w) * [1 - (1 - F)^{-W}] * (1 - F)^{(W_e + 1)}}{W * \ln (1 - F)} \\
 &= 0.320 + \frac{-0.313 * [1 - (0.894)^{-30}] * (0.894)^{(33 + 1)}}{30 * \ln (0.894)} \\
 &= \boxed{0.279} \text{ vps}
 \end{aligned}$$

7. Flow rates at downstream intersection.

$$\begin{aligned}
 q_{pl} &= q_w + (1 - p) * q \\
 &= 0.279 + (1 - 0.80) * 0.20 \\
 &= \boxed{0.319} \text{ vps} \\
 q_p &= \frac{p * q * C - W * q_w}{C - W} \\
 &= \frac{0.80 * 0.20 * 60 - 30 * 0.279}{60 - 30} \\
 &= \boxed{0.041} \text{ vps} \\
 q_s &= q_p + (1 - p) * q \\
 &= 0.041 + (1 - 0.80) * 0.20 \\
 &= \boxed{0.081} \text{ vps}
 \end{aligned}$$

8. Duration of downstream green experiencing platoon arrivals.

$$\begin{aligned}
 G_1 &= O + g = 27 + 30 = 57 \text{ seconds} \\
 G_2 &= O = 27 \text{ seconds} \\
 P_1 &= W_1 + \beta * t = 33 + 0.80 * 30 = 57 \text{ seconds} \\
 P_2 &= W_1 + \beta * t = 3 + 0.80 * 30 = 27 \text{ seconds}
 \end{aligned}$$

check:

$$\begin{aligned}
 G_1 - C &> W_1 + \beta * t; & 57 - 60 &= -3 < 27 \text{ O.K.} \\
 G_2 - C &> 0; & 27 - 60 &= -33 < 27 \text{ O.K.}
 \end{aligned}$$

Therefore, no adjustment is necessary.

$$\begin{aligned}
 g_{pl} &= \text{MIN} \left\{ G_1 \right. & - & \text{MAX} \left\{ G_2 \right. \\
 & \quad \left. P_1 \right\} & & \quad \left. P_2 \right\} \\
 &= \text{MIN} \left\{ 57 \right. & - & \text{MAX} \left\{ 27 \right. \\
 & \quad \left. 57 \right\} & & \quad \left. 27 \right\} \\
 &= \boxed{30} \text{ seconds}
 \end{aligned}$$

$$\text{check: } W = 30 \leq (C - g) = (60 - 30) = 30$$

$$\begin{aligned}
 \text{then } g_{pl} &\geq 0.0 \\
 g_{pl} &= 30 \geq 0.0 \quad \text{O.K.}
 \end{aligned}$$

9. Arrival rate during downstream green and red phases.

$$\begin{aligned}
 q_g &= \frac{q_{pl} * g_{pl} + q_s * (g - g_{pl})}{g} \\
 &= \frac{0.319 * 30 + 0.081 * (30 - 30)}{30} \\
 &= \boxed{0.319} \text{ vps} \\
 q_r &= \frac{q * C - q_g * g}{C - g} \\
 &= \frac{0.20 * 60 - 0.319 * 30}{60 - 30} \\
 &= \boxed{0.081} \text{ vps}
 \end{aligned}$$

10. Platoon performance parameters and delay estimate.

$$R_g = \frac{q_g}{q}$$

$$= \frac{0.319}{0.20}$$

$$= 1.60$$

$$P = \frac{q_g * g}{q * C}$$

$$= \frac{0.319 * 30}{0.20 * 60}$$

$$= 0.80$$

$$PF = \frac{q_r}{q} * \left(1 - \frac{q}{s}\right) * \left(1 + \frac{q_r}{s - q_g}\right)$$

$$= \frac{0.081}{0.20} * \left(1 - \frac{0.20}{0.50}\right) * \left(1 + \frac{0.081}{0.50 - 0.319}\right)$$

$$= 0.35$$

$$d = \frac{C}{2} * \frac{(1 - g/c)^2}{1 - q/s} * PF$$

$$= \frac{60}{2} * \frac{(1 - 30/60)^2}{1 - 0.20/0.50} * 0.35$$

$$= 4.4 \text{ seconds / vehicle}$$

Thus, in this instance, the assumption of uniform arrivals during the cycle (when, in fact, arrivals are platooned and coordinated) has led to a significant overestimation of the actual delay incurred by motorists; i.e., 96 versus 3.4 seconds per vehicle.

A supplemental worksheet (see Figure A-13) has been completed for this example to further illustrate the calculation process. Although these calculations can be done manually, the use of spreadsheets or other computer techniques is recommended.

Converting total delay to stopped delay:

$$\text{stopped delay} = 4.4 / 1.3$$

$$= 3.4 \text{ seconds / vehicle}$$

By comparison, the uniform stopped delay predicted by the first term of Equation 9-18 in the 1985 HCM can be calculated as:

$$\text{stopped delay} = 0.38 * C * \frac{(1 - g/c)^2}{1 - q/s}$$

$$= 0.38 * 60 * \frac{(1 - 30/60)^2}{1 - 0.20/0.50}$$

$$= 9.6 \text{ seconds / vehicle}$$

SUPPLEMENTAL WORKSHEET FOR PROGRESSION ADJUSTMENT FACTOR, PF									
INPUT VARIABLES		EB		WB		NB		SB	
Cycle Length, C (sec)		60							
Effective Green, g (sec)		30							
Upstream Effective Green, g _i (sec)		30							
Offset, 0 (sec)		27							
Travel Time, t (sec)		30							
Progressed Flow Proportion, p		0.80							
Average Flow Rate, q (vpspl)		0.20							
Saturation Flow Rate, s (vpsgpl)		0.50							
Platoon Window, W (sec)		30							
COMPUTATIONS		EB		WB		NB		SB	
$f = 0.064 \cdot \sqrt{t}$		0.350							
$q_u = p \cdot q \cdot [C - f \cdot (g_i - W)] / W$		0.320							
$F = 1 / [1 + \alpha \cdot \beta \cdot t]; \alpha = 0.35 \beta = 0.80$		0.106							
$q_o = 1.26 \cdot p \cdot q \cdot (1 - F)^{(C - g_i)}$		0.007							
$W_1 = \frac{\ln [(p \cdot q - s) / (q_o - s)]}{\ln (1 - F)}$		3							
$W_e = W_1 + W$		33							
$q_w = q_u + \frac{(q_o - q_u)[1 - (1 - F)^W](1 - F)^{(W_e + 4)}}{W \cdot \ln (1 - F)}$		0.279							
$q_{pl} = q_w + (1 - p) \cdot q$		0.319							
$q_p = (p \cdot q \cdot C - W \cdot q_w) / (C - W)$		0.041							
$q_s = q_p + (1 - p) \cdot q$		0.081							
$G_1 = 0 + g$ ^{1.}	$G_2 = 0$ ^{1.}	57	27						
$P_1 = W_e + \beta \cdot t$ ^{2.}	$P_2 = W_1 + \beta \cdot t$ ^{2.}	57	27						
MIN = Minimum of {G ₁ , P ₁ }		57							
MAX = Maximum of {G ₂ , P ₂ }		27							
$g_{pl} = \text{MIN} - \text{MAX}$ ^{3.}		30							
$q_g = [q_{pl} \cdot g_{pl} + q_s \cdot (g - g_{pl})] / g$		0.319							
$q_r = (q \cdot C - q_g \cdot g) / (C - g)$		0.081							
$P = (q_g \cdot g) / (q \cdot C)$		0.80							
$PF = \frac{q_r}{q} \cdot \left(1 - \frac{q}{s}\right) \left(1 + \frac{q_r}{s - q_g}\right)$		0.35							

1. IF $G_1 - C > W_1 + \beta \cdot t$ then $G_1 = 0 + g - C$ and $G_2 = 0 - C$
2. IF $P_1 - C > 0$ then $P_1 = W_e + \beta \cdot t - C$ and $P_2 = W_1 + \beta \cdot t - C$
3. IF $W > (C - g)$ then $g_{pl} \geq W - (C - g)$
IF $W \leq (C - g)$ then $g_{pl} \geq 0$



Figure A-13. Completed Supplemental Worksheet.

APPENDIX B --

FIELD DATA

HOUSTON SUBURBAN SITE

The pilot study and the first suburban arterial study were conducted on two segments of NASA Road 1, a suburban arterial running east and west in Clear Lake, Texas. NASA Road 1 is a four-lane, divided arterial with separate left- and right-turn lanes on both approaches to the controlling intersection, El Camino Road. El Camino Road is a four-lane, divided arterial with separate left-turn lanes on both approaches to NASA Road 1. The secondary intersections to the east and west of El Camino were Space Park and Kings Row, respectively. Both secondary intersections were "Ts" with two-lane, undivided cross-sections. The geometrics and data collection system set-up at the study site are shown in Figure B-1.

The pilot study was conducted on March 15 and 16, 1987, with the first field study following on July 7 through 10, 1987. Four two-hour time periods were studied each day. These study periods were 7-9 A.M., 10 A.M.-12 noon, 1-3 P.M., and 4-6 P.M. Rain occurred on several of the data collection days; however, it only rained during one of the time periods that data were actually collected, the 1-3 P.M. period on July 7. The only effect of the rain on the data collection effort was the loss of some videotape data.

The data collection system for this study consisted of an electronic data collection system (signal timing, traffic counts, and platoon profiles), a manual data collection system (stopped delay, overflow delay, and travel time delay), and a videotape recording system (turning movements vehicle classification, and saturation flow rates). The data collected are summarized in Table B-1.

The traffic signals along NASA Road 1 were controlled by a computer operated by the Texas State Department of Highways and Public Transportation (SDHPT). These signals were capable of operating in either pretimed or semiactuated mode, and a variable phase sequence selection mode. For this study the controllers were set up to operate in the pretimed mode so that the effect on delay of different offsets (quality of progression) could be studied. A summary of the offsets evaluated, by day, is given in Table B-2.

Table B-3 is an example of the collected data after it had been summarized into 15-minute intervals. Table B-3 represents the data collected from the eastbound direction on July 7, 1987.

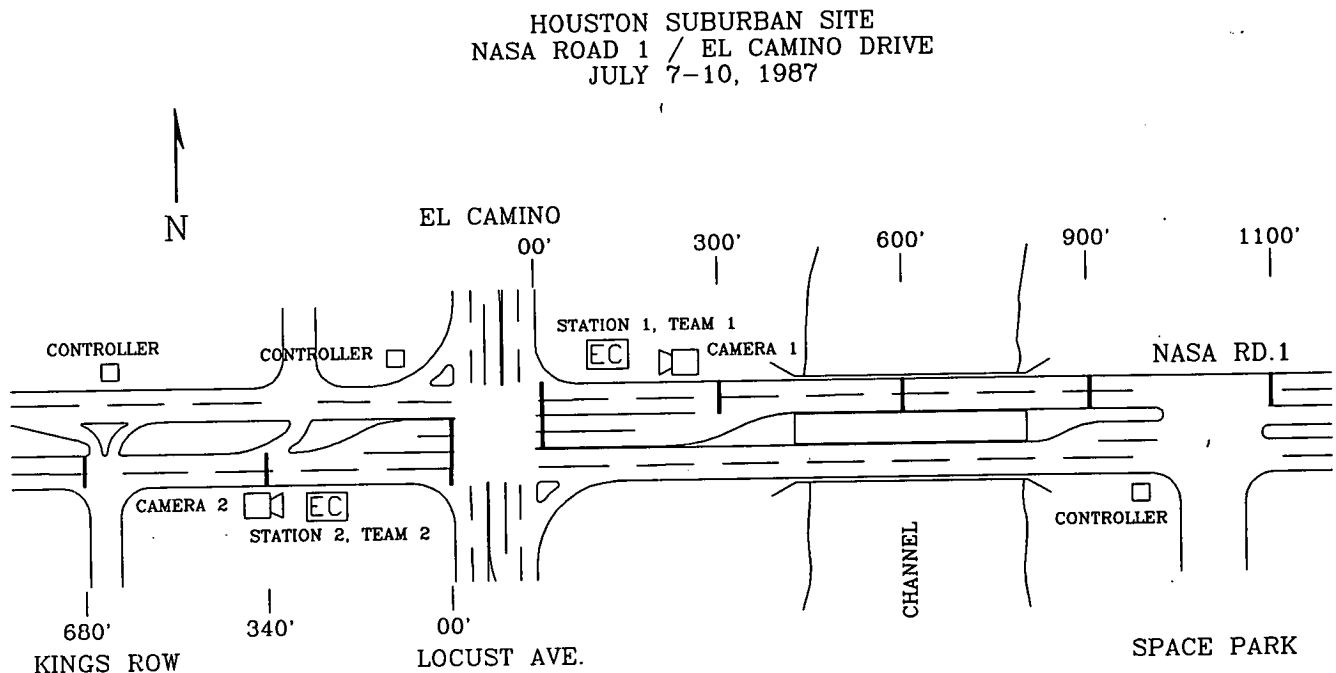


Figure B-1. Houston Suburban Site.

Table B-1. Summary of Data Collected at the Houston Suburban Site.

Day	Data Collected	7:00 - 9:00		10:00 - 12:00		1:00 - 3:00		4:00 - 6:00		TOTAL
		EB	WB	EB	WB	EB	WB	EB	WB	
Tuesday (7/7/87)	Cycles	68	76	100	100	80	80	65	66	635
	Queue Counts	480	480	480	480	480	480	480	480	3840
	Vehicles	2145	1388	1626	1721	1595	1970	1659	1907	14011
Wednesday (7/8/87)	Cycles	73	73	101	100	80	80	66	67	640
	Queue Counts	480	480	480	480	480	480	480	480	3840
	Vehicles	1851	1288	1683	1765	1885	2032	1445	1702	13651
Thursday (7/9/87)	Cycles	75	74	100	102	80	84	66	65	646
	Queue Counts	480	480	480	480	480	480	480	480	3840
	Vehicles	2240	1324	1613	1667	2192	1868	1841	2901	15646
Friday (7/10/87)	Cycles	74	74	101	100	81	80	66	66	642
	Queue Counts	480	480	480	480	480	480	480	480	3840
	Vehicles	2462	1347	1788	2237	1985	2278	1995	3264	17356
TOTAL	Cycles	290	297	402	402	321	324	263	264	2563
	Queue Counts	1920	1920	1920	1920	1920	1920	1920	1920	15360
	Vehicles	8698	5347	6710	7390	7657	8148	6940	9774	60664

Table B-2. Offsets Evaluated at the Houston Suburban Site.

DAY	AM PEAK 7:00-9:00	OFF PEAK 10:00-12:00	OFF PEAK 1:00-3:00	PM PEAK 4:00-6:00
Tuesday (7/7/89)	ORG 9 seconds	ORG 63 seconds	+16 seconds 25.9 seconds	-11 seconds 15.4 seconds
Wednesday (7/8/89)	ORG 9 seconds	+7 seconds 0 seconds	-6 seconds 3.9 seconds	ORG 26.4 seconds
Thursday (7/9/87)	-15 seconds 94 seconds	ORG 63 seconds	ORG 9.9 seconds	+11 seconds 37.4 seconds
Friday (7/10/87)	+15 seconds 24 seconds	-7 seconds 56 seconds	ORG 9.9 seconds	ORG 26.4 seconds

Table B-3. Data Collected at the Houston Suburban Site, Eastbound, July 7, 1987.

15-Minute Time Interval	G1/C (PTG)	Green Time 2	Cycle Length	G2/C (PTG)	Offset (sec.)	Volume on Green	Volume on Red	Total Volume	(PVG)	X-Ratio (QC/SG)	Platoon Ratio, Rp	Measured Delay	Uniform Delay	Incremental Delay	Predicted Delay	Dm - D2 D1
7:00-7:15	0.76	46	100	0.46	16	-	-	-	-	-	-	-	-	-	-	-
7:15-7:30	0.76	44	101	0.44	16	250	188	438	0.57	1.09	1.31	16.78	23.26	64.83	88.09	0.19
7:30-7:45	0.76	44	100	0.44	13	185	189	374	0.49	0.92	1.12	23.70	20.03	18.66	38.69	0.61
7:45-8:00	0.65	44	100	0.44	13	126	299	425	0.30	1.05	0.67	47.84	22.09	48.27	70.36	0.68
8:00-8:15	0.83	44	100	0.44	12	155	130	285	0.54	0.70	1.24	26.63	17.24	3.68	20.92	1.27
8:15-8:30	0.84	44	100	0.44	16	148	89	237	0.62	0.58	1.42	17.09	16.03	1.58	17.61	0.97
8:30-8:45	0.75	46	100	0.46	15	146	52	198	0.74	0.47	1.60	7.65	14.11	0.61	14.72	0.52
8:45-9:00	0.72	32	86	0.37	38	91	101	192	0.47	0.56	1.27	12.50	16.27	1.55	17.82	0.70
10:00-10:15	0.63	26	70	0.37	57	22	174	196	0.11	0.59	0.30	24.26	13.45	1.99	15.45	1.57
10:15-10:30	-	25	70	0.36	58	17	137	154	0.11	0.48	0.31	21.14	13.28	0.91	14.19	1.49
10:30-10:45	-	25	70	0.36	58	26	143	169	0.15	0.53	0.43	24.94	13.55	1.32	14.87	1.68
10:45-11:00	0.64	22	68	0.32	58	19	182	201	0.09	0.69	0.29	27.24	15.25	4.76	20.01	1.36
11:00-11:15	0.64	26	70	0.37	59	14	207	221	0.06	0.66	0.17	30.07	13.95	3.41	17.36	1.73
11:15-11:30	0.70	26	70	0.37	58	18	207	225	0.08	0.68	0.22	24.07	14.04	3.71	17.75	1.36
11:30-11:45	0.70	27	69	0.39	57	20	254	274	0.07	0.78	0.19	25.84	14.00	7.45	21.45	1.20
11:45-12:00	0.58	32	83	0.39	45	86	136	222	0.39	0.64	1.00	22.36	15.83	2.83	18.66	1.20
1:00-1:15	0.70	43	90	0.48	27	204	66	270	0.76	0.63	1.58	6.50	13.34	2.08	15.42	0.42
1:15-1:30	0.81	43	90	0.48	29	179	67	246	0.73	0.57	1.52	8.05	12.84	1.38	14.23	0.57
1:30-1:45	0.62	39	94	0.41	29	142	68	210	0.68	0.56	1.63	9.79	15.96	1.48	17.44	0.56
1:45-2:00	0.76	43	90	0.48	31	92	82	174	0.53	0.41	1.11	11.81	11.57	0.36	11.93	0.99
2:00-2:15	0.75	43	90	0.48	29	149	52	201	0.74	0.47	1.55	6.72	12.02	0.61	12.63	0.53
2:15-2:30	0.75	43	90	0.48	27	107	34	141	0.76	0.33	1.59	6.28	11.06	0.17	11.23	0.56
2:30-2:45	0.76	43	90	0.48	31	114	46	160	0.71	0.37	1.49	4.13	11.35	0.26	11.61	0.36
2:45-3:00	0.76	43	90	0.48	30	136	52	188	0.72	0.44	1.51	6.06	11.80	0.48	12.27	0.49
4:00-4:15	0.74	51	105	0.49	16	133	27	160	0.83	0.36	1.71	4.41	12.76	0.22	12.98	0.34
4:15-4:30	0.72	59	110	0.54	23	150	45	195	0.77	0.39	1.43	7.23	11.39	0.28	11.67	0.62
4:30-4:45	0.74	61	110	0.55	14	150	26	176	0.85	0.34	1.54	5.88	10.25	0.17	10.41	0.56
4:45-5:00	0.74	61	110	0.55	14	141	39	180	0.78	0.35	1.41	5.75	10.30	0.18	10.48	0.55
5:00-5:15	0.74	61	110	0.55	13	164	42	206	0.80	0.40	1.44	7.28	10.67	0.29	10.97	0.66
5:15-5:30	0.74	61	110	0.55	14	177	43	220	0.80	0.43	1.45	5.80	10.89	0.37	11.26	0.52
5:30-5:45	0.74	61	110	0.55	14	208	49	257	0.81	0.50	1.46	6.42	11.49	0.67	12.17	0.53
5:45-6:00	0.72	61	112	0.54	14	204	41	245	0.83	0.49	1.53	4.84	12.01	0.61	12.62	0.38

HOUSTON URBAN SITE

The first urban arterial study was conducted on two segments of Richmond Avenue, an urban arterial running east and west in Houston, Texas. Richmond Avenue is a six-lane, divided arterial with separate left-turn lanes on both approaches to the controlling intersection, Hillcroft Avenue. Hillcroft is a six-lane, divided arterial with separate left-turn lanes on both approaches to Richmond Avenue. The secondary intersections to the east and west of Hillcroft were Unity Drive and Stoneybrook Drive, respectively. Unity Drive intersection was four-legged with a two-lane, undivided cross-section. Stoneybrook Drive was a skewed, four-legged intersection with a four-lane, divided cross-section. The geometrics and data collection system set-up at this study site are shown in Figure B-2.

The Houston urban study was conducted from August 3 through 6, 1987. Four two-hour time periods were studied each day. These study periods were 7-9 A.M., 10 A.M.-12 noon, 1-3 P.M., and 4-6 P.M. The data collection system for this study consisted of an electronic data collection system (signal timing,

traffic counts, and platoon profiles), a manual data collection system (stopped delay, overflow delay, and travel time delay), and a videotape recording system (turning movements, vehicle classification, and saturation flow rates). The data collected are summarized in Table B-4.

The traffic signals along Richmond Avenue were controlled by three-dial, fixed-time controllers operated by the City of Houston's Department of Transportation. City of Houston personnel manually changed the offsets for each two-hour time block so that the effect on delay of quality of progression could be studied. A summary of the offsets evaluated, by day, is given in Table B-5.

Tables B-6 and B-7 are examples of the collected data after it had been summarized into 15-minute intervals. Table B-6 represents data collected from the eastbound direction on August 3, 1987, and Table B-7 represents data collected from the westbound direction on the same day.

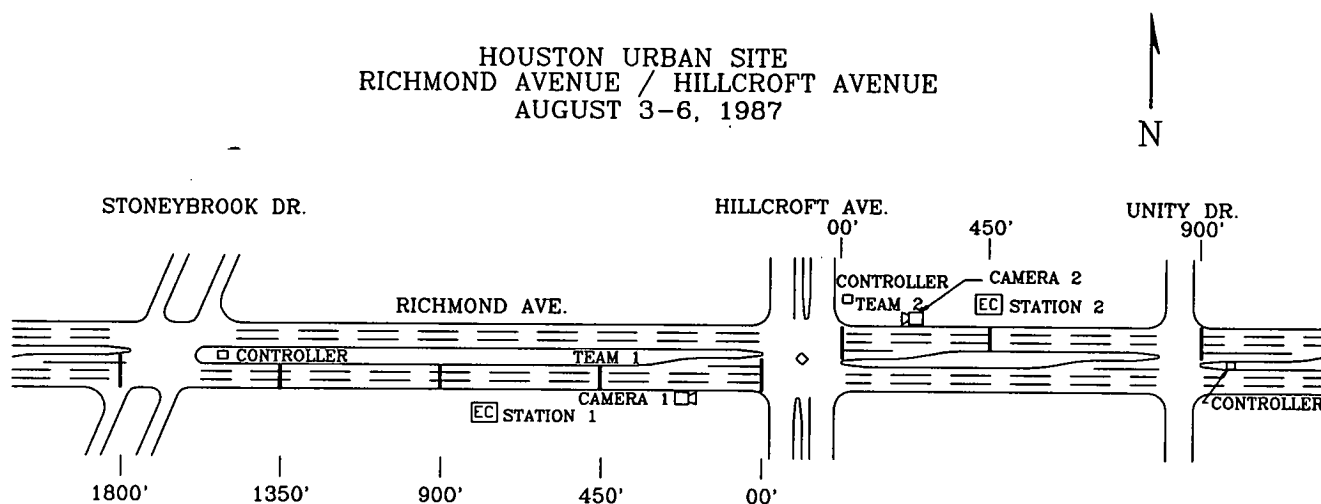


Figure B-2. Houston Urban Site.

Table B-4. Summary of Data Collected at the Houston Urban Site.

Day	Data Collected	7:00 - 9:00		10:00 - 12:00		1:00 - 3:00		4:00 - 6:00		TOTAL
		EB	WB	EB	WB	EB	WB	EB	WB	
Monday (8/3/87)	Cycles	72	72	103	103	103	100	72	72	697
	Queue Counts	480	480	480	480	480	480	480	480	3840
	Vehicles	2832	641	1108	1717	1222	1054	1520	2414	12508
Tuesday (8/4/87)	Cycles	72	75	94	90	103	103	70	71	678
	Queue Counts	480	480	480	480	480	480	480	480	3840
	Vehicles	3200	803	1543	719	1020	1361	1117	3133	12896
Wednesday (8/5/87)	Cycles	72	72	100	103	103	104	72	70	696
	Queue Counts	480	480	480	480	480	480	480	480	3840
	Vehicles	2483	761	872	1100	1484	1521	1675	2757	12653
Thursday (8/6/87)	Cycles	72	72	103	99	102	104	71	72	695
	Queue Counts	480	480	480	480	480	480	480	480	3840
	Vehicles	2640	748	1381	1004	1399	1472	1630	3139	13413
TOTAL	Cycles	288	291	400	395	411	411	285	285	2766
	Queue Counts	1920	1920	1920	1920	1920	1920	1920	1920	15360
	Vehicles	11155	2953	4904	4540	5125	5408	5942	11443	51470

Table B-5. Offsets Evaluated at the Houston Urban Site.

DAY	AM PEAK 7:00-9:00	OFF PEAK 10:00-12:00	OFF PEAK 1:00-3:00	PM PEAK 4:00-6:00
Monday (8/3/87)	-2 seconds 63 seconds	+6 seconds 53.6 seconds	+6 seconds 53.6 seconds	-5 seconds 75 seconds
Tuesday (8/4/87)	ORG 65 seconds	ORG 47.6 seconds	ORG 47.6 seconds	ORG 80 seconds
Wednesday (8/5/87)	ORG 65 seconds	ORG 47.6 seconds	ORG 47.6 seconds	ORG 80 seconds
Thursday (8/6/87)	+20 seconds 85 seconds	-2.1 seconds 45.5 seconds	-2.1 seconds 45.5 seconds	+5 seconds 85 seconds

Table B-6. Data Collected at the Houston Urban Site, Eastbound, August 3, 1987.

15-Minute Time Interval	G1/C (PTG)	Green Time 2	Cycle Length	G2/C (PTG)	Offset (sec.)	Volume on Green	Volume on Red	Total Volume	(PVG)	X-Ratio (QC/SG)	Platoon Ratio, Rp	Measured Delay	Uniform Delay	Incremental Delay	Predicted Delay	Dm - D2 D1
7:00-7:15	0.69	60	100	0.60	38	260	21	317	0.92	0.37	1.54	1.39	7.83	0.13	7.97	0.17
7:15-7:30	0.69	60	100	0.60	38	440	14	399	0.96	0.47	1.61	0.66	8.46	0.31	8.78	0.09
7:30-7:45	0.69	60	100	0.60	38	468	34	520	0.93	0.61	1.56	1.52	9.60	0.94	10.55	0.14
7:45-8:00	0.69	60	100	0.60	38	470	30	500	0.94	0.59	1.57	0.84	9.40	0.79	10.19	0.08
8:00-8:15	0.69	60	100	0.60	38	345	26	371	0.93	0.44	1.55	1.05	8.24	0.24	8.47	0.12
8:15-8:30	0.69	60	100	0.60	38	293	20	313	0.94	0.37	1.56	1.82	7.80	0.13	7.93	0.23
8:30-8:45	0.69	62	100	0.62	38	229	7	236	0.97	0.27	1.57	1.84	6.58	0.04	6.63	0.28
8:45-9:00	0.69	62	100	0.62	38	195	17	212	0.92	0.24	1.48	2.05	6.45	0.03	6.48	0.32
10:00-10:15	0.51	17	70	0.24	34	93	61	111	0.65	0.34	2.67	20.35	16.63	0.26	16.89	1.46
10:15-10:30	0.51	17	70	0.24	34	112	71	119	0.60	0.37	2.46	23.31	16.74	0.33	17.07	1.38
10:30-10:45	0.51	17	70	0.24	34	150	70	160	0.70	0.49	2.88	20.11	17.33	1.00	18.32	0.99
10:45-11:00	0.51	17	70	0.24	34	122	59	196	0.82	0.61	3.36	18.39	17.88	2.29	20.17	0.56
11:00-11:15	0.51	17	70	0.24	34	88	69	157	0.55	0.48	2.28	12.80	17.28	0.92	18.21	0.69
11:15-11:30	0.51	17	70	0.24	34	97	83	128	0.55	0.40	2.25	16.17	16.87	0.43	17.30	0.89
11:30-11:45	0.51	17	70	0.24	34	137	70	143	0.66	0.44	2.74	7.61	17.08	0.65	17.73	0.66
11:45-12:00	0.51	17	70	0.24	34	95	58	99	0.64	0.31	2.62	11.67	16.47	0.17	16.65	1.08
1:00-1:15	0.51	17	70	0.24	34	101	78	171	0.58	0.52	2.41	17.43	17.45	1.20	18.65	0.97
1:15-1:30	0.51	17	70	0.24	34	85	47	141	0.65	0.43	2.66	18.64	17.02	0.57	17.59	1.06
1:30-1:45	0.51	17	70	0.24	34	94	74	166	0.56	0.50	2.31	14.29	17.38	1.07	18.44	0.77
1:45-2:00	0.51	17	70	0.24	34	85	68	151	0.56	0.46	2.29	16.67	17.16	0.74	17.90	0.93
2:00-2:15	0.51	17	70	0.24	34	87	69	154	0.56	0.47	2.30	11.25	17.20	0.80	18.00	0.62
2:15-2:30	0.51	17	70	0.24	34	99	51	148	0.66	0.45	2.73	11.80	17.12	0.68	17.80	0.66
2:30-2:45	0.51	17	70	0.24	34	105	39	143	0.73	0.43	2.99	9.06	17.05	0.60	17.65	0.51
2:45-3:00	0.51	17	70	0.24	34	98	49	145	0.67	0.44	2.75	13.57	17.08	0.63	17.71	0.76
4:00-4:15	0.71	48	119	0.40	63	65	128	144	0.32	0.26	0.79	18.96	17.96	0.06	18.01	1.01
4:15-4:30	0.71	38	100	0.38	63	72	146	150	0.44	0.28	1.16	11.22	16.37	0.08	16.46	0.64
4:30-4:45	0.71	38	100	0.38	63	81	140	221	0.62	0.42	1.63	8.55	17.37	0.33	17.69	0.38
4:45-5:00	0.71	38	100	0.38	63	94	207	200	0.37	0.38	0.97	7.43	17.06	0.23	17.29	0.58
5:00-5:15	0.71	38	100	0.38	63	134	159	221	0.49	0.42	1.29	6.14	17.37	0.33	17.69	0.51
5:15-5:30	0.71	38	100	0.38	63	128	142	190	0.53	0.36	1.39	4.83	16.92	0.19	17.11	0.40
5:30-5:45	0.71	38	100	0.38	63	158	179	217	0.52	0.41	1.37	5.25	17.31	0.30	17.61	0.46
5:45-6:00	0.71	38	100	0.38	63	146	153	188	0.45	0.36	1.18	4.72	16.89	0.18	17.07	0.44

Table B-7. Data Collected at the Houston Urban Site, Westbound, August 3, 1987.

15-Minute Time Interval	G1/C (PTG)	Green Time 2	Cycle Length	G2/C (PTG)	Offset (sec.)	Volume on Green	Volume on Red	Total Volume	(PVG)	X-Ratio (QC/SG)	Platoon Ratio, Rp	Measured Delay	Uniform Delay	Incremental Delay	Predicted Delay	Dm - D2 D1
7:00-7:15	0.77	43	100	0.43	93	28	16	44	0.64	0.07	1.48	14.32	12.74	0.00	12.74	1.12
7:15-7:30	0.77	43	100	0.43	93	24	22	46	0.52	0.07	1.21	17.61	12.75	0.00	12.76	1.38
7:30-7:45	0.77	43	100	0.43	93	39	45	84	0.46	0.14	1.08	20.18	13.11	0.01	13.12	1.54
7:45-8:00	0.77	43	100	0.43	93	44	53	97	0.45	0.16	1.05	15.93	13.24	0.01	13.25	1.20
8:00-8:15	0.77	43	100	0.43	93	52	36	88	0.59	0.14	1.37	13.98	13.15	0.01	13.16	1.06
8:15-8:30	0.77	43	100	0.43	93	52	36	88	0.59	0.14	1.37	14.66	13.15	0.01	13.16	1.11
8:30-8:45	0.77	43	100	0.43	93	58	44	102	0.57	0.16	1.32	16.03	13.29	0.01	13.30	1.21
8:45-9:00	0.77	43	100	0.43	93	58	34	92	0.63	0.15	1.47	9.95	13.19	0.01	13.20	0.75
10:00-10:15	0.69	17	70	0.24	30	93	51	144	0.65	0.44	2.66	9.27	17.08	0.64	17.71	0.52
10:15-10:30	0.69	17	70	0.24	30	77	34	111	0.69	0.34	2.86	8.51	16.62	0.25	16.87	0.50
10:30-10:45	0.69	17	70	0.24	30	68	37	105	0.65	0.32	2.67	7.57	16.54	0.21	16.74	0.45
10:45-11:00	0.69	17	70	0.24	30	84	45	129	0.65	0.39	2.68	8.84	16.87	0.42	17.29	0.51
11:00-11:15	0.69	17	70	0.24	30	90	37	127	0.71	0.39	2.92	7.56	16.84	0.40	17.24	0.44
11:15-11:30	0.69	17	70	0.24	30	104	50	154	0.68	0.47	2.78	9.84	17.22	0.82	18.04	0.55
11:30-11:45	0.69	17	70	0.24	30	87	60	147	0.59	0.45	2.44	5.94	17.12	0.69	17.81	0.33
11:45-12:00	0.69	17	70	0.24	30	113	57	170	0.66	0.52	2.74	6.88	17.45	1.21	18.66	0.37
1:00-1:15	0.69	17	70	0.24	30	155	72	227	0.68	0.68	2.81	3.44	18.27	3.85	22.12	0.16
1:15-1:30	0.69	17	70	0.24	30	126	67	193	0.65	0.58	2.69	3.42	17.75	1.85	19.60	0.17
1:30-1:45	0.69	17	70	0.24	30	145	86	231	0.63	0.69	2.58	5.52	18.34	4.18	22.82	0.25
1:45-2:00	0.69	17	70	0.24	30	150	72	222	0.68	0.67	2.78	5.20	18.19	3.46	21.65	0.24
2:00-2:15	0.69	17	70	0.24	30	153	61	214	0.71	0.64	2.94	4.98	18.07	2.92	20.99	0.24
2:15-2:30	0.69	17	70	0.24	30	96	24	120	0.80	0.36	3.29	5.75	16.71	0.30	17.01	0.34
2:30-2:45	0.69	17	70	0.24	30	81	38	119	0.68	0.36	2.80	7.31	16.70	0.29	16.99	0.43
2:45-3:00	0.69	17	70	0.24	30	90	21	111	0.81	0.33	3.34	7.30	16.59	0.23	16.82	0.43
4:00-4:15	0.70	56	100	0.36	10	161	61	222	0.73	0.43	2.02	6.55	28.85	0.38	29.23	0.22
4:15-4:30	0.70	56	100	0.36	10	205	51	256	0.80	0.50	2.23	6.09	29.98	0.66	30.35	0.20
4:30-4:45	0.70	56	100	0.36	10	212	56	268	0.79	0.52	2.20	6.16	29.99	0.80	30.79	0.20
4:45-5:00	0.70	56	100	0.36	10	248	80	328	0.76	0.64	2.11	8.28	31.63	1.90	33.53	0.25
5:00-5:15	0.70	56	100	0.36	10	242	99	341	0.71	0.67	1.98	8.97	32.01	2.28	34.29	0.26
5:15-5:30	0.70	56	100	0.36	10	199	177	376	0.53	0.73	1.47	15.00	33.07	3.74	36.81	0.41
5:30-5:45	0.68	56	100	0.36	10	162	156	318	0.51	0.62	1.42	13.21	31.34	1.65	32.99	0.40
5:45-6:00	0.62	56	100	0.56	10	247	103	350	0.71	0.44	1.26	8.23	9.75	0.26	10.00	0.82

LOS ANGELES URBAN SITE

The second urban arterial study was conducted on two segments of Normandie Avenue, a major urban arterial running north and south in Los Angeles, California. Normandie Avenue is a four-lane arterial with a continuous two-way left-turn lane. The controlling intersection for this site, Jefferson Boulevard, is also a four-lane arterial with a continuous two-way left-turn lane. The secondary intersections to the north and south of Jefferson were 29th Street and 36th Street, respectively. Both secondary intersections were four-legged with two-lane, undivided cross-sections on the cross streets. The geometrics and data collection system set-up at the study site are shown in Figure B-3.

The Los Angeles urban study was conducted from August 18 through 21, 1987. Four two-hour time periods were studied each day. These study periods were 7-9 A.M., 10 A.M.-12 noon, 1-3 P.M., and 4-6 P.M. On August 20 only three time periods were studied (7-9 A.M., 12:30-3:30 P.M., and 4-6 P.M.). The data collection system for this study consisted of an electronic data collection system (signal timing, traffic counts, and platoon profiles), a manual data collection system (stopped delay, overflow

delay, and travel time delay), and a videotape recording system (turning movements, vehicle classification, and saturation flow rates). The data collected are summarized in Table B-8.

The traffic signals along Normandie Avenue were controlled by computers at the City of Los Angeles' Automated Traffic Surveillance and Control (ATSAC) Center. Thus, signal timing modifications could be made by department personnel at the control center. The signals could be operated in both the pretimed and semiactuated mode, and critical intersection control was an option at the intersection of Normandie and Jefferson. For this study, however, the system was set for pretimed operation. A summary of the offsets evaluated, by day, is given in Table B-9.

Tables B-10 and B-11 are examples of the collected data after it had been summarized into 15-minute intervals. Table B-10 represents data collected from the northbound direction on August 18, 1987, and Table B-11 represents data collected from the southbound direction on the same day.

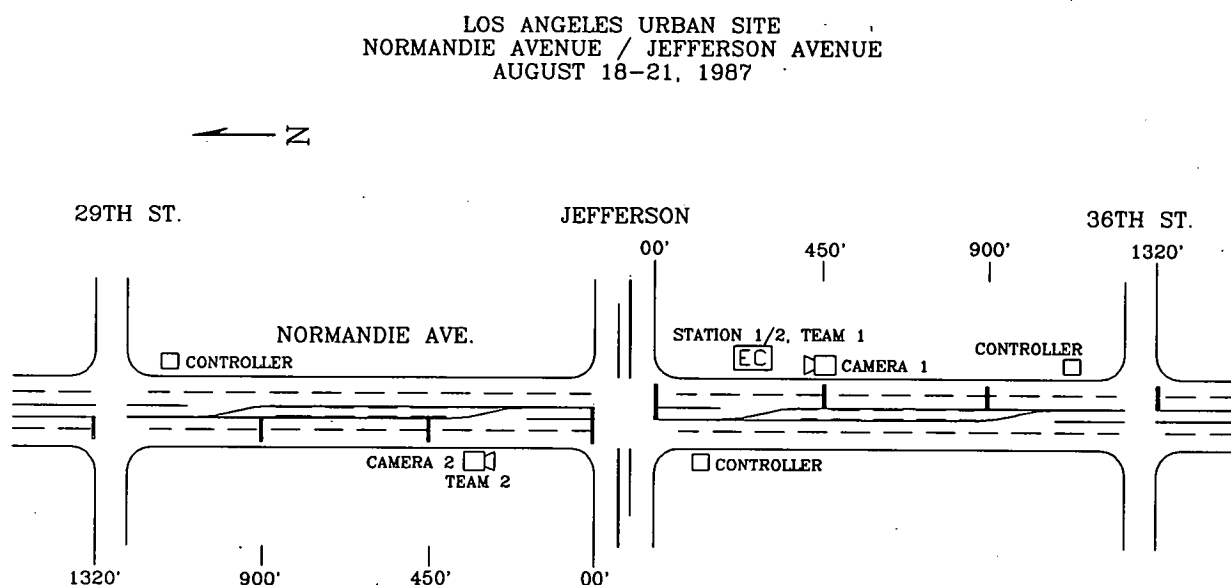


Figure B-3. Los Angeles Urban Site.

Table B-8. Summary of Data Collected at the Los Angeles Urban Site.

Day	Data Collected	7:00 - 9:00		10:00 - 12:00		1:00 - 3:00		4:00 - 6:00		TOTAL
		NB	SB	NB	SB	NB	SB	NB	SB	
Tuesday (8/18/87)	Cycles	120	120	120	120	120	120	120	120	960
	Queue Counts	480	480	480	480	480	480	480	480	3840
	Vehicles	2117	1116	1109	940	1254	1146	1763	1885	11330
Wednesday (8/19/87)	Cycles	120	120	120	120	120	120	120	120	960
	Queue Counts	480	480	480	480	480	480	480	480	3840
	Vehicles	2130	983	1086	946	1250	1147	1611	2355	11508
Thursday (8/20/87)	Cycles	120	120	-	-	180	180	120	120	840
	Queue Counts	480	480	-	-	720	720	480	480	3360
	Vehicles	1977	906	-	-	1775	1809	1535	2590	10592
Friday (8/21/87)	Cycles	120	120	120	120	120	120	120	120	960
	Queue Counts	480	480	480	480	480	480	480	480	3840
	Vehicles	1952	979	1093	958	1318	1426	1737	2455	11918
TOTAL	Cycles	480	480	360	360	540	540	480	480	3720
	Queue Counts	1920	1920	1440	1440	2160	2160	1920	1920	14880
	Vehicles	8176	3984	3288	2844	5597	5528	6646	9285	45348

Table B-9. Offsets Evaluated at the Los Angeles Urban Site.

DAY	AM PEAK 7:00-9:00	OFF PEAK 10:00-12:00	OFF PEAK 1:00-3:00	PM PEAK 4:00-6:00
Tuesday (8/18/87)	ORG 24 seconds	ORG 36 seconds	ORG 36 seconds	-3 seconds 34 seconds
Wednesday (8/19/87)	ORG 24 seconds	+5 seconds 41 seconds	+5 seconds 41 seconds	+3 seconds 40 seconds
Thursday (8/20/87)	-3 seconds 21 seconds	ORG 36 seconds	ORG 36 seconds	ORG 37 seconds
Friday (8/21/87)	+6 seconds 30 seconds	-5 seconds 31 seconds	-5 seconds 31 seconds	ORG 37 seconds

Table B-10. Data Collected at the Los Angeles Urban Site, Northbound, August 18, 1987.

15-Minute Time Interval	G1/C (PTG)	Green Time 2	Cycle Length	G2/C (PTG)	Offset (sec.)	Volume on Green	Volume on Red	Total Volume	(PVG)	X-Ratio (QC/SG)	Platoon Ratio, Rp	Measured Delay	Uniform Delay	Incremental Delay	Predicted Delay	Dm - D2 D1
7:00-7:15	0.72	35	60	0.58	48	214	68	282	0.76	0.54	1.30	4.47	5.77	0.87	6.63	0.62
7:15-7:30	0.70	35	60	0.58	46	243	91	334	0.73	0.64	1.25	4.90	6.30	1.81	8.10	0.49
7:30-7:45	0.70	35	60	0.58	42	241	72	313	0.77	0.60	1.32	4.55	6.07	1.35	7.42	0.53
7:45-8:00	0.74	35	60	0.58	42	217	71	288	0.75	0.55	1.29	4.53	5.82	0.95	6.77	0.62
8:00-8:15	0.71	35	60	0.58	46	210	73	283	0.74	0.54	1.27	4.98	5.78	0.88	6.66	0.71
8:15-8:30	0.69	35	60	0.58	44	187	52	239	0.78	0.46	1.34	4.33	5.39	0.45	5.84	0.72
8:30-8:45	0.82	35	60	0.58	45	159	44	203	0.78	0.39	1.34	4.36	5.11	0.25	5.36	0.80
8:45-9:00	0.74	26	60	0.43	47	84	91	175	0.48	0.45	1.11	6.50	9.09	0.57	9.66	0.65
10:00-10:15	0.75	25	60	0.42	46	77	62	139	0.55	0.41	1.33	4.95	9.38	0.49	9.87	0.48
10:15-10:30	0.75	25	60	0.42	43	70	75	145	0.48	0.43	1.16	5.77	9.46	0.58	10.04	0.55
10:30-10:45	0.71	25	60	0.42	44	71	77	148	0.48	0.44	1.15	6.11	9.51	0.62	10.13	0.58
10:45-11:00	0.72	25	60	0.42	38	69	73	142	0.49	0.42	1.17	5.32	9.42	0.53	9.95	0.51
11:00-11:15	0.65	25	60	0.42	42	82	56	138	0.59	0.41	1.43	3.42	9.36	0.48	9.85	0.31
11:15-11:30	0.69	25	60	0.42	42	86	56	142	0.61	0.42	1.45	4.94	9.42	0.53	9.95	0.47
11:30-11:45	0.65	25	60	0.42	37	65	53	118	0.55	0.35	1.32	6.98	9.09	0.27	9.37	0.74
11:45-12:00	0.74	25	60	0.42	40	76	61	137	0.55	0.41	1.33	6.89	9.35	0.47	9.82	0.69
1:00-1:15	0.77	25	60	0.42	47	96	68	164	0.59	0.49	1.40	5.93	9.75	0.93	10.68	0.51
1:15-1:30	0.74	25	60	0.42	44	78	78	156	0.50	0.47	1.20	6.75	9.63	0.77	10.40	0.62
1:30-1:45	0.68	25	60	0.42	43	104	50	154	0.68	0.46	1.62	5.26	9.60	0.73	10.33	0.47
1:45-2:00	0.68	25	60	0.42	41	79	68	147	0.54	0.44	1.29	5.69	9.50	0.61	10.11	0.53
2:00-2:15	0.67	25	60	0.42	43	101	54	155	0.65	0.46	1.56	4.79	9.61	0.75	10.36	0.42
2:15-2:30	0.66	25	60	0.42	45	117	45	162	0.72	0.48	1.73	4.58	9.72	0.89	10.61	0.38
2:30-2:45	0.66	25	60	0.42	43	92	72	164	0.56	0.49	1.35	7.98	9.75	0.93	10.68	0.72
2:45-3:00	0.67	25	60	0.42	45	67	85	152	0.44	0.45	1.06	6.66	9.57	0.70	10.27	0.62
4:00-4:15	0.67	28	60	0.47	41	125	88	213	0.59	0.51	1.26	7.01	8.50	0.86	9.36	0.72
4:15-4:30	0.67	28	60	0.47	42	118	83	201	0.59	0.48	1.26	6.18	8.35	0.68	9.03	0.66
4:30-4:45	0.67	28	60	0.47	35	139	93	232	0.60	0.55	1.28	6.13	8.74	1.21	9.95	0.56
4:45-5:00	0.58	28	60	0.47	41	111	85	196	0.57	0.47	1.21	5.69	8.29	0.62	8.91	0.61
5:00-5:15	0.60	28	60	0.47	36	134	83	217	0.62	0.52	1.32	5.81	8.55	0.92	9.47	0.57
5:15-5:30	0.55	28	60	0.47	38	158	99	257	0.61	0.61	1.32	6.23	9.08	1.88	10.96	0.48
5:30-5:45	0.68	28	60	0.47	40	131	92	223	0.59	0.53	1.26	5.33	8.62	1.03	9.65	0.50
5:45-6:00	0.63	28	60	0.47	42	133	91	224	0.59	0.53	1.27	5.06	8.64	1.05	9.69	0.46

Table B-11. Data Collected at the Los Angeles Urban Site, Southbound, August 18, 1987.

15-Minute Time Interval	G1/C (PTG)	Green Time 2	Cycle Length	G2/C (PTG)	Offset (sec.)	Volume on Green	Volume on Red	Total Volume	(PVG)	X-Ratio (QC/SG)	Platoon Ratio, Rp	Measured Delay	Uniform Delay	Incremental Delay	Predicted Delay	Dm - D2 D1
7:00-7:15	0.75	35	60	0.58	27	110	8	118	0.93	0.22	1.60	1.02	4.55	0.04	4.59	0.22
7:15-7:30	0.76	35	60	0.58	23	143	7	150	0.95	0.28	1.63	0.80	4.75	0.08	4.83	0.15
7:30-7:45	0.77	35	60	0.58	23	126	18	144	0.88	0.27	1.50	1.56	4.71	0.07	4.78	0.32
7:45-8:00	0.78	35	60	0.58	23	110	16	126	0.87	0.24	1.50	3.09	4.60	0.05	4.65	0.66
8:00-8:15	0.82	35	60	0.58	25	127	6	133	0.95	0.25	1.64	0.45	4.64	0.06	4.70	0.08
8:15-8:30	0.82	35	60	0.58	25	125	12	137	0.91	0.26	1.56	1.42	4.67	0.06	4.73	0.29
8:30-8:45	0.71	35	60	0.58	26	110	8	118	0.93	0.22	1.60	1.02	4.55	0.04	4.59	0.22
8:45-9:00	0.82	26	60	0.43	24	30	51	81	0.37	0.21	0.85	3.52	8.04	0.04	8.08	0.43
10:00-10:15	0.79	25	60	0.42	48	61	36	97	0.63	0.29	1.51	3.71	8.83	0.15	8.98	0.40
10:15-10:30	0.80	25	60	0.42	47	53	44	97	0.55	0.29	1.31	3.40	8.83	0.15	8.98	0.37
10:30-10:45	0.80	25	60	0.42	48	78	42	120	0.65	0.36	1.56	2.75	9.13	0.30	9.44	0.27
10:45-11:00	0.25	25	60	0.42	48	71	33	104	0.68	0.31	1.64	3.89	8.92	0.18	9.11	0.42
11:00-11:15	0.67	25	60	0.42	47	79	42	121	0.65	0.36	1.57	3.84	9.15	0.31	9.46	0.39
11:15-11:30	0.77	25	60	0.42	48	72	31	103	0.70	0.31	1.68	3.35	8.91	0.18	9.09	0.36
11:30-11:45	0.80	25	60	0.42	48	99	58	157	0.63	0.47	1.51	2.39	9.66	0.82	10.48	0.16
11:45-12:00	0.84	25	60	0.42	48	89	60	149	0.60	0.45	1.43	3.83	9.54	0.67	10.21	0.33
1:00-1:15	0.77	25	60	0.42	48	85	44	129	0.66	0.39	1.58	7.91	9.26	0.39	9.65	0.81
1:15-1:30	0.77	25	60	0.42	48	85	34	119	0.71	0.36	1.71	6.81	9.12	0.30	9.42	0.71
1:30-1:45	0.77	25	60	0.42	48	117	34	151	0.77	0.45	1.86	5.26	9.57	0.71	10.28	0.48
1:45-2:00	0.77	25	60	0.42	48	106	29	135	0.79	0.41	1.88	3.33	9.34	0.47	9.81	0.31
2:00-2:15	0.79	25	60	0.42	48	116	32	148	0.78	0.45	1.88	6.59	9.53	0.65	10.18	0.62
2:15-2:30	0.73	25	60	0.42	47	97	42	139	0.70	0.42	1.67	6.48	9.40	0.52	9.92	0.63
2:30-2:45	0.74	25	60	0.42	47	121	39	160	0.76	0.48	1.82	5.63	9.71	0.88	10.59	0.49
2:45-3:00	0.80	25	60	0.42	48	114	51	165	0.69	0.50	1.66	7.82	9.78	0.99	10.78	0.70
4:00-4:15	0.78	28	60	0.47	45	169	80	249	0.68	0.59	1.45	4.55	8.94	1.56	10.50	0.33
4:15-4:30	0.77	28	60	0.47	44	130	96	226	0.58	0.53	1.23	6.37	8.64	1.04	9.68	0.62
4:30-4:45	0.74	28	60	0.47	45	134	104	238	0.56	0.56	1.21	4.24	8.79	1.29	10.08	0.34
4:45-5:00	0.79	28	60	0.47	40	128	120	248	0.52	0.59	1.11	6.90	8.92	1.54	10.46	0.60
5:00-5:15	0.75	28	60	0.47	41	121	107	228	0.53	0.54	1.14	6.08	8.66	1.08	9.74	0.58
5:15-5:30	0.66	28	60	0.47	39	159	100	259	0.61	0.61	1.32	8.88	9.08	1.86	10.93	0.77
5:30-5:45	0.75	28	60	0.47	43	126	99	225	0.56	0.53	1.20	7.92	8.62	1.02	9.65	0.80
5:45-6:00	0.76	28	60	0.47	42	108	104	212	0.51	0.50	1.09	6.03	8.46	0.81	9.27	0.62

LOS ANGELES SUBURBAN SITE

The second suburban arterial study and the semiactuated study were conducted on two segments of Azusa Avenue, a major arterial running north and south in Covina, California. Azusa Avenue is a four-lane, divided arterial with separate left-turn lanes on both approaches to the controlling intersection, San Bernardino Road. San Bernardino is also a four-lane, divided arterial with separate left-turn lanes on both approaches to Azusa. The secondary intersections to the north and south of San Bernardino were Cypress Street and Badillo Street, respectively. The Cypress Street intersection was four-legged with separate left-turn lanes and a four-lane, undivided cross-section. Badillo Street was a four-legged intersection with separate left-turn lanes and a four-lane, divided cross-section. The geometrics and data collection system set-up at this study site are shown in Figure B-4.

The Los Angeles pretimed suburban study was conducted from August 24 through 27, 1987, with the semiactuated study following on August 28, 1987. Four two-hour time periods were studied each day. These study periods were 7-9 A.M., 10 A.M.-12 noon, 1-3 P.M., and 4-6 P.M. The data collection system for this study consisted of an electronic data collection system (signal timing, traffic counts, and platoon profiles), a manual data system (stopped delay, overflow delay, and travel time delay), and a

videotape recording system (turning movements, vehicle classification, and saturation flow rates). The data collected are summarized in Table B-12.

The traffic signals along Azusa Avenue were controlled by Type 170 Controllers operated by the California Department of Transportation (DOT). These signals were operated in a fixed-time mode for four days (August 24 to 27) and a semiactuated mode on the fifth day (August 28). DOT personnel manually changed the offsets for each two-hour time block so that the effects on delay of quality of progression could be studied. A summary of the offsets evaluated, by day, is given in Table B-13.

Tables B-14 and B-15 are examples of the collected data after it had been summarized into 15-minute intervals. Table B-14 represents data collected from the northbound direction on August 26, 1987, and Table B-15 represents data collected from the southbound direction on the same day. Tables B-16 and B-17 give examples of the semiactuated data collected from both directions on August 28, 1987. In addition, Table B-18 gives an example of a portion of the cycle-by-cycle data collected for the northbound direction on August 26, 1987.

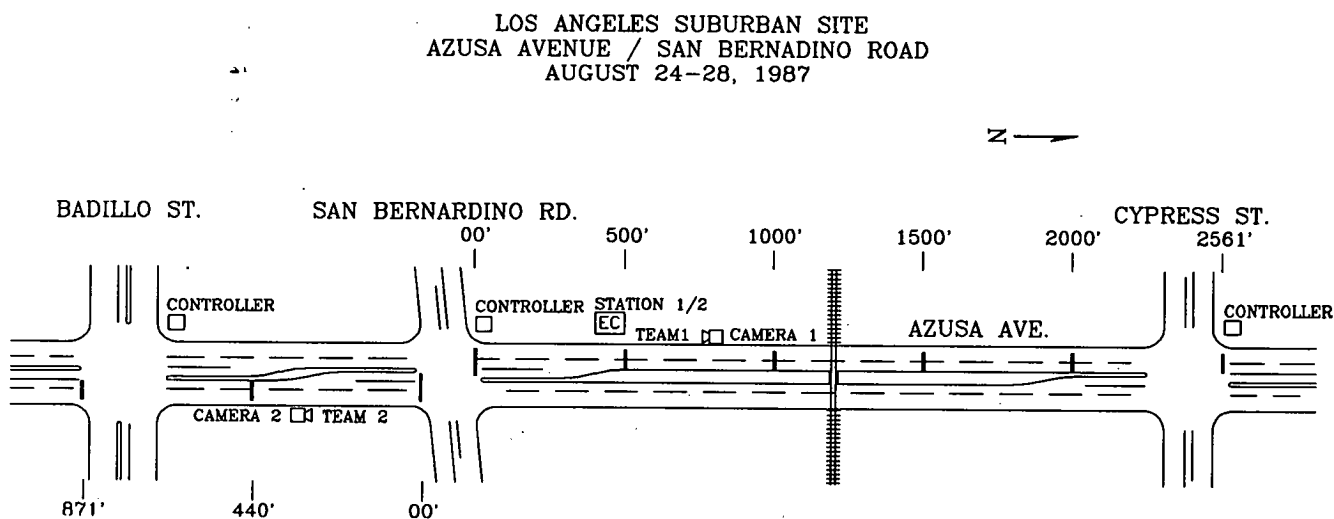


Figure B-4. Los Angeles Suburban Site.

Table B-12. Summary of Data Collected at the Los Angeles Suburban Site.

Day	Data Collected	7:00 - 9:00		10:00 - 12:00		1:00 - 3:00		4:00 - 6:00		TOTAL
		NB	SB	NB	SB	NB	SB	NB	SB	
Monday (8/24/87)	Cycles	80	80	85	85	85	85	73	72	645
	Queue Counts	480	480	480	480	480	480	480	480	3840
	Vehicles	1338	1173	1468	1370	1666	1619	2049	2106	12789
Tuesday (8/25/87)	Cycles	80	80	85	86	85	86	73	73	648
	Queue Counts	480	480	480	480	480	480	480	480	3840
	Vehicles	1456	1160	1397	1358	1628	1605	1986	2013	12603
Wednesday (8/26/87)	Cycles	80	82	86	85	85	85	72	72	647
	Queue Counts	480	480	480	480	480	480	480	480	3840
	Vehicles	1456	1165	1493	1405	1652	1588	1984	2039	12782
Thursday (8/27/87)	Cycles	80	80	85	85	86	85	72	73	646
	Queue Counts	480	480	480	480	480	480	480	480	3840
	Vehicles	1331	1145	1562	1448	1585	1596	2098	2035	12800
Friday (8/28/87)	Cycles	80	80	85	86	85	85	72	72	645
	Queue Counts	480	480	480	480	480	480	480	480	3840
	Vehicles	1442	1221	1618	1540	1858	1794	2185	2119	13777
TOTAL	Cycles	400	402	426	427	426	426	362	362	3231
	Queue Counts	2400	2400	2400	2400	2400	2400	2400	2400	19200
	Vehicles	7023	5864	7538	7121	8389	8202	10302	10312	64751

Table B-13. Offsets Evaluated at the Los Angeles Suburban Site.

DAY	AM PEAK 7:00-9:00	OFF PEAK 10:00-12:00	OFF PEAK 1:00-3:00	PM PEAK 4:00-6:00
Monday (8/24/87)	ORG 34 seconds	ORG 32 seconds	ORG 32 seconds	-10 seconds 22 seconds
Tuesday (8/25/87)	ORG 34 seconds	+5 seconds 37 seconds	+5 seconds 37 seconds	+10 seconds 42 seconds
Wednesday (8/26/87)	-10 seconds 24 seconds	ORG 32 seconds	ORG 32 seconds	ORG 32 seconds
Thursday (8/27/87)	ORG 44 seconds	-5 seconds 27 seconds	-5 seconds 27 seconds	ORG 32 seconds
Friday (8/28/87)	ORG 34 seconds	ORG 32 seconds	ORG 32 seconds	ORG 32 seconds

Table B-14. Data Collected at the Los Angeles Suburban Site, Northbound, August 26, 1987.

15-Minute Time Interval	G1/C (PTG)	Green Time 2	Cycle Length	G2/C (PTG)	Offset (sec.)	Volume on Green	Volume on Red	Total Volume	(PVG)	X-Ratio (QC/SG)	Platoon Ratio, Rp	Measured Delay	Uniform Delay	Incremental Delay	Predicted Delay	Dm - D2 D1
7:00-7:15	0.31	28	90	0.31	9	117	45	162	0.72	0.51	2.3	10.44	19.30	1.17	20.50	0.48
7:15-7:30	0.31	28	90	0.31	9	120	51	171	0.70	0.54	2.3	8.98	19.51	1.45	21.00	0.39
7:30-7:45	0.31	28	90	0.31	9	132	72	204	0.65	0.64	2.1	17.06	20.30	3.10	23.40	0.69
7:45-8:00	0.31	28	90	0.31	9	136	121	257	0.53	0.81	1.7	24.00	21.71	10.07	31.80	0.64
8:00-8:15	0.31	28	90	0.31	9	120	80	200	0.60	0.63	1.9	17.40	20.20	2.84	23.00	0.72
8:15-8:30	0.31	28	90	0.31	9	97	81	178	0.54	0.56	1.8	23.26	19.67	1.71	21.40	1.10
8:30-8:45	0.31	28	90	0.31	9	102	50	152	0.67	0.48	2.2	13.97	19.08	0.91	20.00	0.68
8:45-9:00	0.31	28	90	0.31	9	96	40	136	0.71	0.43	2.3	14.21	18.73	0.60	19.30	0.73
10:00-10:15	0.29	24	85	0.28	19	127	45	172	0.74	0.61	2.6	9.68	20.33	3.60	23.90	0.30
10:15-10:30	0.29	24	85	0.28	19	132	46	178	0.74	0.67	2.6	7.33	20.48	4.21	24.70	0.15
10:30-10:45	0.29	24	85	0.28	19	126	52	178	0.71	0.67	2.5	11.71	20.48	4.21	24.70	0.37
10:45-11:00	0.29	24	85	0.28	19	118	44	162	0.73	0.61	2.6	11.94	20.07	2.76	22.80	0.46
11:00-11:15	0.29	24	85	0.28	19	118	56	174	0.68	0.65	2.4	13.88	20.38	3.80	24.20	0.49
11:15-11:30	0.29	24	85	0.28	19	128	56	184	0.70	0.69	2.5	14.18	20.65	4.92	25.60	0.45
11:30-11:45	0.29	24	85	0.28	19	123	102	225	0.55	0.84	1.9	24.47	21.82	14.21	36.00	0.47
11:45-12:00	0.29	24	85	0.28	19	124	98	222	0.56	0.83	2	22.77	21.73	13.15	34.90	0.44
1:00-1:15	0.29	24	85	0.28	19	133	130	263	0.51	0.98	1.8	16.83	23.03	37.88	60.90	-0.91
1:15-1:30	0.29	24	85	0.28	19	151	56	207	0.73	0.77	2.6	11.81	21.29	8.92	30.20	0.14
1:30-1:45	0.29	24	85	0.28	19	149	44	193	0.77	0.72	2.7	7.31	20.89	6.21	27.10	0.05
1:45-2:00	0.29	24	85	0.28	19	122	71	193	0.63	0.72	2.2	17.95	20.89	6.21	27.10	0.56
2:00-2:15	0.29	24	85	0.28	19	144	46	190	0.76	0.71	2.7	10.03	20.81	5.75	26.60	0.21
2:15-2:30	0.29	24	85	0.28	19	142	72	214	0.66	0.80	2.4	15.42	21.49	10.68	32.20	0.22
2:30-2:45	0.29	24	85	0.28	19	144	61	205	0.70	0.77	2.5	14.20	21.23	8.47	29.70	0.27
2:45-3:00	0.29	24	85	0.28	19	157	73	230	0.68	0.86	2.4	13.83	21.97	16.19	38.20	-0.11
4:00-4:15	0.38	35	100	0.35	18	185	40	225	0.82	0.65	2.3	8.20	20.74	2.85	23.60	0.26
4:15-4:30	0.38	35	100	0.35	18	214	38	252	0.85	0.72	2.4	7.38	21.49	4.93	26.40	0.11
4:30-4:45	0.38	35	100	0.35	18	211	45	256	0.82	0.73	2.4	8.38	21.61	5.34	27.00	0.14
4:45-5:00	0.38	35	100	0.35	18	189	41	230	0.82	0.66	2.3	7.76	20.88	3.16	24.00	0.22
5:00-5:15	0.38	35	100	0.35	18	167	77	244	0.68	0.70	2	13.52	21.26	4.19	25.50	0.44
5:15-5:30	0.38	35	100	0.35	18	211	57	268	0.79	0.77	2.2	9.68	21.97	6.82	28.80	0.13
5:30-5:45	0.38	35	100	0.35	18	189	60	249	0.76	0.71	2.2	10.36	21.41	4.64	26.00	0.27
5:45-6:00	0.38	35	100	0.35	18	201	50	251	0.80	0.72	2.3	9.14	21.46	4.83	26.30	0.20

Table B-15. Data Collected at the Los Angeles Suburban Site, Southbound, August 26, 1987.

15-Minute Time Interval	G1/C (PTG)	Green Time 2	Cycle Length	G2/C (PTG)	Offset (sec.)	Volume on Green	Volume on Red	Total Volume	(PVG)	X-Ratio (QC/SG)	Platoon Ratio, Rp	Measured Delay	Uniform Delay	Incremental Delay	Predicted Delay	Dm - D2 D1
7:00-7:15	0.38	25	90	0.28	46	113	24	137	0.82	0.48	2.97	6.87	20.58	1.01	21.59	0.28
7:15-7:30	0.38	25	90	0.28	46	93	39	132	0.70	0.46	2.54	8.36	20.47	0.88	21.35	0.37
7:30-7:45	0.38	25	90	0.28	46	141	28	169	0.83	0.59	3.00	4.47	21.35	2.36	23.71	0.10
7:45-8:00	0.38	25	90	0.28	46	111	69	180	0.62	0.63	2.22	16.22	21.63	3.11	24.74	0.61
8:00-8:15	0.38	25	90	0.28	46	116	38	154	0.75	0.54	2.71	7.87	20.99	1.60	22.59	0.30
8:15-8:30	0.38	25	90	0.28	46	124	33	157	0.79	0.55	2.84	6.50	21.06	1.73	22.79	0.23
8:30-8:45	0.38	25	90	0.28	46	90	29	119	0.76	0.42	2.72	8.77	20.18	0.59	20.77	0.41
8:45-9:00	0.38	25	90	0.28	46	103	25	128	0.80	0.45	2.90	6.66	20.38	0.78	21.16	0.29
10:00-10:15	0.42	23	85	0.27	57	91	81	172	0.53	0.67	1.96	13.56	20.96	4.35	25.31	0.44
10:15-10:30	0.42	23	85	0.27	57	83	74	157	0.53	0.61	1.95	12.57	20.57	2.89	23.46	0.47
10:30-10:45	0.42	23	85	0.27	58	90	88	178	0.51	0.69	1.87	13.87	21.12	5.11	26.24	0.41
10:45-11:00	0.42	23	85	0.27	57	90	73	163	0.55	0.63	2.04	12.27	20.72	3.41	24.13	0.43
11:00-11:15	0.42	22	85	0.26	57	94	78	172	0.55	0.70	2.11	11.15	21.64	5.59	27.23	0.26
11:15-11:30	0.42	23	85	0.27	57	98	105	203	0.48	0.79	1.78	15.70	21.82	9.95	31.77	0.26
11:30-11:45	0.42	23	85	0.27	57	89	84	173	0.51	0.67	1.90	15.17	20.99	4.47	25.46	0.51
11:45-12:00	0.42	23	85	0.27	57	100	104	204	0.49	0.79	1.81	16.98	21.85	10.22	32.07	0.31
1:00-1:15	0.42	23	85	0.27	57	82	107	189	0.43	0.72	1.60	22.18	21.36	6.38	27.74	0.74
1:15-1:30	0.42	23	85	0.27	57	92	120	212	0.43	0.81	1.60	22.05	22.01	11.69	33.70	0.47
1:30-1:45	0.42	23	85	0.27	57	90	101	191	0.47	0.73	1.74	15.30	21.42	6.72	28.14	0.40
1:45-2:00	0.42	23	85	0.27	50	101	95	196	0.52	0.75	1.90	16.46	21.56	7.67	29.22	0.41
2:00-2:15	0.42	22	85	0.26	57	71	130	201	0.35	0.80	1.36	23.09	22.40	11.54	33.94	0.52
2:15-2:30	0.42	23	85	0.27	57	94	95	189	0.50	0.72	1.84	19.61	21.36	6.38	27.74	0.62
2:30-2:45	0.42	22	85	0.26	57	77	113	190	0.41	0.76	1.57	31.75	22.08	8.54	30.63	1.05
2:45-3:00	0.42	23	85	0.27	57	99	123	222	0.45	0.85	1.65	18.31	22.31	15.22	37.53	0.14
4:00-4:15	0.49	34	100	0.34	61	131	95	226	0.58	0.67	1.70	13.53	21.39	3.37	24.76	0.48
4:15-4:30	0.49	34	100	0.34	61	152	91	243	0.63	0.72	1.84	10.49	21.87	4.79	26.66	0.26
4:30-4:45	0.49	34	100	0.34	61	147	134	281	0.52	0.83	1.54	17.83	23.03	10.61	33.64	0.31
4:45-5:00	0.49	34	100	0.34	61	167	96	263	0.63	0.77	1.87	10.21	22.47	7.26	29.72	0.13
5:00-5:15	0.49	33	100	0.33	62	144	132	276	0.52	0.84	1.58	21.52	23.57	11.68	35.25	0.42
5:15-5:30	0.49	34	100	0.34	61	142	121	236	0.54	0.77	1.59	16.26	22.47	7.26	29.72	0.40
5:30-5:45	0.49	34	100	0.34	61	152	116	268	0.57	0.79	1.67	13.60	22.62	8.06	30.68	0.24
5:45-6:00	0.49	34	100	0.34	61	137	114	251	0.55	0.74	1.61	15.42	22.11	5.65	27.76	0.44

Table B-16. Semiactuated Data Collected at the Los Angeles Suburban Site, Northbound, August 28, 1987.

15-Minute Time Interval	G1/C (PTG)	Green Time 2	Cycle Length	G2/C (PTG)	Offset (sec.)	Volume on Green	Volume on Red	Total Volume	(PVG)	X-Ratio (QC/SG)	Platoon Ratio, Rp	Measured Delay	Uniform Delay	Incremental Delay	Predicted Delay	Dm - D2 D1
7:00-7:15	-	-	-	-	-	149	19	168	0.89	-	-	-	-	-	-	-
7:15-7:30	-	-	-	-	-	164	19	183	0.90	-	-	1.84	-	-	-	-
7:30-7:45	-	-	-	-	-	176	30	206	0.85	-	-	3.15	-	-	-	-
7:45-8:00	-	-	-	-	-	237	39	276	0.86	-	-	4.87	-	-	-	-
8:00-8:15	-	-	-	-	-	137	20	157	0.87	-	-	2.60	-	-	-	-
8:15-8:30	0.43	42	92	0.46	20	154	19	173	0.89	0.37	1.95	2.77	12.44	0.24	12.68	0.22
8:30-8:45	0.47	47	94	0.50	23	128	26	154	0.83	0.30	1.66	3.82	10.52	0.11	10.63	0.35
8:45-9:00	0.48	38	94	0.40	24	107	20	127	0.84	0.31	2.08	4.16	14.49	0.14	14.63	0.28
10:00-10:15	0.39	32	90	0.36	17	133	41	174	0.76	0.52	2.15	5.86	17.40	1.14	18.54	0.27
10:15-10:30	0.34	31	91	0.34	22	132	50	182	0.73	0.56	2.13	7.83	18.61	1.70	20.31	0.33
10:30-10:45	0.39	28	86	0.33	29	151	36	187	0.81	0.61	2.48	5.94	18.52	2.42	20.94	0.19
10:45-11:00	0.35	30	87	0.34	19	149	49	198	0.75	0.61	2.18	8.26	17.94	2.29	20.23	0.33
11:00-11:15	0.41	28	83	0.34	19	133	56	189	0.70	0.59	2.09	9.92	17.30	2.10	19.41	0.45
11:15-11:30	0.36	31	89	0.35	23	162	44	206	0.79	0.62	2.26	8.81	18.35	2.59	20.94	0.34
11:30-11:45	0.34	26	85	0.31	20	129	109	238	0.54	0.82	1.77	18.28	20.78	11.60	32.38	0.32
11:45-12:00	0.32	26	85	0.31	19	131	88	219	0.60	0.76	1.96	16.69	20.24	7.33	27.57	0.46
1:00-1:15	0.33	26	97	0.27	21	135	92	227	0.59	0.89	2.22	16.59	25.97	21.29	47.26	-0.18
1:15-1:30	0.41	25	85	0.29	23	89	142	231	0.39	0.83	1.31	29.42	21.28	12.64	33.93	0.79
1:30-1:45	0.38	24	85	0.28	22	95	145	240	0.40	0.90	1.40	17.31	22.28	21.00	43.28	-0.17
1:45-2:00	0.33	27	85	0.32	21	140	81	221	0.63	0.73	1.99	12.90	19.62	6.11	25.73	0.35
2:00-2:15	0.36	25	85	0.29	21	148	89	237	0.62	0.85	2.12	17.15	21.46	14.70	36.16	0.11
2:15-2:30	0.37	30	85	0.35	17	146	63	209	0.70	0.63	1.98	10.55	17.35	2.57	19.92	0.46
2:30-2:45	0.32	27	85	0.32	19	182	64	246	0.74	0.82	2.33	7.93	20.31	10.94	31.26	-0.15
2:45-3:00	0.36	25	89	0.28	20	147	85	232	0.63	0.87	2.26	13.38	23.16	17.66	40.82	-0.18
4:00-4:15	0.39	36	100	0.36	18	166	75	241	0.69	0.67	1.91	15.56	20.53	3.36	23.89	0.59
4:15-4:30	0.39	35	100	0.35	19	220	46	266	0.83	0.76	2.36	7.10	21.91	6.55	28.45	0.03
4:30-4:45	0.42	36	100	0.36	19	197	75	272	0.72	0.76	2.01	12.85	21.41	6.18	27.60	0.31
4:45-5:00	0.39	35	100	0.35	18	199	71	270	0.74	0.77	2.11	9.39	22.03	7.10	29.13	0.10
5:00-5:15	0.35	36	112	0.32	28	213	89	302	0.71	0.94	2.19	12.52	28.13	25.82	53.95	-0.47
5:15-5:30	0.38	36	100	0.36	17	182	80	262	0.69	0.73	1.93	13.11	21.12	5.07	26.19	0.38
5:30-5:45	0.39	35	100	0.35	18	161	106	267	0.60	0.77	1.72	18.31	21.94	6.68	28.62	0.53
5:45-6:00	0.42	35	100	0.35	27	195	100	295	0.66	0.85	1.89	14.69	22.81	11.92	34.73	0.12

Table B-17. Semiactuated Data Collected at the Los Angeles Suburban Site, Southbound, August 28, 1987.

15-Minute Time Interval	G1/C (PTG)	Green Time 2	Cycle Length	G2/C (PTG)	Offset (sec.)	Volume on Green	Volume on Red	Total Volume	X-Ratio (PVG)	X-Ratio (QC/SG)	Platoon Ratio, Rp	Measured Delay	Uniform Delay	Incremental Delay	Predicted Delay	Dm - D2 D1
7:00-7:15	0.48	36	101	0.36	55	72	70	142	0.51	0.39	1.42	8.45	18.45	0.36	18.80	0.44
7:15-7:30	0.55	33	95	0.35	77	92	52	144	0.64	0.40	1.84	5.67	17.88	0.42	18.31	0.29
7:30-7:45	0.41	33	93	0.35	55	112	64	176	0.64	0.48	1.79	8.80	17.75	0.81	18.56	0.45
7:45-8:00	0.41	31	93	0.33	51	152	49	201	0.76	0.59	2.27	5.79	19.53	1.91	21.44	0.20
8:00-8:15	0.53	32	100	0.32	56	71	59	130	0.55	0.40	1.71	8.68	20.12	0.43	20.54	0.41
8:15-8:30	0.45	33	90	0.37	59	82	56	138	0.59	0.37	1.62	7.30	15.85	0.28	16.13	0.44
8:30-8:45	0.56	34	90	0.38	67	79	60	139	0.57	0.36	1.50	8.55	15.31	0.25	15.57	0.54
8:45-9:00	0.55	31	91	0.34	59	85	72	157	0.54	0.45	1.59	11.62	17.75	0.64	18.38	0.62
10:00-10:15	0.44	26	85	0.31	69	101	69	170	0.59	0.58	1.94	9.88	18.93	2.14	21.07	0.41
10:15-10:30	0.34	25	84	0.30	65	96	84	180	0.53	0.63	1.79	14.08	19.40	3.17	22.58	0.56
10:30-10:45	0.49	25	86	0.29	70	106	91	197	0.54	0.71	1.85	15.91	20.71	5.53	26.24	0.50
10:45-11:00	0.51	24	85	0.28	61	92	89	181	0.51	0.67	1.80	14.92	20.53	4.35	24.88	0.51
11:00-11:15	0.46	24	85	0.28	62	85	89	174	0.49	0.65	1.73	13.88	20.34	3.63	23.97	0.50
11:15-11:30	0.42	25	85	0.29	56	101	114	215	0.47	0.77	1.60	19.33	20.77	8.06	28.83	0.54
11:30-11:45	0.43	24	85	0.28	66	107	105	212	0.50	0.79	1.79	18.82	21.38	9.64	31.02	0.43
11:45-12:00	0.45	24	85	0.28	59	94	122	216	0.44	0.80	1.54	22.71	21.50	10.68	32.18	0.56
1:00-1:15	0.44	23	85	0.27	59	53	182	235	0.23	0.90	0.83	31.40	22.70	21.48	44.18	0.44
1:15-1:30	0.48	23	85	0.27	59	42	173	215	0.20	0.82	0.72	40.88	22.10	12.65	34.75	1.28
1:30-1:45	0.53	24	85	0.28	50	96	124	220	0.44	0.81	1.55	22.50	21.54	10.94	32.47	0.54
1:45-2:00	0.44	28	85	0.33	58	121	94	215	0.56	0.68	1.71	11.44	18.68	3.83	22.51	0.41
2:00-2:15	0.45	28	85	0.33	59	74	154	228	0.32	0.72	0.99	25.79	19.01	5.10	24.11	1.09
2:15-2:30	0.45	25	85	0.29	59	104	106	210	0.50	0.74	1.68	13.43	20.56	6.61	27.17	0.33
2:30-2:45	0.45	25	87	0.29	57	101	124	225	0.45	0.81	1.56	22.53	21.88	11.08	32.96	0.52
2:45-3:00	0.56	24	84	0.29	61	97	158	255	0.38	0.92	1.33	24.35	22.12	24.60	46.72	-0.01
4:00-4:15	0.49	34	100	0.34	61	152	101	253	0.60	0.74	1.77	13.87	22.17	5.89	28.06	0.36
4:15-4:30	0.49	34	100	0.34	61	132	111	243	0.54	0.72	1.60	12.78	21.87	4.79	26.66	0.37
4:30-4:45	0.49	34	100	0.34	61	147	120	267	0.55	0.79	1.62	20.90	22.59	7.89	30.48	0.58
4:45-5:00	0.49	34	100	0.34	61	151	120	271	0.56	0.80	1.64	15.11	22.71	8.58	31.30	0.29
5:00-5:15	0.49	34	100	0.34	61	125	178	303	0.41	0.89	1.21	28.81	23.76	17.04	40.79	0.50
5:15-5:30	0.49	34	100	0.34	61	152	117	269	0.57	0.79	1.66	12.16	22.65	8.23	30.88	0.17
5:30-5:45	0.49	34	100	0.34	61	162	115	277	0.58	0.82	1.72	16.35	22.90	9.74	32.65	0.29
5:45-6:00	0.49	35	100	0.35	72	136	124	260	0.52	0.74	1.49	15.98	21.70	5.69	27.39	0.47

Table B-18. Cycle-by-Cycle Data Collected at the Los Angeles Suburban Site, Northbound, August 26, 1987.

Time Interval	G1/C (PTG)	Green Time	Cycle Length	G2/C (PTG)	Offset (sec.)	Volume on Green	Volume on Red	Total Volume	(PVG)	X-Ratio (QC/SG)	Platoon Ratio, Rp	Measured Delay	Uniform Delay	Incremental Delay	Predicted Delay	Dm - D2 D1
7:09	0.31	28	90	0.31	9	9	6	15	0.60	0.47	1.94	19.33	19.08	0.22	19.30	1.00
	0.31	28	90	0.31	9	9	1	10	0.90	0.32	2.90	5.50	18.05	0.05	18.10	0.30
7:12	0.31	28	90	0.31	9	6	7	13	0.46	0.41	1.49	33.85	18.66	0.13	18.78	1.81
	0.31	28	90	0.31	9	12	1	13	0.92	0.41	2.98	4.62	18.66	0.13	18.78	0.24
7:15	0.31	28	90	0.31	9	11	4	15	0.73	0.47	2.37	11.33	19.08	0.22	19.30	0.58
	0.31	28	90	0.31	9	20	0	20	1.00	0.63	3.23	0.00	20.25	0.74	20.98	-0.04
7:18	0.31	28	90	0.31	9	11	6	17	0.65	0.54	2.09	18.82	19.53	0.36	19.90	0.95
	0.31	28	90	0.31	9	9	0	9	1.00	0.28	3.23	0.00	17.86	0.04	17.89	0.00
7:21	0.31	28	90	0.31	9	9	3	12	0.75	0.38	2.42	9.58	18.45	0.10	18.55	0.51
	0.31	28	90	0.31	9	19	5	24	0.79	0.76	2.55	9.58	21.28	1.90	23.18	0.36
7:24	0.31	28	90	0.31	9	13	9	22	0.59	0.69	1.91	22.27	20.75	1.18	21.93	1.02
	0.31	28	90	0.31	9	11	1	12	0.92	0.38	2.96	5.42	18.45	0.10	18.55	0.29
7:27	0.31	28	90	0.31	9	14	8	22	0.64	0.69	2.05	20.45	20.75	1.18	21.93	0.93
	0.31	28	90	0.31	9	13	11	24	0.54	0.76	1.75	25.21	21.28	1.90	23.18	1.10
7:30	0.31	28	90	0.31	9	14	9	23	0.61	0.73	1.96	18.70	21.01	1.49	22.50	0.82
	0.31	28	90	0.31	9	7	2	9	0.78	0.28	2.51	11.67	17.86	0.04	17.89	0.65
7:33	0.31	28	90	0.31	9	9	5	14	0.64	0.44	2.07	21.79	18.87	0.17	19.04	1.15
	0.31	28	90	0.31	9	19	9	28	0.68	0.88	2.19	13.39	22.43	5.55	27.98	0.35
7:36	0.31	28	90	0.31	9	14	9	23	0.61	0.73	1.96	18.04	21.01	1.49	22.50	0.79
	0.31	28	90	0.31	9	14	10	24	0.58	0.76	1.88	18.75	21.28	1.90	23.18	0.79
7:39	0.31	28	90	0.31	9	11	10	21	0.52	0.66	1.69	25.24	20.50	0.93	21.43	1.19
	0.31	28	90	0.31	9	15	1	16	0.94	0.51	3.02	3.75	19.31	0.28	19.59	0.18
7:42	0.31	28	90	0.31	9	15	12	27	0.56	0.85	1.79	22.96	22.13	4.14	26.27	0.85
	0.31	28	90	0.31	9	11	11	22	0.50	0.69	1.61	23.64	20.75	1.18	21.93	1.08
7:45	0.31	28	90	0.31	9	15	6	21	0.71	0.66	2.30	9.29	20.50	0.93	21.43	0.41
	0.31	28	90	0.31	9	18	8	26	0.69	0.82	2.23	12.69	21.84	3.15	24.99	0.44
7:48	0.31	28	90	0.31	9	16	13	29	0.55	0.92	1.78	23.10	22.74	7.61	30.35	0.68
	0.31	28	90	0.31	9	10	8	18	0.56	0.57	1.79	23.89	19.76	0.46	20.23	1.19
7:51	0.31	28	90	0.31	9	10	18	28	0.36	0.88	1.15	31.07	22.43	5.55	27.98	1.14
	0.31	28	90	0.31	9	15	19	34	0.44	1.07	1.42	24.85	24.40	42.15	66.56	-0.71
7:54	0.31	28	90	0.31	9	11	10	21	0.52	0.66	1.69	23.81	20.50	0.93	21.43	1.12
	0.31	28	90	0.31	9	12	17	29	0.41	0.92	1.33	26.03	22.74	7.61	30.35	0.81
7:57	0.31	28	90	0.31	9	17	9	26	0.65	0.82	2.11	16.15	21.84	3.15	24.99	0.60
	0.31	28	90	0.31	9	15	9	24	0.63	0.76	2.02	16.25	21.28	1.90	23.18	0.67
8:00	0.31	28	90	0.31	9	19	10	29	0.66	0.92	2.11	15.69	22.74	7.61	30.35	0.36

STATISTICAL ANALYSIS

INTRODUCTION

This appendix documents the statistical evaluation of the analytical delay and progression factor equations presented in previous sections of this report. More specifically, this appendix documents how well stopped delay and progression factors estimated from analytical equations compare to actual values measured in the field. The data set used in this analysis contained 860 15-minute observations under pretimed conditions and 55 15-minute observations under semiactuated conditions. These data were used to both calibrate and validate the previously mentioned delay and progression factor equations. The microcomputer version of the Statistical Analysis System (SAS) program package, Release 6.03 (24), was used for all statistical tests performed in this research.

The delay equation analysis examined the use of the current HCM delay equation adjustments (0.38 for the uniform delay term and 173 for the incremental delay term) as well as alternative adjustment factors developed using least squares regression. The first part of the analysis dealt with the adjustment factors currently used in the HCM (1). These factors were used to initially examine the analytical delay equations developed in this research and to check for violations in the assumptions used in linear regression analysis. The second part of the analysis developed two alternative sets of adjustment factors based on a least squares regression fit. These two sets of least squares adjustment factors were then evaluated to determine how closely they predicted measured delay.

The progression factor analysis compared the analytical progression factors to those observed in the field studies. Because progression factors were not actually measured, observed progression factors were obtained by rearranging the terms in the delay equation, substituting the observed values for each of the variables, and solving for the progression factor. The progression factor analysis concludes with a table presenting the progression adjustment factor values recommended as replacements for those currently contained in Table 9-13 of the 1985 HCM (1).

Delay Equations

Appendix A contains the derivation of two equations proposed as possible replacements for the uniform delay portion of the delay equation described in the 1985 HCM (1). The first of these equations is a simplified or approximate equation developed as part of this research, and the second equation is a simplification of more exact equations published by Rouphail (22) in 1988 and Messer and Fambro in 1975 (4). A major benefit of the new formulation of these equations is elimination of the need for a separate table or set of equations for calculating progression factors, as each of the new equations includes a term to implicitly account for the effects of progression.

The current uniform delay equation, as given in the 1985 HCM, is reproduced here for convenience.

$$d_u = 0.38 * C * \frac{(1 - g/C)^2}{(1 - (g/C) * X)} \quad [C-1]$$

where:

- d_u = uniform delay based on an average arrival rate, seconds/vehicle;
- C = cycle length, sec;
- g = effective green time of phase, sec; and
- X = demand volume to signal phase capacity ratio (qC/gs).

The simplified delay equation developed in Appendix A is shown next with a modification made for the purpose of simplifying the statistical analysis. This equation will be referred to as Equation 1 for the remainder of this appendix. The value of f_u is an adjustment or calibration factor developed from the regression analysis of the field data.

$$d_{u1} = f_u * r * \left(\frac{1 - P}{1 - y} \right) \quad [C-2]$$

where:

- d_{u1} = uniform delay for Equation C-2, sec/veh;
- f_u = uniform delay adjustment factor;
- r = effective red time of phase, sec;
- P = proportion of all vehicles in the movement arriving during the green phase ($P = PVG$); and
- y = flow rate of phase (q/s).

The second, more exact equation was also developed in Appendix A with the same modification. This equation will be referred to as Equation 2 from here on and is as follows:

$$d_{u2} = f_u * C * \left(1 - \frac{g}{C} \right)^2 * \left(1 + \frac{q_r}{s - q_g} \right) * \left(\frac{q_r}{q} \right) \quad [C-3]$$

where:

- d_{u2} = uniform delay for Equation C-3, sec/veh;
- q_r = average movement flow rate during effective red time, vps;
- q_g = average movement flow rate during effective green time, vps;
- q = average movement flow rate during cycle, vps; and
- s = saturation flow rate of phase, vps/g.

Due to several limitations of the data set, it was not feasible to develop a replacement for the incremental term of the HCM delay model. As a result, the equation is given as it appears in the 1985 HCM with only a simple modification to allow for calibration.

$$d_i = f_i * X^2 * \left[(X - 1) + \sqrt{(X - 1)^2 + \left(\frac{16 * X}{c} \right)} \right] \quad [C-4]$$

where:

- d_i = incremental delay, sec/veh;
- f_i = incremental delay adjustment factor; and
- c = capacity of the lane group.

For the purpose of clarity, as indicated above, Equation 1 and Equation 2 are also labeled as d_{u1} and d_{u2} , respectively. The incremental delay term shown in Equation C-4 will be labeled as d_i for the remainder of the appendix. The resulting stopped delay equations are also labeled separately as follows:

$$d_1 = d_{u1} + d_i \quad [C-5]$$

$$d_2 = d_{u2} + d_i \quad [C-6]$$

Progression Factor Equations

As stated previously, it is not necessary to calculate a progression factor when using the proposed delay equations. One of the main objectives of this research, however, was to develop either a new set of progression factors or some kind of continuous relationship for estimation of progression factors. The derivation of the delay equations presented in Appendix A also resulted in the development of several analytically based equations for estimating progression factors. The exact formulation that was recommended is reproduced here for convenience.

$$PF = \left(\frac{1 - P}{1 - g/C} \right) \quad [C-7]$$

Given a set of measured and predicted delays, this equation can be rewritten to yield a progression factor as follows:

$$PF = \left(\frac{d_m - d_i}{d_u} \right) \quad [C-8]$$

where:

- d_m = field measured delay, sec/veh;
- d_i = calculated incremental delay, sec/veh; and
- d_u = uniform delay based on an average arrival rate, sec/veh.

By substituting Equations 1 and 2 for the value of d_u , this equation can be rewritten as follows:

$$\text{from Eq. 1:} \quad PF = \left[\frac{d_m - d_i}{f_u * r * (1 - P/1 - y)} \right] \quad [C-9]$$

from Eq. 2:

$$PF = \left[\frac{d_m - d_i}{f_u * C * (1 - g/C)^2 * (1 + (q_r / (s - q_g))) * (q_r / q)} \right] \quad [C-10]$$

For the purpose of this analysis it was necessary to solve for the progression factors embedded in the field data using either Equation C-9 or C-10. Individual observations were used as the variables' values, and the delay measured in the field was used as the value for d_m . The calibration factors (f_u and f_i) used in the delay equations in this case were developed from a regression analysis of the delay equations.

FREQUENCY ANALYSIS

A frequency analysis was performed on several of the more important variables collected during the field studies prior to any detailed statistical analysis of the data. These variables included proportion of the total volume arriving on green (P), green ratio (g/C), volume-to-capacity or X-ratio (X), and measured delay (d_m). The entire pretimed data set, which contained 855 15-minute observations, was analyzed in the initial frequency analysis and then broken down by site for a more detailed analysis. The by-site frequency analyses were used as the basis for selecting the calibration and validation data sets used in the statistical analysis of the delay equations. Because of the set's small size and the fact that it was collected at only one site, the semiactuated data were only analyzed as a complete data set.

Entire Pretimed Data Set

Figure C-1 shows the frequency distribution of green ratios, X-ratios, proportion of the total volume arriving on green, and measured delays for the entire pretimed data set. The green ratio was preset and constant for each two-hour time period of data collection and, as a result, follows a rectangular rather than a normal distribution. As shown in the figure, the actual green ratios observed during the study ranged from 0.25 to 0.65, with most of the observations occurring at green ratios less than 0.60. Because there were too few observations for statistical reliability with green ratios greater than 0.60, only the green ratios between 0.25 and 0.60 were used in subsequent analysis.

The relative frequencies of the observed X-ratios show a normal distribution with values ranging from 0.10 to 1.00. The slightly non-normal behavior from 0.60 to 0.80 was due to the unusually heavy offpeak traffic volumes at the Los Angeles suburban site. The majority of the observations occurred in the range of 0.40 to 0.80. Even though some data from oversaturated operating conditions were desirable and initial consultation with the responsible authorities suggested that oversaturated operating conditions occurred at the study sites, these conditions were not observed during the data collection for this research. The reason for these better than expected operating conditions was that both the signal timing and progression at each of the sites were relatively good, i.e., the signals were timed properly. Additionally, the signal timing adjustments required to achieve a usable number of observations at oversaturated conditions were not considered desirable and were therefore not attempted.

The relative frequencies of the proportion of total volumes arriving on green show a negatively skewed distribution (the bulk of the distribution shows relatively high P values). This distribution was not surprising given the fact that the signal timing was observed to be relatively good at each of the study sites. As

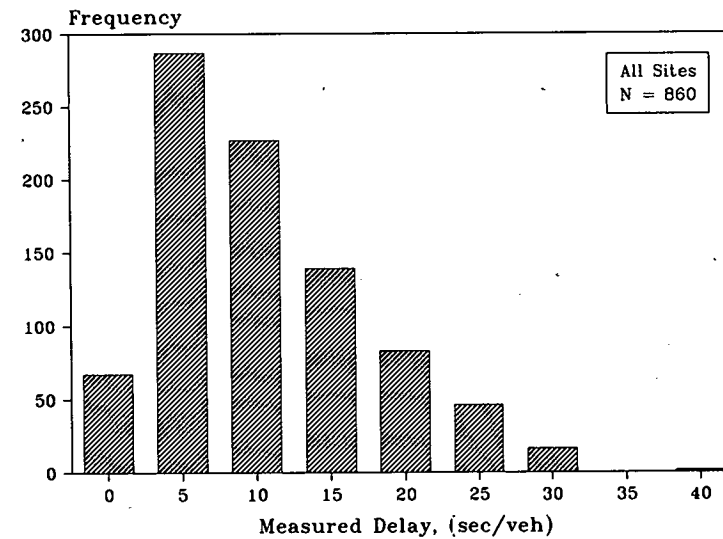
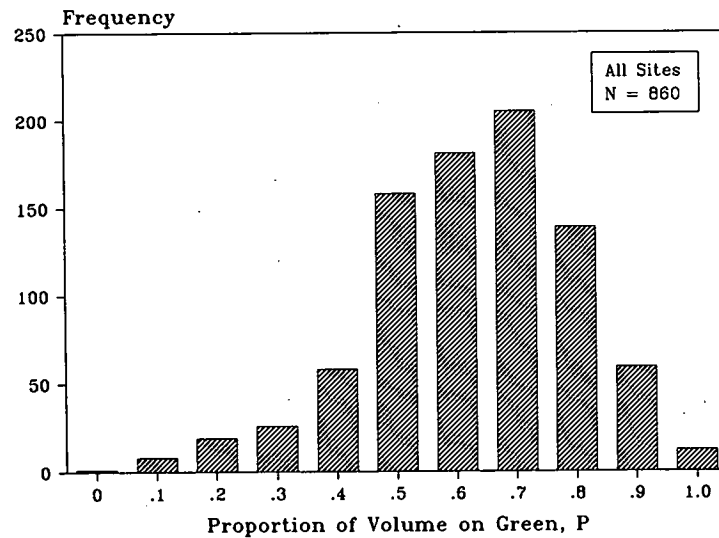
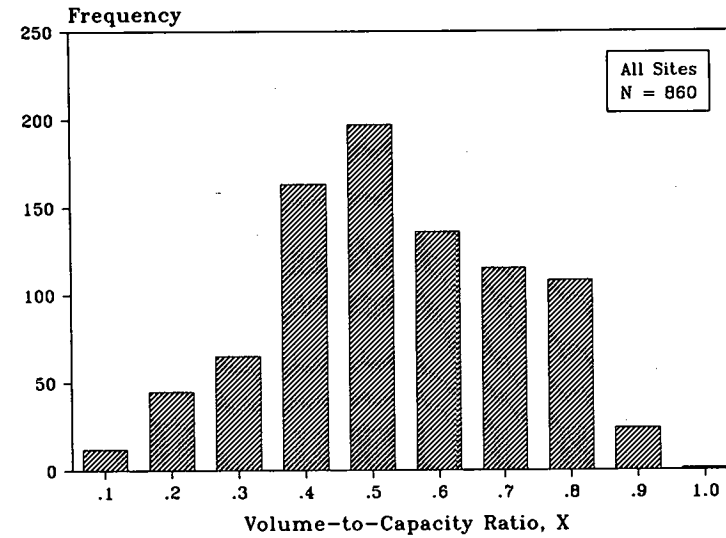
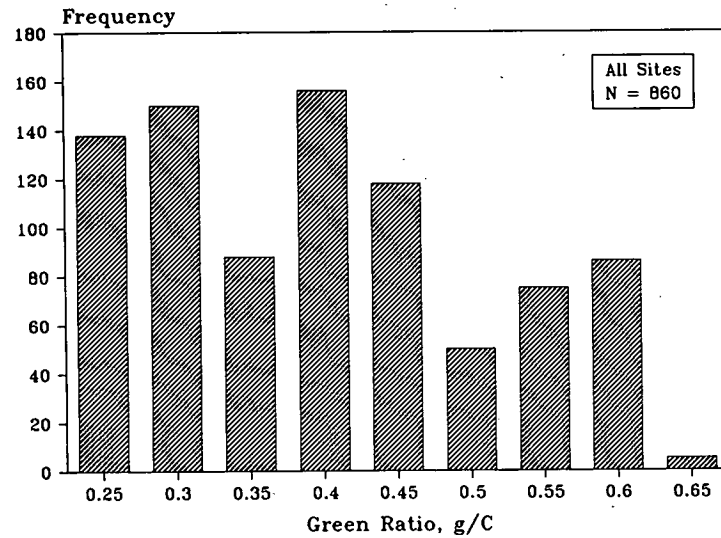


Figure C-1. Frequency Distribution of Important Study Variables, Pretimed Data Set.

shown in the Figure C-1, the measured P values ranged from 0.0 to 1.0, with most of the observations occurring between 0.4 and 0.9. The values of 0.0 and 1.0 are the result of rounding into class intervals. In other words, there were no measurements at either of these two values, although some observations were close enough to be placed in those class intervals. Based on this distribution of observed proportion of total volumes arriving on green, high measured delays would not be expected.

As suggested by the frequency distribution for the proportion of the total volume arriving on green, the measured delays were low and, as a result, the data display a pronounced positive skew (the bulk of the distribution shows relatively low values of delay). As shown, the measured delays covered a range from 0 to 40 seconds per vehicle, with most of the values falling between 0 and 25 seconds per vehicle. This means that all of the observations during the data collection for this study were at level-of-service D or better. Again, the observations with no delay are a result of the rounding performed in setting up the class intervals and not actual field measurements.

By-Site Pretimed Data Set

The frequency distribution of green ratios observed at each of the four field study sites is shown in Figure C-2. It is apparent from these charts that not all of the green ratios were observed at each study site. For example, the two Houston sites showed a broader range of green ratios and, as a result, had fewer observations per value of g/C . The two Los Angeles sites, on the other hand, had only three usable green ratios apiece. The primary reason for this difference is the different signal timing conditions present at each site. The Los Angeles urban site used a two-phase operation with permitted left-turns. This type of operation results in higher green ratios for the thru movements because there are no separate left-turn phases. The Los Angeles suburban site used an eight-phase operation with protected left-turns on all approaches, which results in shorter thru greens and thus lower green ratios. Collectively, however, the Los Angeles sites covered a range of green ratios from 0.25 to 0.60.

The frequency distribution of X-ratios observed at each site is shown in Figure C-3. Again, the Houston sites showed a more even distribution of observations over a broader range of X-ratios than did the Los Angeles sites. The Houston urban site was a six-lane arterial with fairly low volumes and consequently produced lower X-ratios than did the suburban site. The Los Angeles urban site produced a large number of observations at X-ratios of 0.4 and 0.5, the result of relatively low volumes and the previously mentioned high green ratios. The Los Angeles suburban site produced a large number of observations at the X-ratios of 0.4, 0.7, and 0.8. This site was located between two interstate highways and bounded by a large number of commercial businesses. These businesses generated high traffic volumes and correspondingly high X-ratios during a major portion of the day. This figure clearly shows that the non-normality from 0.6 to 0.8 in the X-ratio distribution in Figure C-1 is indeed caused by the operating conditions at the Los Angeles suburban site.

The frequency distribution of the proportion of the total volume arriving on green is shown in Figure C-4. The Ps at the Houston urban and Los Angeles suburban sites appear to be normally distributed and the Ps at the Houston suburban and Los

Angeles urban sites appear to be negatively skewed. The mean of the Ps for the four sites was in the 0.5 to 0.6 range, indicating relatively good progression. It is interesting to note that even with relatively low green ratios and relatively high X-ratios observed at the Los Angeles suburban site, the proportion of the total volume arriving on green remained high, again indicating good progression and low expected delays.

The frequency distribution of measured delays is shown in Figure C-5. The Los Angeles urban site chart shows a very narrow range of measured delays, with most of the observations occurring in the 5 seconds per vehicle range. This narrow distribution was caused by low volumes and the relatively long greens present at this site. The other three sites displayed a wider range of delays. Consistent with the results shown in Figure C-2, but harder to visualize, the measured delay charts show a positive skew with the bulk of the distribution showing relatively low values of delay.

Semiactuated Data Set

The frequency distribution information for the semiactuated data represents 56 observations and is shown in Figure C-6. This data was collected on the last day of the data collection effort at the Los Angeles suburban site. There was a small number of observations at green ratios less than 0.30 and greater than 0.35, and only the green ratios of 0.30 and 0.35 (20 and 29 observations, respectively) contained enough observations to be used in subsequent statistical analyses. When compared to the pretimed data set, the semiactuated data set contained slightly higher green ratios.

The frequency distribution of X-ratios shows a much different distribution from that of the pretimed data set from the same site (Los Angeles suburban in Figure C-3). The major difference in the two distributions is the lower frequency of observations at X-ratios of 0.4 and higher frequency of observations at X-ratios of 0.9 for the semiactuated data, a direct result of semiactuated control making the most efficient use of the available time. The X-Ratios cover a range from 0.3 to 0.9, which is essentially the same range represented in the pretimed data set, with a negative skewness and the bulk of the distribution showing higher values of X.

The proportion of the total volume arriving on green in the semiactuated data set ranged from 0.2 to 0.9 with a mean of around 0.6. This value is similar to the mean observed in the pretimed data set, although, not surprisingly, the range is narrower for the semiactuated data set. The narrower range of the proportion of the total volume arriving on green is another result of semiactuated control making efficient use of the available time. The distribution of the Ps appears to be normal with no skewness.

The measured delays in the semiactuated data set range from 5 to 30 seconds per vehicle. The mean value for the measured delays is around 13 seconds per vehicle, which is approximately the same as that observed in the pretimed data set. This result was somewhat surprising as it was expected that semiactuated control would decrease delays for the thru movements. The distribution of delays in this case, as in the pretimed data, shows a positively skewed distribution (the bulk of the distribution showing relatively low values of delay).

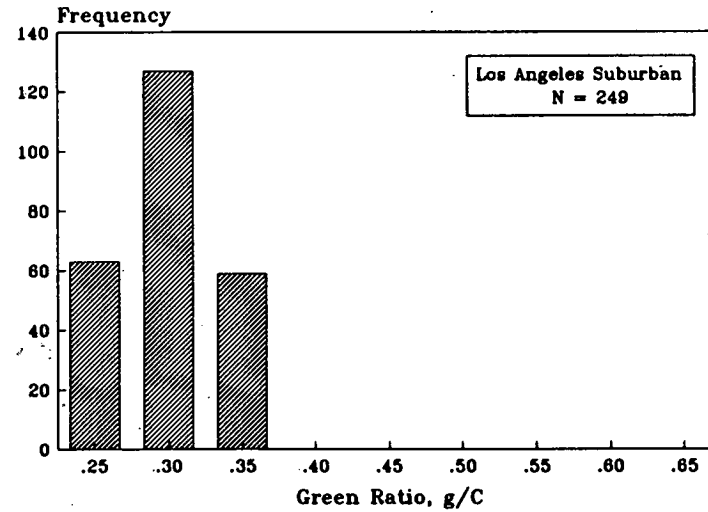
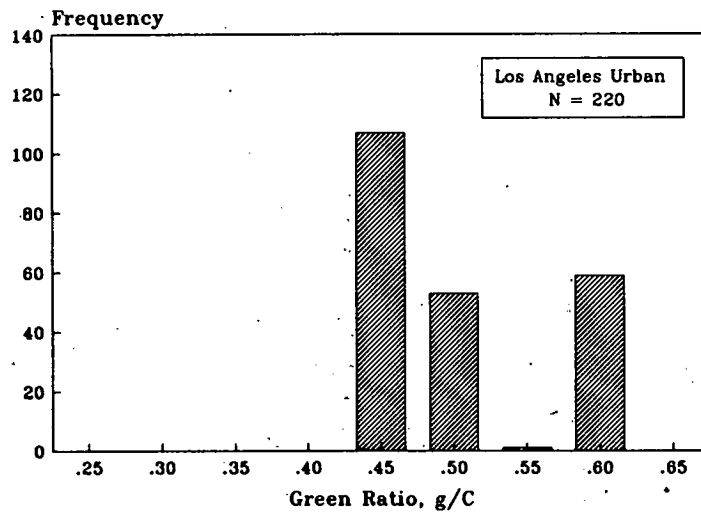
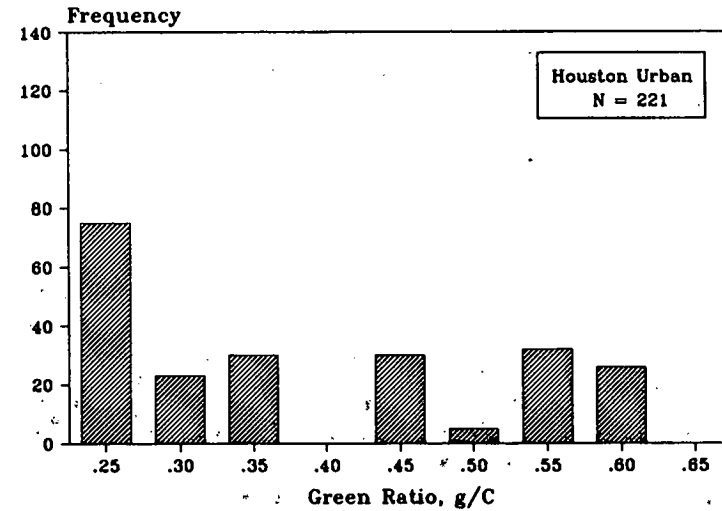
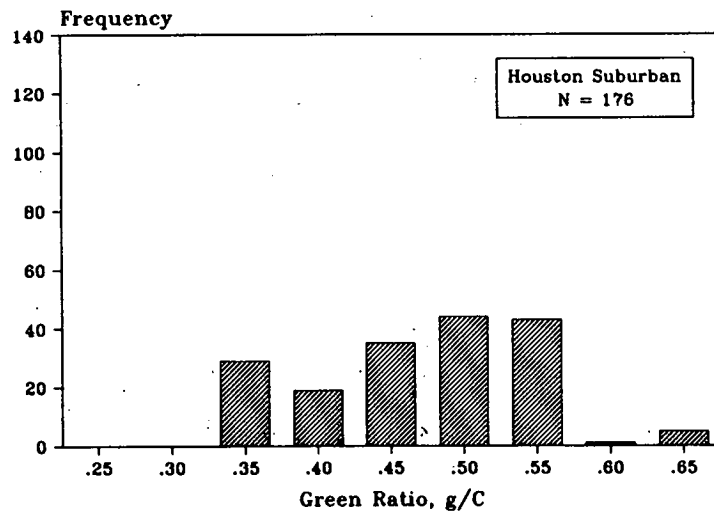


Figure C-2. Frequency Distribution of Observed Green Ratios by Study Site.

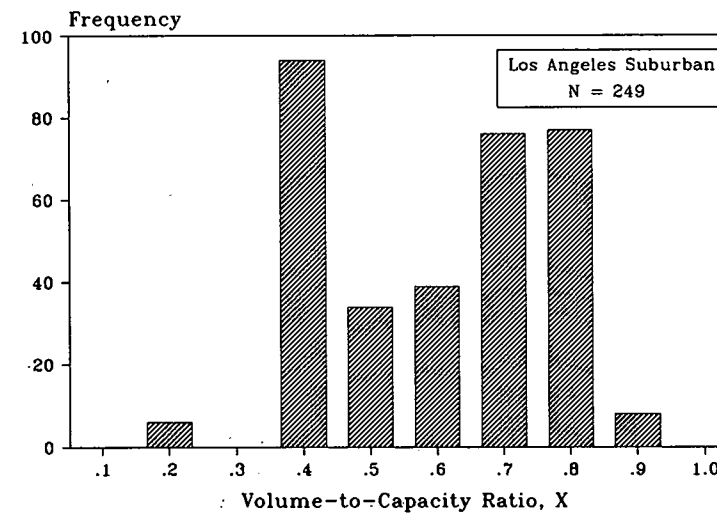
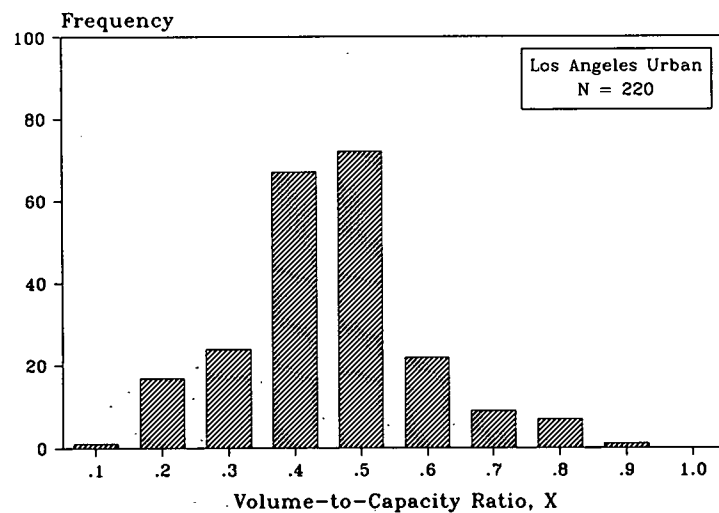
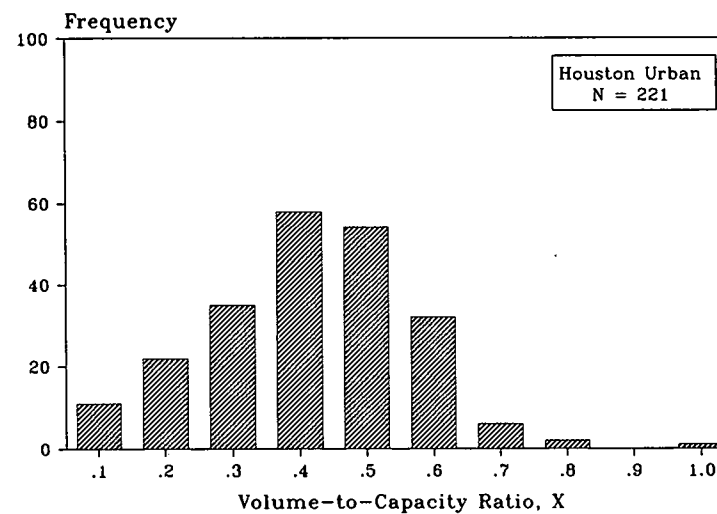
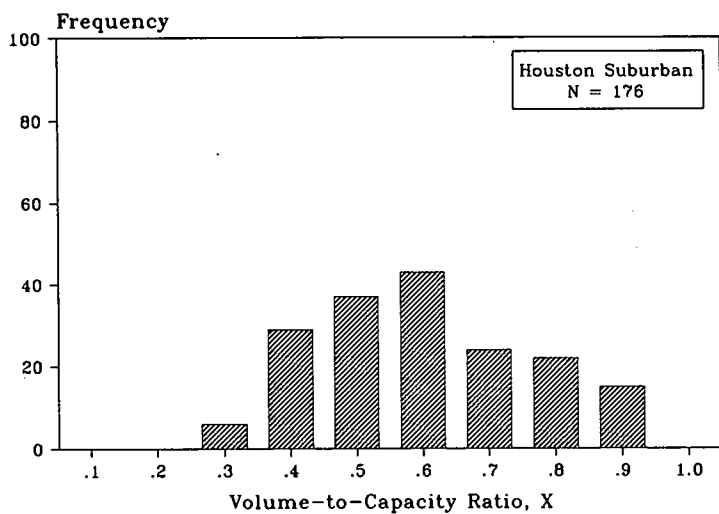


Figure C-3. Frequency Distribution of Observed Volume-to-Capacity Ratios by Study Site.

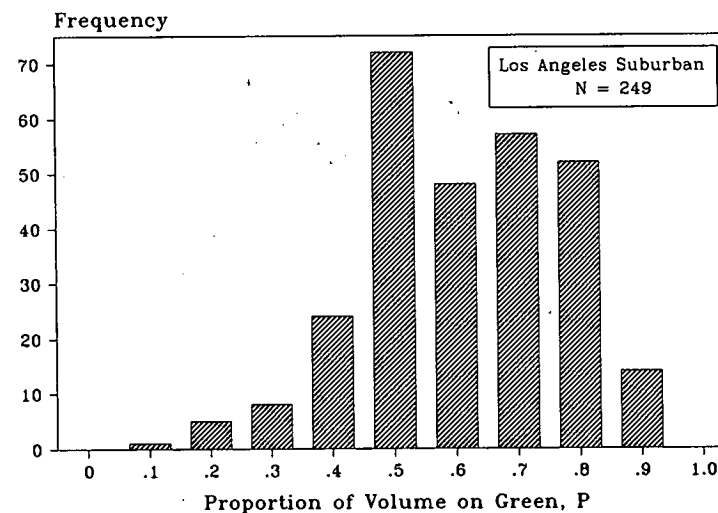
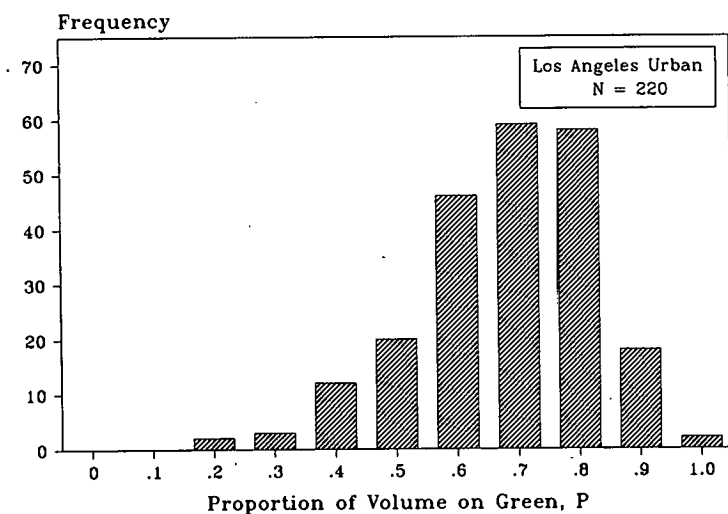
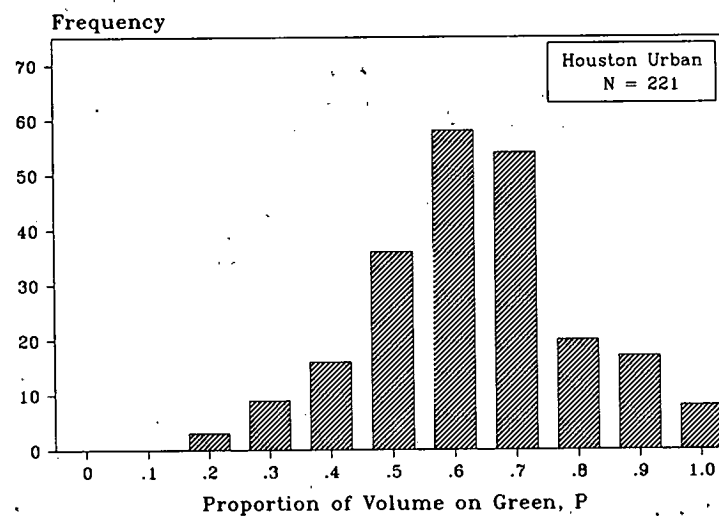
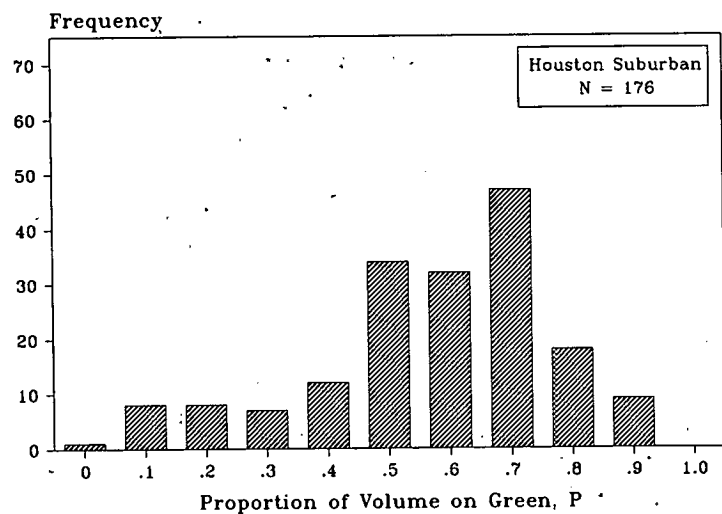


Figure C-4. Frequency Distribution of Observed Proportion of Total Volume Arriving on Green by Study Site.

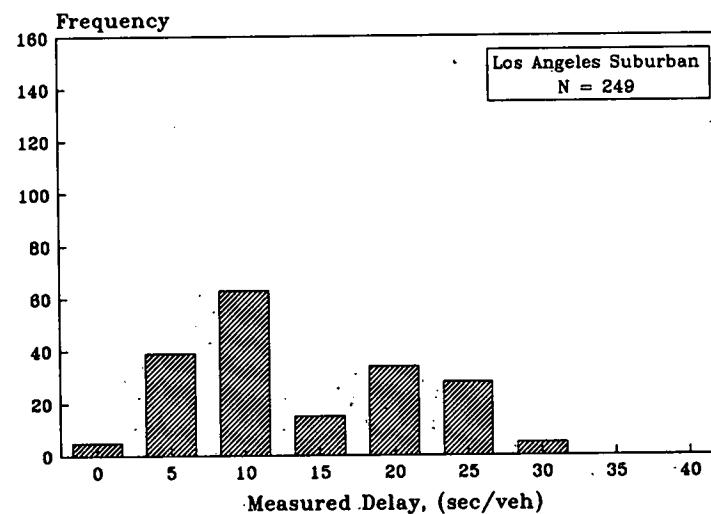
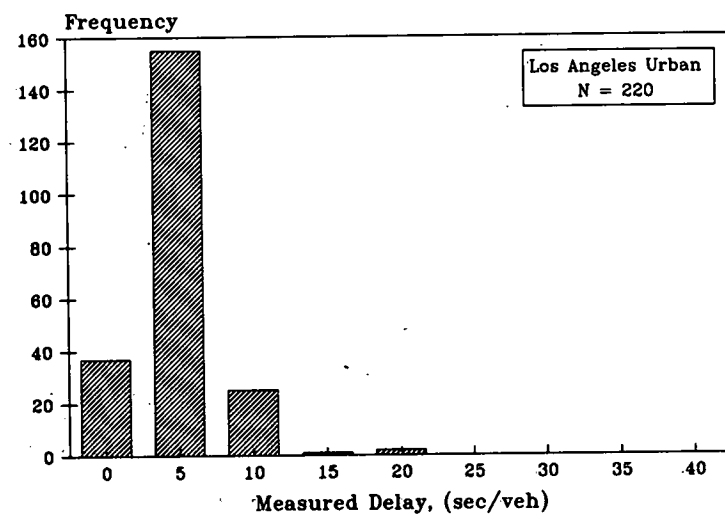
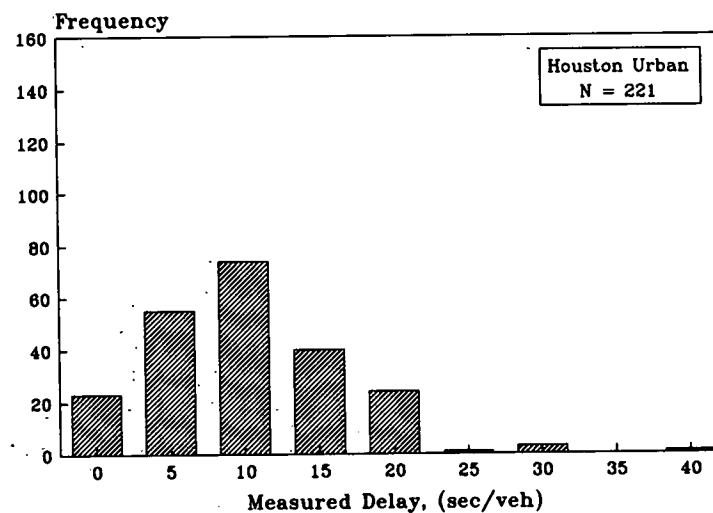
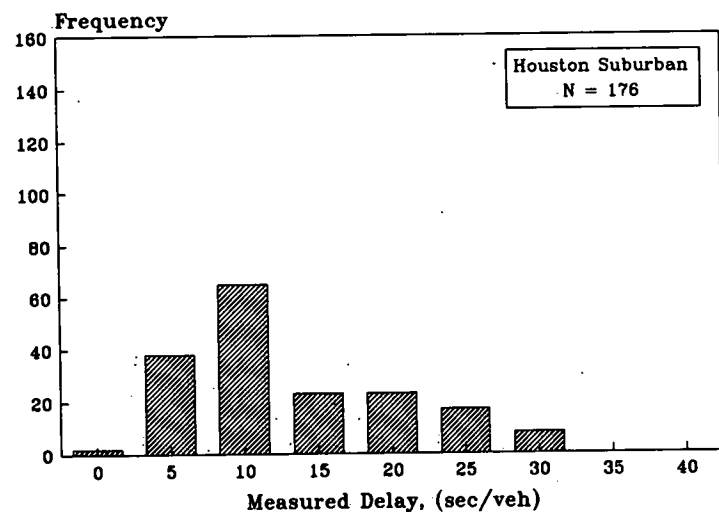


Figure C-5. Frequency Distribution of Measured Delays by Study Site.

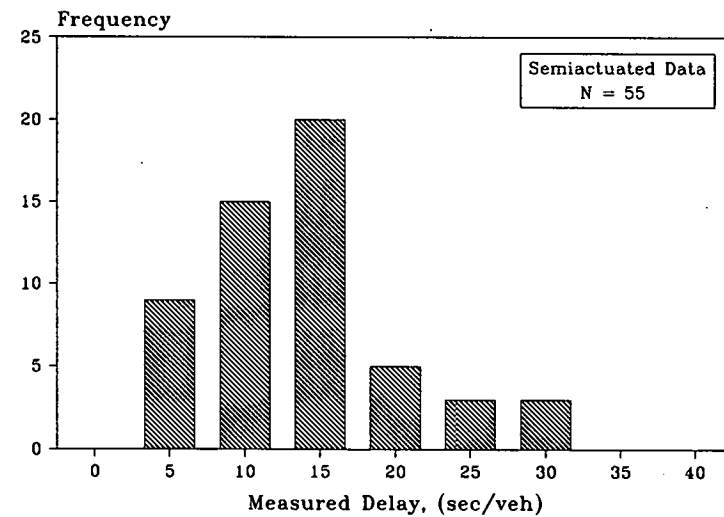
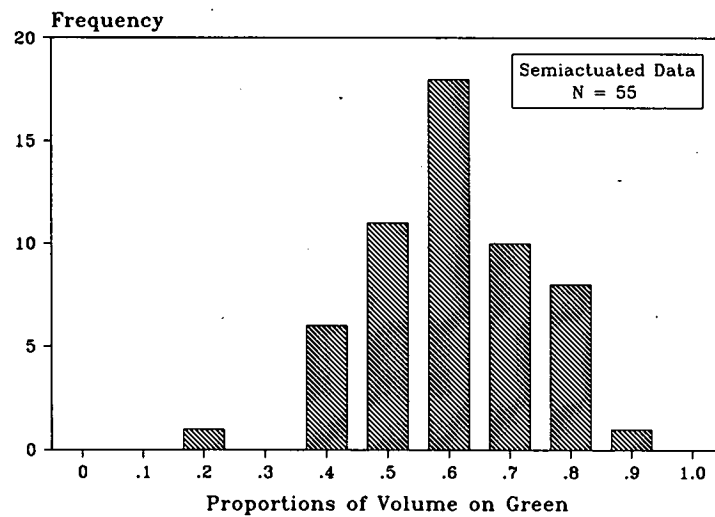
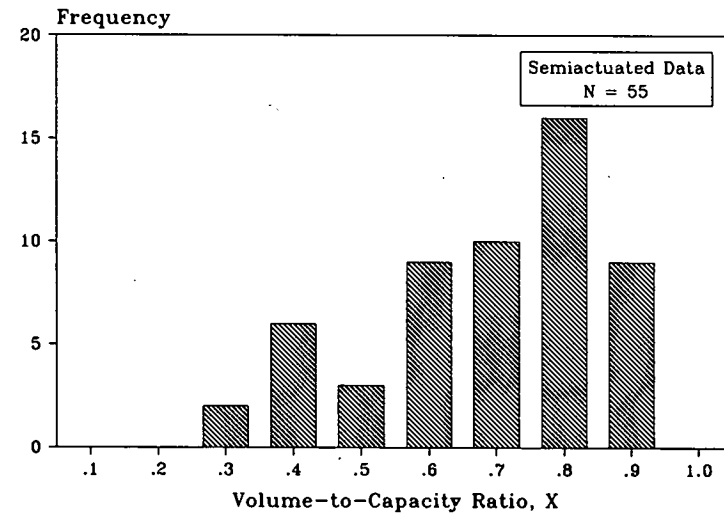
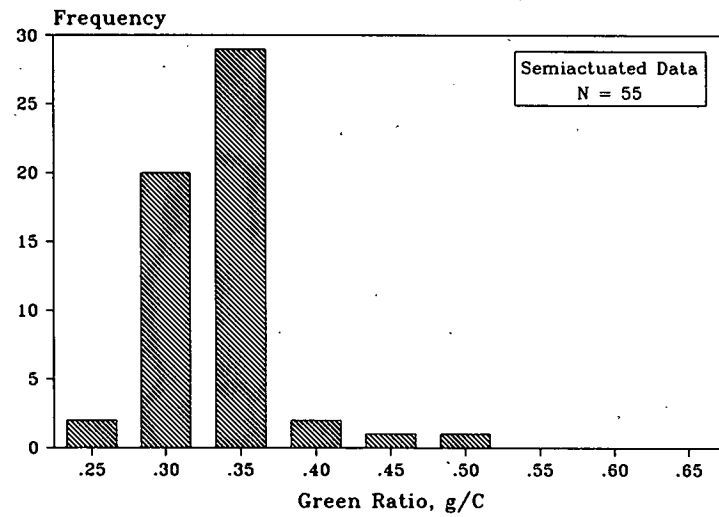


Figure C-6. Frequency Distribution of Import Study Variables, Semiactuated Data Set.

DELAY EQUATION ANALYSIS

The regression analysis examined how well, from statistical and practical points of view, the proposed uniform delay equations were able to predict delays measured in the field under both pretimed and semiactuated operating conditions. This examination was accomplished by first regressing Equations 1 and 2 with the current adjustment factors of 0.38 and 173 against the measured delay. The information resulting from this analysis was then used to determine whether or not any of the assumptions used in the linear regression analysis were violated. This check was done to insure that the results of the regression analysis were appropriately and accurately interpreted.

After the initial analyses were completed, the pretimed data set was broken down into two parts. The first part of the data was used to develop the two sets of least squares fit calibration factors for the uniform and incremental delay terms of the two delay equations. The second part of the data was then used to validate the predictive ability of the two calibrated delay equations using a simple two-tailed T-test for the slope parameter estimate being equal to 1.0. This analysis included a comparison of the delay predictions made by the two calibrated delay equations, each with two sets of adjustment factors, and the delays measured in the field. The same testing procedure was performed on both the pretimed and the semiactuated data. There were not, however, enough semiactuated data to do both calibration and validation analyses; thus, only the validation analysis was performed.

Study Design

The statistical analysis of the delay equations was a combination of linear regression analyses and T-tests. The delay equations were placed into various model forms, based on the different sets of adjustment factors (i.e., 0.38 and 173 or the least squares developed factors), to provide models for the regression analyses. These model forms are described in more detail in the study procedure section. The dependent variable under study in this analysis was the random measured delays from the field study data. The independent variables were the mean predicted delays from the two delay equations. The analysis sought first to determine the predictive ability of the two delay equations using the uniform and incremental delay adjustment factors currently given in the HCM. If these factors proved to be inappropriate, then another set of adjustment factors would be developed by fitting the delay equations to the field data using least squares linear regression analyses.

Statistical Background. Field data often contains variability which either cannot be or is not explained by the variables in an analytical model. Thus, for a given value of mean delay predicted by the delay equations, this unexplained variability shows up as a number of measured delays occurring above and/or below the mean predicted value. In this case, the apparent variation in the values of random measured delay for a given value of mean predicted delay was due to the equation's inability to account for some factor(s) affecting the value of the random measured delay. The predictive ability of the delay equations then became a function of how the assumptions made in developing the model affect the equation's ability to account for the different factors contributing to the random measured delay.

From this explanation, and by definition from least square analyses, it can be said that any point along a regression line comparing random measured delay and mean predicted delay represents an average value of the random measured delay for a given value of predicted delay. The factors affecting delay at signalized intersections are very complex and, given the approximate nature of the equations used in this research, a certain amount of variability was expected. To insure that the equations predicted accurately under different conditions, the statistical tests were performed on each green ratio category, as well as the entire validation data set.

The regression analyses for the delay models were conducted using a no-intercept option in the SAS (26) regression procedure as the interest of the analysis was to determine how much of a contribution the equations made to the explanation of the factors affecting the mean value of the random measured delays. The no-intercept option produced an analysis which had a fixed y-intercept of zero with only the slope of the regression line being allowed to vary. The model's contribution in accounting for the delay-causing factors is explained in terms of a parameter estimate or slope resulting from the least squares regression analysis.

These parameter estimates represent the expected change in the average value of the random measured delay for a unit increase in the value of predicted delay (i.e., the definition of the slope of a line). Thus, if the equations were able to provide a perfect prediction of the average value of the random measured delays for each value of predicted delay, the parameter estimate would equal to 1.0 (i.e., the expected change in the value of average random measured delay would be equal to a unit increase in the predicted value of delay).

The validation or testing procedures, used in determining the predictive ability of the delay equations, consisted of simple (single independent variable) linear regression and T-tests. The uniform and incremental delay terms of the delay models, using the appropriate sets of adjustment factors, were combined prior to the analysis in order to form a single independent variable model. The predictive ability of the two adjusted delay equations was then measured as a function of the parameter estimates (slopes) resulting from the regression analyses.

Given the fact that a perfect delay model would be able to account for all of the factors contributing to the mean value of the random measured delays, a parameter estimate of 1.0 would be the expected result of a regression analysis comparing the random measured and mean predicted delays. Thus, the predictive ability of the delay models could be tested using a simple two-tailed T-test for the parameter estimate being equal to 1.0. The null hypothesis used for this test was that the regression parameter estimates were equal to 1.0. The alternate hypothesis, then, was that the regression parameter estimates were not equal to 1.0.

Confidence Intervals. The parameter estimates developed in the regression analysis were, as the name implies, only estimates of the actual mean values of the random measured delay. The data used to determine the parameter estimates, in this research, are only samples taken from a much larger population.

Thus, any statistical measures obtained from the data were only estimates of the actual value for the entire population. Given this observation, and the previous discussion on variability in field measured data, it is not difficult to imagine how several samples taken from the same population might produce different parameter estimates.

Because of this variation in the parameter estimation, it is often useful to construct a confidence interval on the parameter estimate. This confidence interval is based on the standard error of the regression analysis and the tabular value of a test statistic which is based on a given probability of error. The probability of error is generally given as the percentage of all tests in which the parameter estimates do not reflect the actual value of the population parameter being estimated. The tabular test statistic is multiplied by the standard error from the regression analysis to obtain the value used to construct the confidence interval. This value is added to and subtracted from the parameter estimate to obtain the upper and lower limits of the confidence interval.

The confidence interval forms a set of boundary conditions within which the actual value of the population parameter would be expected to fall (if the null hypothesis holds true). If the null hypothesis for the parameter estimate does not hold true, then the actual value of the population parameter would not be expected to fall within the confidence interval. In this research, confidence intervals are used as an added indication of how well the delay equations are able to predict the actual mean value of the random measured delay. For each parameter estimate calculated, a confidence interval was determined and included with the results.

Analysis Procedures. The initial goal of the statistical analysis was to test the predictive ability of the delay equations using the current adjustment factors for uniform and incremental (0.38 and 173, respectively) delay. Should the results of the regression analysis and T-tests indicate that the new equations were able to accurately predict the mean delay (the null hypothesis holds true), then no further testing would be required. If, however, the results of the analyses showed that the parameter estimates were not equal to 1.0, further analysis would be required using some other adjustment factors.

The second step in the analysis was to check for any violations in the assumptions of linear regression. This check was necessary to insure that the result of the regression analyses provided the most accurate description of the predictive ability of the delay equations possible. Violations of the assumptions of linear regression might require that special corrective measures, such as a weighted least squares, be taken when performing the regression analyses.

Assuming that the null hypothesis was rejected in step one and that no assumptions were violated in step two, the third step in the analysis sought to develop adjustment factors for the incremental term of the delay model only. Fixing the 0.38 factor on the uniform delay term for both of the proposed delay equations, however, required the delay equations be adjusted using only the incremental delay term.

The fourth step in the statistical analysis was designed to develop adjustment factors for both the uniform and incremental delay terms of the delay model. The development of separate

adjustment factors was accomplished by using multiple regression analysis. This analysis required the use of a regression model having one dependent and two independent variables. The two independent variables for this analysis were the unadjusted uniform and incremental terms of the delay models.

The parameter estimates, developed by the multiple regression analysis, for each of the independent variables (uniform delay and incremental delay) represent the expected change in the average value of random measured delay for a unit change in the value of predicted uniform delay with the incremental term being held constant. In simple terms, for a fixed value of predicted incremental delay, the parameter estimate for the predicted uniform delay term is equal to the change in average random measured delay caused by unit change in the delay predicted by the uniform delay term alone.

In statistical terms, these multiple regression parameter estimates are referred to as partial slopes. Because the expected change in average random measured delay for a unit change in the predicted value of delay for one term of the delay model is constant and does not depend on the value of the other term, the effects of the independent variables are assumed to be additive (27). Based on the assumption of additivity, the parameter estimates of the multiple regression analyses then became the adjustment factors for the two terms in the delay models.

HCM Comparison

Initial Analysis. The first step in the statistical analysis was to perform a linear regression on Equations 1 and 2, using the uniform and incremental delay adjustments currently given in the HCM. The resulting parameter estimates were then analyzed to determine how well delays predicted by the new equations with the current adjustments compared to the average values of random measured delay. Table C-1 shows the results of the regression analysis and T-tests performed on the proposed mean delay equations using the full pretimed and semiactuated data sets. Figure C-7 shows, graphically, the location of the regression lines for each delay equation in relation to the perfect prediction line (slope equal to 1.0). The raw data are also plotted in these figures to show their relationship to the regression lines.

It is apparent from the information in the table and figures that the parameter estimates developed using the current uniform and incremental delay adjustments of 0.38 and 173, respectively, are not equal to 1.0, and thus there is sufficient evidence to reject the null hypothesis in all cases. An examination of the R-squares, however, shows that the delay equations do explain a large portion of the variability in the random measured delay. Based on the results given in Table C-1, it was apparent that other adjustment factors were required to obtain more accurate estimates of the mean random measured delay.

Check Assumptions. Before proceeding with additional analysis of the data, the assumptions used in performing the regression analysis were checked to insure that the previous conclusions were valid and data transformations or weighting were not necessary. This check was performed using the pretimed data set and predicted delays from Equations 1 and 2. The primary method of checking these assumptions involves various plots

Table C-1. Results of Regression Analysis for Measured Versus Predicted Delay, $f_u = 0.38$ and $f_l = 173$.

Equation / Interval	Number of Observations	Slope Parameter Estimate	R-Square	Standard Error	Confidence Interval (+/-)	T for Ho: Parameter = 1.0	Level of Significance
PRETIMED							
<i>Equation 1</i>							
All Data	860	0.832	0.89	0.010	0.019	-17.081 *	>0.999
g/C = 0.25	137	0.849	0.89	0.026	0.052	-5.737 *	>0.999
g/C = 0.30	150	0.801	0.91	0.021	0.041	-9.565 *	>0.999
g/C = 0.35	88	0.856	0.93	0.026	0.051	-5.625 *	>0.999
g/C = 0.40	156	0.741	0.91	0.018	0.036	-14.197 *	>0.999
g/C = 0.45	118	0.873	0.84	0.035	0.069	-3.649 *	>0.999
g/C = 0.50	50	0.897	0.91	0.039	0.079	-2.629 *	0.989
g/C = 0.55	75	0.832	0.86	0.039	0.078	-4.280 *	>0.999
g/C = 0.60	86	0.893	0.94	0.025	0.050	-4.216 *	>0.999
<i>Equation 2</i>							
All Data	860	0.843	0.89	0.010	0.020	-15.661 *	>0.999
g/C = 0.25	137	0.862	0.88	0.027	0.053	-5.152 *	>0.999
g/C = 0.30	150	0.819	0.91	0.022	0.043	-8.361 *	>0.999
g/C = 0.35	88	0.865	0.93	0.025	0.050	-5.324 *	>0.999
g/C = 0.40	156	0.748	0.91	0.018	0.037	-13.666 *	>0.999
g/C = 0.45	118	0.883	0.84	0.036	0.070	-3.298 *	0.999
g/C = 0.50	50	0.912	0.91	0.041	0.082	-2.157 *	0.964
g/C = 0.55	75	0.823	0.85	0.041	0.081	-4.339 *	>0.999
g/C = 0.60	86	0.922	0.94	0.026	0.052	-2.964 *	0.996
SEMIACTUATED							
<i>Equation 1</i>							
All Data	55	0.675	0.94	0.025	0.051	-12.805 *	>0.999
g/C = 0.30	20	0.637	0.92	0.043	0.091	-8.434 *	>0.999
g/C = 0.35	29	0.736	0.97	0.025	0.052	-10.419 *	>0.999
<i>Equation 2</i>							
All Data	55	0.687	0.93	0.026	0.053	-11.885 *	>0.999
g/C = 0.30	20	0.644	0.92	0.044	0.092	-8.122 *	>0.999
g/C = 0.35	29	0.756	0.97	0.027	0.055	-9.048 *	>0.999

* Statistically significant difference at the 95 percent confidence level.

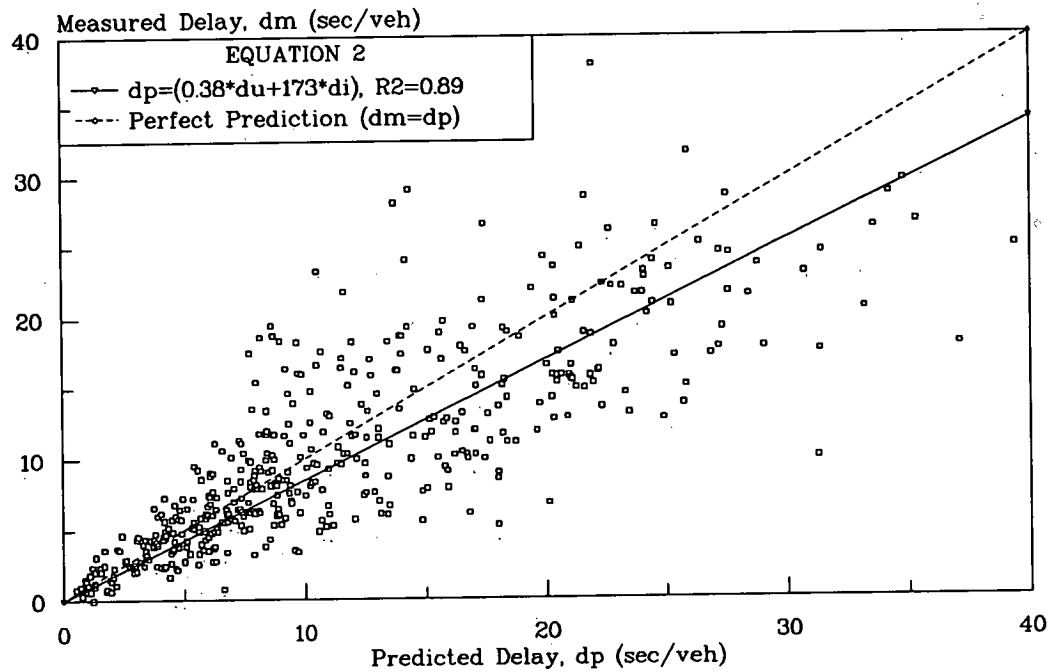
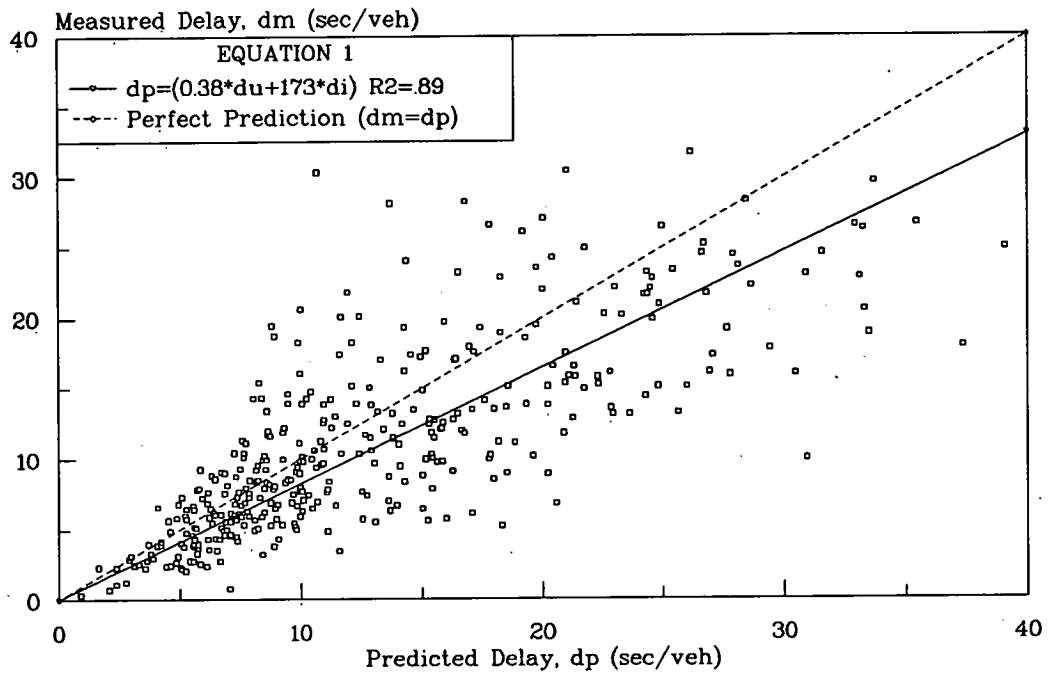


Figure C-7. Comparison of Measured Versus Predicted Delay, HCM Delay Equation.

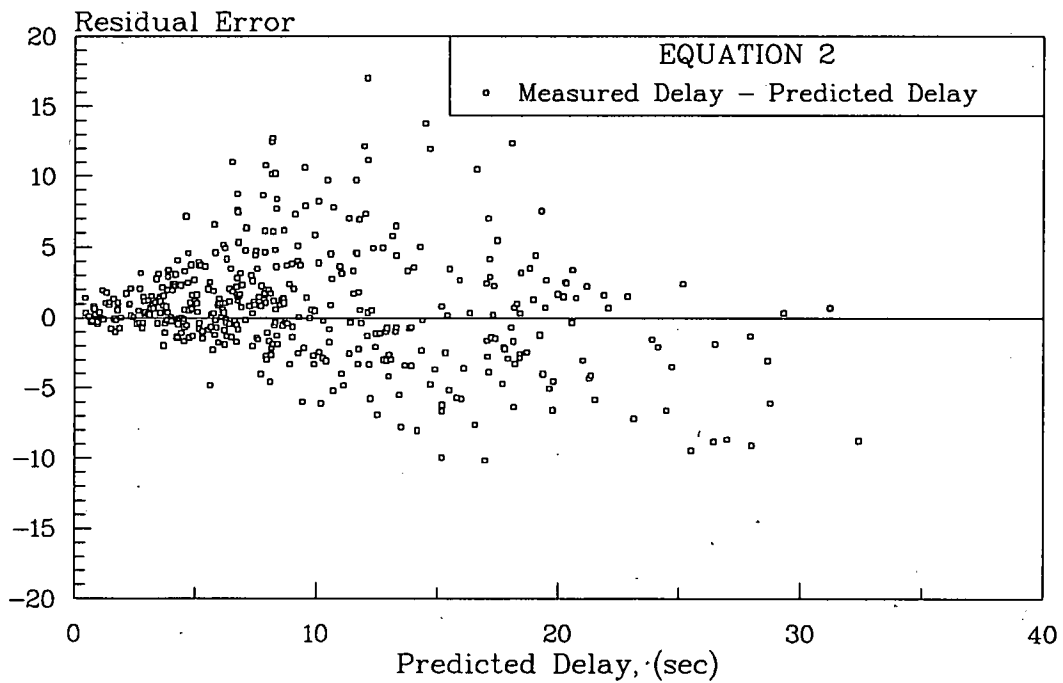
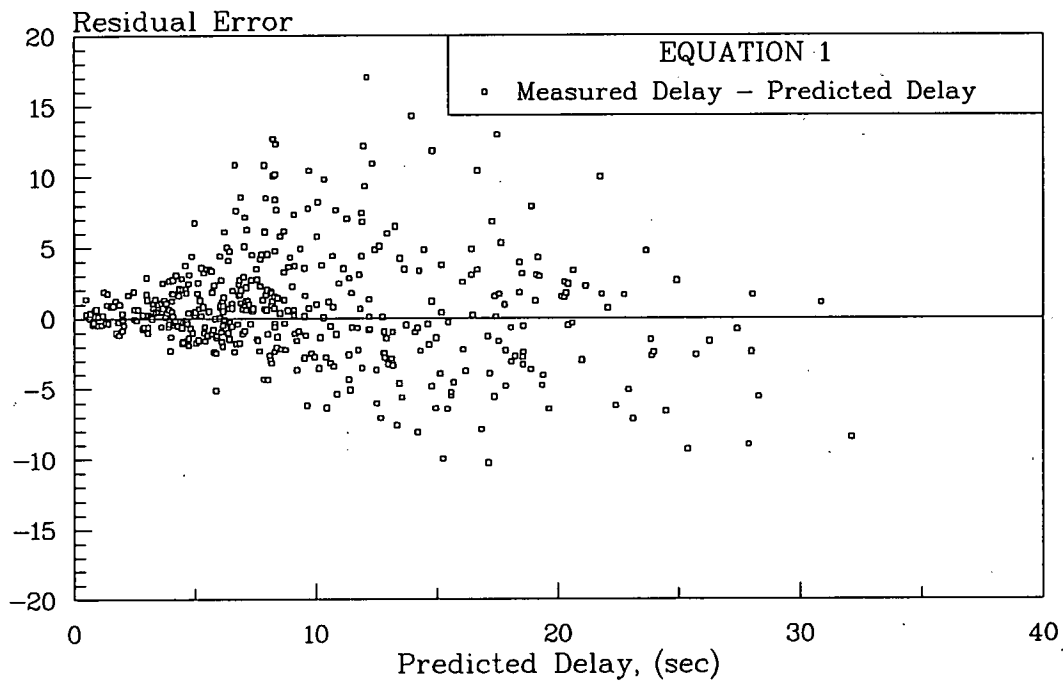


Figure C-8. Residual Errors for Measured and Predicted Delay.

made with the residual errors taken from the regression analysis. The residual error or error of prediction, in this case, is simply the difference between the measured delay and the predicted delay for each observation.

The two assumptions of concern were those of constant variance and normality. Constant variance assumes that the variance of the residual errors is the same for all values of predicted delay. This assumption was checked with a plot of residual error versus the values of predicted delay. This plot would show if there was any increase or decrease in the variance of the residual error for different values of predicted delay. Figure C-8 shows the residual error versus predicted delay plots for Equations 1 and 2. A violation of the constant variance assumption would show a change in the magnitude of scatter about the zero point for changing values of predicted delay. These plots do not show any significant variation in the residual errors, and an overlay of the two plots indicates that the variation for both data sets is the same.

The second assumption that was addressed is that of normal distribution of the residual errors. This assumption was checked by constructing a frequency histogram of the residual errors to reveal any skewness or outliers in the data set. The residual histograms for the two equations are shown in Figure C-9. From this plot, it is apparent that the distributions were normal and there are no significant outliers. Overall, the assumptions of the linear regression analysis were met and further analysis was continued.

Model Calibration

Separating the Data. At this point, it was necessary to separate the pretimed field data into two separate data sets. The data used to develop adjustment factors for the delay equations could not be used to validate their predictive ability and thus two data sets were required. The frequency analysis of the pretimed data broken down by site was used as the basis for determining how to split up the data. Green ratio distribution was used as the primary measure in the selection process. It was desirable to provide as broad a range of operating conditions as possible for both the adjustment factor development and validation data sets and a good distribution of green ratios was considered to provide this range of operating conditions.

Based on the frequency analysis information, the data was separated roughly in half with adjustment factor development and calibration data sets chosen as Houston urban/Los Angeles suburban and Houston suburban/Los Angeles urban, respectively. The Houston urban/Los Angeles suburban data were chosen for the adjustment factor development because of its greater range of green ratios and greater number of observations. The adjustment factors used for Equations 1 and 2 will be given as f_{u1} and f_{i1} , and f_{u2} and f_{i2} , respectively.

Developing Adjustment Factors. The third step in the statistical analysis was to develop an adjustment factor for only the incremental term of the delay models. This task was accomplished by holding the adjustment factor on the uniform delay term at a constant 0.38, then altering the adjustment on the incremental delay term until the regression parameter estimate for the combined terms equaled 1.0. The adjustment factors resulting from this process were then used to test the predictive ability of the two delay equations using the pretimed test and semiactuated data sets.

The fourth step in the analysis was to develop separate adjustment factors for both terms of the delay model using a least squares fit of each term. In order to obtain these factors, it was necessary to perform a multiple regression analysis on the separated and unadjusted uniform and incremental delay terms of the two delay models. This analysis produced parameter estimates for the two independent variables (the uniform and incremental delay terms) of the regression model. These two parameter estimates were then used as the adjustment factors for the two terms of the delay equations. The newly adjusted uniform and incremental delay terms were then combined to form the single independent variable model required for the testing analysis. The single variable delay models for each equation were then tested using the pretimed validation and semiactuated data sets.

An additional step performed at this point was to regress each delay equation against itself using the two different sets of least squares adjustment factors. This analysis was performed to determine whether or not there was any difference in the mean delay predictions made by the two delay models when using the different adjustment factors.

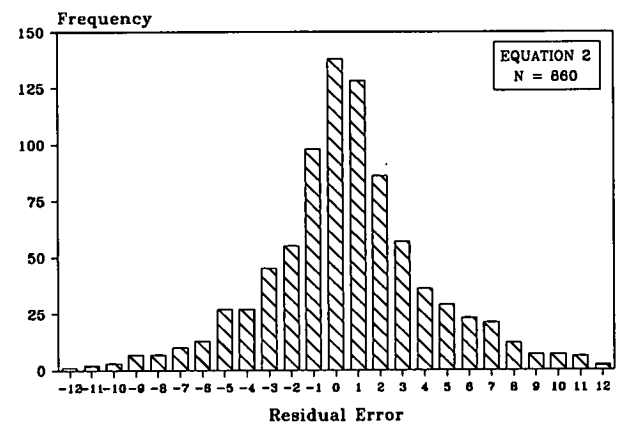
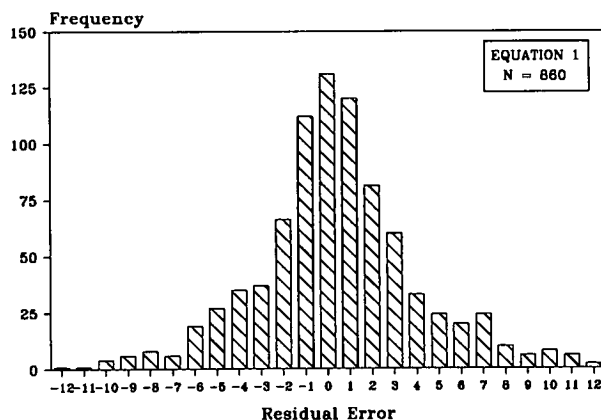


Figure C-9. Frequency Distribution of Residual Errors for Measured and Predicted Delays.

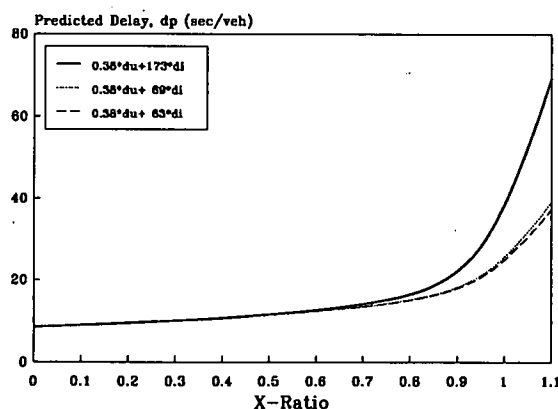
Results of Delay Equation Analysis

The adjustment factors resulting from the least squares adjustment factors analyses described in Steps 3 and 4 of the analysis procedures section are given in Table C-2. From this table, it is apparent that the least squares adjustments developed for the uniform delay terms of Equations 1 and 2 in Step 4 (the lower half of the table) of the analysis were essentially the same as the adjustment used on the HCM uniform delay term (0.38). The adjustment for Equation 1 in the lower half of the table was actually higher than shown in the table, but it does round to 0.38. This slight increase is reflected in the different incremental adjustments in the upper and lower portions of the table, for Equation 1, when using what appears to be the same 0.38 adjustment. This similarity in adjustment factors would seem to indicate that the delays predicted when using Equation 1 are virtually the same for each set of adjustment factors.

The least squares adjustment developed for the uniform delay term of Equation 2 was also greater than the value given in the lower half of Table C-2, but it rounds down to 0.39. The decrease in the adjustments for the incremental term of Equation 2, when combined with the increase in the adjustment for the uniform delay term, would seem to indicate that the two sets of adjustments will result in similar delay predictions.

The rather large decrease in all of the adjustments for the incremental delay term, from the current HCM value of 173, is probably due to the lack of high X-ratio, overflow delay observations in the field data set. The high X-ratio conditions that were observed in the field did not persist long enough to achieve steady state operation. Steady state operation was one of the assumptions used in the development of the delay models.

The effects of the different adjustment factor sets on the delay predictions of Equations 1 and 2 are shown in Figure C-10. These figures show how the current incremental delay adjustment of 173 predicts significantly higher delays at X-ratios over 0.9 than the adjustment factors developed using least squares regression.



Model Validation

The final step in this analysis fitted the calibrated delay models to the pretimed validation and semiactuated data sets and then compared the two delay equations to each other using the different adjustment factors. The first task was accomplished by simply substituting the calibrated delay equations into the regression model as the independent variable and running the model on both the pretimed calibration and semiactuated data sets. This task resulted in four separate analyses for each data set, i.e., there was one analysis for each combination of Equations 1 and 2 and

Table C-2. Calibration Factors Derived from Least Squares Analysis.

Analysis	Equation	f_u	f_i
0.38 fixed d_i varied	Equation 1	0.38	69
	Equation 2	0.38	81
d_u and d_i varied	Equation 1	0.38	63
	Equation 2	0.39	67

alternative adjustment factors. To test the effects of the different adjustment factors, each delay equation was then regressed against itself using the different adjustment factors. This part of the analysis was designed to determine what effect the different adjustment factors had on the predictions made by each equation and involved only the pretimed validation data set.

Figures C-11 and C-12 are included for the purpose of illustrating the relationship between the line with slope parameter equal to 1.0 and the lines formed by the regression analysis parameter estimates for each delay equation adjustment factor combination given in Table C-2. These plots show the regression information for the pretimed validation data set. With these plots, it is somewhat easier to visualize how having slopes greater or less than one affects whether the delay models are predicting mean delays that are either too low or too high. By visual examination of these plots, it would be expected that the null hypothesis holds true for the T-tests conducted on the data represented in the plots. The plots also show the variability in the random measured delays.

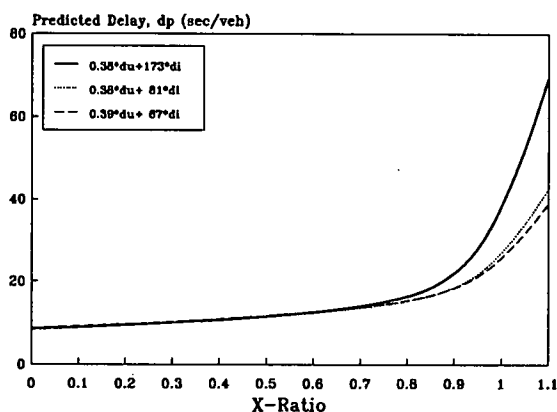


Figure C-10. Comparison of HCM and Calibrated Delay Equations.

Tables C-3 and C-4 summarize the results for the regression analysis and T-tests described in Steps 3 and 4 of the analysis procedures section. Table C-3 shows the results of Step 3 of the analysis (using a 0.38 adjustment fixed on the uniform delay term) on Equations 1 and 2 while Table C-4 shows the same results using the least squares fit adjustments for both the uniform and incremental delay terms. The results given in Tables C-3 and C-4 show that the null hypothesis is not rejected in most of the tests conducted on the pretimed validation data set. In addition to the T-test results, the R-square values show that the equations fit the data very well. The failure of the null hypothesis, in the cases given for the pretimed data, could be the result of conditions at the site where the observations were collected. Research by Rouphail (22) indicates that it is possible to observe different delays for the same set of operating conditions. The difference in the delays is caused by the platoon of vehicles arriving at different points during the cycle of the downstream intersection. If a set of random measured delays contained only observations with arrivals at one particular point during the cycle, a possible failure of the null hypothesis would be expected. In order to account for the effects of these different arrivals, it would be necessary to develop additional factors for adjusting the delay equations.

The test results for the semiactuated data in Tables C-3 and C-4 do, however, present some possible problems. Table C-3 shows that the null hypothesis is rejected in all cases when testing the semiactuated data, even though the equations fit the semiactuated data better than the pretimed data (i.e., the equations explain more of the variability in the semiactuated data than the pretimed data). When both terms of the delay equations use the least squares developed adjustment factors, as shown in the bottom of Table C-4, there is some improvement in the mean delay predictions made by the equations. This result was expected given the fact that the regression program was allowed to fit each term of the model separately, thus accounting for a larger portion of the variation in the values of the random measured delays.

Because it was not possible to both develop adjustment factors for and test the semiactuated data set, it is possible that the adjustments developed for the pretimed data set are not appropriate. There is also a potential for problems in the small size of the data set and the fact that the semiactuated data was only collected

on one day at one of the sites. The conditions under which the semiactuated data were collected do not represent a very broad range of conditions and, as a result, may contain some bias (i.e., arrival time).

Table C-5 summarizes the results of the comparison between the different adjustment factors for each equation on the pretimed test data set. The results of the T-tests indicate that the least squares developed adjustment factors will generally produce statistically different estimates of the actual mean value of delay. Visual inspection of the parameter estimates and standard errors, however, indicates that these differences are not practically significant. For practical purposes then, the mean delay estimates produced, when using the two different sets of least squares adjustments, are the same.

Conclusions

There appears to be very little difference in the predictive ability of either of the two equations for either set of adjustment factors. The predictive ability of the equations using the 173 adjustment on the incremental delay term, however, might be better in the presence of high X-ratio overflow delay observations. Conversely, the predictions made using the least squares adjustments might be outside the acceptable error limits given the same high X-ratio overflow delay conditions.

The proposed delay equations show some error in prediction; but, given their simplicity and intended usage, this error is within practical limits. The practical limits established for the validation of these equations describe how much error can be expected in the equations; thus, it is possible to determine a confidence interval for any value of predicted delay.

Both equations contain a term for the inclusion of a continuous progression adjustment factor, eliminating the need for a separate table or set of equations. This fact in itself should be seen as a major advantage in the consideration of their future application. In summary, either equation would provide a suitable replacement for the HCM equation. Equation 1, using the current uniform delay adjustment of 0.38, is recommended for subsequent use because of its greater simplicity.

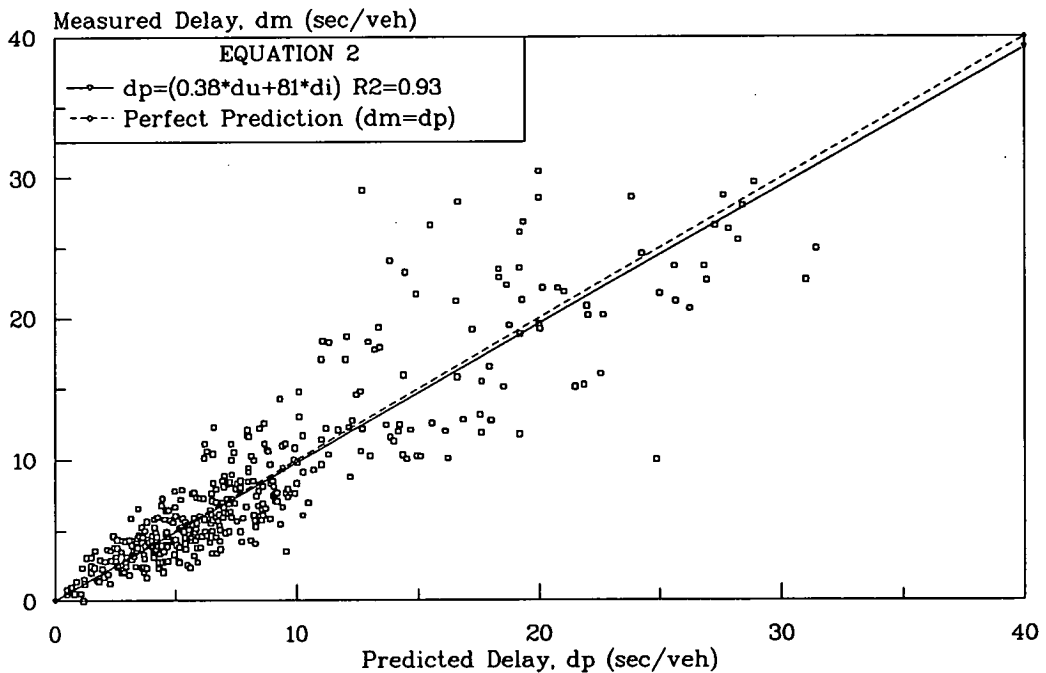
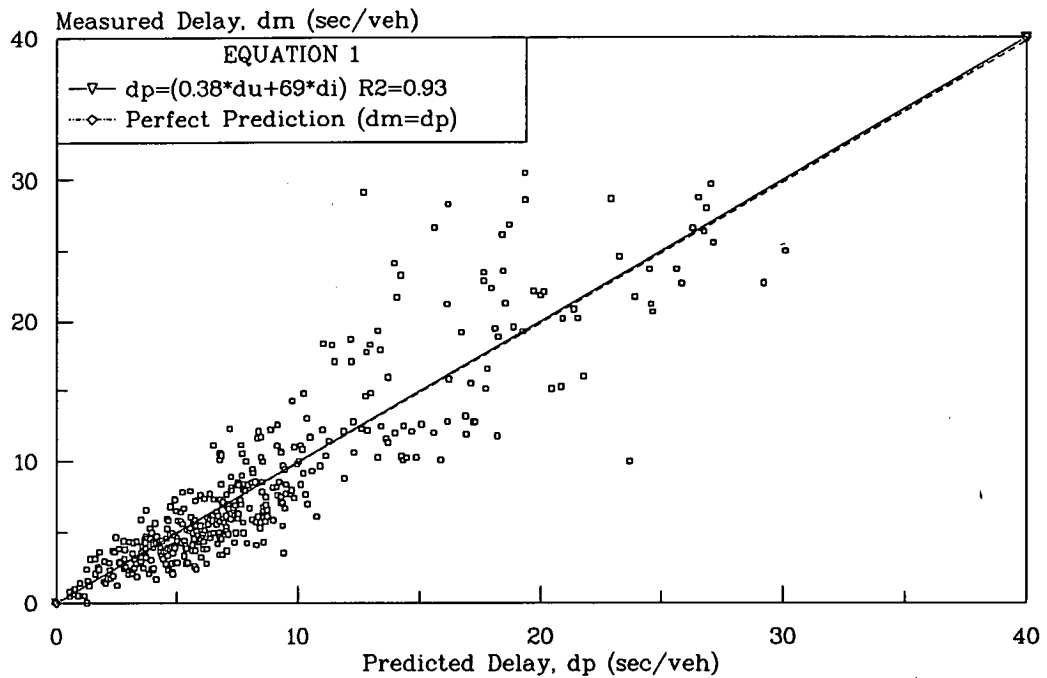


Figure C-11. Comparison of Measured Versus Predicted Delay, Calibrated Delay Equations, $f_u = 0.38$ and f_i Variable

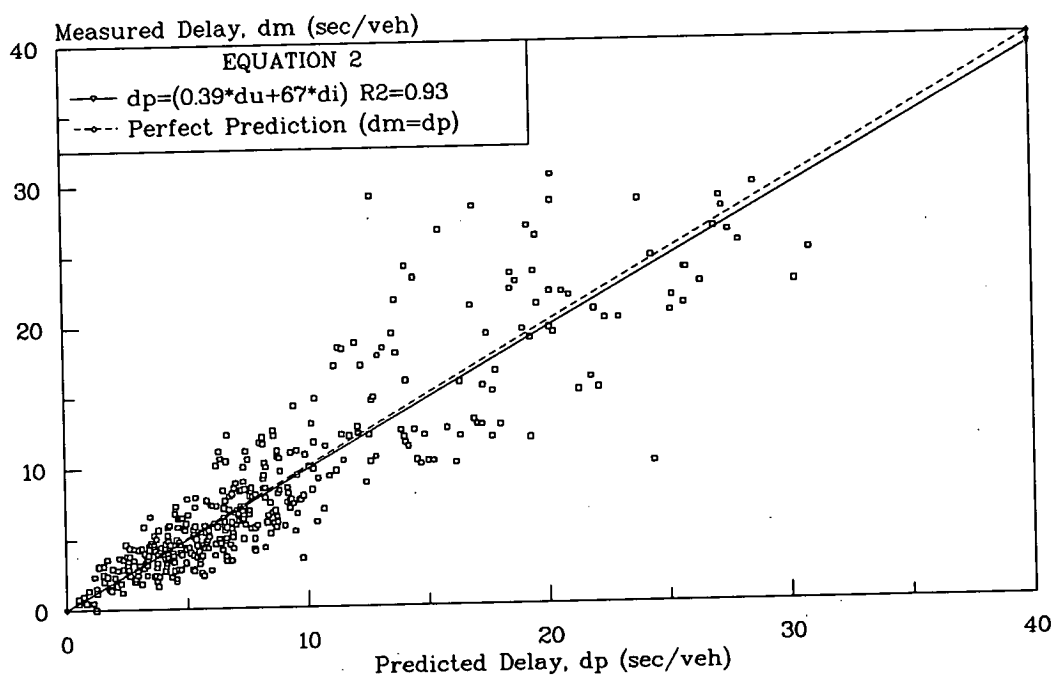
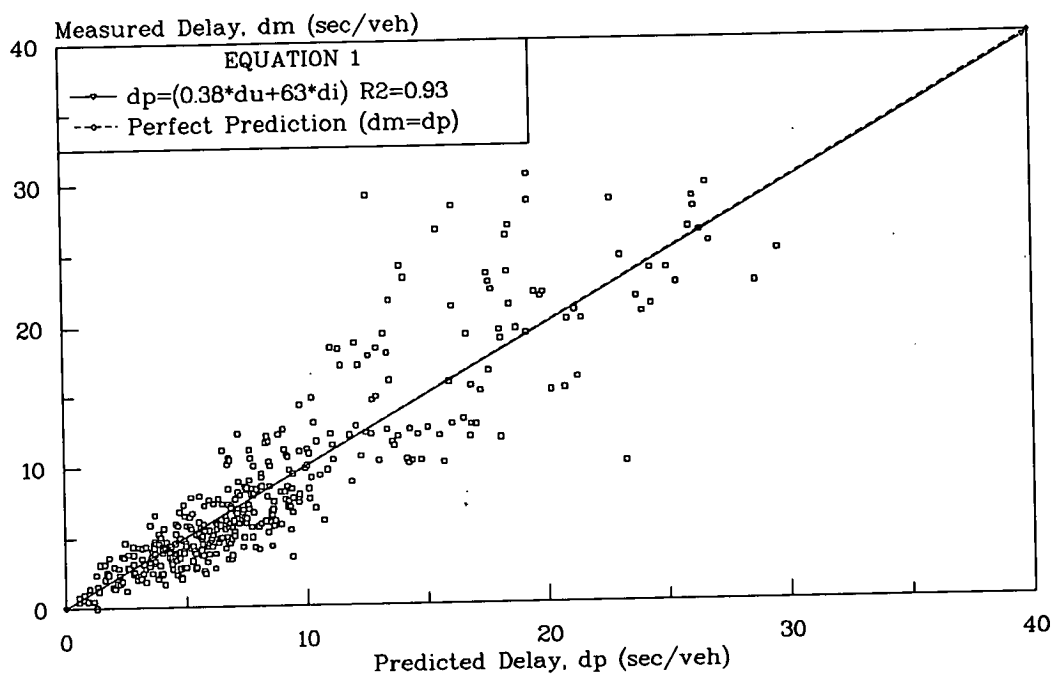


Figure C-12. Comparison of Measured Versus Predicted Delay, Calibrated Delay Equations, f_u and f_l Variable

Table C-3. Results of Regression Analysis for Measured Versus Predicted Delay, $f_u = 0.38$ and f_l Variable.

Equation/Interval	Number of Observations	Slope Parameter Estimate	R-Square	Standard Error	Confidence Interval (+/-)	T for Ho: Parameter = 1.0	Level of Significance
PRETIMED							
<i>Equation 1</i>							
Test Data	391	0.996	0.93	0.014	0.028	-0.308	0.242
$g/C = 0.35$	29	1.128	0.95	0.047	0.097	2.704 *	0.988
$g/C = 0.40$	126	0.910	0.95	0.018	0.035	-5.057 *	>0.999
$g/C = 0.45$	88	0.964	0.93	0.028	0.055	-1.320	0.810
$g/C = 0.50$	45	1.055	0.94	0.040	0.08	1.380	0.825
$g/C = 0.55$	43	0.931	0.88	0.054	0.108	-1.284	0.794
$g/C = 0.60$	60	0.984	0.93	0.036	0.072	-0.450	0.346
<i>Equation 2</i>							
Test Data	391	0.980	0.93	0.014	0.028	-1.420	0.844
$g/C = 0.35$	29	1.087	0.95	0.046	0.095	1.888	0.931
$g/C = 0.40$	126	0.910	0.96	0.018	0.035	-4.873 *	>0.999
$g/C = 0.45$	88	0.952	0.93	0.028	0.056	-1.723	0.912
$g/C = 0.50$	45	1.054	0.93	0.042	0.085	1.280	0.793
$g/C = 0.55$	43	0.900	0.87	0.054	0.108	-1.857	0.930
$g/C = 0.60$	60	1.018	0.92	0.039	0.078	0.471	0.361
SEMIACTUATED							
<i>Equation 1</i>							
All Data	49	0.905	0.96	0.027	0.054	-3.540 *	>0.999
$g/C = 0.30$	20	0.896	0.95	0.045	0.094	-2.323 *	0.969
$g/C = 0.35$	29	0.917	0.97	0.033	0.067	-2.558 *	0.984
<i>Equation 2</i>							
All Data	49	0.893	0.96	0.028	0.055	-3.894 *	>0.999
$g/C = 0.30$	20	0.871	0.95	0.046	0.096	-2.847 *	0.990
$g/C = 0.35$	29	0.924	0.97	0.033	0.068	-2.312 *	0.972

* Statistically significant difference at the 95 percent confidence level.

Table C-4. Results of Regression Analysis for Measured Versus Predicted Delay, f_u and f_l Variable.

Equation / Interval	Number of Observations	Slope Parameter Estimate	R-Square	Standard Error	Confidence Interval (+/-)	T for Ho: Parameter = 1.0	Level of Significance
PRETIMED							
<i>Equation 1</i>							
Test Data	391	1.006	0.93	0.014	0.028	0.419	0.325
$g/C = 0.35$	29	1.137	0.95	0.048	0.098	2.871 *	0.992
$g/C = 0.40$	126	0.918	0.95	0.018	0.036	-4.569 *	>0.999
$g/C = 0.45$	88	0.977	0.93	0.028	0.055	-0.823	0.587
$g/C = 0.50$	45	1.064	0.94	0.040	0.080	1.616	0.887
$g/C = 0.55$	43	0.941	0.88	0.054	0.109	-1.085	0.716
$g/C = 0.60$	60	0.992	0.93	0.036	0.072	-0.217	0.171
<i>Equation 2</i>							
Test Data	391	0.981	0.93	0.014	0.027	-1.364	0.827
$g/C = 0.35$	29	1.081	0.95	0.046	0.094	1.755	0.910
$g/C = 0.40$	126	0.910	0.95	0.018	0.035	-5.034 *	>0.999
$g/C = 0.45$	88	0.963	0.93	0.028	0.055	-1.352	0.820
$g/C = 0.50$	45	1.052	0.94	0.041	0.083	1.248	0.781
$g/C = 0.55$	43	0.903	0.87	0.053	0.108	-1.828	0.925
$g/C = 0.60$	60	1.016	0.92	0.039	0.077	0.411	0.317
SEMIACTUATED							
<i>Equation 1</i>							
All Data	49	0.922	0.96	0.027	0.054	-2.877 *	0.994
$g/C = 0.30$	20	0.916	0.96	0.045	0.094	-1.863	0.922
$g/C = 0.35$	29	0.929	0.97	0.034	0.069	-2.118 *	0.957
<i>Equation 2</i>							
All Data	49	0.915	0.96	0.027	0.055	-3.132 *	0.997
$g/C = 0.30$	20	0.900	0.96	0.044	0.093	-2.251 *	0.964
$g/C = 0.35$	29	0.934	0.96	0.034	0.070	-1.935	0.937

* Statistically significant difference at the 95 percent confidence level.

Table C-5. Results of Regression Analysis for Predicted Delay from Equation 1 Versus Predicted Delay from Equation 2.

Equation / Interval	Number of Observations	Slope Parameter Estimate	R-Square	Standard Error	Confidence Interval (+/-)	T for Ho: Parameter = 1.0	Level of Significance
<i>Equation 1</i>							
Test Data	391	1.015	1.00	0.002	0.004	7.662 *	>0.999
g/C = 0.35	29	0.987	1.00	0.005	0.009	-2.986 *	0.994
g/C = 0.40	126	1.029	1.00	0.003	0.006	9.916 *	>0.999
g/C = 0.45	88	1.030	1.00	0.004	0.007	8.545 *	>0.999
g/C = 0.50	45	1.029	1.00	0.007	0.013	4.468 *	>0.999
g/C = 0.55	43	1.001	1.00	0.005	0.010	0.292	0.228
g/C = 0.60	60	1.066	1.00	0.005	0.009	14.421 *	>0.999
<i>Equation 2</i>							
Test Data	391	1.004	1.00	0.002	0.004	2.122 *	0.966
g/C = 0.35	29	0.973	1.00	0.006	0.013	-4.379 *	>0.999
g/C = 0.40	126	1.017	1.00	0.003	0.006	5.188 *	>0.999
g/C = 0.45	88	1.025	1.00	0.004	0.007	6.867 *	>0.999
g/C = 0.50	45	1.016	1.00	0.007	0.014	2.401 *	0.979
g/C = 0.55	43	0.992	1.00	0.005	0.009	-1.732	0.909
g/C = 0.60	60	1.052	1.00	0.004	0.009	11.927 *	>0.999

* Statistically significant difference at the 95 percent confidence level.

PROGRESSION FACTOR ANALYSIS

The progression factor (PF) analysis determined how the progression factors calculated from the field data (observed progression factors) compared to progression factors calculated from the analytical equations (analytical progression factors). Equation C-9, with $f_{u1} = 0.38$ and $f_i = 69$, was used to calculate the progression factors embedded in the pretimed and semiactuated field data. This equation/adjustment factor combination was chosen because it proved to be a good predictor of delay and retained the HCM's uniform delay adjustment factor.

Arrival Types

As mentioned earlier in this report, the proportion of the total volume arriving on green, P , is recommended as a replacement for platoon ratio when describing quality of progression. The rationale behind this recommendation is the use of fixed boundary conditions for P (between 0.0 and 1.0), whereas the boundary conditions for platoon ratio are dependent on the green ratio. One complication of this recommendation is that when examining a plot of measured delay, d_m , or progression factors, PF, versus P , it is possible to observe different values of d_m or PF for a given value of P . This effect, as noted in the simulation analysis, is caused by the point in time at which the front and rear of the platoon arrives at the downstream intersection. In other words, the observed delay for a given P depends on whether the platoon's arrival is before or after the start of green (i.e., early or

late arrivals). As a result, it was necessary to develop some method of identifying whether the observations represented in the data set were early or late arrivals.

Figure C-13 and Table C-6 illustrate the methodology and relationships used in determining these "arrival type" designations. This methodology is similar in concept to that used in the 1985 HCM(1), but the actual designation of arrival types is different. Basically, the travel time and offset data collected during the field studies were used to determine the time, relative to the start of green, that the lead vehicles in the platoon should have arrived at the downstream intersection. The green and red times for the observed cycle length were then divided into thirds as shown in the figure. This division resulted in six arrival type designations with a seventh arrival type designation added to cover vehicles arriving near the start of green, i.e., perfect progression.

Simply comparing the arrival time to the segregated green and red times, however, results in arrival type estimates that were dependent on the cycle length. By dividing the length of green and red intervals and the arrival time by the cycle length, a more generic arrival type designation was achieved. In other words, the vehicles were said to arrive before or after the start of green by a certain percentage of the total cycle length. Arrival Type 4, however, was not designated by a percentage of the cycle length, but instead represented the start of green plus or minus 2 seconds. This arrival type represented the least amount of and

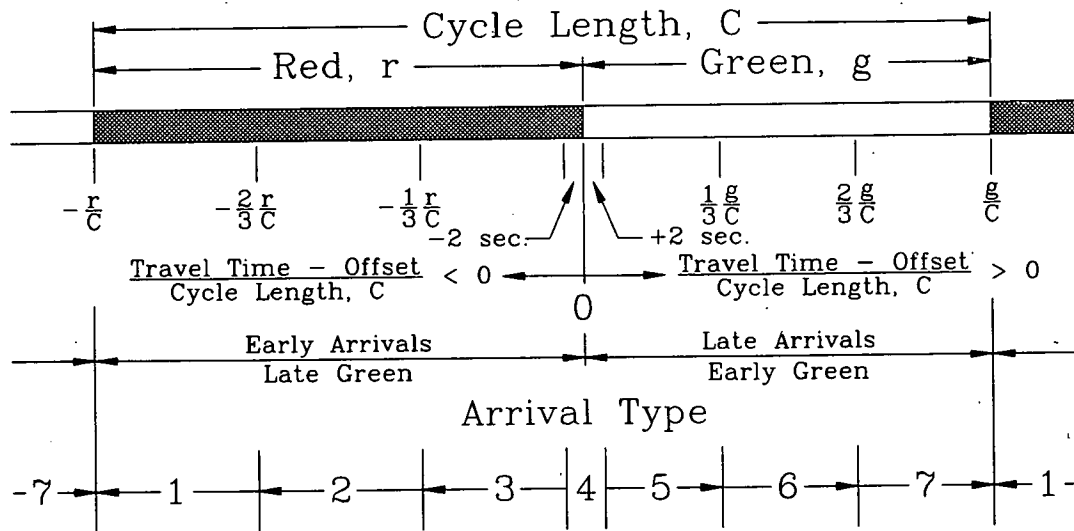


Figure C-13. Pictorial Representation of Arrival Type Designations.

Table C-6. Relationship Between Arrival Type and Platoon's Arrival at the Downstream Intersection.

Arrival Type	Progression Type	Description	
1	Bad	Front of platoon arrives during first third of red.	} Early Arrivals or Late Green
2	Poor	Front of platoon arrives during middle third of red.	
3	Good	Front of platoon arrives during last third of red.	
4	Perfect	Front of platoon arrives near the start of green.	
5	Good	Front of platoon arrives during first third of green.	} Late Arrivals or Early Green
6	Poor	Front of platoon arrives during middle third of green.	
7	Bad	Front of platoon arrives during last third of green.	

variation in delay for a platoon arriving at the downstream intersection. Figure C-13 also shows the relationship between early arrivals/late green and late arrivals/early green. Arrival Types 1, 2, and 3 represent early arrivals or a late green while Arrival Types 5, 6, and 7 represent late arrivals or an early green. Note that this relationship is cyclic, i.e., vehicles arriving before the start of red can also be thought of as vehicles arriving at the end of green.

Figure C-14 is an illustration of this concept that was developed from results of the simulation analysis presented earlier in the report. The arrival type point symbols used on the plot are actual data points from the simulation analysis and illustrate how different delays could be measured for the same value of P . The entire set of data points form a boundary or envelope within which measured delays are expected to fall, and the location of delays within the envelope are a function of when the platoon of vehicles

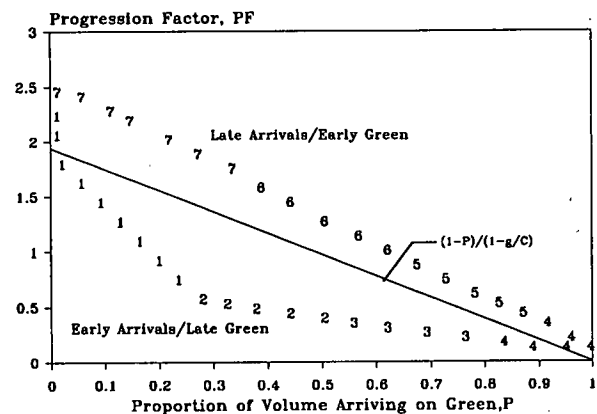


Figure C-14. Effects of Early and Late Platoon Arrivals on Progression Factors.

arrives at the downstream intersection. Arrival Types of 1, 2, and 3 (early arrivals) represent the lower than expected delays on the bottom of the envelope while the Arrival Types of 5, 6, and 7 (late arrivals) represent the higher than expected delays on the upper portion of the envelope.

The solid line shown in Figure C-14 represents the progression factors predicted by the analytical equation, $PF = (1 - P) / (1 - g/C)$. Any point along this line represents an average progression factor for the given value of P . It is this average value of PF that up to this point has been used in the various delay equation and progression factor tables. From this figure, however, it is apparent that any data set containing disproportionate numbers of early or late arrivals would produce regression analysis parameter estimates (slopes) different than that given by the analytical equation. For example, a data set containing a high percentage of early arriving platoons would produce a regression line with a slope less than that predicted by the analytical equation, and a data set containing a high percentage of late arriving platoons would produce a regression line with a slope greater than that predicted by the analytical equation. With this information in mind, a frequency analysis of arrival types should give an indication of how close and in which direction the parameter estimates for the regression and analytical lines would be expected to fall.

Study Procedure

The first step in this analysis was to calculate the observed progression factors for both the pretimed and semiactuated data sets. This calculation was accomplished by entering the progression factor equations (Equations C-9 and C-10) into SAS and running the program to solve for an observed progression factor for each value of measured delay. SAS was then run using a series of statements, based on Figure C-13, to estimate the arrival type for each measured delay.

The next step in the analysis was to develop frequency distributions for the seven arrival types. Histograms were prepared for the entire pretimed and semiactuated data sets and also for each green ratio contained in the two data sets. The data sets were broken down by green ratio because the analytical equation indicates that the progression factor is a function of green ratio and

thus each green ratio will have a different set of progression factors.

Regression analyses were then performed for each green ratio in the two data sets. These analyses used the proportion of the total volume arriving on green (a field-measured value) as the independent variable and observed progression factor as the dependent variable. The result of these analyses was a slope parameter estimate for each value of green ratio. This parameter estimate was then compared to the slope produced by the analytical equation for the same green ratio. Simple two-tailed T-tests at the 95 percent confidence level were used to test whether the parameter estimates were equal.

Results

Figure C-15 shows the frequency distribution of arrival types for the pretimed and semiactuated data sets. The pretimed plot indicates that there were some observations for each of the seven arrival types. The bulk of the observations, however, could be classified as Arrival Types 3, 4, and 5, i.e., good progression. These three arrival types are expected to produce relatively low delays given the information in Table C-6 and Figure C-14. These results confirm the observation that the data were collected under conditions of good progression and low delays. The relatively few number of observations for Arrival Type 4 is the result of its covering a disproportionately smaller amount of the cycle length than the other arrival types. The semiactuated data set frequency plot in Figure C-15 shows that the arrival types for the semiactuated data only covered a range from Arrival Type 2 to 5, with most of the observations occurring for Arrival Types 3 and 4 (early arrivals). From this distribution of arrival types, the slopes for the regression lines from the semiactuated data were expected to be less than the slopes of the analytical lines.

Table C-7 gives the results of the regression analysis and T-test for the pretimed and semiactuated data sets. For the pretimed data, four of the eight green ratios tested showed that the parameter estimates for the observed PF regression line and the analytical line were equal. The R-squares for these tests are all greater than or equal to 0.88, which indicates that the regression line satisfactorily explains the variability in the observed progres-

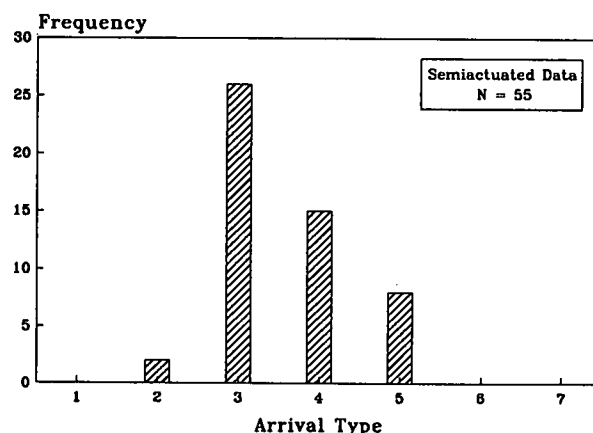
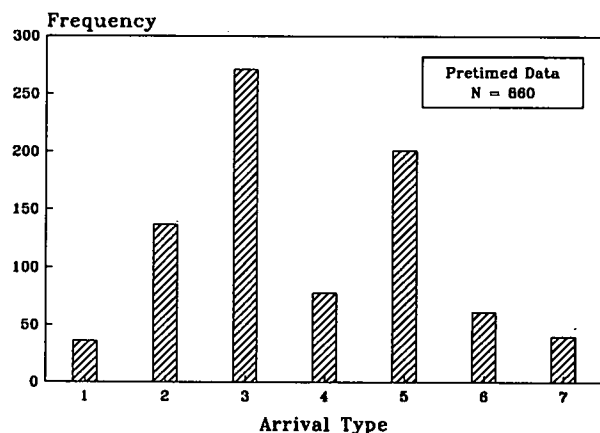


Figure C-15. Frequency Distribution of Arrival Types for Pretimed and Semiactuated Data Sets.

sion factors. It should be mentioned, however, that some of the difference between the two slopes may be due to possible inaccuracies in the delay equation (more specifically the incremental delay term) used to calculate the progression factors. The semiactuated data, as expected, showed that the slopes for the regression lines were lower than those for the analytical line. The R-squares for this semiactuated data, however, were higher than those for the pretimed data. This observation is a result of there being less variability in the semiactuated data set.

Figures C-16 through C-20 illustrate the relationship between the different arrival types, regression lines, simulation envelopes, and arrival type frequency distribution for each green ratio in the pretimed and semiactuated data sets. Each graph shows the raw data points, least squares regression line, analytical line, and simulation envelope for a given green ratio. To the right of each graph is the frequency distribution for the arrival types observed at that green ratio. With these plots, it is easier to visualize how the variation in the distribution of arrival types effects the relationship between the observed regression line and the analytical line. The plots for the pretimed green ratios of 0.25, 0.35, 0.40, and 0.50, and semiactuated green ratio of 0.35, for which the null hypothesis was rejected, all show a disproportionate amount of either early or late arrivals.

Another observation which can be made from these plots is the change in the boundary conditions of the simulation envelopes for the different green ratios. The lower limit of P for the simulated boundaries in these plots increases as the green ratio

increases indicating that, for a given platoon, it becomes more difficult to obtain low Ps at high g/Cs. This trend is further supported by the increase in the lowest measured Ps at high g/Cs in the field data. Given some basic mathematical estimations of flow rate over time for a platoon of a given length and density, this relationship should not be surprising. In simple terms, the longer the green the shorter the red, and the shorter the red, the fewer the number of vehicles that can arrive on red.

Figures C-16 through C-20 show some mixing of the arrival types caused by the travel time values used, the effects of platoon dispersion, and the fact that many of the observations (especially for Arrival Types 3, 4, and 5) occur on the boundaries set up for the different arrival types. The travel times used for the estimation of arrival type were based on average estimates for each time period of each direction at each study site and, as a result, contain some error when applied over the full data set. The effects of platoon dispersion can be characterized as producing different Ps for a given value of arrival type. For example, a platoon with an Arrival Type 4 and a large amount of dispersion has a lower P than the same platoon with a lesser amount of dispersion. In regard to the different arrival types, Figure C-21 shows a frequency analysis of travel time minus offset for a range of plus or minus 15 seconds. As shown, a significant number of observations occur near the boundaries between Arrival Types 3 and 4, and 4 and 5 (plus or minus 2 seconds of perfect progression). The closeness of these values is expected to produce some mixing because the data are continuous and not discrete for each arrival type.

Table C-7. Results of Regression Analysis for Observed Versus Predicted Progression Factors.

Green Ratio	Number of Observations	Slope Parameter Estimate	R-Square	Standard Error	Confidence Interval (+/-)	T for Ho: Parameter = 1.0	Level of Significance
PRETIMED							
0.25	137	1.12	0.88	0.0354	0.07	3.342 *	0.999
0.30	150	0.98	0.87	0.0315	0.06	-0.665	0.493
0.35	88	1.09	0.94	0.0307	0.06	3.038 *	0.997
0.40	154	0.82	0.92	0.0200	0.04	-9.140 *	>0.999
0.45	113	1.06	0.87	0.0383	0.08	1.594	0.886
0.50	46	1.09	0.93	0.0431	0.09	2.072 *	0.956
0.55	75	1.04	0.88	0.0454	0.09	0.884	0.599
0.60	83	1.02	0.92	0.0319	0.06	0.758	0.549
SEMIACTUATED							
0.30	20	0.90	0.93	0.0571	0.12	-1.826 *	0.916
0.35	29	0.89	0.95	0.0390	0.08	-2.869	0.992

* Statistically significant difference at the 95 percent confidence level.

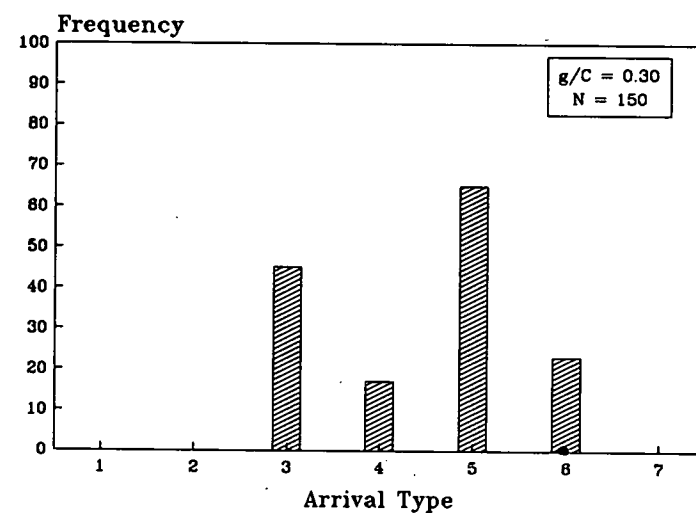
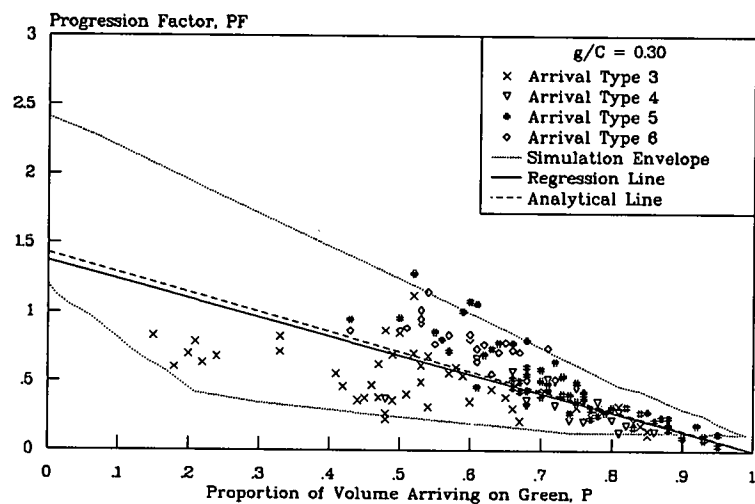
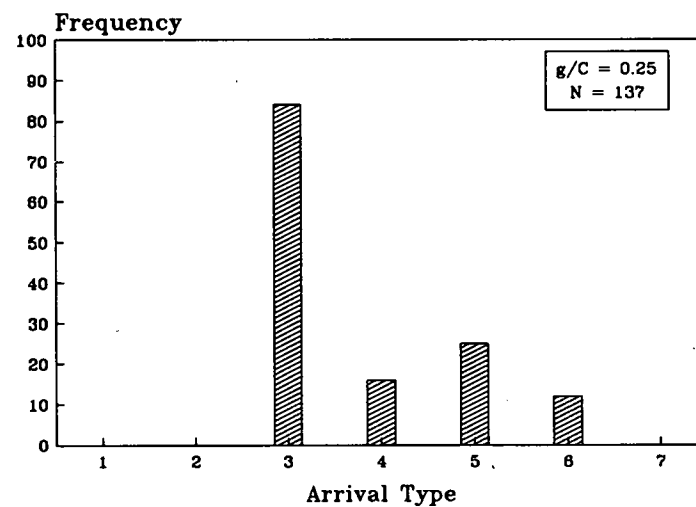
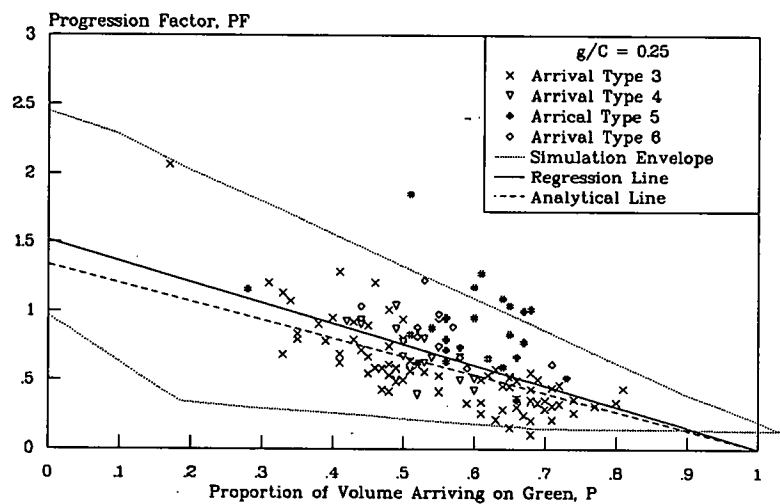


Figure C-16. Relationship Between Progression Factors and Proportion Total Volume Arriving on Green, g/C of 0.25 and 0.30.

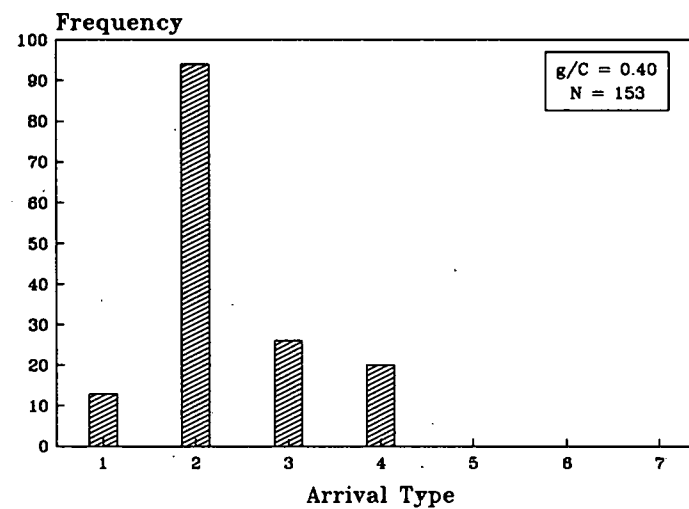
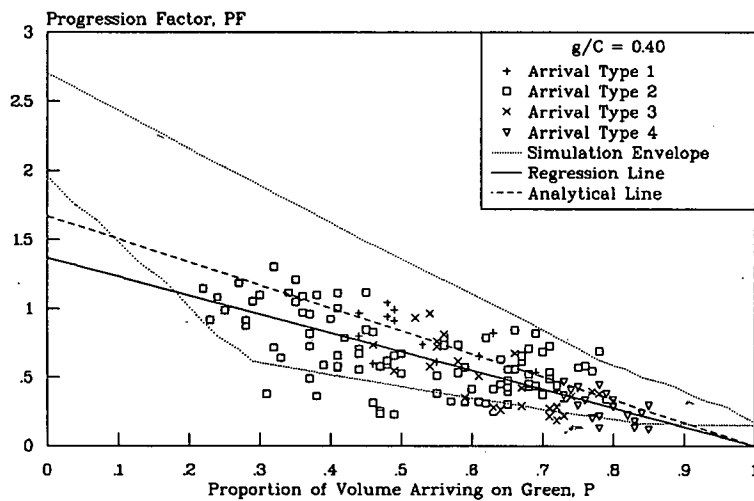
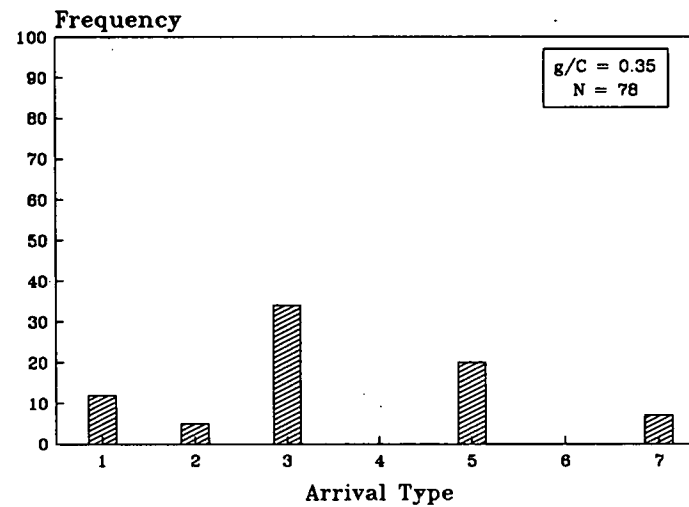
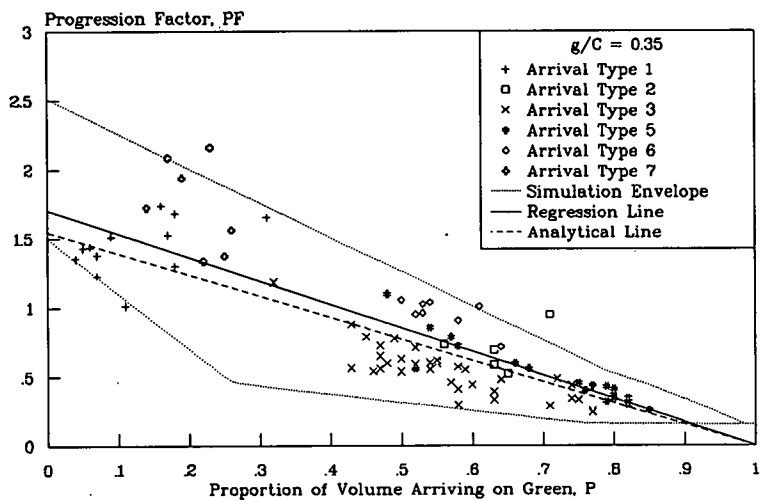


Figure C-17. Relationship Between Progression Factors and Proportion Total Volume Arriving on Green, g/C of 0.35 and 0.40..

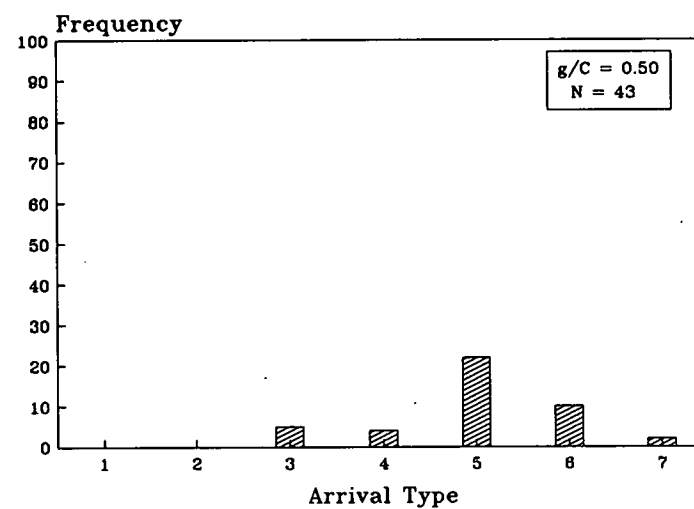
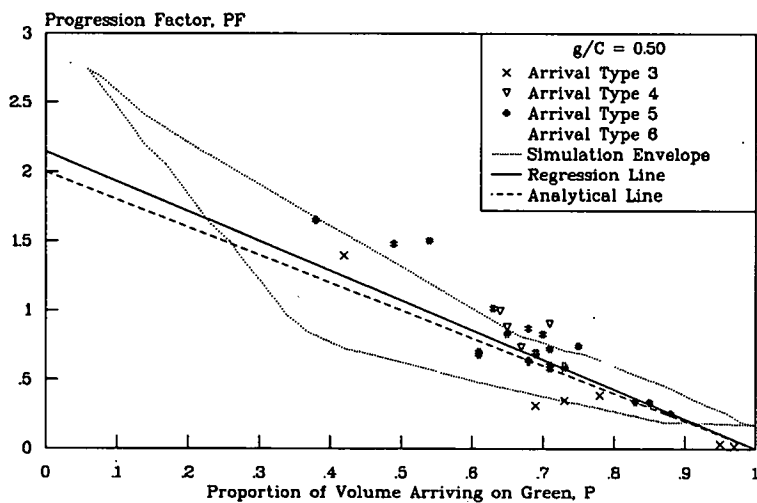
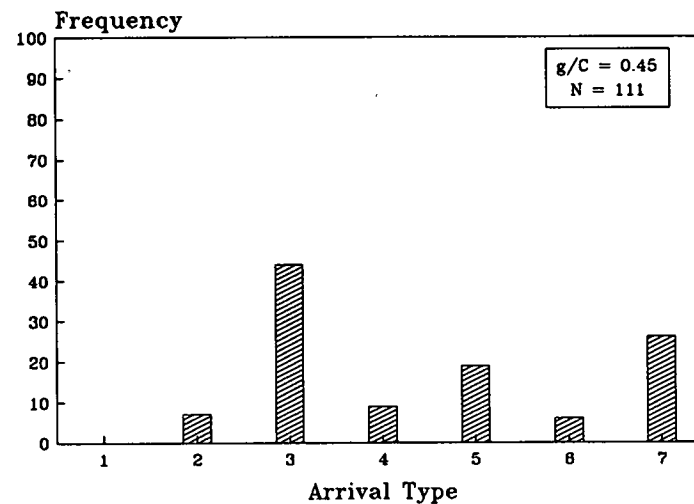
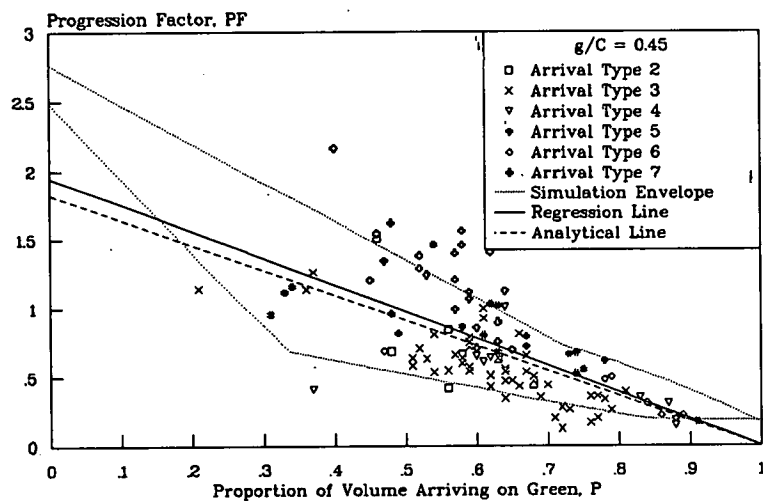


Figure C-18. Relationship Between Progression Factors and Proportion Total Volume Arriving on Green, g/C of 0.45 and 0.50.

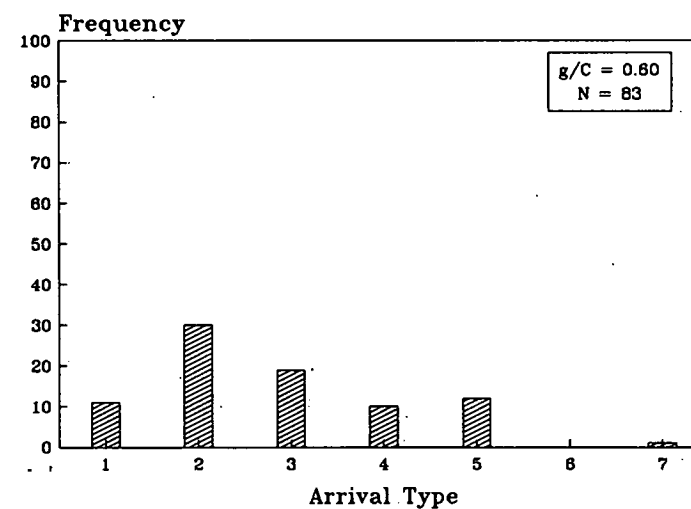
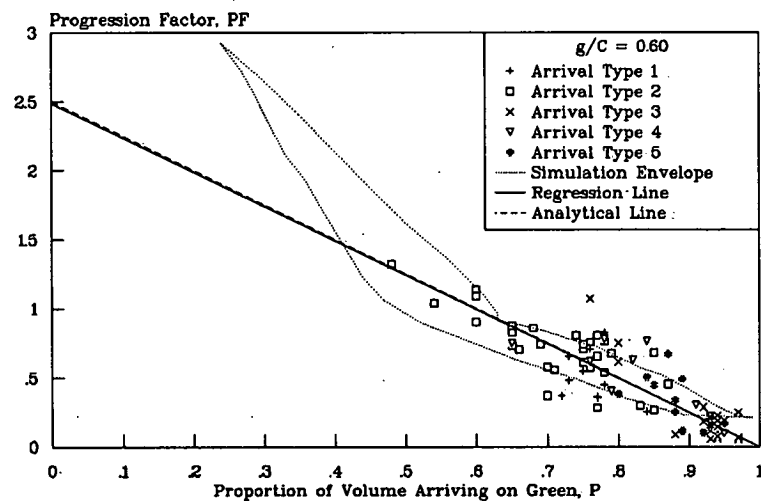
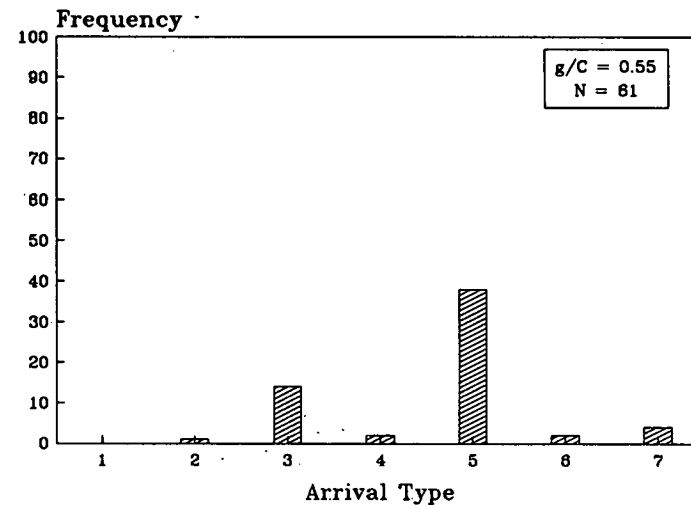
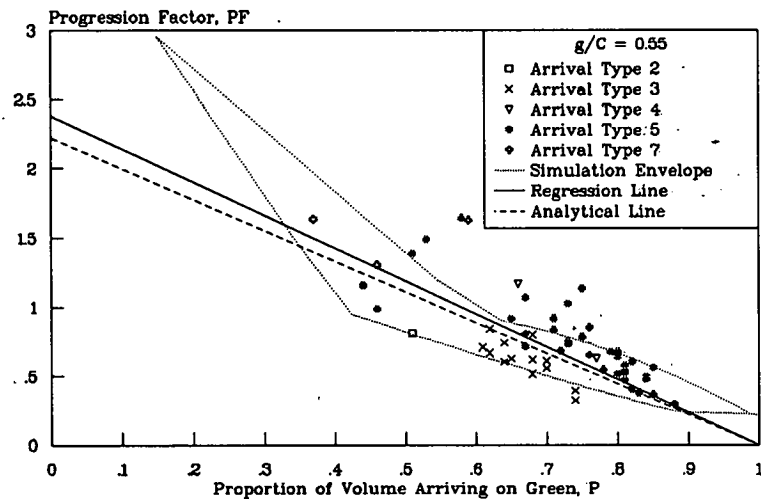


Figure C-19. Relationship Between Progression Factors and Proportion Total Volume Arriving on Green, g/C of 0.55 and 0.60.

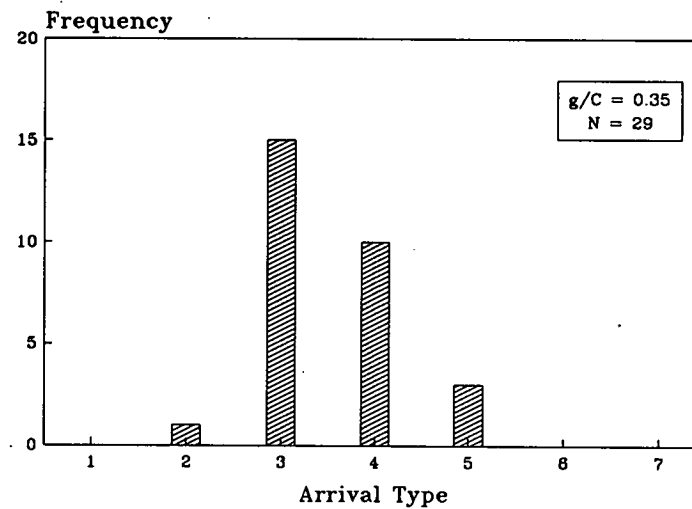
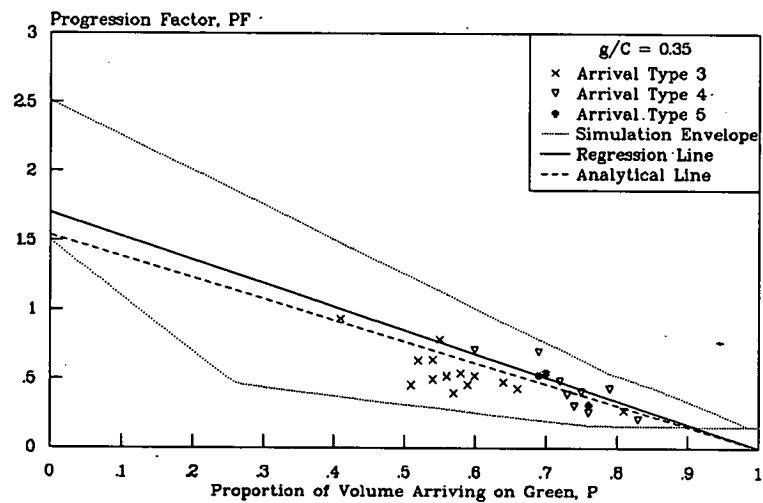
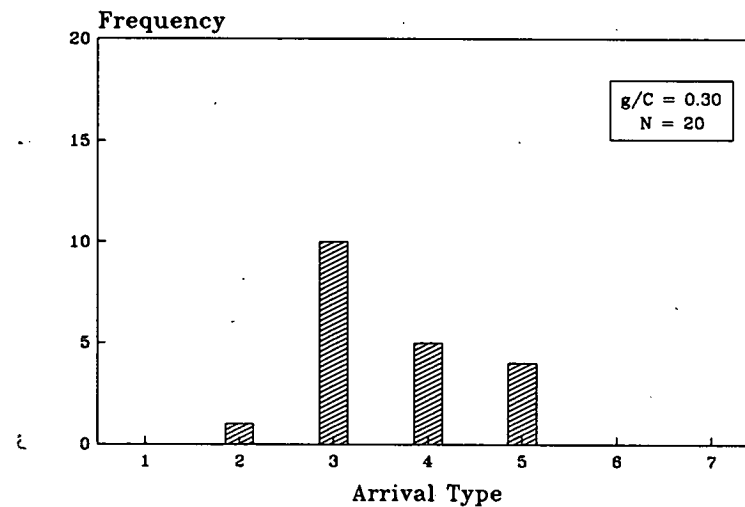
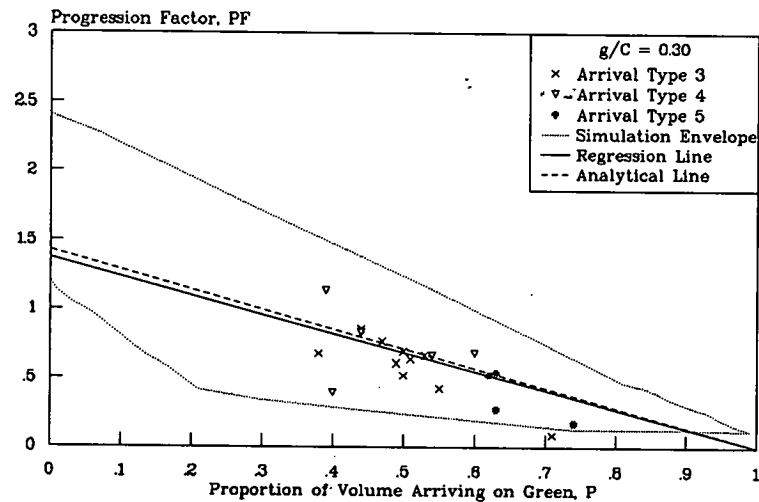


Figure C-20. Relationship Between Progression Factors and Proportion Total Volume Arriving on Green, Semiactuated Data.

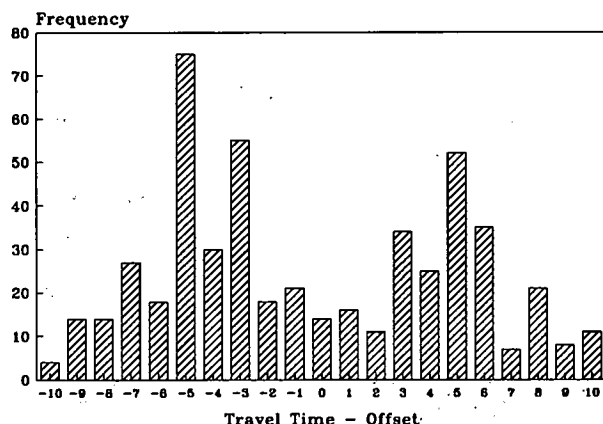


Figure C-21. Partial Histogram of the Variable Travel Time Minus Offset.

To further analyze the effects of early and late arrivals, the pretimed data set was separated by those two categories for further analysis. Regression analyses were then performed for both types of arrivals and each green ratio in the pretimed data set. The results are shown in Table C-8. Note that five of the nine equations for early arrivals predict lower progression factors (less delay) than the analytical equation and seven of the nine equations for late arrivals predict higher progression factors (more delay) than the analytical equation. Thus, it appears that an additional adjustment factor to account for early and late arrivals would further improve the accuracy of the delay equation. This factor, f_{AT} , could be applied to the proposed uniform delay equation as shown below:

$$d = (.38 * d_u * PF * f_{AT}) + (173 * d_u)$$

where:

$$d_u = r * \left(\frac{1-g/C}{1-y} \right)$$

and

$$PF = \left(\frac{1-P}{1-g/C} \right)$$

Table C-8. Results of Regression Analysis for Observed Versus Predicted Progression Factors for Early and Late Arrivals in the Pretimed Data Set.

	Number of Observations	Slope Parameter Estimate	R-Square	Standard Error	Confidence Interval (+/-)	T for Ho: Parameter = 1.0	Level of Significance
EARLY ARRIVALS							
All Data	475	0.873	0.91	0.012	0.02	-10.19 *	>0.999
$g/C = 0.25$	84	0.971	0.91	0.034	0.06	-0.85	0.602
$g/C = 0.30$	45	0.719	0.90	0.036	0.06	-7.85 *	>0.999
$g/C = 0.35$	53	0.985	0.94	0.033	0.06	-0.45	0.345
$g/C = 0.40$	134	0.818	0.91	0.022	0.04	-8.41 *	>0.999
$g/C = 0.45$	58	0.830	0.93	0.030	0.05	-5.60 *	>0.999
$g/C = 0.50$	10	0.935	0.95	0.071	0.13	-0.91	0.613
$g/C = 0.55$	29	0.810	0.91	0.048	0.08	-3.96 *	>0.999
$g/C = 0.60$	62	1.013	0.93	0.035	0.06	0.37	0.287
LATE ARRIVALS							
All Data	302	1.309	0.93	0.021	0.03	14.91 *	>0.999
$g/C = 0.25$	37	1.550	0.92	0.076	0.13	7.26 *	>0.999
$g/C = 0.30$	88	1.314	0.96	0.029	0.05	10.84 *	>0.999
$g/C = 0.35$	35	1.339	0.97	0.038	0.06	8.92 *	>0.999
$g/C = 0.45$	51	1.357	0.92	0.055	0.09	6.46 *	>0.999
$g/C = 0.50$	34	1.107	0.93	0.053	0.09	2.03 *	0.95
$g/C = 0.55$	44	1.294	0.93	0.054	0.09	5.41 *	>0.999
$g/C = 0.60$	13	1.014	0.87	0.112	0.20	0.12	0.094

* Statistically significant difference at the 95 percent confidence level.

Based on the data in Table C-8, the recommended values for f_{AT} are 0.85 for early arrivals and 1.30 for late arrivals. Although use of these discrete adjustment factors for arrival type creates a discontinuity in the delay equation, the discontinuity occurs near the minimum delay point (i.e., perfect progression) which corresponds to the smallest progression adjustment factors. Thus, because the arrival type adjustment factor is being multiplied by an already small progression adjustment factor, the magnitude of the discontinuity in predicted delay is usually negligible.

Conclusions

Based on the preceding results, it is apparent that the analytical equation developed in this research is a good estimator of progression adjustment factors. Table C-9 contains the progres-

sion factor values calculated from the analytical equation and recommended as a replacement for Table 9-13 in the HCM(1). These factors should be somewhat easier to use than the platoon ratio/arrival type factors currently in use as P can be measured in the field or estimated for one of several analytical procedures. If P is neither known nor estimable, however, the progression factor, PF , should be set equal to 1.0.

The delay prediction equations with which these factors would be used is such that the analytical equation for calculating progression factors provides adequate accuracy; i.e., more complicated equations do not significantly improve the accuracy of the delay prediction. The analytical equation also is easy to use and provides a continuous estimate of PF , thus eliminating the problem of discrete thresholds. The boundary conditions for the variables in the table are also wider than those given in the HCM.

Table C-9. Recommended Progression Adjustment Factors, PF^a , for both Pretimed and Semiactuated Signals.

Green Ratio, g/C	Proportion of Total Volume Arriving on Green, P							
	.20	.30	.40	.50	.60	.70	.80	.90
.60	N/A ^b	1.75	1.50	1.25	1.00	0.75	0.50	0.25
.55	1.78	1.56	1.33	1.11	0.89	0.67	0.44	0.22
.50	1.60	1.40	1.20	1.00	0.80	0.60	0.40	0.20
.45	1.45	1.27	1.09	0.91	0.73	0.55	0.36	0.18
.40	1.33	1.17	1.00	0.83	0.67	0.50	0.33	0.17
.35	1.23	1.08	0.92	0.77	0.62	0.46	0.31	0.15
.30	1.14	1.00	0.86	0.71	0.57	0.43	0.29	0.14
.25	1.07	0.93	0.80	0.67	0.53	0.40	0.27	0.13

Note: If P cannot be estimated by field data or a valid analytical procedure, $PF = 1.0$.

^a $PF = (1 - P) / (1 - g/C)$

and $d = (.38 * d_u * PF * f_{AT}) + (173 * d_l)$

where:

$f_{AT} = 0.85$ if the front of the platoon arrives before the start of green and the rear of the platoon arrives before the start of red (early arrivals);

$f_{AT} = 1.00$ if the front and rear of the platoon both arrive on either green or red; and

$f_{AT} = 1.30$ if the front of the platoon arrives after the start of green and the rear of the platoon arrives after the start of red (late arrivals).

^b N/A indicates a condition that simulation analysis shows to be extremely unlikely.

THE TRANSPORTATION RESEARCH BOARD is a unit of the National Research Council, which serves the National Academy of Sciences and the National Academy of Engineering. It evolved in 1974 from the Highway Research Board which was established in 1920. The TRB incorporates all former HRB activities and also performs additional functions under a broader scope involving all modes of transportation and the interactions of transportation with society. The Board's purpose is to stimulate research concerning the nature and performance of transportation systems, to disseminate information that the research produces, and to encourage the application of appropriate research findings. The Board's program is carried out by more than 270 committees, task forces, and panels composed of more than 3,300 administrators, engineers, social scientists, attorneys, educators, and others concerned with transportation; they serve without compensation. The program is supported by state transportation and highway departments, the modal administrations of the U.S. Department of Transportation, the Association of American Railroads, the National Highway Traffic Safety Administration, and other organizations and individuals interested in the development of transportation.

The National Academy of Sciences is a private, nonprofit, self-perpetuating society of distinguished scholars engaged in scientific and engineering research, dedicated to the furtherance of science and technology and to their use for the general welfare. Upon the authority of the charter granted to it by the Congress in 1863, the Academy has a mandate that requires it to advise the federal government on scientific and technical matters. Dr. Frank Press is president of the National Academy of Sciences.

The National Academy of Engineering was established in 1964, under the charter of the National Academy of Sciences, as a parallel organization of outstanding engineers. It is autonomous in its administration and in the selection of its members, sharing with the National Academy of Sciences the responsibility for advising the federal government. The National Academy of Engineering also sponsors engineering programs aimed at meeting national needs, encourages education and research and recognizes the superior achievements of engineers. Dr. Robert M. White is president of the National Academy of Engineering.

The Institute of Medicine was established in 1970 by the National Academy of Sciences to secure the services of eminent members of appropriate professions in the examination of policy matters pertaining to the health of the public. The Institute acts under the responsibility given to the National Academy of Sciences by its congressional charter to be an adviser to the federal government and, upon its own initiative, to identify issues of medical care, research, and education. Dr. Stuart Bondurant is acting president of the Institute of Medicine.

The National Research Council was organized by the National Academy of Sciences in 1916 to associate the broad community of science and technology with the Academy's purpose of furthering knowledge and advising the federal government. Functioning in accordance with general policies determined by the Academy, the Council has become the principal operating agency of both the National Academy of Sciences and the National Academy of Engineering in providing services to the government, the public, and the scientific and engineering communities. The Council is administered jointly by both Academies and the Institute of Medicine. Dr. Frank Press and Dr. Robert M. White are chairman and vice chairman, respectively, of the National Research Council.

TRANSPORTATION RESEARCH BOARD

National Research Council
2101 Constitution Avenue, N.W.
Washington, D.C. 20418

ADDRESS CORRECTION REQUESTED

NON-PROFIT ORG.
U.S. POSTAGE
PAID
WASHINGTON, D. C.
PERMIT NO. 8970